Characterisation Of Androgen Receptor Function In The Male Reproductive System Through Conditional Gene Targeting

Laura O'Hara

Thesis submitted to the University of Edinburgh for the degree of Doctor of Philosophy

February 2011

Declaration

The studies used in this thesis were the unaided work of the author, except where acknowledgement is made by reference. The work described in this thesis has not been previously accepted for, or is currently being submitted for another degree or qualification.

Laura O'Hara
February 2011

Acknowledgements

Several times during the course of my PhD I was convinced that I would never be writing these acknowledgements! So the people that have inspired me to keep going deserve these heartfelt dedications.

First I would like to thank Dr. Lee Smith, for being a supervisor who has taught me so much about how to think like a scientist, for never turning me away when I had a stupid question to ask and for his bad jokes, which (usually) make me smile.

I would also like to thank Prof. Philippa Saunders for her supervision. Philippa's comments have changed my perspective on several results in my PhD and inspired alternative directions in the work.

I would like to thank other members of the Smith group over the past 3 years: Nancy, Lindsey, Lindsay, Martin, and particularly Michelle, who has taught me so much in the lab and been a great friend throughout my PhD. Thanks to Mark Fisken, Mike Millar, Sheila MacPherson, Arantza Esnal, Nancy Evans, Ian Swanston and Marion Walker, all who have assisted me with animal work, histology, serum hormone assays and the ubiquitous stupid questions. Thanks to Prof. Richard Sharpe and Dr. Pamela Brown who have contributed to valuable discussions on my results.

Thanks to the friends I have made in the HRSU for their support, laughs, tea breaks, trips to Starbucks and Assembly (!) particularly Sharon, Vicky, Afshan, Kirsten, Michelle and Lindsey.

Thanks to my parents for never asking when I am going to get a 'proper job': I hope you take great pleasure in telling friends and family that I have finally submitted!

This thesis is dedicated to Andy: thanks for your amazing support and love. I couldn't have done this without you.

Abstract

Androgen receptor (AR) signalling is essential for the development and function of the male reproductive system. Conditional gene ablation using the Cre-*loxP* system has previously assisted in the elucidation of the role of AR in different cell types. The aim of this study was to examine the effects of the ablation of AR in previously untargeted cell types, with the hypothesis that this will have significant and novel effects on reproductive development and function that have not been previously documented by current models of androgen disruption.

In these studies, three Cre recombinase lines were empirically validated for action in the male reproductive system, before being used to ablate AR and the phenotypes of the resulting lines were characterised. Endothelial-specific receptor tyrosine kinase (Tie2)-Cre was shown to target the vascular and endothelial cells of the testis, and used to ablate AR in these cells. The testes of the resulting Tie2-ARKO line were morphologically similar to controls, with normal spermatogenesis and mature spermatozoa present in the cauda epididymis. Aquaporin 2 (Aqp2)-Cre was shown to target the post-meiotic germ cells of the testis, and was used to ablate AR in these cells. The testes of the resulting Aqp2-ARKO line were morphologically similar to controls, with normal spermatogenesis and mature spermatozoa present in the cauda epididymis. It was concluded that the *Ar* gene was dispensable in the endothelial cells and post-meiotic germ cells of the testis for normal spermatogenesis.

Forkhead box protein G1 (FoxG1)-Cre was shown to target the caput epididymal epithelium and pituitary, and used to ablate AR in these cells. d100 FoxG1-ARKO mice had a severe testicular phenotype, with sloughing of the seminiferous epithelium, atrophy of some seminiferous tubules and distension of the rete testis with spermatozoa. Despite the severe testis phenotype, ablation in the testis was incomplete and restricted to a small percentage of Leydig cells, with no ablation in Sertoli cells. Ablation of AR in the embryonic pituitary did not cause adult serum testosterone or LH concentrations to change, nor did it cause changes in other

pituitary hormone transcripts. Mosaic ablation of AR in the caput epididymal epithelium was shown to impair epididymal development, with failure of initial segment (segment I) development and a significant decrease in epithelial cell height and lumen diameter in the remaining proximal caput epididymis (segment II).

Dysfunction of the caput epididymis resulted in the failure of spermatozoa to transit the efferent ducts into the epididymis correctly: instead they were found to stall in the efferent ducts and produce a block. The testicular phenotype could be explained as the result of fluid backpressure effects resulting from the efferent duct block. Consequently, low concentration of spermatozoa in the cauda epididymis resulted in infertility in the FoxG1-ARKO, which represents a new model of obstructive azoospermia.

Publications relating to this thesis

O'Hara L., Welsh M., Saunders P. T. K. and Smith L. B.

Androgen receptor expression in the caput epididymal epithelium is essential for development of the initial segment and epididymal spermatozoa transit. *Endocrinology* 2011, 152(2):718-29.

Bound in this thesis with permission of co-authors.

Presentations relating to this thesis

Ablation of androgen receptor in the caput epididymis epithelium (CEE-ARKO) contributes to a novel mouse model of obstructive azoospermia

Oral presentation at the 15th European Testis Workshop, Elba, Italy, 2010

Ablation of pituitary androgen receptor from male mice results in infertility due to obstructive azoospermia.

Oral presentation at the 5th International Workshop Molecular Andrology, Giessen, Germany, 2009

Table of Contents

List of Figures

List of Tables

Abbreviations

Abbreviation	Definition
17βHSD	17β-hydroxysteroid dehydrogenase
3βHSD	3β-hydroxysteroid dehydrogenase
ACTH	adrenocorticotrophic hormone
AGD	anogenital distance
AIS	androgen insensitivity syndrome
AMH	anti-Müllerian hormone
ALC	adult Leydig cell
Aqp2	aquaporin 2
AR	androgen receptor
ARE	androgen response element
ARKO	androgen receptor knockout
ArKO	aromatase knockout
BSA	bovine serum albumin
CAIS	complete androgen insensitivity syndrome
cDNA	complementary deoxyribonucleic acid
Cre	Cre recombinase
d	postnatal day
DAB	3, 3 diaminobenzidine
DHT	dihydrotestosterone
DNA	deoxyribonucleic acid
e	embryonic day
ER	endoplasmic reticulum
ERKO	estrogen receptor knockout
ERα	estrogen receptor alpha
ERβ	estrogen receptor beta
EtOH	ethanol
FLC	fetal Leydig cell
FoxG1	forkhead box protein G1
FSH	follicle stimulating hormone
FSHβ	follicle stimulating hormone beta subunit
FSHβKO	follicle stimulating hormone beta subunit knockout
FSHR	follicle stimulating hormone receptor
FSHRKO	follicle stimulating hormone receptor knockout
GH	growth hormone
GHR	growth hormone receptor
H&E	haematoxylin and eosin
Hox	homeobox transcription factor
HPG	hypothalamus-pituitary-gonadal

Abbreviation	Definition
ILC	immature Leydig cell
Insl3	insulin-like protein 3
LBD	ligand binding domain
LH	luteinising hormone
LHβ	luteinising hormone beta subunit
LHβKO	luteinising hormone beta subunit knock-out
LHR	luteinising hormone receptor
LHRKO	luteinising hormone receptor knock-out
MD	Müllerian duct
mRNA	messenger ribonucleic acid
n	number
OA	obstructive azoospermia
PAIS	partial androgen insensitivity syndrome
PBS	phosphate buffered saline
PCR	polymerase chain reaction
PLC	progenitor Leydig cell
pnd	post-natal day
POMC	pro-opiomelanocortin
PTM	peri-tubular myoid
qRT-PCR	quantitative reverse transcription polymerase chain reaction
R26YFP	Rosa26 yellow fluorescent protein transgene
RT	reverse transcription
RT-PCR	reverse transcription polymerase chain reaction
SEM	standard error of the mean
SF-1	steroidogenic factor 1
SMA	alpha smooth muscle actin
Sox9	sex determining region Y-box 9
Sry	sex determining region Y
StAR	steroid acute regulatory protein
TBS	tris buffered saline
Tfm	testicular feminisation
Tie2	endothelial receptor tyrosine kinase 2
TSH	thyroid stimulating hormone
TSHβ	thyroid stimulating hormone beta subunit
TSHβKO	thyroid stimulating hormone beta subunit knock-out
TSHR	thyroid stimulating hormone receptor
TSHRKO	thyroid stimulating hormone receptor knock-out
UGS	urogenital sinus
WD	Wolffian duct
WT-1	Wilms' tumour suppressor protein 1
YFP	yellow fluorescent protein

1. Literature review

1.1 The mouse as a model organism for reproductive biology

1.1.1 The mouse as a model organism

The use of the house mouse, *Mus musculus* as a mammalian model organism for human disease has been growing in popularity since the beginning of the 20th century (Paigen, 2003a). The striking similarity between the anatomy and physiology of humans and mice was recognised long before the sequencing of the mouse genome discovered that there are mouse homologues of around 99% of human genes (Waterston et al., 2002). Mice and humans are estimated to have diverged from a common ancestor around 75 million years ago, comparatively recently in evolutionary terms (Paigen, 2003b). The advantages of using the mouse as a model organism are numerous. Its small size, basic needs (food, water, bedding, controlled temperature and light regimens and a small amount of environmental enrichment), short generation time (approximately 10 weeks from being born to giving birth) and a large litter number (an average of 5-10 pups) allows for rapid generation of large numbers of experimental animals (Silver, 1995). This makes them advantageous when compared to model organisms such as sheep and cows, which, although phylogenetically closer to humans, are expensive to maintain as experimental animals (Gama Sosa et al., 2010). Another advantage is the availability of congenic inbred strains generated from at least 20 generations of sibling inter-crosses (Beck et al., 2000) which are essentially genetically identical and homozygous at all loci, limiting any influence of genetic variation on experimental outcome. More recently, the generation of transgenic mice by oocyte pro-nuclear microinjection and gene targeting in embryonic stem (ES) cells has proven highly successful in mice but less adaptable in other species (Gama Sosa et al., 2010), resulting in an exponential increase in the number of transgenic mouse lines. The International Knockout Mouse Consortium aims to mutate all protein-encoding genes in the mouse using a combination of gene trapping and gene targeting in mouse ES cells (Collins et al.,

2007). As of December 2010 it has generated mutant ES cell lines for 15526 out of 24646 protein coding genes (http://www.knockoutmouse.org).

1.1.2 The Cre-*loxP* system

The Cre-*loxP* system is a genetic tool based on a method of site-specific recombination occurring in P1 bacteriophage (Nagy, 2000). Cre recombinase is an enzyme that catalyses the recombination of DNA between two *loxP* sites. The 34 bp *loxP* site consists of a directional element surrounded by palindromic binding sites for Cre. The directionality of the loxP sites affects the result of recombination: recombination between two inverted loxP sites will cause inversion of the DNA between them and recombination between two repeated loxP sites will cause deletion of the DNA between them. If *loxP* sites are on different chromosomes, a chromosomal translocation can occur.

Transgenes consisting of Cre recombinase driven by cell specific promoters allow cell-specific expression of Cre. These can be either 'knock-in' lines where Cre has been targeted to the endogenous locus of the promoter of interest, or 'random insertion' lines where both Cre and the cloned promoter that will drive it are inserted at a random locus in the genome. Both methods have problems associated with them (Matthaei, 2007). Knock-ins can produce an insertional deletion of the gene controlled by the promoter to be used which may result in a haploinsufficiency phenotype. However, the insertional deletion can be avoided if the construct uses an internal ribosome entry site (IRES) followed by the transgene placed between the stop codon and the polyadenylation signal of the target gene resulting in production of a bicistronic transcript. Random insertions may be significantly influenced by the local environment at the integration site which can lead to the ectopic expression or silencing of the transgene due to modification of the specificity of the promoter, or a more severe phenotype due to disruption of an unknown gene by insertion of the transgene (insertional mutagenesis). A further level of control can be introduced by fusing Cre to a ligand-inducible nuclear translocation signal such as that found in the nuclear hormone receptor family. Under the control of a cell-specific promoter Cre is

generated, but will not be transported to the nucleus to execute recombination unless a ligand to the hormone receptor of choice is applied (Garcia and Mills, 2002).

The corresponding 'floxed' line is created so that the sequence to be recombined is surrounded with direct *loxP* repeats. If cell-specific ablation of a gene of interest is required, this sequence can be a gene, or part of a gene such as an exon that is critical to the gene's action. This strategy can also be utilised for activation of a gene of interest, for example, a 'reporter gene' such as which results in a chromogenic (e.g. *E. coli* β-galactosidase) or fluorescent (e.g. *A. victoria* green fluorescent protein, GFP) product. Reporter genes can be part of a transgenic construct inserted into a ubiquitously expressed locus with an upstream stop codon flanked by *loxP* sites. Recombination between the *loxP* sites by Cre results in excision of the stop codon and expression of the reporter gene. Mating of a 'Cre' line with a 'floxed' line results in offspring with a cell-specific knock-out or activation of the gene of interest, as illustrated in Figure 1-1.

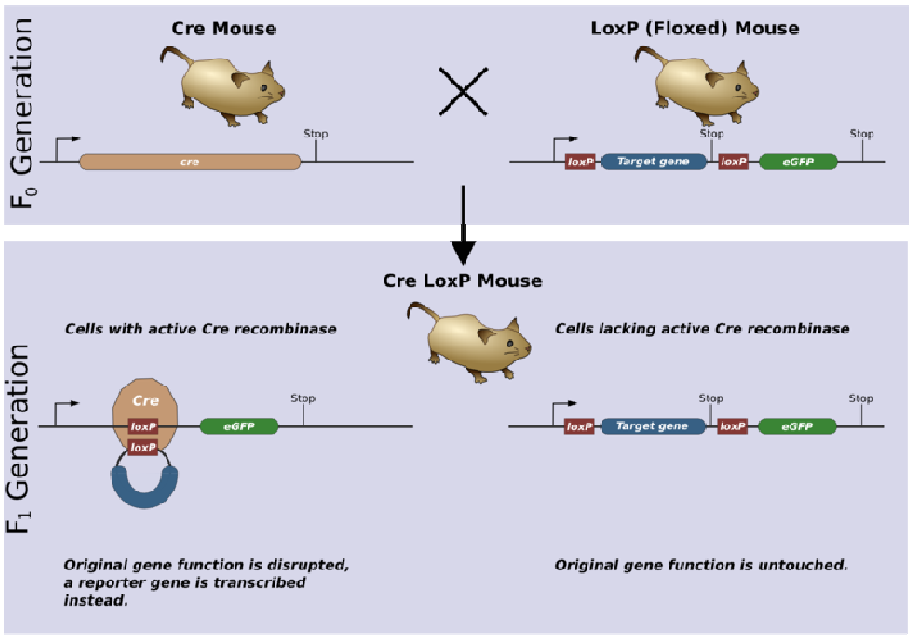

Figure 1-1: Mating of a mouse line expressing Cre under a tissue specific promoter with a mouse line containing a floxed gene of interest generates mice with the gene of interest conditionally ablated in the target tissue.

Image obtained through Wikimedia Commons (http://commons.wikimedia.org, author: Matthias Zepper)

1.1.3 The mouse reproductive system

The reproductive system of the male mouse (summarised in Figure 1-2) is located in the posterior abdomen and exists to produce and deliver haploid male gametes into the female tract for fertilisation. The testes are the male organs of gametogenesis. The testes produce spermatozoa (the male haploid gametes) and testosterone that is vital for correct development and function of the male reproductive system. In mice, the testes are retractable, and can either be found in the posterior abdominal cavity on either side of the urinary bladder, or in the scrotum which is an extension of the body cavity located between the penis and the anus, by travelling through the inguinal canal. Position of the testes is controlled by the cremaster muscle reflex in response to temperature or perineal pressure stimulus (Kojima and Ohe, 1986). Also found inside the scrotum are the excurrent ducts: the efferent ducts, epididymis and vas deferens. Spermatozoa exit the testis and are transported into the efferent ducts (involved in concentration of sperm) and into the epididymis (pl. epididymides), which is a single, highly coiled tubule located on the dorsal side of each testis. The epididymis provides a place for maturation and storage of spermatozoa in the mouse. Up until the point of ejaculation, spermatozoa are stored in the epididymis, and during ejaculation they pass into the vas deferens (pl. vasa deferentia). This is straight tubule that exits the epididymis on the posterior side of the testis and travels through the inguinal canal to connect with the urethra near the neck of the bladder. The vas deferens is surrounded with layers of contractile smooth muscle that force the sperm towards the urethra during ejaculation. The neck of the bladder and the anterior end of the urethra are surrounded by accessory glands and their ducts: the seminal vesicles, coagulating glands, ampullary glands, and the dorsal and ventral lobes of the prostate. These glands and ducts provide secretions to bathe and activate the spermatozoa on ejaculation. In mice, the secretions of these glands also cause the formation of a copulatory plug. During ejaculation, spermatozoa are released from the cauda epididymis, combine with secretions from these glands and enter the urethra. The urethra is the common outlet for urine and semen and extends from the urinary bladder to an opening on the top of the penis. The penis is the male intromittent organ that is used to transmit sperm into the male reproductive tract. In

mice, it contains a small bone: the os penis, as well as corpus cavernosum tissues. The bulbourethral glands secrete a fluid that lubricates the urethra and removes any traces of urine so the urethral environment facilitates the transit of the spermatozoa. In the final stages of ejaculation during mating, sperm pass down the urethra, through the penis and into the female reproductive tract.

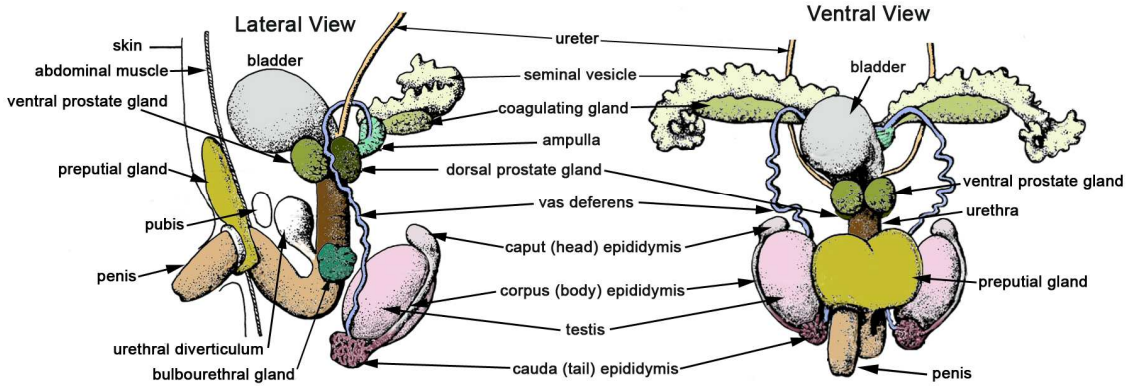

Figure 1-2: Lateral and ventral views of the male mouse reproductive system

Adapted from R. Rugh (1964) Vertebrate Embryology

1.2 Steroidogenesis

Steroid hormones are vital for normal reproductive development and function in both males and females (Johnson and Everitt, 2000). The web of enzymatic conversions that take place in steroidogenesis are summarised in Figure 1-3.

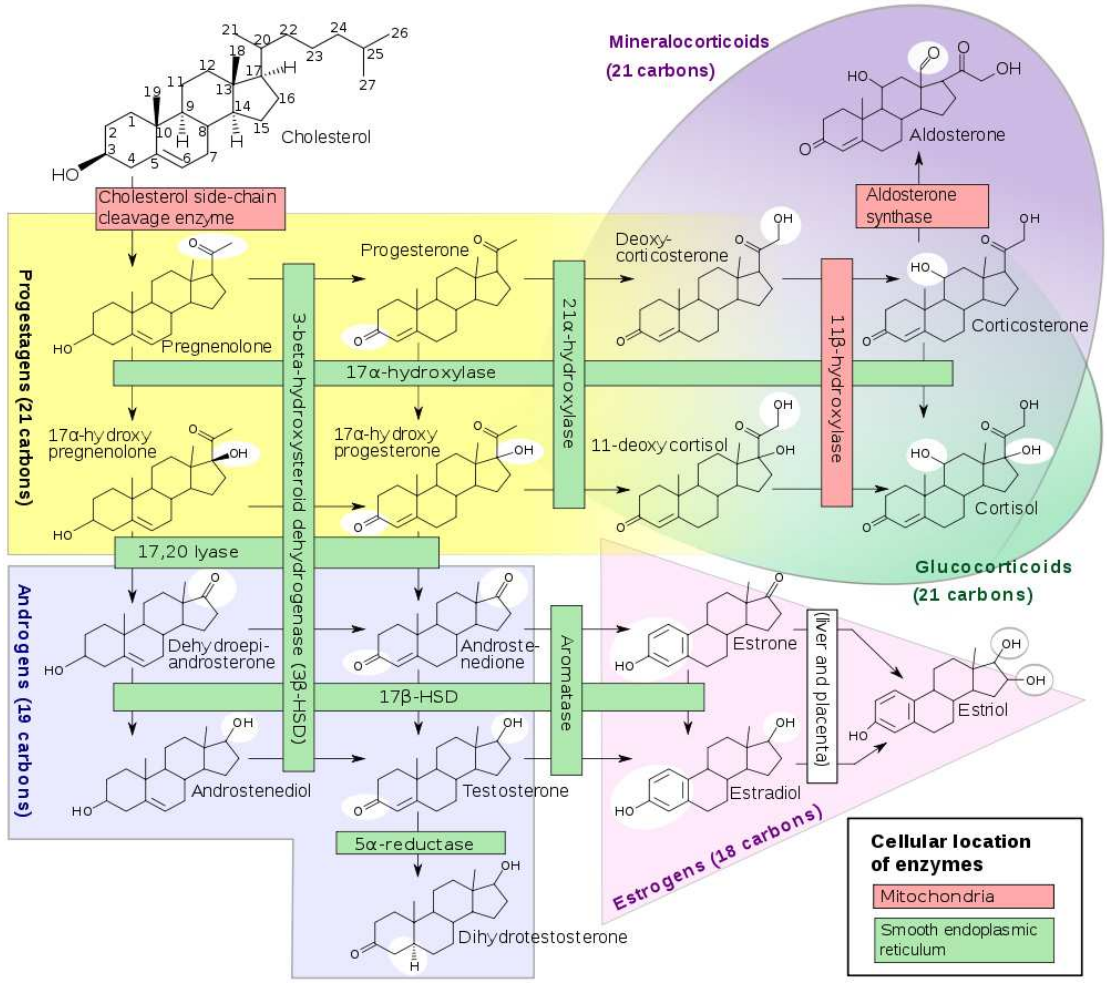

Figure 1-3**: **Synthesis of steroid hormones from cholesterol

Indicating the classes of hormones, enzymes involved and cellular locations (from http://commons.wikimedia.org/, author: Mikael Häggström).

Although it is possible for all steroid hormones to be synthesised from pregnenolone, the hormones produced by a steroidogenic cell largely depend on which of the steroidogenic enzymes it expresses. Synthesis of all steroid hormones begins with the

shuttling of cholesterol from the outer to the inner mitochondrial membrane by steroidogenic acute regulatory protein (StAR), this is the rate-limiting step of steroidogenesis (Stocco, 2001). Cholesterol is then converted to pregnenolone, catalysed by the enzyme cytochrome P450, family 11, subfamily a, polypeptide 1 (commonly known as P450scc, encoded by the *Cyp11a1* gene) (Porter and Coon, 1991). Pregnenolone then exits the mitochondria and can be converted into progestogens, estrogens, androgens, mineralocorticoids and glucocorticoids in the smooth endoplasmic reticulum.

1.2.1 Testicular testosterone biosynthesis

Androgens are the class of steroid hormones responsible for masculinisation and function of the adult reproductive tract. The Leydig cells are the source of androgens in the testes. Due to the web of potential steroid conversions mediated by enzymes that can catalyse multiple steps in the web, production of testosterone by the testis is a dynamic process involving multiple substrates and dynamic equilibria established between intermediate products of the reaction. In the mouse Leydig cell, pregnenolone is converted to progesterone by the action of hydroxy-Δ5-steroid dehydrogenase, 3β- and steroid Δ-isomerase (commonly known as 3β-HSD), types I (encoded by the *Hsd3b1* gene) and VI (encoded by the *Hsd3b6* gene)(Baker et al., 1999). 17α-hydroxylase/17,20 lyase/17,20 desmolase (commonly known as 17α-hydroxylase, encoded by the *Cyp17a1* gene) then catalyses first the hydroxylation of progesterone at C_{17} followed by the cleavage of the two-carbon side-chain to yield the C_{19} steroid, androstenedione, the immediate precursor of testosterone (Nakajin and Hall, 1981). The final reaction is the reduction of the 17-ketone of androstenedione by 17β-hydroxysteroid dehydrogenase (commonly known as 17β-HSD) type III (encoded by the *Hsd17b3* gene)(Geissler et al., 1994). Leydig cells also express cytochrome P450, family 19, subfamily A, polypeptide 1 (commonly known as aromatase, encoded by the *Cyp19a1* gene), which catalyzes the aromatisation of testosterone to 17β-estradiol. Testosterone biosynthesis begins around e13 in the mouse and 6-7 week of pregnancy in the human and is secreted at high levels by fetal Leydig cells during embryonic life to enable masculinisation of the male reproductive tract during development (section 1.3)(O'Shaughnessy et al.,

2006). There is then a reduction of testosterone secretion after birth before adult Leydig cells begin to secrete testosterone around puberty (section 1.5).

Testosterone can act as an autocrine, paracrine or endocrine hormone after binding its receptor, androgen receptor (AR, encoded by the *Ar* gene, see section 1.2.2). As well as having local effects in the testis, testosterone can diffuse into the blood and lymph vessels in the testicular interstitium and be transported around the body in the systemic circulation to reach other endocrine target tissues. It can also diffuse into the seminiferous tubules of the testis, where it may enter Sertoli cells or be carried to the excurrent ducts in seminiferous tubule fluid. During transport in the blood or testicular fluid, testosterone is bound to androgen binding protein (ABP) in rodents, or sex-hormone binding globulin (SHBG) in humans (Joseph, 1994).

1.2.1.1 Conversion of testosterone to DHT

Testosterone can also be converted to dihydrotestosterone (DHT) by the action of steroid 5α-reductase. DHT also binds to the AR and is considered a more 'potent' AR agonist because it has a higher binding affinity for the AR but a lower dissociation rate, making it ideal to stimulate a response at low concentrations (Grino et al., 1990). Conversion occurs locally in tissue-specific sites, and is thought to facilitate the action of testosterone in tissues receiving low concentrations. Two isoforms of steroid 5α-reductase transcribed from separate genes were identified in humans and termed type 1 (encoded by the *Srd5a1* gene) and type 2 (encoded by the *Srd5a2* gene)(Andersson et al., 1991; Andersson and Russell, 1990; Labrie et al., 1992). Mice also have two isoforms (Jenkins et al., 1991). Type 1 is present in non-genital skin, liver and brain and type 2 is present in fetal and adult genitals and adult liver. Males with mutations in the 5α-reductase type 2 gene are born with female external genitalia, and often (but not invariably) with undescended inguinal testicles (Imperato-McGinley and Zhu, 2002). Despite this, the Wolffian duct differentiates normally, with distinct epididymis, vas deferens and seminal vesicles. At puberty patients often undergo a slight virilisation with growth of the phallus and scrotum, and occasionally descent of the testicles due to an increase in circulating testosterone

levels. However the prostate is reduced in size, and although ejaculation is often possible, semen is very viscous. Despite this, normal sperm concentrations and motility are possible, and intra-uterine insemination has been performed successfully with sperm from men with 5α-reductase type 2 (Katz et al., 1997). The phenotype of these males implies that DHT is vital for external genitalia differentiation in humans, as well as growth and function of the prostate, but that it does not seem to have a vital role in sperm production or maturation. In contrast, mice with a knock-out of both 5α-reductase type 1 and type 2 genes have normal external and WD virilisation but with smaller seminal vesicles and prostate (Mahendroo et al., 2001). They are fertile, albeit with a slight decrease compared to controls, and have normal sperm morphology and movement. The relatively mild phenotype in these mice suggests that testosterone is the only androgen required for the differentiation of the male urogenital tract in mice and that the synthesis of DHT serves largely as a signal amplification mechanism.

1.2.1.2 Conversion of testosterone to 17β-estradiol

Testosterone can also be converted to 17β-estradiol in the male mouse reproductive system by the action of aromatase in the Leydig cells and round and elongating spermatids of the testis (Nitta et al., 1993), and epididymal sperm (Janulis et al., 1996). 17β-estradiol acts by binding to its receptors, estrogen receptor α (ERα, encoded by the *Esr1* gene) and estrogen receptor β (ERβ, encoded by the *Esr2* gene) (Heldring et al., 2007). The actions of estrogens in the male reproductive system will be referred to in more detail in sections 1.4 and 1.6.

1.2.2 The androgen receptor (AR)

Steroid hormones can enter almost all cells in the body by diffusing through the lipid bilayer of the cell membrane. Once inside, they bind to receptors that are members of the ligand-activated transcription factor super-family. These intracellular receptors can become activated upon ligand binding allowing interaction with regulatory regions in the genome specific to that receptor (section 1.2.3.1). They can also act in

the absence of a ligand through a non-classical pathway (section 1.2.3.2). All steroid hormone receptors share a similar structure made up of 4 main functional domains (from N to C terminal): the variable domain, DNA-binding domain, hinge region and ligand-binding domain (Ribeiro et al., 1995).

Androgen receptor (NR3C4; nuclear receptor subfamily 3, group C, gene 4) is a single copy gene present on the X chromosome in mice and men (Brown et al., 1989). The length of the ORF is 2697 nucleotides over eight coding exons, which produces a peptide of 899 amino acids (Faber et al., 1991).

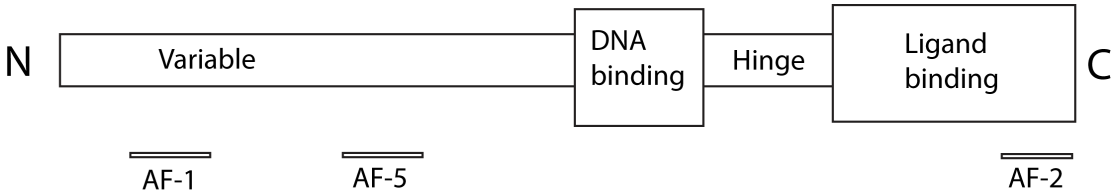

Figure 1-4: Structure of the androgen receptor

Note its four functional domains and three transcriptional activation regions (AF-1, AF-2 and AF-5)

The DNA, hinge and ligand binding domains of the mouse AR are virtually identical to the human AR, but there is approximately 15% variation in the N-terminal variable region (Gaspar et al., 1990). Despite this, mice with a transgenic knock-in of human AR show normal development and fertility (Albertelli et al., 2006). AR and both the ligand binding and DNA binding domains are identical between the two species. The N-terminal variable region of the AR comprises over half of the receptor protein. This region is poorly conserved both in length and sequence similarity among the members of the steroid receptor family (Faber et al., 1989). Within this domain are two transcription activation regions (AF-1 and AF-5) which can bind co-regulator proteins to increase or decrease transcription of downstream genes (Jenster et al., 1995; McEwan, 2004). It also contains a variable polyglutamine stretch that may be important in transcriptional regulation (Lieberman et al., 2002). The AR DNA-binding domain has the greatest sequence similarity with other steroid receptors (Brinkmann, 2009). It is composed of two zinc finger motifs: the first is

responsible for recognition of the target DNA sequence while the second stabilises DNA-receptor interaction by contact with the DNA phosphate backbone (Berg, 1989; Freedman, 1992). Between the two zinc fingers is an amino acid sequence that can recognise specific DNA response elements thus making this domain vital for transcription of downstream genes (Beato et al., 1996). At the overlap between the between the DNA binding and hinge regions is a nuclear targeting sequence that is responsible for androgen dependent translocation from the cytosol to the nucleus (Jenster et al., 1993). The hinge region is responsible for androgen dependent conformational changes of the AR. The ligand binding domain (LBD) is at the C-terminus of the AR. Its sequence is less conserved between other steroid hormone receptors to ensure specific, high affinity binding of androgens (Mangelsdorf et al., 1995). The LBD contains another transcription activation region (AF-2) which can bind coregulator proteins to increase or decrease transcription (Beato et al., 1996). The LBD also contains a binding region for heat-shock protein 90 (HSP90) that is common to all steroid hormone receptors: HSP90 and other HSPs are thought to be involved in maintaining the structure of the receptor in the absence of ligand and preventing the receptor from associating with AREs on DNA in the absence of ligand (Jenster et al., 1993; Picard et al., 1990).

1.2.3 Mechanisms of AR action

1.2.3.1 Classical mechanism of AR action

The current model for genomic androgen action involves a multi-step mechanism (see Figure 1-5). Upon entry of testosterone into the androgen target cell, binding occurs to the androgen receptor either directly or after its conversion to DHT. Binding of the androgen ligand to the receptor is followed by dissociation of the 3'-bound heat shock proteins in the cytoplasm (Jenster et al., 1993). HSP release unmasks the DNA binding motifs and the nuclear localisation signal (Kuil and Mulder, 1995). Androgen binding promotes AR hyper-phosphorylation which induces coactivator recruitment and transcriptional activation (Gioeli et al., 2002;

Kuiper and Brinkmann, 1995). The complex then translocates to the nucleus (Georget et al., 1997).

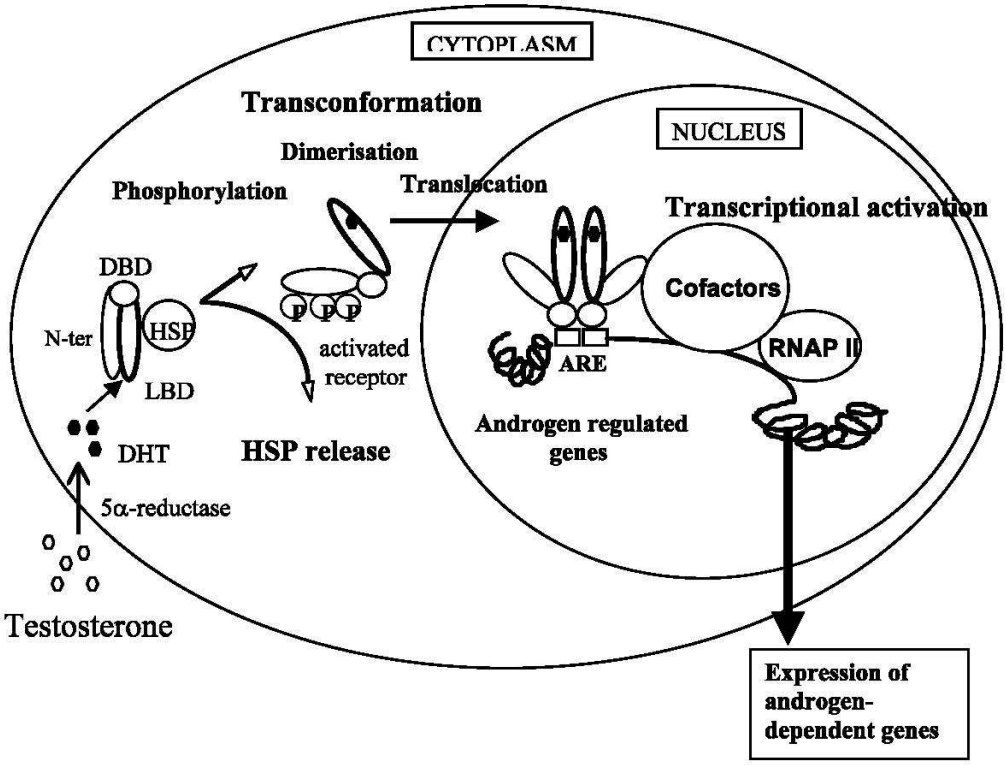

Figure 1-5: The classical mechanism of AR action

Testosterone enters the cell. It can bind to the ligand binding domain (LBD) of cytoplasmic AR either as testosterone or after conversion to DHT. Loss of bound heat-shock proteins (HSP) occurs, along with phosphorylation of the receptor, dimerisation and translocation to the nucleus.The DNA binding domain (DBD) binds to androgen response elements (ARE) in the genome, and cofactors and RNA polymerase (RNAP) II bind to the receptor complex, resulting in expression of androgen dependent genes.(Gobinet et al., 2002)

It is widely accepted that the receptor/ligand complex requires dimerisation to bind to androgen response elements (AREs) located in the regulatory regions of androgen responsive genes (Jones, 1990). Classical AREs are 15 bp sequences with two imperfect 6 bp repeats that are almost identical to glucocorticoid response elements so will also bind glucocorticoids (Roche et al., 1992). More recently, androgen-specific response elements have been discovered that will only bind activated AR.

Reproductive homeobox on the X chromosome 5 (*Rhox5*) is a well-characterised androgen-responsive gene with two androgen-specific AREs in its promoter (Barbulescu et al., 2001). Rhox5 itself is a transcription factor found in Sertoli cells that is thought to direct some of the actions of AR in the testes (Hu et al.). In order to modify transcription of genes with AREs, the AR/ligand homodimer complex further recruits additional proteins that form a transcription activation/repression complex at discrete sites on the chromatin (McKenna et al., 1999). Cofactors are thought to be cell specific so AR signalling can elicit particular responses in a wide variety of different tissues.

1.2.3.2 Non-classical and ligand independent actions of androgens and AR

Androgens and AR can act in a rapid non-classical way without binding to genomic AREs. Non-classical effects of testosterone have now been demonstrated convincingly in several tissues, in particular in the reproductive, cardiovascular, immune and musculoskeletal systems (Rahman and Christian, 2007). It is thought that non-classical signalling may explain the relative lack of genes discovered that contain AREs compared to the wide range of effects that testosterone can produce within a cell (Walker, 2010). In the reproductive system, evidence from both Sertoli cells and the prostate cancer LNCaP cell line show that testosterone can produce intracellular calcium influx *via* membrane depolarisation, leading to cytoskeletal rearrangement (Kampa et al., 2002; Lyng et al., 2000). It can also activate the mitogen-activated protein kinase (MAPK) pathway to regulate numerous transcription factors including cAMP response element binding protein (CREB), independently of AR binding to DNA. This is thought to occur by binding of testosterone-activated AR to Src tyrosine kinase, which subsequently activates the MAPK pathway through the EGF receptor (Cheng et al., 2007; Fix et al., 2004).

AR can also act ligand-independently. A set of constitutively-active AR splice variants that lack the ligand-binding domain have been discovered in hormone-refractory prostate cancer cells (Hu et al., 2009). In the absence of ligand or in the presence of low androgenic concentrations, AR can also be stimulated by growth

factors or proinflammatory cytokines including interleukin-6 and insulin-like growth factor 1 (Kim and Lee, 2009; Malinowska et al., 2009).

1.2.4 Disruption of AR action

1.2.4.1 Clinical mutations

Androgen insensitivity syndrome (AIS) consists of a spectrum of masculinisation disorders in XY individuals from a fully female external phenotype (complete (C)AIS) to an undervirilised male phenotype (partial (P)AIS). In most cases, AIS is caused by a mutation of the *Ar* gene (Quigley et al., 1995). CAIS (historically known as testicular feminisation or *Tfm*) individuals have inguinal undescended testes with incomplete spermatogenesis: embryonic testicular development is not affected by lack of androgens but testicular descent and adult function is dependent on it (section 1.3). Due to lack of AR signalling during development, they have female external genitalia, a blind ending vagina and no Wolffian duct-derived structures (Quigley et al., 1995). Because the Sertoli cells of the testes still produce AMH they have no uterus or oviducts. PAIS is a spectrum of undervirilisation, and testicular maturation of seminiferous tubules and Sertoli cells tends to be more advanced in patients with PAIS than ones with CAIS (Muller, 1984).

As of November 2010, more than 1000 mutations in human *AR* have been identified (http://www.mcgill.ca/androgendb/). Many of these mutations lead to androgen insensitivity *via* different mechanisms: incomplete synthesis of the AR protein, inability of androgen binding by the AR or abnormalities in binding of the androgen–AR complex to AREs (Gottlieb et al., 2004). Some of them are ‘silent’ and do not have a phenotypic effect, others are implicated in prostate cancer (Marcelli et al., 2000) and Kennedy’s disease (X-linked spinal and bulbar muscular atrophy) (Lumbroso et al., 1997). Kennedy’s disease results in an expansion of the polyglutamine tract in the N-terminal variable region of the AR. Symptoms include progressive flaccid proximal paralysis and muscle atrophy as well as endocrine disturbances including gynaecomastia and progressive infertility (La Spada et al., 1991). A number of mutations in the AR have also been reported that result in

patients that present with oligozoospermia or azoospermia despite an otherwise normal male phenotype (Hiort and Holterhus, 2003). For example, in one patient, the mutation prevented interaction of the AR with a TIF2, Sertoli-cell specific co-activator, thus impeding the genomic actions of AR in Sertoli cells only (Ghadessy et al., 1999).

1.2.4.2 Transgenic animal models

The first animal model of androgen insensitivity was described in 1970 by Lyon and Hawkes, who reported an X-linked gene for *Tfm* in the mouse (Lyon and Hawkes, 1970). It was subsequently discovered that male *Tfm* mice carry a single nucleotide deletion in exon 1 of their *Ar* gene, the resulting frameshift introduces a premature termination codon (Charest et al., 1991; Gaspar et al., 1991). With the advent of Cre-*loxP* technology (section 1.1.2), mice with a total androgen receptor knock-out (ARKO) genotype have been produced by four groups. By mating a mouse line with floxed region of the *Ar* gene to one expressing Cre recombinase under the control of a constitutively active gene, genetic ablation of part of the AR resulting in loss of functional protein was achieved in all cells of the resulting offspring (De Gendt et al., 2004; Notini et al., 2005; Sato et al., 2004; Yeh et al., 2002). Both ARKO and *Tfm* mice have a phenotype similar to that of CAIS, with small, inguinal testes, lack of Wolffian duct structures and external feminisation. Testicular histology consists of some tubules with Sertoli cells only and the others containing a few spermatogonia, but no post-meiotic germ cells. Normal spermatogenesis does not occur. This is analogous to testicular histology in CAIS patients (Hannema et al., 2006; Yeh et al., 2002).

Studies of global androgen receptor ablation mice have been vital in gaining information on the function of androgens during development, but since adult spermatogenesis is incomplete and Wolffian duct-derived structures (epididymis, vas deferens and seminal vesicles) are absent, little knowledge can be gained about the post-natal role of androgens in these tissues. Cre-*loxP* transgenic mice are ideal for studying the post-natal actions of androgens and also for elucidating the specific roles of androgens in different cell types, as the promoter that drives Cre can be

selected to be active post-natally, or in specific cell types. Mouse lines with cell-specific knock-outs of AR in Sertoli cells (Chang et al., 2004; De Gendt et al., 2004; Holdcraft and Braun, 2004), peri-tubular myoid cells (Welsh et al., 2009a; Zhang et al., 2006), Leydig cells (Xu et al., 2007), germ cells (Tsai et al., 2006), vascular smooth muscle (Welsh et al., 2010b), prostate epithelium (Simanainen et al., 2008; Wu et al., 2007), seminal vesicle smooth muscle (Welsh et al., 2010a) and nervous system (Raskin et al., 2009) have been characterised.

1.3 Androgens and reproductive development

1.3.1 Formation of the fetal testis and initiation of androgen production

Sex determination in mammals results from the action of the Sex-determining region Y (*Sry*) gene (Sinclair et al., 1990). *Sry* is normally found on the Y chromosome but translocations may occur that cause individuals with an XX genotype to develop into males (Koopman et al., 1991). Prior to action of *Sry* at e10.5 embryos develop 'bipotential' gonads independent of chromosomal sex, but expression of *Sry* causes the gonads to form into testes and begin production of androgens, which act to masculinise the male reproductive tract.

The intermediate mesoderm thickens to form a pair of urogenital ridges first identifiable at e10 either side of the aorta. Three segments emerge from each ridge, the transient pronephros, the mesonephros and the metanephros, which later develops into the kidney (Kuure et al., 2000). The gonads begin to form on the ventromedial side of the mesonephros beneath the coelomic epithelium at e10.5 and grow quickly over the next 48 hours through recruitment of somatic and germ cells. The primordial germ cell gamete precursors move from the allantois to the hindgut and then actively migrate to the developing urogenital ridges *via* the dorsal mesentery, where they continue to proliferate. Germ cell migration completes between e10-11.5 (Bendel-Stenzel et al., 1998). The somatic supporting cell population of the bipotential gonad at this stage is recruited from the coelomic epithelium (Karl and Capel, 1998).

Several genes have been identified that are necessary for development of the bipotential gonad. Mutations in genes encoding steroidogenic factor 1 *(Sf-1),* Wilms' tumour suppressor 1 *(WT-1),* Lim homeobox gene 9 *(Lhx9)* and empty-spiracles homeobox gene 2 *(Emx2)* result in regression of both XX and XY gonads before differentiation (Wilhelm et al., 2007).

The first stage of testis differentiation involves the expression of the transcription factor *Sry* at e10.5 in a sub-population of cells that have migrated from the coelomic epithelium to the gonad. At e11.5 the gonad is undifferentiated and only 6 cells thick, but by e12.5 the testis is easily discernable on the ventro-medial side of the mesonephros and the newly-formed seminiferous cords can be identified (Smith and Mackay, 1991). Early stages of testis formation include complex positive and negative feedback loops resulting in proliferation and recruitment of the supporting cell lineage of the testis (Sekido and Lovell-Badge, 2009). Cells expressing Sry differentiate into Sertoli cells (Palmer and Burgoyne, 1991). Sry combines with SF-1 to upregulate expression of Sry-like HMG box 9 (*Sox9)* in pre-Sertoli cells almost immediately after *Sry* expression (Kent et al., 1996; Morais da Silva et al., 1996).

Sry initiates a feed-forward loop between Sox9 and fibroblast growth factor 9 (Fgf9), which represses two independent signalling pathways, one involving the R-spondin1 (Rspo1)/ wingless-type MMTV integration site family, member 4 (Wnt4)/β-catenin pathway and the other involving Foxl2. This results in differentiation of more Sertoli cells and commitment to a testis-specific fate (Kim et al., 2006). In females, the absence of the Sry stimulus prevents the feed-forward loop between Sox9 and Fgf9, and thus allows the Rspo1/Wnt4/β-catenin pathway and Foxl2 to block further *Fgf9* transcription, initiating the female-specific pathway. Thus, gonadal fate is dependent on which way the balance is tipped between the mutual antagonism of the male and female pathways. The ‘tipping point’ is the expression of *Sry* (Nef and Vassalli, 2009).

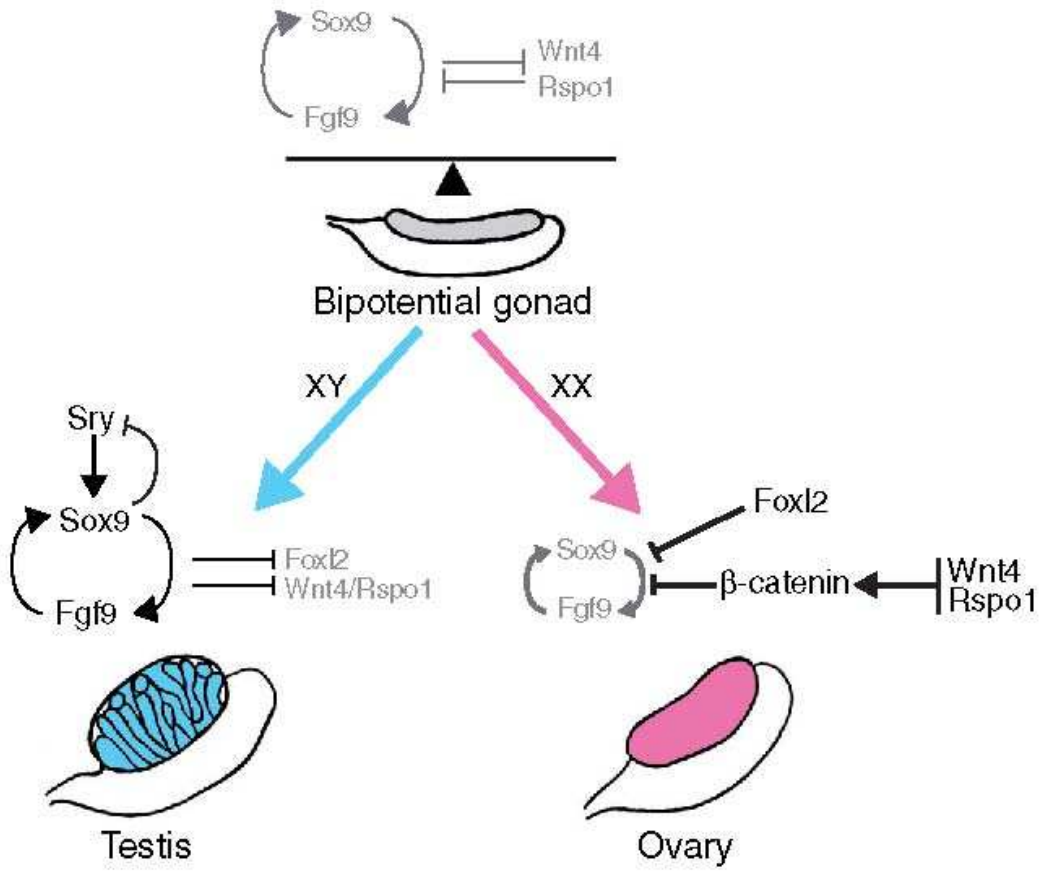

Figure 1-6: A genetic model of sex determination

The mutual antagonism of Sox9/Fgf9 and Foxl2/Rspo1/Wnt4 acts as a 'balance' that can tip the bipotential gonad towards either a testicular or ovarian fate. Arrows indicate stimulation; T bars indicate inhibition (Nef and Vassalli, 2009).

The next stage of testis development involves the polarisation and aggregation of pre-Sertoli cells around the newly-migrated germ cells to form the seminiferous cords. Peri-tubular myoid (PTM) cells are induced to differentiate and surround the cords, depositing the basal lamina (Frojdman et al., 1992). PTM differentiation, formation of the testis-specific vasculature and differentiation of fetal Leydig cells are all developmentally intertwined, and disruption of one of these processes often results in disruption of the other. For example, disruption in PTM cell differentiation resulting from a knockout of the desert hedgehog (*Dhh)* gene causes impairment of testis cord formation and fetal Leydig cell differentiation (Yao and Capel, 2002).

Migration of cells from the mesonephros induces cord formation (Tilmann and Capel, 1999) and differentiation of PTM cells from the interstitial cells derived from the coelomic epithelium (Cool et al., 2008). Inhibition of the development of the testis-specific coelomic vessel results in the absence of testis cords (Combes et al., 2009). Fetal Leydig cells (FLCs) first appear in the mouse at around e12.5 as an inter-cord population expressing p450scc (Greco and Payne, 1994). There are several theories that FLCs arise from cells migrating from the neural crest, adreno-gonadal primordium, coelomic epithelium or mesonephros, or that they are present in the bipotential gonad but induced to differentiate by an unknown signal upon male sex determination. Currently none of these putative migratory populations, nor a resident gonadal population have been demonstrated to be an exclusive source of FLCs (Griswold and Behringer, 2009). Differentiation and development of FLCs is known to depend on a number of factors including the Sertoli cell products *Dhh* (Yao et al., 2002) and *platelet derived growth factor A (PdgfA)* (Brennan et al., 2003), the PTM/endothelial product *aristaless related homeobox gene (Arx)* (Kitamura et al., 2002) and *steroidogenic factor 1 (SF-1)* which is specifically required for induction of steroidogenic enzyme expression in FLCs (Jeyasuria et al., 2004). Onset of expression of the necessary steroidogenic enzymes from e12.5 onwards (Greco and Payne, 1994) results in secretion of testosterone from e13 (Pointis et al., 2010).

1.3.2 Masculinisation of the Wolffian duct by androgens

The internal genitalia develop from the paired Wolffian ducts in the male and Müllerian ducts in the female. Initial formation of these ducts is common to both male and female embryos. The Wolffian ducts initially develop from the transient embryonic pronephroi at e9.5 (Smith and Mackay, 1991). From e9 to e10.5, each Wolffian duct extends caudally through the mesonephros by the process of mesenchymal to epithelial transition, connecting with the cloaca (later the urogenital sinus) at its posterior end. Extension of the Wolffian duct induces condensation of surrounding mesenchyme into mesonephric tubules that lie perpendicular to the duct and elongating towards the coelomic epithelium. Mesonephric tubules form along the whole length of the Wolffian duct, but whilst cranial tubules are attached to the duct,

the more caudal tubules are unattached (Sainio et al., 1997). Caudal tubules degenerate by apoptosis between e11 and e12, leaving cranial tubules attached to the Wolffian duct at one end and terminating close to the lateral edge of the developing gonad. The Müllerian (paramesonephric) ducts form alongside the Wolffian ducts at e12 from invaginations of the mesonephric surface epithelium (Smith and Mackay, 1991). Müllerian ducts grow in a cranial-caudal direction. At the cranial pole of the gonad they are lateral to the Wolffian ducts, but cross over as they reach the caudal mesonephros to appear on the medial side of the Wolffian ducts before termination in the urogenital sinus (Staack et al., 2003). The two ducts and mesonephric tubules persist alongside each other until the developing testes start to produce anti-Müllerian hormone (AMH) and testosterone.

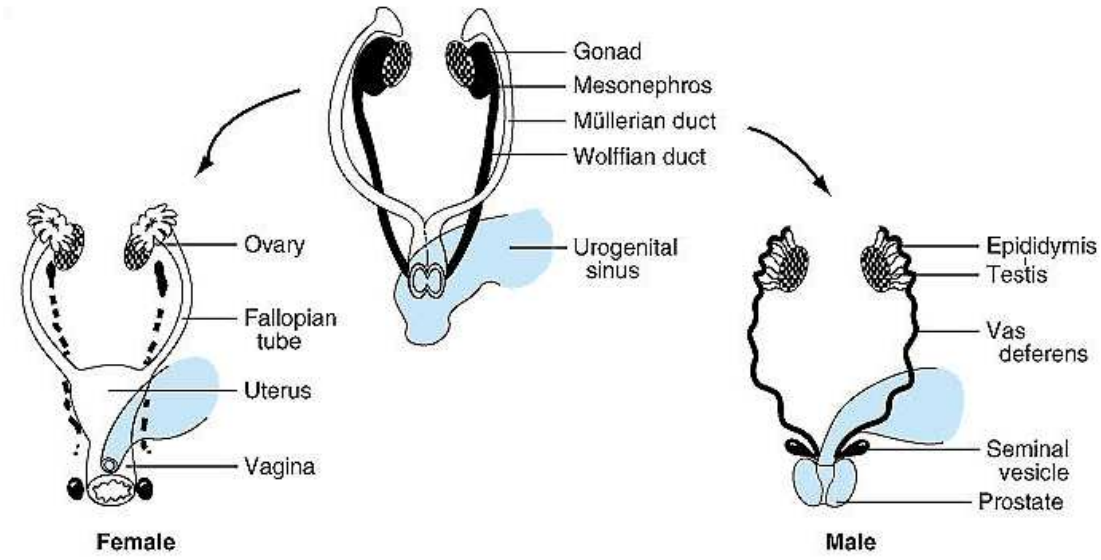

Figure 1-7: Development of the bipotential gonad, ducts and urogenital sinus into either a female-specific or male-specific physiology

The male-specific fate of the bipotential duct system is regression of the Müllerian ducts and stabilisation and differentiation of the Wolffian ducts (Figure 1-7). The Wolffian duct is morphologically similar in male and female mice until e13-e14 (Staack et al., 2003). Around this time, the fetal Leydig cells of the testes begin to produce testosterone and the Wolffian duct in male embryos starts to increase in size

compared to that of female embryos (Smith and Mackay, 1991). Wolffian duct growth is due to testosterone prevention of programmed cell death (Welsh et al., 2009b). Around e12.5 the Sertoli cells of the fetal testis begin to produce AMH (Munsterberg and Lovell-Badge, 1991), which causes regression of the Müllerian duct in a cranial-caudal direction between e13 and e14 (Kobayashi and Behringer, 2003). Regression occurs due to a combination of apoptosis and subsequent basement membrane disruption and epithelial-mesenchymal transition (Allard et al., 2000). AMH receptor (*Amhr2*) is expressed in the peri-Müllerian mesenchyme, but not in the duct epithelium itself, implying that the regression is mediated by mesenchymal-epithelial signalling (Baarends et al., 1994) .

Stabilisation of the male Wolffian duct is also due to mesenchymal-epithelial signalling, in this case by androgen signalling *via* androgen receptor (AR). Adult ARKO mice lack any Wolffian duct-derived structures due to the failure of the WD to stabilise (Welsh et al., 2009b; Yeh et al., 2002). Since both humans and mice with knock-out mutations in 5α-reductase develop a fully differentiated Wolffian duct, it is thought that testosterone rather than DHT is the androgen involved in Wolffian duct stabilisation and differentiation (Imperato-McGinley and Zhu, 2002; Mahendroo et al., 2001). *AR* mRNA is first identified in the mesonephric mesenchyme at e12.5 (Crocoll et al., 1998), with functional protein identified at e13.5 (Cooke et al., 1991). *AR* mRNA has been identified in the Wolffian duct epithelium from e15.5 (Crocoll et al., 1998) but onset of significant levels of functional epididymal AR protein expression occurs in stages in a cranio-caudal direction from epididymis and vas deferens at e19.5, and seminal vesicles at post-natal day 2 (Cooke et al., 1991). This pattern of AR protein expression onset is also seen in rats (Bentvelsen et al., 1995). Since onset of AR protein production in the epithelium of the WD occurs after its stabilisation at e15.5 (Welsh et al., 2009b) it has been theorised that AR signalling within the mesenchyme is sufficient for initial stabilisation of the WD in fetal life. AR protein is not present in the mesenchyme or epithelium of the Müllerian duct (Drews et al., 2001). The expression of AR during development is thought to be induced by the presence of androgens (Bentvelsen et al., 1995).

Once the Wolffian duct has stabilised it then begins to differentiate into its three terminal organs: the epididymis, the vas deferens and the seminal vesicles. Differentiation proceeds in a cranial-caudal direction. At e16, the cranial Wolffian duct begins the process of coiling and elongation that will result in the differentiation of the highly convoluted epididymis (Joseph et al., 2009; Welsh et al., 2009b). Three-dimensional coiling of the caput epididymis begins at e18. The straight tubule of the vas deferens arises from the medial region of the Wolffian and is surrounded by three layers of smooth muscle. At around e17 the caudal segment of the WD begins to distend and elongate in the initial stages of seminal vesicle formation (Staack et al., 2003). Initial differentiation of the three organs of the WD also occurs before onset of epithelial AR protein expression, implying that epithelial androgen receptor is also not required for these early patterning events. Tissue recombination experiments by Cunha and colleagues have provided insight into the relationship between the Wolffian duct epithelium and mesenchyme during this critical period of development. When epithelium from the anterior portion of the Wolffian ducts (which will form the epididymides), was grafted onto mesenchyme from the posterior Wolffian ducts (which will form the seminal vesicles), the epithelium was transformed to a seminal vesicle-like phenotype (Higgins et al., 1989). Grafting experiments have also confirmed the importance of mesenchymal AR by recombining Wolffian duct epithelium from androgen-insensitive *Tfm* embryos onto wild-type urogenital sinus mesenchyme. The *Tfm* epithelium of these recombinants, still underwent ductal and cellular differentiation resembling that of the prostate (Sugimura et al., 1986).

AR signalling is vital for the early differentiation events of the three WD organs: male rats given the AR antagonist flutamide during development undergo WD stabilisation (possibly due to the dose of flutamide not being high enough to abolish all AR action) but the epididymal part of the Wolffian duct does not undergo its distinctive coiling (Welsh et al., 2006). Other genes that have been shown to be involved in patterning of the WD are inhibin beta A (*Inhba*) and some homeobox (*Hox*) genes. Inhba protein is present in a cranial to caudal gradient in the WD

mesenchyme, and epididymides of *Inhba* knockout mice do not undergo coiling, so it is possible that Inhba is induced to activate epididymal coiling by AR signalling in the mesenchyme (Tomaszewski et al., 2007). Both *Hoxa10* and *Hoxa11* mutant mice have a partial homeotic transformation of vas deferens to epididymis (Benson et al., 1996; Hsieh-Li et al., 1995).

The epithelium of the mesonephric tubules expresses AR protein at e16.5, three days before the Wolffian duct epithelium (Cooke et al., 1991). However, testosterone is not required to stabilise the mesonephric tubules, as they are often seen as peri-ovarian remnants (also known as the paroophron) in female mice (Rosenfeld et al., 2000).

The female specific pathway of duct differentiation in the absence of testosterone and AMH results in the regression of the Wolffian duct and persistence of the Müllerian duct, which develops into the oviduct, uterine horns, cervical canal, and upper vagina (Kobayashi and Behringer, 2003).

1.3.3 Masculinisation of the prostate and external genitalia by androgens

Masculinisation of the remainder of the reproductive organs is also dependent on the action of testosterone. The prostate begins to develop from budding of the epithelium lining the UGS and cloaca at around e17 (Staack et al., 2003). The buds become tubular, branch and fuse behind the urethra forming its lobed structure (Thomson and Marker, 2006). The mesenchyme of the UGS expresses AR protein from e13.5, but it is not seen in the prostate epithelium until d4, implying that the prostate morphogenesis, like WD patterning, is dependent on mesenchymal not epithelial AR signalling (Cooke et al., 1991). In females, absence of androgen signalling results in the UGS developing into the lower portion of the vagina (Marker et al., 2003). This is also seen in the ARKO mouse model (Yeh et al., 2002).

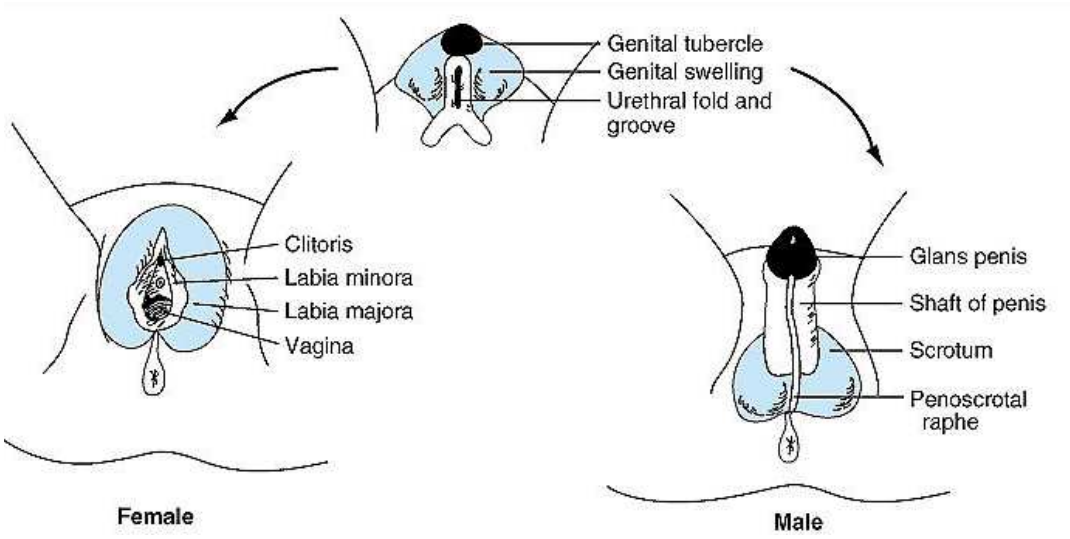

Figure 1-8: Development of the bipotential external genitalia into either a female-specific or male-specific physiology

The male and female external genitalia develop from the same anlagen, namely the genital tubercle, genital swellings and urethral folds, all of which express mesenchymal AR (Drews et al., 2001). Under the influence of androgens the genital tubercle elongates to form the body of the penis, the urethral folds elongate and fuse to form the penile urethra and the urogenital swellings fuse to form the scrotum (Johnson and Everitt, 2000). In females, absence of androgen signalling results in the genital tubercle becoming the clitoris, urethral folds become the labia minora and the urogenital swellings form the labia majora. A female pattern of external genitalia development is also seen in the ARKO mouse model (Yeh et al., 2002). Hypospadias (the incomplete fusion of the urethral folds resulting in incorrect placement of the urethral meatus) is present in rats treated with the AR-antagonist flutamide (Welsh et al., 2008). DHT is thought to be the androgen that masculinises both the prostate and external genitalia during embryonic development in humans, as both are under-developed in men with 5α-reductase type 2 mutations (Imperato-McGinley and Zhu, 2002). However, mice with genetic ablation of both 5α-reductase isoforms have an under-developed prostate, but normally virilised external genitalia, suggesting that testosterone is sufficient for external genitalia masculinisation in mice (Mahendroo et al., 2001).

1.3.4 Descent of the testes under the influence of androgens

Testis descent occurs in two phases: the trans-abdominal phase when testes migrate from the urogenital ridge to above the inguinal ring occurs from e16 until just before birth, and the inguinoscrotal phase when testes migrate through the inguinal canal into the scrotum, occurs at around d21 (Hughes and Acerini, 2008). The trans-abdominal phase requires the action of the Leydig cell-derived insulin-like 3 (Insl3) which promotes thickening of the gubernaculum, the ligament that connects the testis to the inguinal canal (Nef and Parada, 1999; Zimmermann et al., 1999). This results in the testis being drawn towards the inguinal ring. Androgens are also known to play a role in trans-abdominal descent preventing the outgrowth of the cranial suspensory ligament and so allowing the embryonic testis to move caudally from the diaphragm (Emmen et al., 1998; van der Schoot and Elger, 1992). The inguinoscrotal phase of descent is predominantly controlled by androgens, occurring just after birth at the same time as the neonatal surge in testosterone levels. ARKO mice are cryptorchid with testes found in the low abdominal area close to the internal inguinal ring (Yeh et al., 2002). The gubernaculum contracts and relaxes in response to a concentration gradient of calcitonin gene-related peptide (CGRP) released from the sensory neurons of the genital branch of the genitor-femoral nerve (GFN) (Park and Hutson, 1991). Androgens are thought to mediate a sex-dimorphic differentiation of the GFN as prenatal administration of an AR-antagonist in rats inhibited the development of the GFN nucleus in the spinal cord and resulted in cryptorchidism (Shono et al., 2004).

1.4 Actions of androgens in the adult testis

1.4.1 Testicular histology: an overview

The testes of mammals are paired organs that perform two functions: the production of spermatozoa (spermatogenesis) and synthesis of steroid hormones (steroidogenesis). The testis consists of numerous u-shaped seminiferous tubules that begin and end in the rete testis, a network of anastomotic channels lined with

cuboidal epithelium located at the vascular pole of the testis through which sperm pass as they exit the testis into the efferent ducts. The seminiferous tubules are embedded in a vascularised interstitial stroma and the structure is encased by a connective tissue capsule: the tunica albuginia. Spermatogenesis takes place in the seminiferous epithelium lining the seminiferous tubules, and is supported by intratubular somatic Sertoli cells (Figure 1-9). The seminiferous epithelium interfaces with a lumen into which spermatozoa are released. Seminiferous tubules are surrounded by a basement membrane and a layer of contractile peri-tubular myoid (PTM) cells that cause peristalsis to move the luminal spermatozoa towards the rete testis. The interstitium consists of steroidogenic Leydig cells, mesenchymal cells, macrophages and blood and lymphatic vessels. Communication between the interstitium and the tubules is possible *via* release of paracrine factors that are transported between the compartments. Blood vessels are not found inside the seminiferous tubules and the tubule is divided into physiologically distinct adluminal and basal layers separated by the ‘blood-testis barrier’: junction complexes between Sertoli cells that act to keep maturing haploid germ cells separate from the rest of the testis. This helps avoid an adverse immune response to spermatozoal antigens, and to regulate the conditions specific to the germ cells.

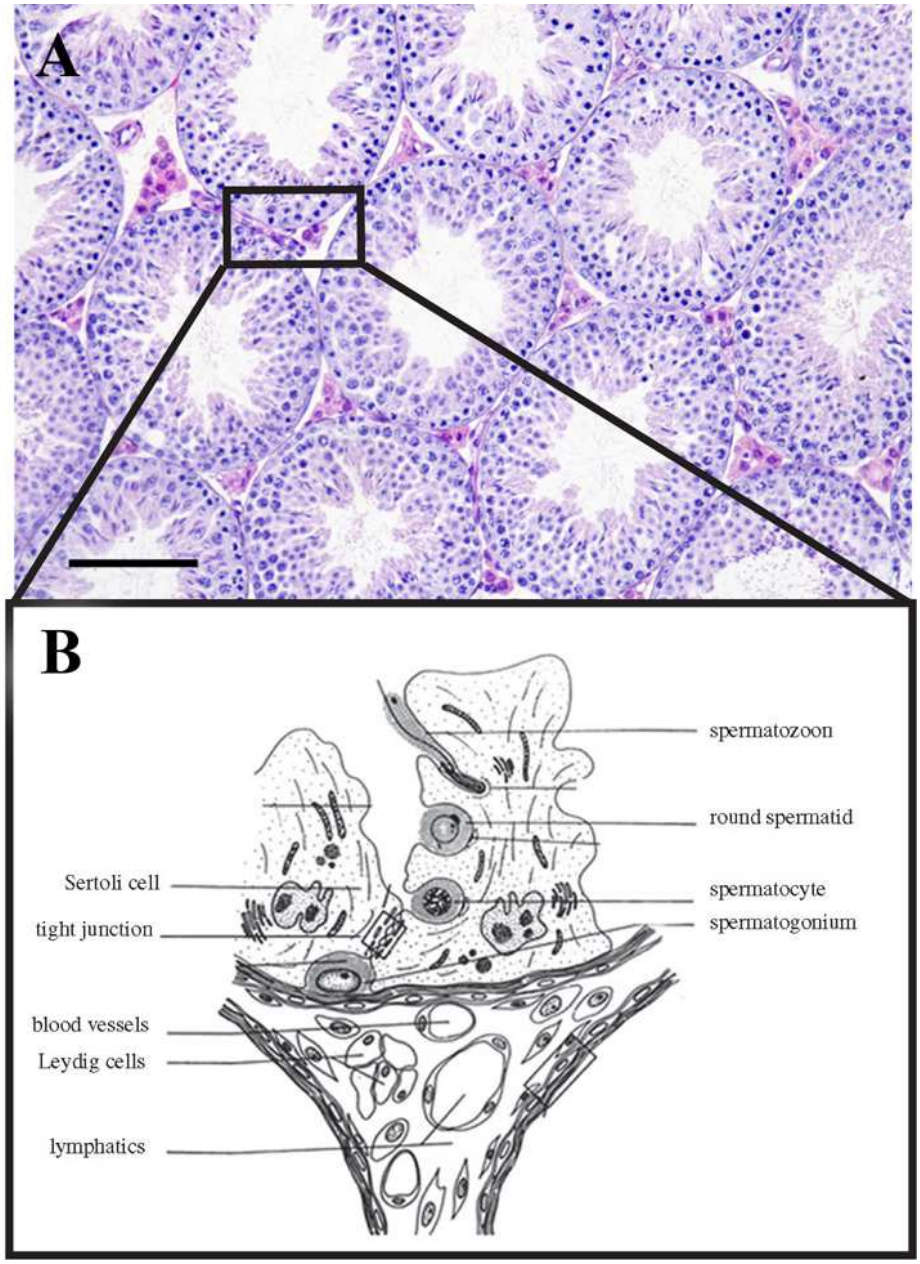

Figure 1-9: Architecture of the testis

(a): haematoxylin and eosin stained thin-section of the testis, showing the arrangement of the seminiferous tubules (scale 100µm) (b): schematic diagram showing the cell types of the seminiferous epithelium and testicular interstitium, adapted from (Walker, 2010)

1.4.2 Spermatogenesis

After puberty begins, quiescent pro-spermatogonial germ cells undergo a process of mitotic proliferation followed by meiotic division to produce spermatozoa: the mature sperm cells. Spermatogenesis in mice can be summarised as three distinct phases:

- Mitosis of one spermatogonia to form many spermatocytes
- Meiosis of each spermatocyte to form 4 haploid spermatids
- Metamorphosis of round spermatids into elongated spermatids and then spermatozoa involving a process of cellular remodelling.

1.4.2.1 Mitosis: spermatogonia to spermatocytes

The mitotic phase of spermatogenesis (also known as spermatocytogenesis) takes place in the basal compartment of the seminiferous tubule. There are three different types of spermatogonia, the undifferentiated stem cell spermatogonia, dividing spermatogonia and differentiating spermatogonia (Hermo et al., 2010). Type A single (A_s) spermatogonia are the diploid spermatogonial stem cells found proximal to the basement membrane in the seminiferous epithelium. When an A_s spermatogonia undergoes mitosis it forms a pair of daughter cells connected by an intracellular cytoplasmic bridge. These cells either separate to become two A_s cells (and thus renew the A_s stem cell population), or continue to remain connected as A paired (A_{pr}) spermatogonia. A_{pr} spermatogonia both undergo mitosis to form 4 A aligned (A_{al}) spermatogonia, arranged side by side. These undergo two further mitoses to form a string of 16 A_{al} spermatogonia, and a further mitosis differentiates them into a clone of 32 A_1 spermatogonia. Further mitoses form A_2, A_3, A_4, Intermediate (I) and type B spermatogonia. In mice, A, I and B-type spermatogonia can be identified in thin section, with type A having a pale nucleus, type I a ‘speckled’ nucleus and type B a dark nucleus. B spermatogonia further divide to give primary spermatocytes in the last mitotic division of spermatogenesis. Through the process of these mitotic divisions one spermatogonium should theoretically yield 2048 spermatocytes. The actual number of spermatocytes generated by one spermatogonium is estimated to be much lower due to apoptosis (Billig et al., 1995). Points of this theory are contested

between research groups. It is still debated whether A_s cell division is symmetrical (forming two daughter cells committed to renewal or differentiation) or asymmetrical (producing one daughter cell committed to renewal and one committed to differentiation) (Oatley and Brinster, 2008) and whether or not A_{pr} and A_{al} spermatogonia, in case of cell loss, for example because of irradiation or the administration of a cytostatic drug, can 'de-differentiate' and become stem cells again (Nakagawa et al., 2007).

The microenvironment of spermatogonial stem cells is called their 'niche', and is formed by the contributions of surrounding cells. Of particular note are the contributions of Sertoli cells, which produce glial cell line derived neurotrophic factor (GDNF) which stimulates spermatogonial self-renewal and proliferation, and stem cell factor (SCF) which promotes spermatogonial differentiation (de Rooij, 2009). Retinoic acid is essential for male fertility and deficiency leads to degeneration of spermatogenesis through arrest of normal spermatogonial differentiation (Ghyselinck et al., 2006)

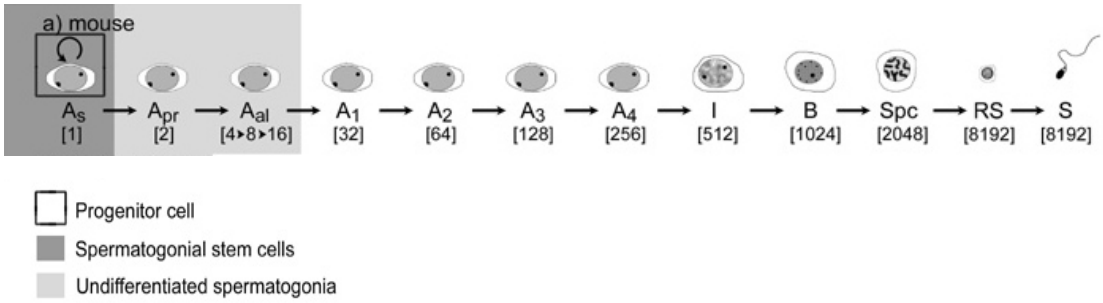

Figure 1-10: Stages of spermatogenesis in the mouse

Note the number of germ cells present after each step (Ehmcke et al., 2006).

1.4.2.2 Meiosis: spermatocytes to spermatids

The primary spermatocytes migrate from the basal compartment of the seminiferous tubule and enter the adluminal compartment, where each undergoes a round of meiosis to form four haploid spermatids. Meiosis is a process unique to germ cells

that involves one round of DNA replication followed by two consecutive cell divisions, allowing diploid germ cells to form haploid germ cells (Kerr et al., 2006). The two cell divisions are known as meiosis I and meiosis II (Figure 1-11).

Primary spermatocytes undergo meiosis I. The prophase of meiosis I takes up 90% of the time of meiosis. It is at this stage that DNA synthesis takes pace to replicate chromosomes, and that the chromosomes of the diploid cell undergo crossing over (recombination of portions of DNA between homologous chromosome pairs). During prophase chromosomes condense (leptotene), come together in their homologous pairs (zygotene) *via* a protein complex called the synaptonemal complex (Zickler and Kleckner, 1999), undergo crossing over at chiasmata (pachytene) and begin to separate (diplotene). During the diakinesis phase of meiosis the nuclear membrane begins to disintegrate and the spindle beings to form. Recombination during crossing over introduces genetic variation into the population of sperm. Pachytene spermatocytes are particularly obvious in testicular thin sections because they appear very large after a period of sudden cytoplasmic and nuclear growth in this phase. Next, during metaphase I, homologous chromosomes align along an equatorial plane that bisects the spindle. Alignment is random, which adds more genetic variation to the population of sperm. During anaphase I, the microtubules that make up the spindles shorten, pulling the homologous chromosomes apart towards opposing poles of the cell. During telophase I, the chromosomes arrive at the cell poles, the spindle disappears and new nuclear membranes form around each haploid set of chromosomes. Cytokinesis is the process of the division of the cell cytoplasm into two separate daughter cells, each containing a haploid set of chromosomes, still present as sister chromatids.

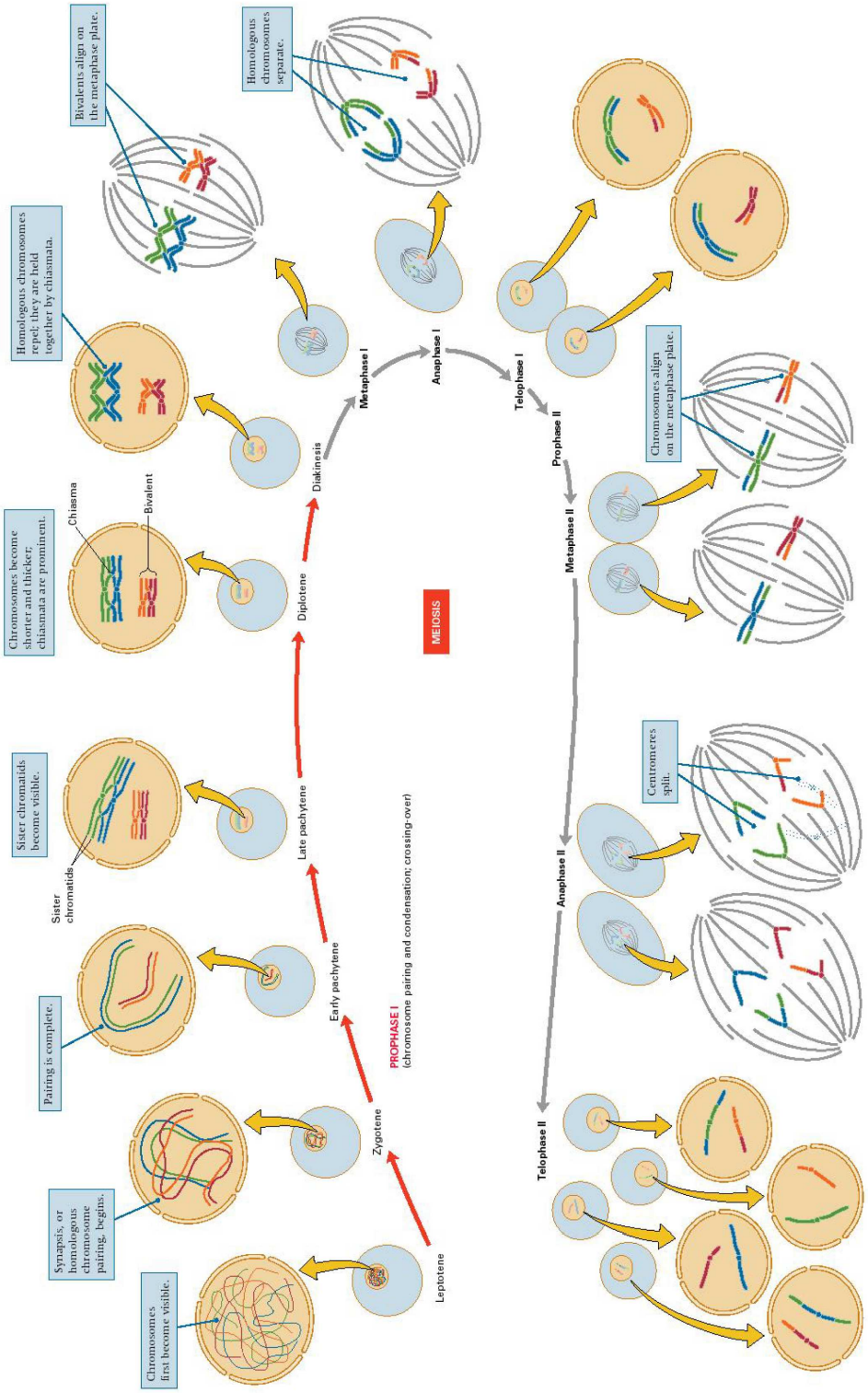

Figure 1-11: Schematic of meiosis, showing the different stages of meiosis I and meiosis II and the distinct cellular events that define them *(http://www.cbs.dtu.dk, Dave Ussery)*

After a period of rest (interphase) in which the chromosomes are present as decondensed chromatin, the cell enters meiosis II, which is similar to mitosis. Cells that are undergoing meiosis II are known as secondary spermatocytes, but this cell type is rarely seen in testicular thin sections because of the fast progression of meiosis II. In prophase II the nuclear envelope again breaks down and the chromatids begin to condense. In metaphase II, the individual chromosomes (still consisting of two chromatids) line up on the spindle in the same orientation. In anaphase II the two sister chromatids of each chromosome are pulled apart to opposite poles of the cell. The process ends with telophase II, which is similar to telophase I, and is marked by uncoiling and lengthening of the chromosomes and the disappearance of the spindle. Nuclear envelopes reform and cleavage or cell wall formation eventually produces a total of four haploid daughter cells, known as spermatids.

1.4.2.3 Metamorphosis: spermatids to spermatozoa

The metamorphic stage of spermatogenesis (also known as spermiogenesis) is where spermatids undergo a profound morphological change from radially symmetrical cells with large nuclei to elongated polar cells with tails and highly condensed heterochromatin before being released into the lumen of the seminiferous tubules and into the reproductive tract (Figure 1-12).

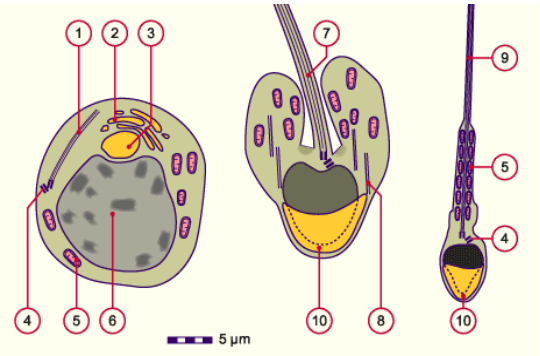

Figure 1-12 Morphological changes of the spermatid during spermiogenesis *(http//www.embryology.ch) 1= axonemal primordium, 2= Golgi apparatus 3=Golgi vesicles, 4= pair of centrioles 5= mitochondrion, 6= nucleus, 7= developing axoneme, 8=manchette microtubules, 9=tail piece, 10= acrosome*

During spermiogenesis, the size of the spermatid head decreases to approximately 5% of the size of a somatic cell nucleus (Brewer et al., 1999). This occurs through replacement of the major nuclear proteins: the histones, with transition proteins, and finally protamines. Protamines are small, basic proteins that are thought to allow denser DNA packaging than histones and maintain the majority of the DNA in a highly condensed transcriptionally-inactive state (Braun, 2001). Despite this, between 2 and 15% of the genome essential for early embryonic development remains bound to histones (Ward, 2010).

The acrosome is a membrane bound lysosomal organelle that contains digestive enzymes including hyaluronidase and acrosin to allow a mature spermatozoa to break through the zona pellucida of the ovum (Abou-Haila and Tulsiani, 2000). The acrosome begins to form in the round spermatid when vesicles produced by the Golgi apparatus accumulate and fuse at one pole of the spermatid. The acrosome is closely associated with the nuclear membrane, and as the head elongates it stretches it to form a 'cap'. In the mouse, head elongation occurs in the latter half of spermiogenesis (from step 9) and gives rise to elongating spermatids. Head elongation occurs at the same time as the formation of the manchette, a perinuclear ring linked to bundles of microtubules that is thought to be involved in head elongation and tail formation (Toshimori and Ito, 2003). In mice and rats the head of the spermatozoa containing the acrosome is shaped like a hook (Breed, 2004). Abnormalities in sperm head shaping result in teratozoospermia, including the specific disorder globozoospermia, which occurs when the sperm does not develop an acrosome (Borg et al., 2010).

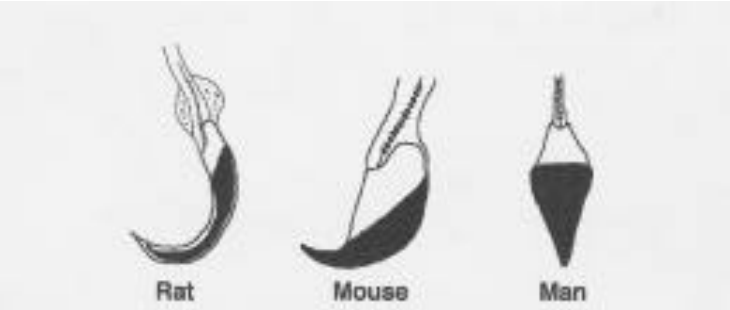

Figure 1-13: Variations in acrosome morphology in rat, mouse and man

(Rex Hess)

The distinctive flagellum (tail) of the sperm originates from a pair of centrioles (proximal and distal). The motile core of the flagellum, called the axoneme (Kierszenbaum, 2002), originates from extension of the distal centriole, assisted by a structure called the manchette. The axoneme consists of a bundle of nine peripheral double microtubules with two single ones in the centre. During its development, through the rotation of the nucleus and acrosomal vesicle, the flagellum primordium comes to lie on the opposite side of the acrosome. The mature flagellum consists of a neckpiece closest to the nucleus, which contains the centriole, a midpiece which consists of a sheath of mitochondria surrounding the axoneme to provide energy for movement, a principal piece consisting of ring fibres around the axoneme and an endpiece which consists only of the axoneme (Borg et al., 2010). Spermatozoa orientate so that their tails point towards the centre of the lumen, away from the epithelium.

During spermiogenesis the spermatid cytoplasm is displaced to the caudal end of the elongating nucleus. Just before spermiation (release of sperm into the lumen of the seminiferous tubule) the majority is sloughed off as the residual body, though some remains attached as the cytoplasmic droplet. The cytoplasmic droplet contains aromatase (Janulis et al., 1996), and is retained in rodents until it is lost during epididymal transit, coinciding with maturation (Hermo et al., 1988). The residual body is phagocytosed by Sertoli cells under the influence of androgens (Beardsley and O'Donnell, 2003). They can be clearly seen in stage IX seminiferous tubule sections as basophilic vesicles being drawn down towards the basement membrane by Sertoli cells (Borg et al., 2010). Also thought to be involved in cytoplasmic reduction are tubulobulbar complexes (TBCs): long tubular projections of the spermatid plasma membrane that end in a bulbous swelling in the apical process of the supporting Sertoli cell (Russell, 1979). Spermiation involves complex remodelling of the Sertoli-germ cell junctional complexes (Mruk and Cheng, 2004). These spermatozoa are morphologically mature but lack motility.

1.4.2.4 The cycle of the seminiferous epithelium and the spermatogenic wave

The mechanism and duration of spermatogenesis shows differences between species. It takes a mouse 35 days to produce a mature clone of spermatozoa from one type A spermatogonia and 64 days for a human (Johnson and Everitt, 2000; Oakberg, 1956). In mice, a transverse section through a seminiferous tubule reveals that germ cells at specific maturational stages are always found together. These 'sets' of germ cells can be classed into one of 12 different stages in mice. A seminiferous tubule cross section can always be designated at one of these stages because spermatozoa in that vicinity initiate a new round of spermatogenesis at the same time: known as the cycle of the seminiferous epithelium. If an individual seminiferous tubule is dissected and laid out longitudinally, it appears that adjacent tubule segments have entered the spermatogenic process slightly out of phase with each other. For example, a segment of the seminiferous tubule that can be classified at stage V will have a segment at stage IV on one side and VI on the other. This is known as the spermatogenic wave. These levels of organisation allow a constant supply of mature spermatozoa to be available for fertilisation. In humans it is slightly different, a cross section through a seminiferous tubule will show 'wedges' of delinearisation containing similar cell associations in the same way as the mouse seminiferous tubule, but several different sets of cell associations could be present in the same tubule cross section (Johnson and Everitt, 2000) .

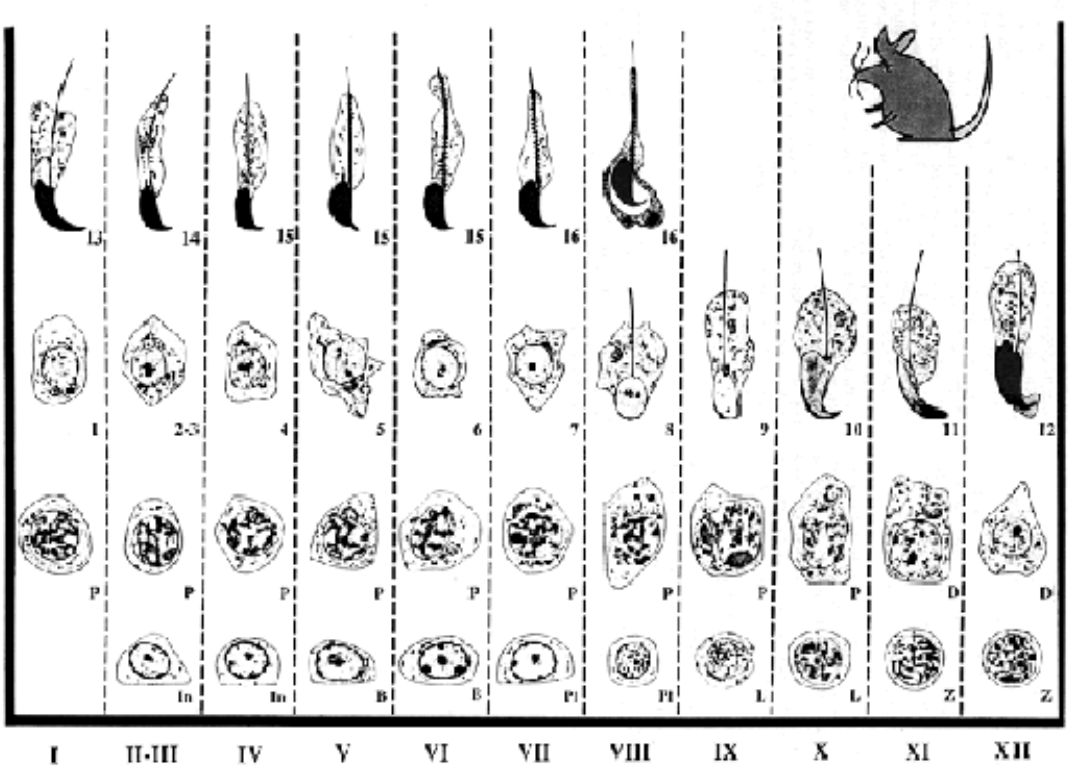

Figure 1-14: The cycle of the seminiferous epithelium in mice

Stages are indicated by roman numerals (In= intermediate spermatogonium, B= type B spermatogonium, Pl= preleptotene spermatocyte, L= leptotene spermatocyte, P= pachytene spermatocyte, D= diplotene spermatocyte, 1-16= stages of spermatid morphogenesis) From (Russell et al., 1990).

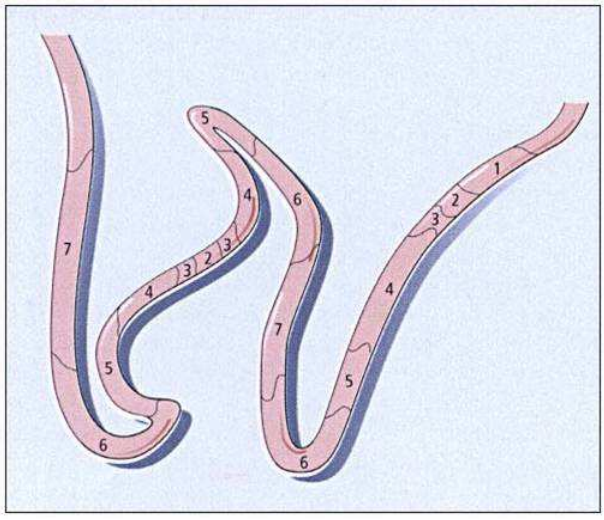

Figure 1-15: The spermatogenic wave

Note that whole segments of the tubule are at the same stage of the cycle of the seminiferous epithelium, and that adjacent segments tend to be either just advanced or just retarded (Johnson and Everitt, 2000).

1.4.3 Somatic cell types of the adult testis and their control by androgens

Dependence of spermatogenesis on the action of androgens has been documented in models of hypophysectomy (Russell and Clermont, 1977), interference with gonadotropin action (Russell et al., 1981) and Leydig cell ablation by administration of ethane dimethanesulfonate (EDS) cells (Bartlett et al., 1986). Local testicular testosterone levels are much higher those found in serum (Maddocks et al., 1993). Despite their dependence on androgens for their survival and maturation, the germ cells of the murine testis do not express androgen receptors (O'Donnell et al., 2006) and germ cell specific androgen receptor expression is not required for their normal maturation (Johnston et al., 2001; Tsai et al., 2006). However, the somatic Sertoli, peri-tubular myoid (PTM) and Leydig cells of the mature testis do express androgen receptor (Zhou et al., 2002), and it is likely that the requirement of testosterone for germ cell maturation is mediated by these cell types. Global models of androgen disruption can describe what processes in the testis rely on AR signalling, but they cannot elucidate which cell type(s) mediate these processes. It must also be noted that aromatisation of androgens to estradiol also occur in the testis, and reduction of androgen levels also results in changes in estradiol levels. Cell-specific ablation of AR in the testis using the Cre-loxP system is an ideal technique to elucidate both the cell and AR-specific actions of androgens in the testis, and information gained using this technique is described here.

1.4.3.1 Sertoli cells

Sertoli cells are known as the ‘nurse’ cells of spermatogenesis, as they are mesoepithelial somatic cells that coordinate and structurally support the maturing germ cells. Each Sertoli cells spans the tubule from the basement membrane to the tubule lumen, and is tightly linked to a set of germ cells at specific stages by different types of junction protein complexes (Mruk and Cheng, 2004). Sertoli cells have a very large surface area, but their cytoskeleton is well-developed and assists in maintaining their shape (Vogl et al., 1993) as well as providing a scaffold for the movement of germ cells (Lie et al., 2010). The level of organisation of

spermatogenesis implies temporal and spatial organisation among the maturing germ cells that is likely to be controlled by Sertoli cells. Adjacent Sertoli cells are in continuity *via* connexin gap junction complexes so communication *via* exchange of small molecules and ions could synchronise adjacent Sertoli cells (Pointis et al., 2010).

Tight junctions between adjacent Sertoli cells above the level of leptotene spermatocytes form the blood-testis barrier (BTB), a structure that partitions the adluminal compartment of the seminiferous tubule from the basal compartment so haploid germ cells can mature in an immunologically privileged site with a specialised environment (Dym and Fawcett, 1970). Maturing sperm move apically along the Sertoli cell, traversing the BTB during meiosis, then elongating spermatids appear to be drawn back down towards the basement membrane in Sertoli cell crypts before being released into the lumen during spermiation. Cell movement across the BTB is thought to be controlled by transforming growth factor β (TGFβ) and tumour necrosis factor α (TNFα) mediated perturbation, and testosterone-promoted reformation of the BTB junctions (Li et al., 2006; Lui et al., 2003; Wang et al., 2006). Movement of elongating spermatids across the seminiferous epithelium is largely assisted by ectoplasmic specialisations (‘ES’, a type of adherens junction unique to the testis) between the spermatids and their supporting Sertoli cell (Wong et al., 2008). It has been postulated that spermatids can use their ES junctions to move along the microtubules of their supporting Sertoli cell like a train on a track (Guttman et al., 2000). Release of the sperm from the seminiferous epithelium during spermiation involves the replacement of the apical ES by TBCs: it has been hypothesised that TBCs function to internalise components from disassembled apical ES junctions in preparation for the release of spermatids (Guttman et al., 2004). Evidence is accumulating that fragments of laminin chains produced during spermiation induce remodelling of the BTB, thus intimately coordinating these two processes (Cheng and Mruk, 2009).

Mature Sertoli cells are also highly active synthetic and secretory cells. Sertoli cells synthesise and secrete the endocrine hormones inhibins and activins which work together to regulate FSH secretion. They are required to synthesise and secrete products that are essential for growth and differentiation of developing germ cells: due to the BTB the post-meiotic germ cells cannot obtain these from the systemic circulation. An example is transferrin, a protein required for iron delivery (Sylvester and Griswold, 1994). At puberty the Sertoli cells begin to secrete fluid that opens and maintains the lumen of the seminiferous tubules (Rato et al., 2010). Sertoli cells also produce androgen binding protein (ABP) which binds to testosterone to sequester it at high concentrations in Sertoli cells and can also be exocytosed into luminal fluid and carried to the epididymis (Munell et al., 2002). Sertoli cells also influence their neighbouring spermatogonia by producing growth factors that stimulate stem-cell self-renewal (including GDNF) and differentiation (de Rooij, 2009).

Androgen receptors are not present in the Sertoli cells of the mouse until d4-6 of postnatal life (Willems et al., 2009). After maturation, the expression of AR in Sertoli cells fluctuates in a seminiferous tubule stage-specific manner (Zhou et al., 2002), appearing strongest at in stages VI–VII weakest at stages I–III and VIII–XII. The Sertoli-cell specific AR knockout (SCARKO) mouse line was created by two groups using an inserted Cre recombinase coding sequence driven by an anti-Müllerian hormone promoter (Chang et al., 2004; De Gendt et al., 2004). Until the advent of the SCARKO mouse it was difficult to pinpoint how androgens acted *via* Sertoli cells to promote normal spermatogenesis without having to resort to *in vitro* models and their unavoidable limitations with regard to physiological relevance. The SCARKO mouse demonstrated that action of androgens in Sertoli cells is vital for progression of germ cells through meiosis.

The testes of SCARKO mice develop normally with an external phenotype and weight similar to their control male littermates, with fully descended testes and intact Wolffian duct-derived structures, unlike the ARKO model where they are absent (Yeh et al., 2002). However at post-natal day 50 their testes were approximately a

third of the weight of their wild type littermates' and were found to contain few post-meiotic germ cells more advanced than pachytene primary spermatocytes indicating a meiotic block. A subsequent study suggested that tight junctions in the SCARKO can form, but BTB formation is delayed and incomplete (Willems et al., 2010). A decrease in levels of cytoskeletal and junctional proteins was also seen in a study of the Chang SCARKO (Wang et al., 2006). Gene expression comparison studies have also indicated that genes related to cytoskeletal dynamics and junction formation are differentially expressed between SCARKO and control animals (Denolet et al., 2006; Eacker et al., 2007). Changes in cytoskeletal genes are also seen in the *Tfm* mouse (O'Shaughnessy et al., 2007). Data suggest that ablation of AR in Sertoli cells results in early changes in gene expression (Denolet et al., 2006; Willems et al., 2009) so it is likely that transcriptional changes soon after the onset of AR expression induce maturational changes.

It is important to note that mice with a Sertoli cell-specific ablation of the second zinc finger domain (vital for DNA binding) display a similar post-meiotic block phenotype, indicating that progression of spermatocytes through meiosis is an event dependent on classical genomic signalling of androgens (Lim et al., 2009). The two groups differed in analysis of the levels of testosterone and LH in their SCARKO models; where De Gendt and colleagues found these two hormones to be normal in adult mice, the Chang group found LH to be high and testosterone to be low. Spermatogonia (De Gendt et al., 2004) and Sertoli cell numbers do not differ between SCARKOs and controls (Tan et al., 2005) but Leydig cell numbers in this model are lower than controls (De Gendt et al., 2005). Another study created a 'hypomorphic' SCARKO with Sertoli cell-specific ablation of AR action, but also a general reduction in levels of AR protein throughout the whole body due to a phenotypic effect from the placing of the *loxP* sites in the transgenic AR (Holdcraft and Braun, 2004). The germ cells of these mice do go through meiosis but have a block at the round spermatid stage, which is surprising as this is a less severe phenotype than mice with SCARKO which do not have a reduction in AR protein in the remainder of the testis and other organs of the reproductive system.

Because of the presence of the post-meiotic block in SCARKO mice it is impossible to pinpoint the contribution of Sertoli cell AR signalling to subsequent stages of spermatogenesis. Rats with implants containing low-dose testosterone and estradiol reduce testicular T levels to 3% of control *via* suppression of LH (McLachlan et al., 2002). 'TE implanted' rats have been used to determine that both spermatid maturation and spermiation are dependent on androgens. TE implantation results in a complete block in conversion of round spermatids into elongating spermatids (O'Donnell et al., 1994). Large numbers of round spermatids accumulate in cauda epididymis indicating that they are detaching from the seminiferous epithelium (O'Donnell et al., 1996). Despite this, ES in these mice are normal so it is likely to be defects in adhesion molecules that are causing detachment (O'Donnell et al., 2000). Spermiation is very sensitive to testosterone or FSH withdrawal in rats (Matthiesson et al., 2006). Spermiation failure is noted in TE rats, characterised by spermatid retention with subsequent phagocytosis by Sertoli cells (Saito et al., 2000). Tubulobulbar complexes and removal of ES are not affected by hormone withdrawal, but final disengagement is affected (Beardsley and O'Donnell, 2003). A similar phenotype is seen in the 'hypomorphic' AR mice with a reduction in AR protein throughout the body, with a reduction in numbers of round and elongating spermatids and evidence of spermiation failure (Holdcraft and Braun, 2004). Although defects in spermatid adhesion and spermiation cannot be definitively assigned to AR signalling in the Sertoli cell (because AR signalling is reduced in all testicular cell types), it is likely that the Sertoli cell is responsible due to the isolated environment in which post-meiotic germ cells develop due to the BTB.

1.4.3.2 PTM cells

Seminiferous tubules are surrounded by a layer of peri-tubular myoid (PTM) cells. PTM cells are contractile: this is thought to produce peristaltic waves in the seminiferous tubules that propel mature spermatozoa towards the rete testis (Farr and Ellis, 1980). Contractility is stimulated by endothelin-1 and inhibited by adrenomedullin, both of which are produced by the Sertoli cells (Romano et al., 2005; Tripiciano et al., 1996). PTM cells also synthesise the basement membrane

components laminin, collagen and fibronectin in co-operation with Sertoli cells (Richardson et al., 1995; Skinner et al., 1985). These functions illustrate that, like other tissues in the reproductive system, a reciprocal relationship exists between the mesenchymal (PTM) and epithelial (Sertoli) cells of the testis, which is vital for the structure and function of both cell types. Like the developing reproductive tract, the mesenchymal PTM cells are the first cell in the testis to express AR: at or before e16.5 in the mouse (Drews et al., 2001) and at e18.5 in the rat (Majdic et al., 1995; You and Sar, 1998). Cell-specific ablation of AR in the PTM cells has been achieved using Cre/*loxP* transgenic mice (PTM-ARKO), and has shown that AR in PTM cells is essential for male fertility (Welsh et al., 2009a). PTM-ARKO testes are 70% smaller than controls because of a reduction in numbers of all germ cell stages including the spermatogonia, so it is likely that spermatogonia number may be regulated by AR signalling in PTM cells, which are in intimate proximity to the spermatogonia. The decrease in germ cells is not due to a decrease in Sertoli cell number, as SC is not reduced in PTM-ARKO mice. However, levels of Sertoli cell-specific gene products including *Rhox5*, eppin (*Epp*) and β-tubulin (*tubb3*) are reduced in PTM-ARKO testes, implying that AR signalling in PTM cells has an effect on the neighbouring Sertoli cells. Since PTM cells in the PTM-ARKO also demonstrate a progressive loss of desmin and SMA it is likely that loss of AR is affecting the smooth muscle phenotype in PTM cells, and a disruption of laminin indicates problems with the basement membrane of the seminiferous tubules.

In vitro evidence has demonstrated that androgens can stimulate PTM cells to secrete a factor dubbed P-mod-S (Skinner and Fritz, 1985) that modulates Sertoli cell function (Norton and Skinner, 1989). Attempts have been made to purify (Skinner et al., 1988) and classify (Norton et al., 1994) P-mod-S but it remains as yet unidentified, and is disputed by some investigators (Verhoeven et al., 2000).

1.4.3.3 Leydig cells

The Leydig cells are the steroidogenic cells of the testis (section 1.2). In rodents there are two phases of Leydig cell development: fetal Leydig cells (FLCs) and adult Leydig cells (ALCs) (Lording and De Kretser, 1972). Both populations are

steroidogenic and synthesise and secrete androgens, although there is variation in nature of steroids secreted and control mechanisms regulating cell function. FLC development is discussed in section 1.3.1. FLCs produce testosterone during embryogenesis to masculinise the reproductive tract. FLCs do not express AR (Drews et al., 2001) so it is unlikely that fetal steroidogenesis is influenced by androgen signalling. Testosterone output of fetal Leydig cells drops sharply around birth (O'Shaughnessy et al., 2009) but they appear to persist in the adult testis (Kerr and Knell, 1988). The adult population of Leydig cells begins to differentiate at pnd7 in the mouse (Baker et al., 1999; Nef and Parada, 1999).

Experiments in rats have led to the characterisation of several stages of ALC maturation: progression from stem Leydig cells (SLCs) to progenitor Leydig cells (PLCs) to immature Leydig cells (ILCs) then finally to ALCs (Chen et al., 2009a). Each stage of maturation involves morphological and transcriptional changes. There is conflicting evidence for the location of the SLC population: although some evidence is present for vascular smooth muscle cells/pericytes (Davidoff et al., 2004) it is commonly accepted that SLC population is present in peritubular mesenchymal cells (O'Shaughnessy et al., 2008; Siril Ariyaratne et al., 2000). PLCs are cells that have committed to the ALC lineage. They are still spindle-shaped but express low levels of Leydig cell markers including p450scc 3βHSD and 17α-hydroxylase. They also begin to express luteinising hormone receptor (LHR) and AR, expression of which then persists into the adult stage. Morphological and functional maturation of the adult Leydig cell population is dependent on LH stimulation: mice lacking gonadotropin signalling only develop 10% of the control ALC number (Baker and O'Shaughnessy, 2001). PLCs secrete mainly androsterone (Shan et al., 1995). Their transformation to ILCs involves a morphological change with an increase in smooth ER and levels of steroidogenic enzymes (Dupont et al., 1993; Shan et al., 1995). But ILCs also express high levels of androgen metabolising enzymes, so their primary steroid product is the androgen metabolite androstanediol rather than testosterone (Ge and Hardy, 1998). The adult Leydig cell population results from a decrease in androgen metabolising enzymes and continued increase in steroidogenic enzymes,

resulting in predominance of testosterone biosynthesis. These stages have been characterised *in vitro* in mice (Wu et al., 2010). Mouse ALC precursors do not begin to proliferate extensively until p11 (Vergouwen et al., 1991) and do not express steroidogenic genes until around d30, corresponding with an increase in circulating LH levels (O'Shaughnessy et al., 2000; O'Shaughnessy and Sheffield, 1991; O'Shaughnessy et al., 2002b).

It is difficult to identify the age of onset of AR expression in the post-natal Leydig cells populations due to changes in morphology and gene expression of the differentiating Leydig cell types. Interstitial cells AR staining is evident throughout fetal (Drews et al., 2001) and early postnatal life (Willems et al., 2009), but since SLCs and PLCs share their spindle-shaped cell morphology with mesenchymal stromal cells it is difficult to differentiate between the two cell populations. Obvious ILC staining is present from d21 onwards (Zhou et al., 1996). Intensity of its expression is variable (Zhou et al., 2002). An attempt to create a Leydig cell-specific AR knock-out mouse using the Cre/*loxP* system used AMHR2-Cre as the promoter for Cre (Xu et al., 2007). LC-ARKOs demonstrated a reduction in testosterone secretion and testicular size and a block at the round spermatid stage which led to infertility. However, since AMHR2 is also present in Sertoli cells the contribution of AR ablation in this cell type complicates the phenotype (Jeyasuria et al., 2004). Because of this, most current knowledge about the role of AR in Leydig cells has been gained from the *Tfm* mouse.

Leydig cell number in *Tfm* mice is 60% of controls (O'Shaughnessy et al., 2002a) and serum testosterone levels are severely decreased despite high levels of LH (Goldstein and Wilson, 1972; Murphy and O'Shaughnessy, 1991). Levels of steroidogenic enzyme mRNAs (Murphy et al., 1994; O'Shaughnessy et al., 2002b) and protein activities (Blackburn et al., 1973; Murphy and O'Shaughnessy, 1991) are severely reduced in the *Tfm* testis, Since there is no defect of testosterone synthesis in the fetal *Tfm* testis, it is likely that AR is required for maturation of adult Leydig cells and the increase in steroidogenic enzyme expression that this brings (Blackburn et

al., 1973), further backed up by the positive effect of testosterone on maturation of rat Leydig cells *in vitro* (Hardy et al., 1990). It is currently thought that LH and androgens work together to support pubertal maturation of PLCs to steroidogenically active ILCs (Hardy et al., 1990; Murphy et al., 1994).

There is also evidence for paracrine regulation of Leydig cells by AR signalling in other testicular cell types. In SCARKO mice there is a reduction in Leydig cell number but LH and testosterone levels are identical to controls, explained by the fact that steroidogenic genes are upregulated in SCARKO Leydig cells (De Gendt et al., 2005). The mechanism of how Sertoli cells regulate Leydig cell number is unclear at this time. PTM-ARKO mice have normal levels of serum testosterone but elevated levels of serum LH, suggesting that there is compensatory Leydig cell failure (Welsh et al., 2009a). Further work indicated that this was due to the presence of two populations of Leydig cells in the adult PTM-ARKO testis, both normal ALCs and 'abnormal' Leydig cells which are potentially arrested in their development at a less mature stage (Welsh et al., 2011). This evidence points towards a role for AR signalling in PTM (or vascular smooth muscle) cells in Leydig cell maturation.

1.4.4 Role of estrogens in spermatogenesis

Testosterone can also be converted to 17β-estradiol in the male mouse reproductive system by the action of aromatase in the Leydig cells and round and elongating spermatids of the testis (Nitta et al., 1993), and epididymal sperm (Janulis et al., 1996). 17β-estradiol acts by binding to its receptors, ERα and ERβ (Heldring et al., 2007). In the mouse, ERα is found in the Leydig cells, some peri-tubular cells and the epithelium of the efferent ducts and epididymis, whereas ERβ is found in Leydig, Sertoli, some peritubular cells and pre-meiotic germ cells (Zhou et al., 2002). Evidence for cell-specific localisation of estrogen receptors varies between species and even between studies in a particular species, most likely due to differences in the antibodies used in these studies (Carreau and Hess, 2010). ERβ knock-out mice have no significant disruption of spermatogenesis (Dupont et al., 2000; Krege et al., 1998). ERα or ERα/ ERβ double knock-out mice have degeneration of the seminiferous

epithelium with ageing (Dupont et al., 2000; Eddy et al., 1996), though this was later shown to be a result of the failure of the efferent ducts to absorb testicular fluid, resulting in atrophy of the seminiferous tubules due to back-pressure of the fluid (Hess et al., 1997).

Interestingly, a knockout of the aromatase gene (cyp19) did not display fluid-related seminiferous tubule atrophy (Fisher et al., 1998a) and maintained normal efferent duct morphology (Toda et al., 2008), suggesting that ERα signals in a ligand-independent manner in the efferent ducts to control fluid reabsorbtion. However, the testes of aromatase knock-out animals displayed a heterogeneous failure of spermiogenesis from 18 weeks of age, with germ cells arresting and undergoing apoptosis at early spermiogenic stages, often concurrent with abnormalities in acrosome development (Robertson et al., 1999). This phenotype also occurs in a mouse with an inactivating mutation in the ligand binding domain of ERα (ENERKI), implying that the tropic effects of estrogens on spermiogenesis are dependent on estrogens binding to ERα (Sinkevicius et al., 2009). Interestingly, ablation of ERα signalling increases Leydig cell steroidogenesis (Akingbemi et al., 2003) increases in plasma testosterone levels are seen in ERα knock-out, aromatase knock-out and ENERKI mice (Akingbemi et al., 2003; Fisher et al., 1998a; Sinkevicius et al., 2009). Lack of estrogen feedback at the pituitary also results in a slightly increased serum LH level in these three models. The change in levels of LH and testosterone may be contributing to the disruption in spermatogenesis.

More studies are clearly needed to clarify the distinct roles of estrogens and androgens in the testis and the Cre/loxP system is an ideal tool to answer these questions. The function of AR in Leydig cells is still not fully elucidated. Floxed ERα mice have just become available to examine the action of estrogens in individual cell populations (Chen et al., 2009c). More information will provide a fuller picture of how these two hormones act in balance to control spermatogenesis.

1.5 Control of testicular function by the hypothalamus-pituitary-gonad (HPG) axis

The hypothalamus and pituitary, located in the brain, secrete the gonadotropin endocrine hormones: luteinising hormone (LH) and follicle stimulating hormone (FSH), that are vital for male reproductive function, and are in turn regulated by hormones produced by the testes in a feedback loop that is known as the hypothalamus-pituitary-gonadal (HPG) axis (Figure 1-16).

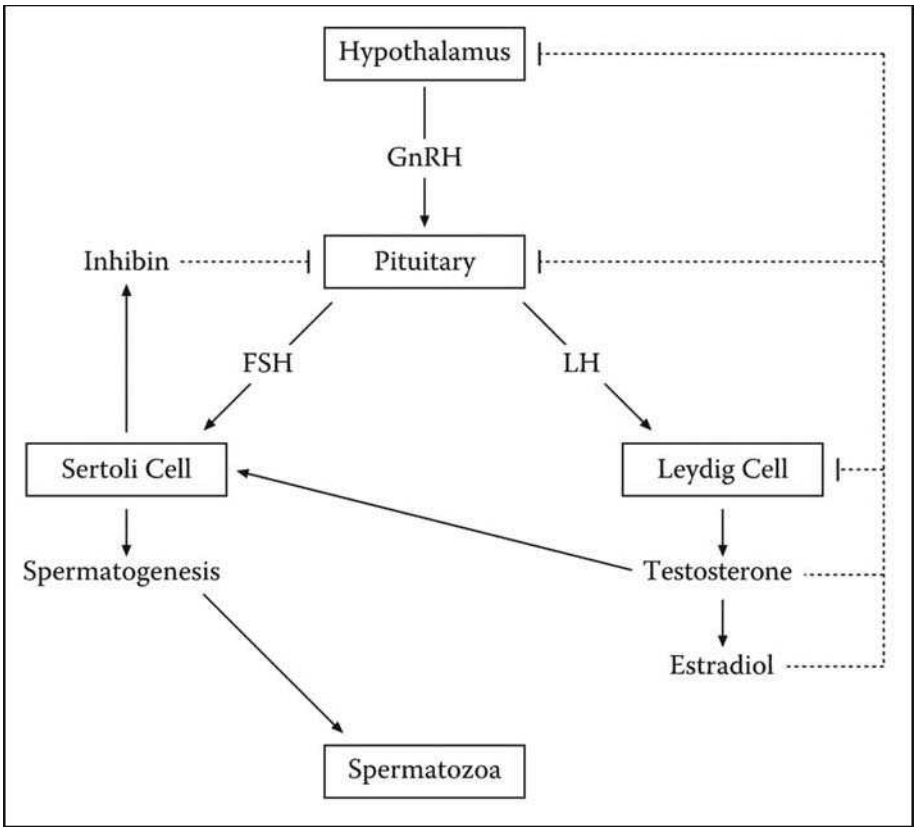

Figure 1-16: Diagram summarising the regulatory pathways of the HPG axis *(Ge et al., 2008)*

1.5.1 The pituitary and hypothalamus

The pituitary gland (also known as the hypophysis) makes LH and FSH under the control of the hypothalamus. The pituitary is located in the hypophyseal fossa of the sphenoid bone of the skull (Page, 2006). It lies beneath the hypothalamus and is connected to it by the infundibulum (pituitary stalk). The mammalian pituitary gland has three lobes. The anterior pituitary (adenohypophysis) is glandular tissue that contains several different cell types, each of which secrete a different endocrine hormone. Gonadotrophs produce LH and FSH, lactotrophs produce prolactin, somatotrophs produce growth hormone, corticotrophs produce adrenocorticotropic hormone (ACTH) and thyroid-stimulating hormone (TSH) is produced by thyrotrophs (Savage et al., 2003). FSH, TSH and LH consist of two subunits, the α subunit is common to all three hormones, and the β subunit specific to each hormone (Ryan et al., 1988). The posterior pituitary lobe (neurohypophysis) is derived from neuroectoderm and extends to the infundibulum; it stores arginine vasopressin (antidiuretic hormone, ADH) and oxytocin. The intermediate lobe produces melanocyte stimulating hormone (MSH).

The hypothalamus consists of many small nuclei which control functions such as sexual and ingestive behaviours, control of temperature and integration of cardiovascular and hormonal responses to stress (Page, 2006). The hypothalamus has both neural and vascular links to the pituitary. Magnocellular secretory neurons traverse the infundibulum to connect the paraventricular nucleus of the hypothalamus to the posterior pituitary. Oxytocin and arginine vasopressin are synthesised in these neurons then stored in the posterior pituitary before release into the blood stream. Conversely, there are no neural connections between the hypothalamus and the anterior pituitary and communication between these two compartments is by vascular transport of neurohormones.

1.5.2 GnRH regulates gonadotropin secretion

Parvocellular secretory neurons in the hypothalamus synthesise neurohormones that are released into the portal vessels in the median eminence that pass down into the

anterior pituitary (Herbison, 2006). These hormones act upon trophic cells to regulate synthesis and release of their hormones. Gonadotropin-releasing hormone (GnRH) is the hormone released from the hypothalamus and acts on its receptor (GnRHR) found on pituitary gonadotrophs to stimulate LH and FSH biosynthesis and release (Millar, 2005). Destruction of GnRH synthesising neurons results in gonadal atrophy, which is reversed by intravenous doses of synthetic GnRH. The hypogonadal (*hpg*) mouse model has a naturally occurring mutation that results in undetectable gonadotropin secretion (Cattanach et al., 1977). The mutation was later found to be a truncation of the gene for the biosynthetic precursor of GnRH (Mason et al., 1986). GnRH and LH are secreted in a pulsatile manner, with a high degree of concordance between GnRH and LH pulses. The synthesis of FSH is clearly stimulated by GnRH but the extent to which its secretion depends on pulses of GnRH is less clear, as a relationship between GnRH pulses and FSH secretion is not always found (Tilbrook and Clarke, 2001). Initiation of pulsatile GnRH secretion by a ligand called kisspeptin in the hypothalamus is concurrent with pubertal maturation of the HPG axis (d'Anglemont de Tassigny and Colledge, 2010). Loss-of-function mutations in the kisspeptin receptor (GPR54) cause hypogonadotropic hypogonadism and failure to progress through puberty.

1.5.3 Feedback loop of LH and testosterone

LH binds to specific, high-affinity receptors (LHR) on the surface of testicular Leydig cells (Dufau, 1988). Knock-out mice have been created for both the β subunit of LH (Ma et al., 2004) and the LHR (Lei et al., 2001; Zhang et al., 2001) and display a similar phenotype, with normal pre-natal masculinisation of the reproductive tract, but a decrease in testis size, Leydig cell hypoplasia, and spermatogenesis blocked at the round spermatid stage in adults. Expression levels of testicular steroidogenic genes, StAR and Insl3 were reduced in LHR knock-out (LuRKO) mouse testis (Zhang et al., 2004). Binding of LH has been shown to rapidly induce the synthesis of testosterone by increasing the phosphorylation of StAR and therefore its translocation across the mitochondrial membrane (Evaul and Hammes, 2008). Binding of LH also results in transcriptional upregulation of *StAR*,

Hsd3b and the *Cyp11a1* gene that codes for p450scc (Lavoie and King, 2009). In humans, androgen production by fetal Leydig cells is under the control of LH: humans with a completely inactivating LHR mutation do not undergo masculinisation but humans with an inactivating mutation of LHβ undergo masculinisation of the male reproductive tract due to the presence of placental human chorionic gonadotropin (HCG) which can also activate the LHR receptor (O'Shaughnessy et al., 2009).

Testicular factors are known to negatively regulate the release of LH from the pituitary. Immunisation of male rhesus monkeys against testosterone results in consistently high plasma LH levels (Wickings and Nieschlag, 1978), and administration of exogenous testosterone causes a decrease in circulating LH and a decrease in Leydig cell synthesis of testosterone (Keeney et al., 1988). AR is found in both the hypothalamus and pituitary in the mouse (Miyamoto et al., 2007). Attempts to elicit the site of action of feedback by testosterone in rams and rhesus monkeys has led to the conclusion that it acts by decreasing the pulse rate of GnRH at the level of the hypothalamus and has negligible pituitary effects (Tilbrook and Clarke, 2001). A study in men with hypogonadotropic hypogonadism (GnRH-deficiency) revealed that both testosterone and estradiol can act at the hypothalamus to suppress LH release, but only estradiol can act at the pituitary (Pitteloud et al., 2008). However, AR colocalises with FSHβ and LHβ in rat and monkey gonadotrophs (Okada et al., 2003), testosterone has been shown to suppress LH secretion in rat gonadotroph cultures (Kotsuji et al., 1988; Starzec et al., 1996) and AR can suppress transcription of the LHβ subunit by interacting with SF-1 (Jorgensen and Nilson, 2001): all evidence that AR potentially has a role in controlling pituitary gonadotropin release. Mouse models of global or specific AR ablation do add little to clarification of how testosterone feedback acts on the HPG axis. In *Tfm* mice, levels of serum LH and FSH are increased (Amador et al., 1986) due to a failure of testosterone to limit LH expression and an excess of LH then stimulating more testosterone production. Despite this, pituitaries of ARKO mice have apparently normal pituitary expression of LHβ and FSHβ at both the mRNA

and protein levels (Miyamoto et al., 2007), but this was recorded qualitatively not quantitatively. Mice with cell-specific inactivation of AR in the nervous system (but not pituitary) also have increased LH and testosterone levels and a slight decline in fertility mainly thought to be due to reduction in male-specific mating behaviours (Raskin et al., 2009). GnRH releasing neurons do not express AR, but hypothalamic KiSS-1 neurons which send projections to GnRH neurons are AR+ so feedback could be acting at this site (Raskin et al., 2009). Aromatisation to estradiol has been postulated to play a part in the feedback (Tilbrook and Clarke, 2001), but ERα and ERβ knockout mice do not appear to have defects in their HPG axis (Eddy et al., 1996; Temple et al., 2003). More work is clearly required to elucidate the site and mechanism of regulation of LH release by testosterone.

1.5.4 Feedback loop of FSH and inhibin B

FSH acts *via* a specific G protein coupled receptor (FSHR) present in the testis exclusively in Sertoli cells (Heckert and Griswold, 1991; Vannier et al., 1996). Knock-out mice have been created both for the FSHβ subunit (Dierich et al., 1998; Kumar et al., 1997), and the FSHR (Abel et al., 2000; Dierich et al., 1998). Both types have a decrease in testicular size with reduced germ cell numbers but show complete spermatogenesis. Despite this, fertility is either normal (Abel et al., 2000) or slightly reduced (Dierich et al., 1998). In FSHβKO mice testosterone production and Leydig cell numbers are normal (Wreford et al., 2001) but aged FSHRKO mice have reduced testosterone production (Krishnamurthy et al., 2001) Leydig cell numbers and steroidogenic enzyme expression (Baker et al., 2003). These results show that FSHR signalling in Sertoli cells has a paracrine affect on Leydig cells and that binding to FSH is not required for these actions (Haywood et al., 2002). The decrease in testis size and germ cell number in FSHR and FSHβ mice is thought to be due to a decrease in testicular Sertoli cell number (Wreford et al., 2001). FSH has a tropic effect on Sertoli cell numbers that is independent of LH actions (Allan et al., 2004). Transgenic FSH expression can restore Sertoli cell number in *hpg* mice (Allan et al., 2001) and neonatal FSH treatment is sufficient to increase Sertoli cell number in *hpg* mice, as long as it is given within the normal perinatal window of Sertoli cell

proliferation (Singh and Handelsman, 1996a, b). Examination of double *hpg*/SCARKO mice has confirmed that stimulation of spermatogonial number by FSH is due to direct effects of FSH on the Sertoli cells, and not due to any increase in testosterone production by the Leydig cells acting on Sertoli cell ARs (O'Shaughnessy et al., 2010). FSH also stimulates the production of GDNF by Sertoli cells, thus promoting the renewal and proliferation of spermatogonial stem cells (Tadokoro et al., 2002).

Based on current evidence, it is thought that although testosterone is sufficient to induce initiation and maintenance of spermatogenesis in the absence of FSH (Singh et al., 1995), FSH is needed for quantitatively normal spermatogenesis and the two hormones act synergistically (Abel et al., 2008; Haywood et al., 2003). In contrast to mice, men with a deletion of the FSHβ gene are azoospermic and infertile (Layman et al., 2002; Phillip et al., 1998), but those with an inactivating mutation in the FSHR are oligozoospermic: their fertility is severely reduced but some have managed to sire children (Tapanainen et al., 1997). FSH appears to work *via* different mechanisms in mice and men.

Inhibin B is a glycoprotein produced by the testes that was originally identified from its ability to inhibit FSH secretion by the pituitary (Burger, 1988). Although it is produced by the testis, the location of its production is disputed: most evidence points towards the Sertoli cells but there is some evidence for the Leydig and germ cells (Meachem et al., 2001). It is putatively thought to act *via* betaglycan as a receptor in the pituitary to reduce FSH secretion (Wiater et al., 2009). In some species with seasonal breeding, testosterone is thought to interact with inhibin to negatively regulate FSH secretion (Tilbrook and Clarke, 2001).

1.5.5 Establishment of fetal Leydig cell testosterone production is independent of the HPG axis

It is currently believed that, although fetal rat and mouse Leydig cells do express a functional LHR (Zhang et al., 1994), their function is not intimately dependent on this stimulus. Evidence for this includes the fact that gonadotroph development and

secretion has not occurred at the time of induction of fetal Leydig cell testosterone production (Savage et al., 2003) and the fact that normal masculinisation of the reproductive system occurs in mice with a total failure of pituitary development (Pakarinen et al., 2002), genetic ablation of LHβ (Ma et al., 2004) and LHR (Lei et al., 2001; Zhang et al., 2001). Despite normal reproductive tract masculinisation, mice with a failure in pituitary development have decreased testicular androgen levels in fetus implying that a pituitary hormone other than LH is involved in regulation of fetal Leydig cell function. This hormone is postulated to be adrenocorticotropic hormone (ACTH), which can stimulate FLC function through the melanocortin type-2 receptor, however mice lacking ACTH have normal FLC development, so it is likely that FLCs, whilst responsive to ACTH, are not dependent on it (O'Shaughnessy et al., 2003). In contrast to rodents, humans are dependent on LH action in FLCs for testosterone production (O'Shaughnessy et al., 2009).

1.6 Structure and function of the adult efferent ducts and epididymis and influence of steroid hormones

1.6.1 Anatomy and physiology of the efferent ducts

1.6.1.1 Structure of the efferent ducts

The efferent ducts (also referred to in the literature as the ductuli efferetes, vasa efferentia or efferent ductules) are a series of tubules that conduct sperm from the rete testis to the epididymis. They develop from the mesonephric tubules (Rosenfeld et al., 2000). They number between 3 and 5 in the mouse (Guttroff et al., 1992). The proximal zone comprises the efferent ducts where they exit the rete testis and are slightly convoluted. They become more and more convoluted towards the epididymis in the region called the conus vasculosi, which is marked by a widening of the connective tissue capsule bundle. The efferent ducts anastomose in this region, with fusion points randomly spaced along the length of the ducts. This results in one common duct called the terminus, which is moderately coiled, and continues into the most proximal lobe of the epididymal capsule. The ducts are lined with a pseudostratified epithelium consisting of ciliated and non-ciliated (secretory) cells. They are surrounded by a thin layer of smooth muscle and connective tissue stroma (Ilio and Hess, 1994).

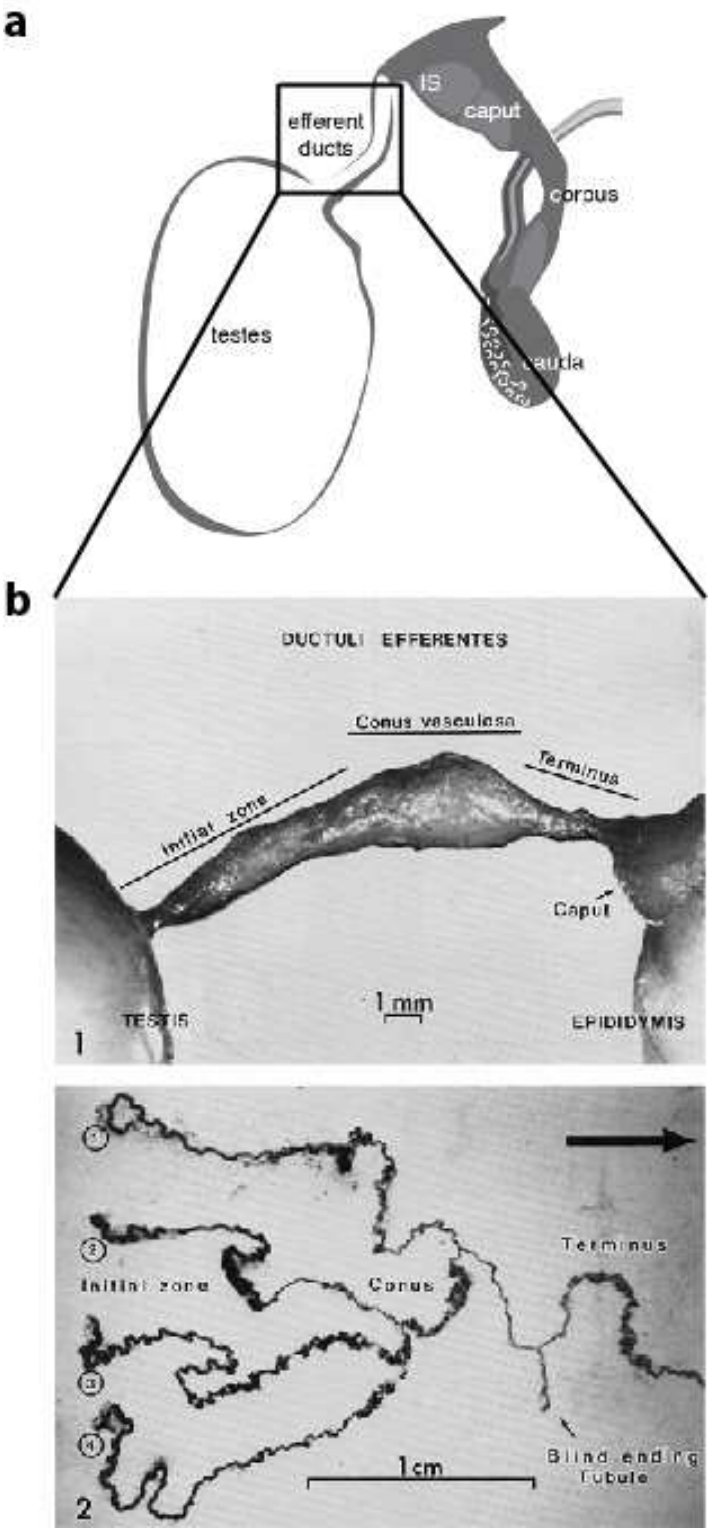

Figure 1-17: Anatomy of the efferent ducts

(a) The efferent ducts connect the testis to the epididymis. Modified from Joseph et al., 2010b. (b) Four efferent ducts exit the testis and anastomose into one duct in the 'conus vasculosa' region before entering the epididymis. Modified from Guttroff et al., 1992.

1.6.1.2 Function of the efferent ducts

The main function of the efferent ducts is to concentrate post-testicular spermatozoa by absorption of testicular fluid secretions. The efferent ducts reabsorb more than 90% of the fluid coming from the testis (Clulow et al., 1994). Several ion transporters (Hansen et al., 1999; Ilio and Hess, 1992; Lee et al., 2001; Leung et al., 2001; Zhou et al., 2001) and aquaporin (AQP) water channels (Badran and Hermo, 2002; Fisher et al., 1998b; Hermo et al., 2004; Pastor-Soler et al., 2001), are also found in the efferent duct epithelium and may participate in the transcellular movement of water, in addition to passive diffusion of water by paracellular pathways. ERα knock-out mice have impaired fluid reabsorbtion in their efferent ducts and several of these proteins have been shown to be regulated by estrogen or impaired in the ERα knock-out (Joseph et al., 2010a; Ruz et al., 2006). It has been proposed that the ciliated cells of the efferent duct epithelium assist in the movement of spermatozoa towards the epididymis, but this has been contradicted by evidence that suggests the cilia do not beat in one direction, and in fact exist to 'stir' the testicular fluids to allow for more homogeneous reabsorbtion. Movement of testicular sperm is now thought to occur due to pressure from testicular fluid and contraction of the PTM cells surrounding the seminiferous tubules (Ilio and Hess, 1994). The efferent ducts appear particularly sensitive to environmental toxicants which have been reported to result in the formation of occlusions of the ducts and obstructive azoospermia (Hess, 1998).

1.6.2 Anatomy and physiology of the epididymis

1.6.2.1 Structure of the epididymis

The epididymis is the organ distal to the efferent ducts and proximal to the vas deferens in the male excurrent duct system. It consists of a single, highly convoluted, tightly packed duct lined with pseudostratified columnar epithelium, embedded in vascularised stroma and surrounded by a connective tissue capsule (Robaire et al., 2006). In rodents, it appears to have three sections when viewed macroscopically: a lobular head at the apical pole of the testis which receives the efferent ducts, a

delicate, thin body that follows the dorsal side of the testis and a lobular tail at the basal pole of the testis which takes a sharp convex curve into the vas deferens. Commonly, these sections are called the caput, corpus and cauda epididymis respectively. The duct and its epithelium vary in morphology between these sections and when viewed in thin-section it is obvious that the caput can be further subdivided into an ‘initial segment’ most proximal to the efferent ducts and the caput proper (Nicander and Glover, 1973; Soler et al., 2005). Each of these 4 regions is divided into segmental lobes by the presence of stromal connective tissue septa. The lobes of the initial segment and caput are the most well characterised, with general agreement that the initial segment is one lobe, designated segment I, the proximal caput consists of two lobes, designated segments II and III, and the distal caput also consists of two lobes, designated segments IV and V (Abou-Haila and Fain-Maurel, 1984; Avram and Cooper, 2004). Each segment is defined by distinct features such as epithelial height and chemical or immunostaining patterns. The connective tissue septa are thought to act as physical barriers between these segments limiting the expression of genes to particular segments of the epididymis (Turner et al., 2003).

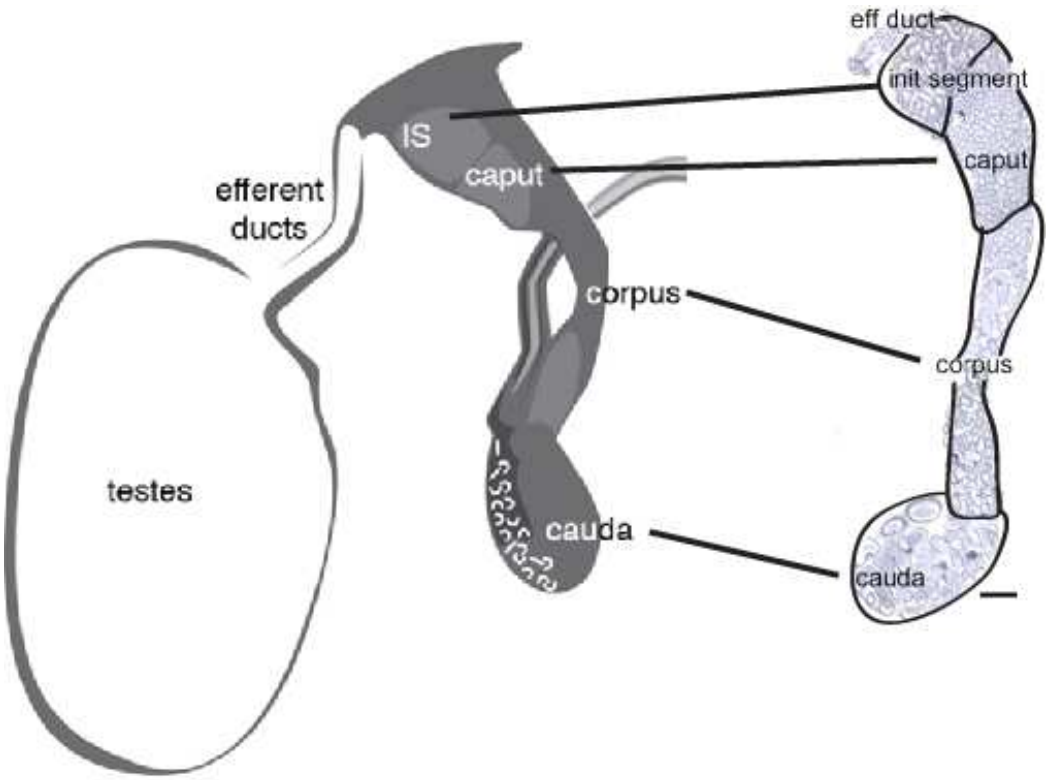

Figure 1-18: Anatomy of the epididymis

The epididymis is commonly divided into 4 regions, the initial segment (which receives the efferent ducts), the caput, the corpus and the cauda. Modified from (Joseph et al., 2010b)

Six different cell types are seen in the epididymal epithelium, some are common to all segments and some are specific, or found in higher numbers in specific segments.

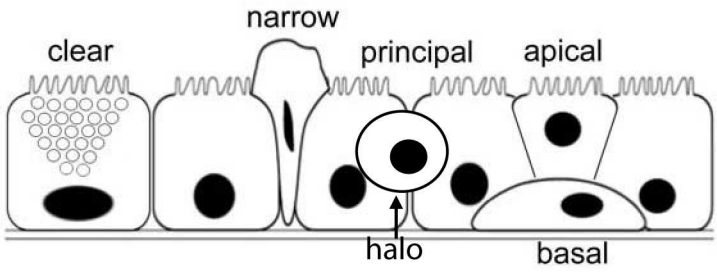

Figure 1-19: Cell types of the epididymal epithelium

Modified from (Joseph et al., 2010b)

Principal cells are found in all epididymal regions and are the most numerous cell type, contributing between 65% and 80% in the rat depending on the region (Robaire and Hermo, 1988). They span the depth of the epithelium from basement membrane to lumen, with a medial to basally located nucleus. In the initial segment they are tall columnar but cell height is reduced in each subsequent segment (Abou-Haila and Fain-Maurel, 1984). Principal cells are very active with respect to transport and secretion of small organic molecules, protein synthesis, and absorption of both fluid and particulate matter (Robaire and Viger, 1995). Narrow cells are found only in the initial segment and proximal caput epididymis, and have an apically located nucleus and a distinctive morphology with a narrow cell body that tapers further towards the basement membrane, but a thicker apical pole that may bulge into the lumen. Apical cells are also found in the initial segment and proximal caput epididymis, and appear morphologically similar to principal cells, but have an apically located nucleus. They have historically either been classified as a type of principal cell or narrow cell. However they do not share the ultra-structural features of the principal cells, or the carbonic anhydrase activity of the narrow cells, so currently are considered to be a distinct cell population (Adamali and Hermo, 1996). Both narrow and apical cells are thought to be involved in H+ secretion and bicarbonate reabsorbtion to maintain the luminal pH. Clear cells are found in the caput, corpus and cauda epididymis. Due to the presence of numerous apical structures including coated pits, vesicles, endosomes and lysosomes their function is thought to be primarily in endocytosis (Hermo et al., 1988; Sun and Flickinger, 1979). Basal cells are found throughout the epididymis and constitute 15-20% of the epithelial population. The flat cell bodies containing nuclei are found along the basement membrane and contact the apical surface of the epithelium through narrow projections. Their function is thought to be in regulation of principal and clear cells by the release of paracrine factors, for example, expression of angiotensin type II receptor indicating a response to angiotensin (Shum et al., 2009). Halo cells are also found in all regions of the epididymis, and have a

distinct dense nucleus surrounded by a pale-staining cytoplasm. Halo cells are thought to function as intra-epithelial leukocytes (Serre and Robaire, 1999).

1.6.2.2 Functions of the epididymis

It is well defined that testicular spermatozoa that have not passed through the epididymis are non-motile and unable to fertilise an oocyte *in vivo*. During transit, spermatozoa undergo morphological and functional changes including increased rigidity due to stiffening of flagellum and neck region (Yeung et al., 2002) movement of cytoplasmic droplet from sperm head to midpiece (Cooper and Yeung, 2003) and change in morphology of the acrosome (Olson et al., 2003). These characteristics are not acquired intrinsically but come about due to associations with the complex mixes of proteins and ions secreted and absorbed by the epididymal epithelium (Cornwall, 2009). Mouse knock-out models with defects in the proteins that mediate luminal protein and ion concentrations are often infertile due to defects in sperm morphology that lead to an inability to function in the female tract or fertilise an oocyte (Cooper et al., 2004). Each stage of spermatozoa maturation is thought to occur in a discrete region of the epididymis and is thought that epididymal septa act to constrain protein localisation to specific epididymal regions as well as providing structural support (Turner et al., 2003). This segment-specific expression of particular genes is illustrated in Figure 1-20.

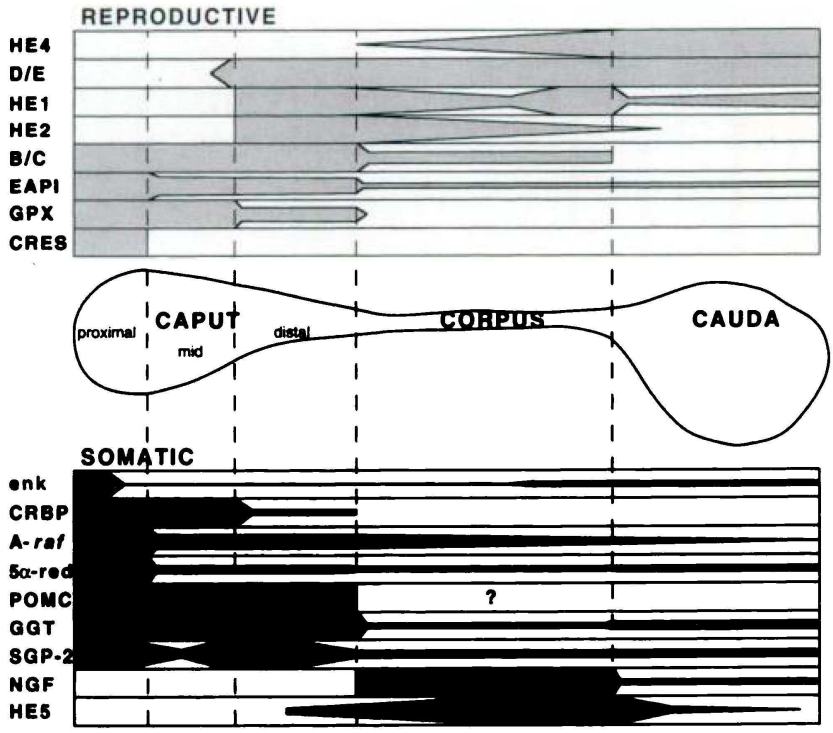

Figure 1-20: Diagram illustrating the specific regions of expression of epididymal gene products

(Cornwall and Hann, 1995)

1.6.3 Action of androgens in the efferent ducts and epididymis

Testosterone produced in the Leydig cells reaches the efferent ducts and epididymis by both transport through the seminiferous tubules to the rete, and in the systemic circulatory system.

1.6.3.1 Expression of AR in the efferent ducts and epididymis

Expression of AR in stromal mesenchymal cells during development is present from e13.5 and is vital for the stabilisation and early development of the Wolffian duct (section 1.3.2). Epithelial expression of AR begins around e16.5 in the efferent ducts and e19.5 in the epididymis (Cooke et al., 1991). In adult tissues, AR is present in the ciliated and non-ciliated cells of the efferent duct epithelium, the periductal smooth muscle cells and most other stromal cells in the efferent ducts of both the mouse (Zhou et al., 2002) and the rat (Oliveira et al., 2004). In most other non-rodent species studied to date including humans (Ungefroren et al., 1997), monkeys (Roselli et al., 1991)

and goats (Goyal et al., 1997) AR has limited or no expression in efferent duct epithelium. Post-natal mouse epididymides express AR in both the epithelial and stromal compartments of all regions in both the mouse (Zhou et al., 2002) and the rat (Yamashita, 2004). All epithelial cell types except halo cells have been reported to express AR. In the stroma, peri-tubular cells are generally AR+, with remaining stromal cells being a mix of AR+ and AR-.

1.6.3.2 Effects of androgen withdrawal on the epididymis and efferent ducts

In 1926, Benoit first reported that bilateral castration (orchidectomy) causes epididymides to regress, and concluded that a testicular factor must be important in epididymal maintenance. It was several years before testosterone was discovered. Many studies since have confirmed the trophic effects of testosterone on the epididymis and other male reproductive organs (Robaire et al., 2006).

Castration causes a reduction in luminal diameter and epithelial height of the efferent ducts. Supplementation with exogenous testosterone did not cause a recovery in lumen diameter, but caused a partial recovery in the height of the epithelium (Oliveira et al., 2004). Castration decreases epididymal weight (Brooks, 1979) and elicits morphological changes in the principal cells of the epididymis including reduction of apical membrane stereocilia and cell organelles including endoplasmic reticulum, lysosomes and Golgi cisternae (Moore and Bedford, 1979b) and increased endocytosis (Moore and Bedford, 1979a). Epididymal lumen diameter and epithelial cell height are both decreased in castrated animals (Fawcett and Hoffer, 1979; Hamzeh and Robaire, 2009). These changes are mediated by a wave of apoptosis of principal cells of the epididymal epithelium that peaks in the initial segment on the first day of castration and then sequentially in the caput, corpus and cauda epididymis in the following days (Fan and Robaire, 1998). Castration also causes any spermatozoa left in the epididymis to lose mobility and ability to fertilise an egg (Dyson and Orgebin-Crist, 1973).

Replacement of testicular testosterone with exogenous testosterone can restore some, but not all of the weight of the epididymis (Brooks, 1979). Several subsequent studies have shown that exogenous testosterone given at the time of castration can rescue the changes associated with epididymal apoptosis and regression in all segments apart from the initial segment (Avram et al., 2004; Fan and Robaire, 1998; Fawcett and Hoffer, 1979; Hamzeh and Robaire, 2009) and preserve the fertilising ability of the epididymal sperm (Dyson and Orgebin-Crist, 1973). A similar pattern of initial segment degradation and apoptosis despite normal appearance of the remainder of the epididymis is seen when efferent ducts are ligated in non-castrated animals, preventing luminal fluid from reaching the epididymis but maintaining circulatory androgens (Abe and Takano, 1989; Avram et al., 2004; Fawcett and Hoffer, 1979; Turner and Riley, 1999). Conclusions of this work have been that circulatory testosterone is enough to maintain the structure and function of the caput, corpus and cauda epididymis, as well as the fertilising ability of spermatozoa (which is most probably an indirect effect on the spermatozoa *via* interactions with the epididymal epithelium), but the initial segment requires a lumicrine factor to maintain epithelial integrity. There is debate as to whether this factor is lumicrine testosterone or some other, as yet unidentified testicular factor (Fawcett and Hoffer, 1979). Several microarray studies have been performed that have attempted to identify genes that mediate the action of testosterone in the epididymis, and their results have led to the discovery and characterisation of several androgen-controlled epididymis-specific genes (Chauvin and Griswold, 2004; Ezer and Robaire, 2003; Robaire et al., 2007; Sipila et al., 2006; Snyder et al., 2009; Turner et al., 2007).

The epididymis can produce both DHT and estradiol (section 1.2) as it expresses both 5α-reductase (Robaire and Viger, 1995) and aromatase (Shayu and Rao, 2006). It has been postulated by some investigators that DHT is the principal androgen in the epididymis (Robaire and Henderson, 2006), but sperm from men with a 5α-reductase type II mutation can result in pregnancy after intrauterine fertilisation (Katz et al., 1997) and 5α-reductase knock-out mice maintain fertility (Mahendroo et al., 2001) so testosterone appears to be the predominant androgen in ensuring normal

epididymal function. Estradiol is also important for the absorptive function of the epididymis as well as the efferent ducts (Joseph et al., 2010b).

So far, no transgenic mice have been created to explore the roles of AR in the function of the efferent ducts and epididymis. Withdrawal of androgens *via* castration has a significant effect on epididymal function, but it is difficult to prove whether androgens are acting *via* stromal AR, epithelial AR, or both to maintain the function and morphology of the epididymis.

1.7 Hypothesis, objectives, rationale and experimental approach

The action of androgens *via* their receptor AR is essential for the correct development and function of the male reproductive system. Studies using rodents with systemic ablation of androgen-action including mice with a systemic genetic ablation of AR (*Tfm* and ARKO) (Lyon and Hawkes, 1970; Yeh et al., 2002) or rats treated with the anti-androgen flutamide (Welsh et al., 2008; Welsh et al., 2006) have been very informative in gaining information on the function of androgens during development and function of the testis. But as adult spermatogenesis is incomplete, the testes of these animals are cryptorchid, and Wolffian duct-derived structures (epididymis, vas deferens and seminal vesicles) are absent, it is difficult to draw conclusions about the relative contributions of androgen action in specific cells to the overall androgen-dependent function and development of the male reproductive system. Models in which AR is genetically ablated in specific cell types have contributed to an exponential increase in our understanding of its role in different organs of the body, but, perhaps unsurprisingly, no one cell specific knockout has a phenotype that recapitulates every aspect of the global ablation models.

1.7.1 Hypothesis

The proposed hypothesis is that ablation of AR function in previously untargeted cell types of the male reproductive system, or in previously characterised cell types at different ages, will have significant and novel effects on reproductive development and function that have not been previously documented by current models of androgen disruption.

1.7.2 Objectives

1. To identify and empirically validate new Cre lines that will permit ablation of AR from previously untargeted cell types in the male reproductive system, or previously targeted cell types at different ages.

2. To ablate AR specifically in these cell types.

3. To use data generated from analysis of the resulting phenotypes to establish the role of AR in these cell types in male reproductive function.

1.7.3 Rationale

The key tool in this approach is the use of the transgenic Cre *loxP* system. Cre-*loxP* transgenic mice are appropriate models for elucidating the specific roles of androgens in different cell types, as the promoter that drives Cre can be selected to be active in a specific cell type, or at a specific age (Smith, 2011). Mouse lines with cell-specific knock-outs of AR in Sertoli cells (Chang et al., 2004; De Gendt et al., 2004; Holdcraft and Braun, 2004), PTM cells (Welsh et al., 2009a; Zhang et al., 2006), Leydig cells (Xu et al., 2007), germ cells (Tsai et al., 2006), vascular smooth muscle (Welsh et al., 2010b), prostate epithelium (Simanainen et al., 2008; Wu et al., 2007), seminal vesicle smooth muscle (Welsh et al., 2010a) and nervous system (Raskin et al., 2009) have been characterised, with varying success, proving that the *Cre loxP* system is an appropriate method for cell-specific AR ablation that has

resulted in new insights into signalling of AR in several of the cell types of the testis and male reproductive tract.

1.7.4 Experimental approach

The first step is to identify novel Cre lines with the potential to express Cre in cell-types of interest that have not previously been targeted for AR ablation. Empirical validation of the spatiotemporal expression pattern is essential. This will be undertaken using a fluorescent reporter gene system that will label cells in which the Cre is active. If validation proves that these Cre lines target novel cell types, they will then be used to generate cell-specific ARKOs. Phenotypes of cell-specific ARKO lines will be analysed using physiological, histological, cellular and molecular techniques and compared to controls to determine the pathophysiological basis of any significant phenotype.

2. Materials and Methods

2.1 Mouse line breeding

2.1.1 Mouse husbandry and welfare

Mice were bred and maintained in the BRF Little France Animal Facility, University of Edinburgh. Mice were kept in a 12 hour Light/Dark regime with humidity maintained at 55% and temperature between 20 and 25 °C. Food and water were available *ad libitum*. Mice were maintained under conditions specified in the Animals (Scientific Procedures) Act, 1986. All procedures were undertaken according to UK Home Office regulations, under project license 60/3544 held by Professor Philippa Saunders. Daily animal husbandry and setting up of timed matings was carried out under my direction by Mark Fisken, for which I am extremely grateful.

2.1.2 Timed matings

When embryos of a specific age were required, vaginal plug checks of breeding females were undertaken at 8 am each morning to allow accurate calculation of their stage of gestation. One male and one female mouse were paired together in cages in the afternoon, then the female examined for a post-copulatory vaginal plug on subsequent mornings. Since mice are expected to mate during the middle of their dark period (overnight), the day of discovery of the plug was designated e0.5.

2.1.3 Breeding of Cre/*loxP* transgenic lines

The Cre/*loxP* system of conditional gene ablation is discussed in section 1.1.2. Several lines are used in this thesis.

2.1.3.1 AR^{flox}, a Cre-conditional AR-ablation line

Two separate groups have constructed a floxed AR line (henceforth referred to as AR^{flox}) by homologous recombination of a transgene constructed to contain a *loxP* site in both intron 1 and intron 3 of the AR genomic sequence, flanking exon 2 (De Gendt et al., 2004; Yeh et al., 2002) (Figure 2-1). When a female homozygous AR^{flox} mouse is mated to a male mouse with a single-insertion Cre transgene under the control of a cell-specific promoter, all of the male offspring will carry the AR^{flox} transgene, as it is on the X chromosome and this is always maternally inherited. Half of the male offspring will carry the Cre transgene and will undergo cell-specific recombination of AR. Upon the cell-specific action of Cre in these animals, the DNA between the two *loxP* sites is recombined and lost, resulting in genomic AR without exon 2. Exon 2 encodes the first zinc finger region of the AR DNA-binding domain, and its deletion causes a frame-shift and introduction of a premature stop codon resulting in premature termination of AR transcription (Hellwinkel et al., 1999). Because the *loxP* sites have been inserted into the introns of the genomic AR they do not interfere with AR transcription and translation in cells that do not express Cre. The AR^{flox} line used in the experiments in this thesis was obtained from Karel de Gendt and Guido Verhoeven, University of Leuven, Belgium.

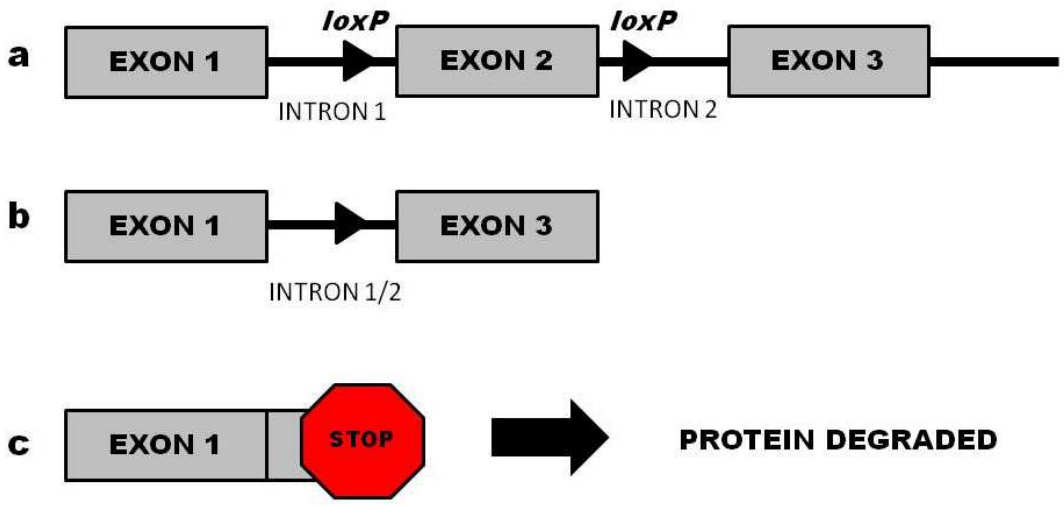

Figure 2-1: Genetic ablation of AR action using the AR^{flox} line

(a) The AR^{flox} transgene was constructed to contain a loxP site in both intron 1 and intron 3 of the AR genomic sequence, flanking exon 2. (b) Upon the cell-specific action of Cre, the DNA between the two loxP sites is recombined and lost, resulting in genomic AR with ablation of exon 2. (3) This causes a frame-shift, introduction of a stop codon and premature termination of AR transcription.

2.1.3.2 Rosa26YFP, a Cre-conditional fluorescent reporter line

The Rosaβgeo26 (Rosa26) mouse strain was produced by random retroviral gene trapping in embryonic stem cells. The β-galactosidase gene carried by the gene trap was shown to be ubiquitously expressed in all tissues (Friedrich and Soriano, 1991; Zambrowicz et al., 1997). The locus itself was mapped and found to produce two, non-coding transcripts. Mice homozygous for Rosa26 insertions are viable and fertile. Because of this, the locus has been exploited for the targeting of transgenes that are required to be ubiquitously expressed. To introduce cell-specific control into genes expressed from this locus, a Rosa26 line was constructed with a transgene consisting of the yellow fluorescent protein (YFP) gene downstream from a stop codon flanked by loxP sites (Srinivas et al., 2001) (Figure 2-2). When a female homozygous Rosa26YFP (R26YFP) mouse is mated to a male mouse with a single-insertion Cre transgene under the control of a cell-specific promoter, all of the offspring will carry one copy of the transgene inherited from the mother. Half of the

offspring will carry the Cre transgene and will undergo cell specific expression of YFP. Upon the cell-specific action of Cre in these animals, the stop codon between the two loxP sites is recombined and lost, resulting in constitutive transcription of the YFP transgene.

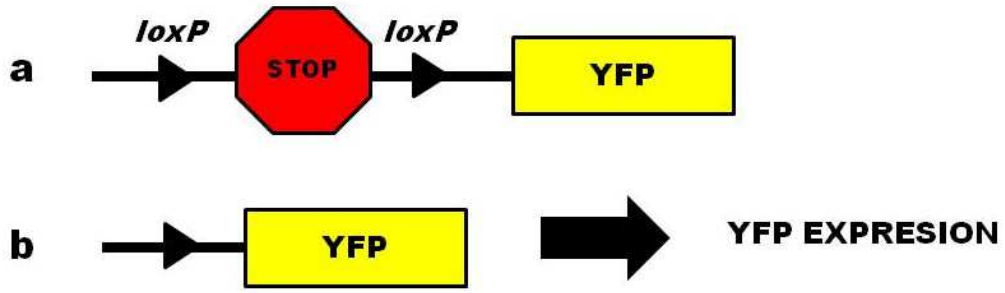

Figure 2-2: Fluorescent reporter gene expression using the R26YFP line.
(a) The R2YFP line consist of the YFP gene downstream from a stop codon flanked by loxP sites. (b) Upon the cell-specific action of Cre, the stop codon between the two loxP sites is recombined and lost, resulting in constitutive transcription and translation of the YFP transgene.

2.1.3.3 FoxG1-ARKO and FoxG1-YFP

The FoxG1-ARKO line used in this thesis is a congenic 129/SvEv mouse line carrying a knock-in of Cre Recombinase at one copy of the FoxG1 locus (Hebert and McConnell, 2000) resulting in hemizygosity of endogenous FoxG1. The line was obtained from Norah Spears, University of Edinburgh.

FoxG1-ARKO mice used in this study were generated by mating FoxG1-Cre male mice to AR^{flox} female mice (De Gendt et al., 2004). Genotype was determined by PCR of DNA purified from ear clips for the presence of Cre (section 2.6). The +/Cre, AR^{flox} /y male offspring from these matings were termed 'FoxG1-ARKO' and the +/+, AR^{flox} /y littermates were termed 'control'.

FoxG1-YFP mice used in this study were generated by mating FoxG1-Cre male mice to R26YFP female mice (Srinivas et al., 2001). Genotype was determined by PCR of DNA purified from ear clips for the presence of Cre (section 2.6), or by viewing tissues under a fluorescent microscope with a YFP filter post-necroscopy. The +/Cre, + /R26YFP male offspring from these matings were termed 'FoxG1-YFP'. +/+, + /R26YFP littermates from these matings were termed 'control'.

2.1.3.4 Tie2-ARKO and Tie2-YFP

The Tie2-Cre line used in this thesis is on a mixed (C57BL/6 x SJL) background. Founder mice were genetically modified to contain one or more copies of a transgene consisting of Cre downstream of the murine endothelial-specific receptor tyrosine kinase (Tie2) promoter inserted into a random locus in the genome. This Tie2-*Cre* line expresses Cre recombinase specifically in endothelial cells (Kisanuki et al., 2001).

Tie2-ARKO mice used in this study were generated by mating Tie2-Cre male mice to AR^{flox} female mice. Genotype was determined by PCR of DNA purified from ear clips for the presence of Cre section 2.6). The +/Cre, AR^{flox} /y male offspring from these matings were termed 'Tie2-ARKO' and the +/+, AR^{flox} /y littermates were termed 'control'.

Tie2-YFP mice used in this study were generated by mating Tie2-Cre male mice to R26YFP female mice. Genotype was determined by PCR of DNA purified from ear clips for the presence of Cre (section 2.6), or by viewing tissues under a fluorescent microscope with a YFP filter post-necroscopy. The +/Cre, + /R26YFP male offspring from these matings express YFP in any cells that express Tie2-Cre and were termed 'Tie2-YFP'. +/+, + /R26YFP littermates from these matings were termed 'control'.

2.1.3.5 Aqp2-ARKO and Aqp2-YFP

The Aquaporin-2 Cre (Aqp2-*Cre)* mouse line used in this thesis is on a mixed (C57BL/6 x CBA) background. Founder mice were genetically modified to contain one or more copies of a transgene consisting of Cre downstream of 14 kb of human AQP2 5'-flanking region (including a TATA box and transcription initiation sites) inserted into a random locus in the genome. This Aqp2-*Cre* line expresses Cre recombinase in the principal cells of the renal collecting duct, post-meiotic germ cells and vas deferens epithelial cells (Nelson et al., 1998).

Aqp2-ARKO mice used in this study were generated by mating Aqp2-Cre male mice to AR^{flox} female mice. Genotype was determined by PCR of DNA purified from ear clips for the presence of Cre. The +/Cre, AR^{flox} /y male offspring from these matings were termed 'Aqp2-ARKO' and the +/+, AR^{flox} /y littermates were termed 'control'.

Aqp2-YFP mice used in this study were generated by mating Aqp2-Cre male mice to R26YFP female mice. Genotype was determined by PCR of DNA purified from ear clips for the presence of Cre (section 2.6), or by viewing tissues under a fluorescent microscope with a YFP filter post-necroscopy. The +/Cre, + /R26YFP male offspring from these matings were termed 'Aqp2-YFP'. +/+, + /R26YFP littermates from these matings were termed 'control'.

2.1.3.6 AMH-YFP

The AMH-Cre mouse line used in this thesis is on a mixed (C57BL/6 x SJL) background. Founder mice were genetically modified to contain one or more copies of a transgene consisting of bacteriophage Cre recombinase downstream of 3.6 kbp of the human anti-Müllerian hormone (AMH) promoter inserted into a random locus in the genome (Lecureuil et al., 2002). Sertoli cells from e15 of embryonic life express AMH, therefore Cre recombinase is also expressed in these cells, and can act to recombine DNA between two loxP sites. It has previously been used to selectively ablate AR in pre-natal Sertoli cells (De Gendt et al., 2004).

AMH-YFP mice used in this study were generated by mating AMH-Cre male mice to homozygous R26YFP female mice. Genotype was determined by PCR of DNA purified from ear clips for the presence of Cre (section 2.6). The +/Cre, + /R26YFP male offspring from these matings expressed YFP in any cells that expressed AMH, and were termed 'AMH-YFP'. +/+, + /R26YFP littermates from these matings were termed 'Controls'.

2.1.4 Evaluation of fertility

To investigate fertility, males were each housed with an adult wild-type C57BL/6 female for 4 days and the presence of a post-copulatory vaginal plug was recorded. This process was repeated with 3 subsequent wild-type CD1 female mice per male. Female mice were monitored for 25 days for litters to be born. Matings were scored as successful if one or more pups were born. Groups were compared with GraphPad Prism software (version 5; GraphPad Software Inc., San Diego, CA, USA) using a Chi squared test.

2.2 Dissection and gross physiological measurements

2.2.1 Culling of mice

Postnatal mice were killed by inhalation of carbon dioxide in a rising concentration and subsequent cervical dislocation. Neonates were killed by decapitation.

2.2.2 Gross physiological observations

Each mouse was weighed and anogenital distance (AGD) was measured using digital callipers (Faithfull Tools, Kent, UK) as this represents a lifelong marker of normal testosterone action within the masculinisation programming window of development (Welsh et al., 2008). The mouse was examined externally to check for nipples, non-scrotal testis and any evidence of penile hypospadias, which are all signs of disrupted testosterone action.

2.2.3 Serum hormone analysis

To obtain serum for hormone analysis, a blood sample was taken from the mouse as soon as possible after cervical dislocation using a 1ml syringe (Becton Dickinson, UK) and 21 gauge needle (Becton Dickinson, UK) pre-treated with heparin to slowly remove blood from the left ventricle whilst the heart was still beating. The blood samples were then centrifuged at 10,000g for 10 minutes in a microcentrifuge, which separated the blood into serum (supernatant) and cellular (pellet) components. Sera were separated and stored at -20°C until assayed for testosterone and luteinising hormone (LH) as previously published (Corker and Davidson, 1978; McNeilly et al., 2000). The within-assay and between-assay coefficients of variation were all less than 10%. Serum hormone assays were performed by Ian Swanston and Nancy Evans at the MRC-HRSU, for which I am extremely grateful.

2.2.4 Recovery of tissues

Individual organs were dissected as described in the following sections. Tissue was either snap-frozen for subsequent RNA analysis (section 2.7) or fixed in Bouin's fixative (Clin-Tech, Guildford, UK) for subsequent embedding and histological analysis (section 2.3).

2.2.4.1 Brain tissues and pituitary

Brain tissues were removed first to minimise RNA degradation. The mouse was decapitated and all fur and skin removed from the skull. The skull was then cut from dorsal to ventral along the midline with a pair of sharp scissors, trying to avoid damage to the brain as much as possible. The anterior surface of the skull was then cut away. The brain was lifted out of the skull by pushing the dorsal side upwards with a blunt object, and the optic nerves cut from the posterior surface to allow the brain to be lifted out of the skull. After removal of the brain the pituitary could then be seen on the floor of the skull between the two large trigeminal nerves that run longitudinally along the bone. The pituitary is a 2 x 1 mm strip of pale tissue running crosswise between these two nerves, covered by a membrane. The pituitary was then frozen by direct contact with dry ice and stored at -80°C. The area of the brain

containing the hypothalamus was then dissected by taking a segment of the median eminence posterior to the optic chiasm about 4mm caudally and 2mm deep. This was frozen as before. The rest of the brain was cut into small pieces to aid freezing and frozen as before.

2.2.4.2 Testis/epididymis/vas deferens

The abdomen was moistened with 70% ethanol to wet the fur, then an incision made across the abdomen through the external skin and peritoneal membrane. The testis was pulled out from the scrotal sac through the abdomen using the attached fat pad then the testis, epididymis and a section of vas deferens were removed as a whole by cutting through the surrounding fat and cutting midway along the vas deferens. After removal, one testis/epididymis/vas deferens was fixed in Bouin's fixative (Triangle Biomedical Sciences Ltd, Lancashire, UK) for 6 hours and then micro-dissected post-fixation, and the other testis/epididymis/vas deferens was micro-dissected, each part weighed and all parts frozen separately by direct contact with dry ice and stored at -80°C.

2.2.4.3 Penis

External fur and skin was removed and the penis was cut midway across the sigmoid flexure. The penis length was measured using digital callipers (Faithfull Tools, Kent, UK) and weighed then either fixed in Bouin's fixative for 6 hours or frozen by direct contact with dry ice and stored at -80°C.

2.2.4.4 Seminal vesicles (SV)

The seminal vesicles and coagulating glands were cut at the junction with the mesentery just behind the bladder, taking care not to pierce the vesicles, weighed (intact, including seminal fluid) and either fixed in Bouin's fixative for 6 hours or frozen.

2.2.4.5 Ventral prostate (VP)

The two lobes of the ventral prostate were cut from around the urethra, weighed, and either fixed in Bouin's fixative for 6 hours or frozen.

2.2.4.6 SV/VP in pre-pubertal animals

In mice culled at day 21 or younger, the SV are small, as testosterone has not yet reached a level high enough to induce proliferation of the SV epithelium. In these animals the bladder, urethra, prostate and SV were dissected out together and fixed in Bouin's fixative for 6 hours. Because of variation in the point of dissection the tissues were not weighed.

2.2.4.7 Adrenal gland and kidney

The adrenal gland was removed by grasping the fat pad above the kidney and trimming the adrenal free of as much fat as possible. It was then weighed and either fixed in Bouin's fixative for 6 hours or frozen. The remaining kidney was trimmed free of mesentery and vessels.

2.2.4.8 Gravid uterus and embryos

After culling of the pregnant dam by inhalation of carbon dioxide and subsequent cervical dislocation, the pregnant dam was positioned supine and the abdomen opened to allow removal of the intact uterus. Embryos were removed from their individual amniotic sacs and the umbilical cord cut prior to embryo immersion in ice-cold PBS. Embryos were then either fixed whole in Bouin's solution (up to e14.5) or subjected to fine dissection to remove gonads and ducts. Fine dissected tissues were then either processed by snap freezing or fixed in Bouin's solution for one hour.

2.2.4.9 Tissue weight analysis

Values from at least 5 tissue weights for each group were averaged and plotted on a graph with the standard error of the mean (SEM). Groups were compared to each other in GraphPad Prism software (version 5; GraphPad Software Inc., San Diego, CA, USA) using a 2-tailed unpaired t test.

2.3 Histology

2.3.1 Fixing, embedding and sectioning

After fixation for 6 hours in Bouin's fixative, the tissues were placed into 70% ethanol where they were stored until processing. Automated processing of tissue was performed in a Leica TP1050 processor (Leica Microsystems, Milton Keynes, UK). Processed tissue was then embedded by hand in liquid paraffin wax and the cooled wax block was stored at room temperature until required. Processing and embedding was performed in-house by Mike Millar, Sheila MacPherson and Arantza Esnal, for which I am very grateful.

Paraffin embedded tissues were sectioned at 5µm using a microtome (Leica, model RM 2135), floated on a water bath (Lamb RA, model E/65) set to 50 °C to smooth out any wrinkles, and mounted on electrostatically charged glass slides (BDH, cat no: 406/0179/00) to facilitate adherence of the sections. The slides where then dried overnight at 50 °C and allowed to cool to room temperature before staining using either a H&E stain to visualise tissue and cell morphology (section 2.3.2) or an immunohistochemistry protocol to visualise localisation of a particular protein of interest (section 2.3.3).

2.3.2 Haematoxylin and Eosin (H&E) staining.

Gross histological analysis of tissues was performed on sections stained with haematoxylin and eosin. Slides were dewaxed by immersion in xylene (BDH) for 5 minutes, then rehydrated by immersion in a series of decreasing concentrations of ethanol at 100%, 95% and 75% for 30 seconds each, were briefly washed and then immersed in Harris's haematoxylin (section 2.9.1.1) for 5 minutes to stain nuclei blue. The slides were then washed in tap water, then 1% acid alcohol (to remove non-specific cytoplasmic staining, section 2.9.1.3), tap water, Scotts Tap Water (to allow the blue dye to develop, section 2.9.1.4), tap water, eosin (section 2.9.1.2), for 30 seconds to stain cell cytoplasm pink), tap water, and then dehydrated by immersion in a series of increasing concentrations of ethanol at 70%, 80%, 95% and

100%. Finally slides were immersed in xylene for 5 minutes to clear, then mounted with a glass cover slip (VWR, UK) and Pertex (Cell Path, UK).

2.3.3 Immunohistochemistry

2.3.3.1 General principles

Immunohistochemistry is the visualisation of a protein of interest in thin-sections of tissue by utilising an antibody to the protein of interest and a chromogenic or fluorescent detection system.

A standard immunohistochemical protocol on tissues that have already been fixed, embedded and sectioned on to slides first involves the process of antigen retrieval. Fixed tissues have undergone chemical processes that induce molecular cross-linking in order to preserve tissue integrity. Exposing fixed tissue to high temperature and pH change unmasks these antigens. The next step is blocking of any endogenous peroxidases using hydrogen peroxide and methanol. Many detection systems use peroxidase enzymes to catalyse a chromogenic or fluorescent reaction and if endogenous peroxide is not blocked this can result in background fluorescence or production of a non-specific chromogenic product. A non-specific antigen blocking step is also included using a serum from the same species that the secondary antibody used is raised in. This helps reduce non-specific binding of the antibodies. After the block the sections are incubated with a primary antibody against the antigen of interest, then a secondary antibody against the species your primary antibody is raised in. The secondary antibody is conjugated with a signal amplification system. Two commonly used ones are streptavidin/biotin for chromogenic detection or peroxidase/tyramide for fluorescent detection. Here the protocols diverge.

Chromogenic detection is the standard detection system to visualise one antigen at a time. It involves first incubating a secondary antibody in this case conjugated to biotin, a glycoprotein, then incubating with streptavidin conjugated horse-radish peroxidase (HRP) enzyme, then a substrate that is modified by the peroxidase to

produce a chromogenic product, in this case 3, 3'-diaminobenzene (DAB) which gives a brown product. The streptavidin/biotin step can be omitted by using a secondary antibody directly conjugated to HRP but inclusion of this step results in a larger amplification of the resulting colour and so a lower concentration of primary antibody is needed.

Fluorescent detection can be used when two antigens need to be visualised at the same time, when the antigen is at a very low concentration (the amplification is generally larger and the detection method more sensitive), or when distribution of the antigen is in a very specific cellular location (for example cytoskeletal proteins). The protocol is identical up until the secondary antibody. For fluorescent detection this can be directly conjugated to a fluorophore if the antigen is abundant, or conjugated to HRP then used with the Tyramide signal amplification (TSA) system (Perkin Elmer, http://las.perkinelmer.com/tsa) if the antigen is present at low levels. When a TSA reagent is applied after a HRP-conjugated secondary antibody, HRP catalyses the production of free radicals from the tyramide. These free radicals covalently bond to electron-rich tyrosine and tryptophan residues of the antigens that the primary/secondary antibody complex has bound to. This provides a greater signal amplification than avidin/biotin methods. The tyramide is bound to a fluorophore which is used to fluorescently localise the signal. Fluorophores are excited and emit light at particular wavelengths when excited by a laser, so two or more fluorophores with different emission spectra can be used on the same section to visualise more than one antigen at the same time.

Before visualisation of the antigen, the tissue sections are counter-stained with a DNA-binding dye. In chromogenic protocols this is usually haematoxylin, as used in an H and E stain, in fluorescent protocols a DNA binding fluorophore such as propidium iodide can be used.

It is prudent to run negative controls when a new antibody or tissue is being investigated, to check for non-specific binding of the antibodies used at each stage.

Running the protocol with a negative control for each step involves substituting the diluted primary antibody, secondary antibody or amplification reagent for the diluent only. All other steps are processed as normal. This must be carried out in each tissue of interest, as non-specific binding can differ between tissues.

2.3.3.2 Standardised chromogenic (DAB) protocol

Slides were dewaxed by immersion in two xylene baths for 5 minutes. They were then dehydrated by immersion in ethanol baths at 100%, 95% and 75% for 30 seconds each, then washed in tap water. For antigen retrieval, slides were boiled for 5 minutes in 0.01M citrate buffer pH 6.0 in a domestic pressure cooker (Clypso, Tefal), then left to stand for 20 minutes before cooling under cold water. To block endogenous peroxidase, slides were incubated in a solution of 30% w/v hydrogen peroxide (Fisher Scientific) diluted 1 in 10 in methanol (Fisher Scientific) for 30 minutes at room temperature with mechanical agitation, then washed in tap water for 5 minutes. Slides were wiped then the appropriate normal serum (NS)/TBS/BSA (section 2.9.3) was dropped on to the slides above the tissue sections. Using a plastic Pasteur pipette. Slides were then incubated for 30 minutes at room temperature in a humidified chamber. Excess blocking serum was carefully wiped from the slides before a solution of primary antibody diluted in appropriate blocking serum to an optimised concentration was pipetted onto the sections. The slides were incubated overnight (16 hours) in a humidified chamber at 4°C. Concentrations of primary antibodies are detailed in Table 2-1. The next day, slides were washed three times with TBS for 5 minutes with agitation to remove residual primary antibody. Excess buffer was carefully wiped from the slides before a biotinylated secondary antibody diluted 1:500 in appropriate NS/TBS/BSA was pipetted onto the sections. Slides were then incubated for 30 minutes at room temperature in the humidified chamber. Slides were then washed as before. Excess buffer was wiped from the slides before streptavidin-conjugated HRP reagent (Dako, UK) diluted 1:1000 in TBS was applied. Slides were incubated for 30 minutes at room temperature in a humidified chamber. After washing as before, antibody localisation was determined using DAB diluted in its supplied buffer (Vector, UK) just prior to use according to

manufacturer's instructions. Sections were incubated with DAB until staining was optimally detected in control sections: this varied depending on the antibody and target tissue. Slides were counterstained with haematoxylin, dehydrated and mounted, as detailed in H and E staining (section 2.3.2). Sections were visualised and photographs taken using a Provis AX70 (Olympus Optical, London, UK) fitted with a Canon DS6031 camera (Canon Europe, Amsterdam).

Table 2-1: Details of antibodies used with DAB chromogenic detection

Protein	Species raised	Company details	Conc. used	Serum diluent	Secondary used	Detection system
AR	Rabbit	Santa Cruz # sc-816	1:200	Goat	GaRb*	Strep-HRP, DAB
CD45	Rabbit	Abcam ab10558	1:20	Goat	GaRb*	Strep-HRP, DAB
ERα	Mouse	Novacastra #NCL-ER-6F11	1:500	Goat	GaMb*	Strep-HRP, DAB
YFP/GFP	Mouse	Abcam # ab38689	1:200	Goat	GaMb*	Strep-HRP, DAB

**Key: GaMb= goat anti-mouse biotinylated (Vector, UK), GaRp= goat anti-rabbit biotinylated (Vector, UK)*

2.3.3.3 Standardised fluorescent tyramide protocol (for single or double antibody staining)

Slides were dewaxed by immersion in two xylene baths for 5 minutes each. They were then dehydrated by immersion in ethanol baths at 100%, 95% and 75% for 30 seconds each, then washed in tap water. For antigen retrieval, slides were boiled for 5 minutes in 0.01M citrate buffer pH 6.0 in a domestic pressure cooker (Clypso, Tefal), then left to stand for 20 minutes before cooling under cold water. To block endogenous peroxidase, slides were incubated in a solution of 3% hydrogen peroxide in methanol for 30 minutes at room temperature with mechanical agitation, then washed in tap water for 5 minutes. Slides were wiped, then appropriate blocking

serum/PBS/BSA (section 2.9.3) was dropped on to the slides above the tissue sections. Using a plastic Pasteur pipette. Slides were then incubated for 30 minutes at room temperature in a humidified chamber. Excess blocking serum was carefully wiped from the slides before a solution of primary antibody diluted in appropriate blocking serum to an optimised concentration was pipetted onto the sections. The slides were incubated overnight (16 hours) in a humidified chamber at 4°C. Concentrations of primary antibodies used are detailed in Table 2-2. The next day, slides were washed three times with PBS for 5 minutes with agitation to remove residual primary antibody. Excess buffer was carefully wiped from the slides before an appropriate peroxidase-conjugated secondary antibody diluted 1:200 in appropriate normal serum/TBS/BSA was pipetted onto the sections. Slides were then incubated for 30 minutes at room temperature in the humidified chamber. Slides were then washed as before. Excess buffer was wiped from the slides before TSA Fluorescein (Perkin Elmer, UK) diluted 1:50 in its own buffer (as manufacturer's instructions) was applied. Slides were incubated for 10 minutes at room temperature in a humidified chamber. All subsequent steps were carried out limiting exposure to light as much as possible to avoid degradation of the fluorophore. At this stage, slides were washed and either counterstained if a single antibody was used, or the protocol repeated from the methanol/ hydrogen peroxide block stage with a second antibody if double-antibody colocalisation staining was required. The second antibody was detected as above but with TSA Cy5 (a TSA reagent that fluoresces at a different wavelength).

To counterstain and mount, buffer was wiped from the slides before propidium iodide (Sigma, UK) diluted 1 in 1000 in PBS was applied as a nuclear counterstain. Slides were incubated for 10 minutes in a humidified chamber, washing again, and mounted with Permafluor mounting medium (Thermo Scientific, UK) and a glass cover slip (VWR, UK). Fluorescent images were captured using a Zeiss LSM 510 Meta Axiovert 100M confocal microscope (Carl Zeiss Ltd, Welwyn Garden City, UK).

Table 2-2: Details of antibodies used with single fluorescent tyramide detection

Protein	Species raised	Company details	Conc.	Serum diluent	Secondary used	Detection system
AR	Rabbit	Santa Cruz # sc-816	1:1000	Goat	GaRp*	Tyramide
FoxG1	Rabbit	Abcam #ab18259	1:200	Goat	GaRp*	Tyramide
YFP/GFP	Mouse	Abcam # ab38689	1:400	Goat	GaMp*	Tyramide

**Key: GaRp= goat anti-rabbit peroxidase conjugated (Dako, UK), GaMp= goat anti-mouse peroxidase conjugated (Dako, UK).*

Table 2-3: Details of antibodies used with double fluorescent tyramide detection

Protein	Species raised	Company details	Conc.	Serum diluent	Secondary used	Detection system
1. AR	Rabbit	Santa Cruz # sc-816	1:1000	Chicken	ChaRp*	Tyramide
2. 3βHSD1	Goat	Santa Cruz #sc-30820	1:2000	Chicken	ChaGp*	Tyramide
1. AR	Rabbit	Santa Cruz # sc-816	1:1000	Goat	GaRp*	Tyramide
2. SMA	Mouse	Sigma # A2547	1:4000	Goat	GaMp*	Tyramide
1. AR	Rabbit	Santa Cruz # sc-816	1:1000	Goat	GaRp*	Tyramide
2. YFP/GFP	Mouse	Abcam # ab38689	1:400	Goat	GaMp*	Tyramide

**Key: ChaRp= chicken anti-rabbit peroxidase conjugated (Santa Cruz, USA), ChaGp= chicken anti-goat peroxidase conjugated (Santa Cruz, USA), GaRp= goat anti-rabbit peroxidase conjugated (Dako, UK), GaMp= goat anti-mouse peroxidase conjugated (Dako, UK).*

2.3.3.4 Automated immunohistochemistry for smooth muscle actin (SMA)

An automated immunostaining machine was utilised for antibodies with an optimised protocol. The Bond-max automated immunostaining machine (Leica Microsystems, UK) can run up to 30 slides at one time, and is based on a polymer rather than a streptavidin-based amplification system. For SMA, automated immunohistochemistry was performed using an α-SMA (Sigma A2547) primary antibody at 1:10,000 concentration and a Polymer Refine Detection kit according to the manufacturer's instructions. Assistance with this machine was provided by Nancy Evans and Lindsey Rutherford, for which I am very grateful.

2.4 Stereology

In the context of these experiments, stereology refers to the quantification of length or counting of cells on 5µm sections of tissue using a microscope (Leitx DBRB), an automatic stage (Prior Pro-Scan automatic stage, Prior Scientific Instruments Ltd., Cambridge, UK) and computer software (Image-Pro Plus 6.2 software with a Stereology 5.0 plug-in (Media Cybernetics U.K., Berkshire, UK). This equipment is applied to the following problems with the assistance of Mike Millar and Marion Walker (MRC HRSU) for which I am extremely grateful.

2.4.1 Quantification of AR ablation in epididymal cells

AR ablation was quantified in the epithelium of FoxG1-ARKO epididymis sections that had been immunostained for AR. Briefly, a slide from each epididymis showing a clear segment II was identified. The slide was examined with a x10 objective and the software used to isolate the area of interest (segment II) and divide it into a grid of squares corresponding to the field of view of the x63 objective. Each field of view was examined using the x63 objective and the 'Count (NV)' setting was used. The nuclei of all AR+ epithelial cells were identified by using a mouse click to place a marker above each nucleus as the software kept a tally. This was then repeated on the

same field of view for AR- epithelial cells. This was repeated for each field of view in the grid, covering the whole area of interest.

2.4.2 Quantification of epithelial cell height in AR+ and AR- cells of the epididymis

Epithelial cell height was quantified in the epithelium of control and FoxG1-ARKO epididymis sections that had been immunostained for AR. Briefly, a slide from each epididymis showing a clear segment II was identified. The slide was examined with a x10 objective and the software used to isolate the area of interest (either segment I or segment II) and divide it into a grid of squares corresponding to the field of view of the x40 objective. Each square was examined using the x40 objective and the 'no experiment' setting was used. For each tubule cross-section present in the field of view, the height of every 5^{th} epithelial cell was measured, starting at 12 o'clock and working clockwise. Cell height was defined as stretching from the basement membrane to the apical luminal cell surface. Each height measurement was designated from an AR+ or an AR- cell based on the staining of the cell nucleus. This was repeated for each tubule cross section in the field of view, then for each field of view in the grid, covering the whole area of interest.

2.4.3 Quantification of epididymal lumen radius

Lumen radius was quantified in the epithelium of control and FoxG1-ARKO epididymis sections that had been AR immunostained. Briefly, a slide from each epididymis showing a clear segment II was identified. The slide was examined with a x10 objective and the software used to isolate the area of interest (either segment I or segment II) and divide it into a grid of squares corresponding to the field of view of the x20 objective. Each square was examined using the x20 objective and the 'no experiment' setting was used. For each epididymal tubule cross-section present in the field of view, the software prompted the user to designate the centre of the lumen, before prompting the user to click at the apical epithelial membrane interface with the lumen on 6 random axes designated by the software. The software then

normalised these measurements to come up with an average lumen radius for each tubule cross-section. This was repeated for each tubule cross section in the field of view, then for each field of view in the grid, covering the whole area of interest.

2.4.4 Quantification of seminiferous tubule radius and tubule lumen radius

Seminiferous tubule and tubule lumen radii were quantified in the epithelium of control and FoxG1-ARKO testis sections that had been H&E stained. Briefly, a slide from each testis sectioned near the midline was examined with a x10 objective and the software used to divide it into a grid of squares corresponding to the field of view of the x20 objective. Each square was examined using the x20 objective and the 'Nucleator' setting was used. When measuring the seminiferous tubule lumen radius: for each tubule cross-section present in the field of view the software prompted the user to designate the centre of the lumen, before prompting the user to click at the apical epithelial membrane interface with the lumen on 6 random axes designated by the software. The software then normalised these measurements to come up with an average lumen radius for each tubule cross-section. This was repeated for each tubule cross section in the field of view, then for each field of view in the grid, covering the whole area of interest. For entire seminiferous tubule radius a similar process was employed, but the axes originating from the centre of the tubule were clicked at the basement membrane of the tubule.

2.4.5 Statistical analysis

Values from at least 3 slides for each group (refer to individual experiments for numbers) were averaged and plotted on a graph with the standard error of the mean. Groups were compared to each other in GraphPad Prism software (version 5; GraphPad Software Inc., San Diego, CA, USA) using a 2-tailed unpaired t test.

2.5 Testis cell dissociation and fluorescence-activated cell sorting (FACS)

The technique of fluorescence activated cell sorting is commonly used to separate cells in a single cell suspension by presence or absence of a fluorescent antibody bound to a cell surface marker. Because of this it is particularly suitable for separating populations of immune cells that are transported in blood or lymph and are defined by the cell surface proteins that they carry. In this case the technique of FACS is applied to the problem of sorting a population of cells in a solid organ (the testis) that are expressing a transgenic fluorescent protein (YFP). In order to sort cells expressing YFP in a testis from other cells that do not, the testis must first be dissociated into a single-cell suspension. FACS can then be used to isolate this single-cell suspension into YFP+ and YFP- cells.

2.5.1 Testis cell dissociation

The protocol used here is based on a previously published protocol for FACS of testicular cells (Deitch et al., 1986). Testes from a litter of mice were separated into fluorescent (AMH-YFP) and non-fluorescent (control) by examination under a dissecting scope fitted with a fluorescent filter. Each population was then processed as follows: the testes were washed in 70% ethanol to sterilise them, then washed twice in PBS (section 2.9.2.1) before removal of the tunica albuginea of each testis using fine forceps. The remaining tubules were minced up into small pieces using small dissection scissors that had been sterilised with 70% ethanol. The minced testes were added to 5 ml of collagenase (section 2.9.4.1) in a flat-bottomed glass tube and incubated at 32°C in a shaking water bath for 15 minutes. After 15 minutes a 200 µl aliquot of DNase (section 2.9.4.2) was added to the testis suspension, and incubation continued for another 15 minutes. The suspension was then transferred to a 15ml Falcon tube and spun at 500g for 5 minutes. The pellet was resuspended and pelleted twice in PBS and then resuspended in 5 ml trypsin/DNase (section 2.9.4.3) in another flat-bottomed glass tube. The suspension was incubated for 5 minutes in a shaking

water bath at 32°C before being dispersed with a 1 ml pipette and filtered through a 70 μm cell strainer (BD Biosciences, UK). The resulting cells were spun and washed twice with PBS as above. The pellet was resuspended in 1 ml PBS and filtered with a 40 μm cell strainer (BD Biosciences, UK). Concentration of cells per ml was checked with a haemocytometer and the volume adjusted with PBS to give 5 x 10^6 cells/ml.

2.5.2 FACS

Fluorescence-activated cell sorting (FACS: trademarked by Becton, Dickinson and Company www.bd.com) is a specialized type of flow cytometry for sorting a population of single cells into two or more sub-populations, based on the specific fluorescent characteristics of each cell. The FACS experiment in this thesis was performed on a BD FACS Calibur at the CALM facility, university of Edinburgh. I am extremely grateful to Fiona Rossi for calibrating the machine to my requirements. Briefly, the two testis cell suspensions (AMH-YFP and control) were taken immediately to the FACS machine after preparation (section 2.5.1). The control testes were used to calibrate the machine. The AMH-YFP testis cell suspension was then placed into the machine for sorting. Once inside the machine, the cell suspension is entrained in the centre of a narrow, rapidly flowing stream of liquid. A vibrating mechanism causes the stream of cells to break into individual droplets. Just before the stream breaks into droplets, the flow passes through a fluorescence measuring station where the fluorescence of each cell is measured at the wavelength of interest. An electrical charging ring is placed just at the point where the stream breaks into droplets. A charge is placed on the ring based on the fluorescence intensity measurement of the cell passing through, which results in the droplet becoming charged with the opposite charge as it breaks from the stream. The charged droplets then fall through an electrostatic deflection system that diverts droplets into containers based upon their charge. The stream is then returned to neutral after the droplet breaks off. The two sorted populations were designated YFP+ and YFP-. RNA was extracted from both cell populations using the Qiagen RNeasy micro kit (section 2.7.1.3).

2.6 PCR genotyping

To determine presence of Cre and the recombination status of genomic *Ar* exon 2 in offspring of transgenic matings, DNA was prepared from ear punches or tail clips and subjected to a PCR assay containing primers for *Cre* and interleukin-2 (*IL2*) as an endogenous control (Welsh et al., 2009a), or Ar exon 2.

2.6.1.1 Lysis of tissue from ear clips and tail tips

First, a rough DNA preparation was obtained by placing either an ear punch in 25 µl TE-Tween (section 2.9.2.5) and 2 µl of 10 mg/ml proteinase K ('PK', Sigma), or 2 mm of tail tip in 50 µl TE-Tween and 5 µl of 10 mg/ml PK and heating to 55 °C for 2 hours (to allow PK to digest proteins) then 95 °C for 7 minutes (to destroy PK activity). Samples were vortexed to mix the digested tissue then spun at 4000 rpm for 5 minutes to pellet undigested tissue. 10 µl of supernatant was removed from the top of the tube then added to 90 µl of PCR-clean water. This dilution was used for any genotyping PCR reactions.

2.6.1.2 PCR assay for *Cre* and *IL2*

PCR was performed on this rough DNA preparation with the following protocol:
10 µl of Biomix Red PCR buffer (Bioline) 0.2 µl of each of the Cre/IL-2 primers (Table 2-4), 7.2 µl of PCR-clean water (BDH, UK) and 2 µl of DNA were combined in a sterile, thin-walled 0.2 ml tube (Continental Lab Products, Oxford, UK) and run on a PCR programme designed to amplify both the *Cre* and *IL2* sequences (94 °C for 3 minutes, followed by 35 cycles of 94 °C for 30 seconds, 57 °C for 30 seconds and 72 °C for 30 seconds, followed by a final incubation at 72 °C for 5 minutes). Samples were run on an agarose gel [2% of agarose (Bioline) in 1x TAE buffer (section 2.9.2.3)] with a 100 base pair ladder (NEB) as a size reference. Expected product sizes were approximately 100 bp for Cre and 300 bp for IL-2.

Table 2-4: PCR primers for Cre recombinase genotyping

Name	5' primer	3' primer
IL2	CTAGGCCACAGAATTGAAAGATCT	GTAGGTGGAAATTCTAGCATCATCC
Cre	GCGGTCTGGCAGTAAAAACTATC	GTGAAACAGCATTGCTGTCACTT

2.6.1.3 PCR assay for *Ar* exon 2

PCR was performed for Ar exon 2 as described in section 2.6.1.2, but instead using the following programme: 94 °C for 3 minutes, followed by 35 cycles of 94 °C for 45 seconds, 64 °C for 60 seconds and 72 °C for 60 seconds, followed by a final incubation at 72 °C for 5 minutes. Primers were 5': GCTGATCATAGGCCTCTCTC and 3': TGCCCTGAAAGCAGTCCTCT, designed to flank Ar genomic exon 2. Samples were run on a QIAxcel automated DNA fragment size analyser (http://www.qiagen.com/products/qiaxcelsystem.aspx). Expected product sizes were approximately 1.2 kb for 'floxed' genomic exon 2 and 0.6 kb for recombined genomic exon 2.

2.7 RNA extraction and reverse transcription (RT)

Extracting RNA from a tissue of interest allows gene expression transcriptome of the tissue to be explored. Commercial spin column kits such as the Qiagen RNeasy mini kit (Qiagen, UK) are based on the lysis of cells and subsequent binding of RNA to a spin column membrane. Once bound, the membrane is washed to purify the RNA, before the RNA is eluted from the membrane by ribonuclease (RNase) free water. RNases are ubiquitous RNA-degrading enzymes, and their effect on RNA quality was minimised by cleaning pipettes and surfaces that may come into contact with the tissue with a RNaseZAP (Ambion, UK), a RNase-denaturing product, and proceeding through an isolation protocol as quickly as possible after the cell-lysis step.

Reverse transcription utilises the reverse transcriptase enzyme to make complementary (c)DNA using RNA as a template, along with random hexamer primers that bind throughout the RNA to allow complete RNA coverage.

2.7.1 RNA extraction from tissues

2.7.1.1 Tissue lysis in preparation for RNA extraction

Tissues were either ground up into powder under liquid nitrogen then homogenised in RLT buffer (part of the Qiagen RNeasy kit) using a QiaShredder column (Qiagen, Crawley, UK) or lysed in RLT buffer using a Qiagen TissueLyser homogeniser (Qiagen, Crawley, UK).

2.7.1.2 RNA extraction using Qiagen RNeasy mini kit

RNA was isolated from frozen tissue pieces up to 30mg in weight by using the RNeasy mini extraction kit (Qiagen, Crawley, UK) according to the manufacturer's instructions. The resulting RNA was eluted in two elutions of 30 µl of RNase-free water, the two aliquots were combined then quantified (section 2.7.1.4) and either reverse transcribed immediately (section 2.7.2) or stored at -80 °C until further use.

2.7.1.3 RNA extraction using Qiagen RNeasy micro kit

To extract RNA from pieces of tissue smaller than 5mg, or up to $5x10^5$ cells from FACS experiments, the Qiagen RNeasy micro kit (Qiagen, Crawley, UK) was used, according to manufacturer's instructions. The binding membrane on the micro columns is smaller than the mini kit, and the resulting RNA is eluted in 15ul RNase-free water to compensate for the smaller amount of starting tissue. Eluate was then quantified (section 2.7.1.4) and either reverse transcribed immediately (section 2.7.2) or stored at -80 °C until further use.

2.7.1.4 Quantification of RNA using a Nanodrop spectrophotometer

In order to correct for differences in amounts of RNA recovered from each sample, RNA concentration was quantified using a Nanodrop ND-1000 spectrophotometer (LabTech International, UK).

2.7.2 Reverse transcription (RT)

Random hexamer primed cDNA was prepared using the Applied Biosystems TaqMan reverse transcription kit (Applied Biosystems, Foster City, CA) according to manufacturer's instructions. Briefly, 400 ng of RNA was made up to 9 µl with RNase-free water, 2 µl PCR buffer II, 4 µl magnesium chloride, 2 µl dNTPs, 1 µl RNase inhibitor, 1 µl of random hexamers and 1 µl of reverse transcriptase. The reagents were added together in a 0.2 ml sterile thin walled PCR tube (Continental Lab Products, Oxford, UK) and cycled in a thermo-cycler through the following programme: 25 °C for 20 minutes, 42 °C for 60 minutes and 95 °C for 5 minutes. The resulting cDNA was frozen at -20 °C until further use.

2.8 Quantification of gene expression using RT-PCR or TaqMan®

To determine whether cDNA prepared from tissues contained transcripts of a gene of interest, two approaches can be undertaken. RT-PCR, like PCR on genomic DNA, utilises two specifically designed oligonucleotide primers, DNA polymerase enzyme and dNTPs to make copies of the sequence of DNA between the two primers. However, RT-PCR uses cDNA rather than genomic DNA as a template, so is representative of the transcriptome of the tissue rather than the genome. RT-PCR is suitable for qualitative or semi-quantitative analysis of a gene of interest, but quantitative analysis requires quantitative (q)RT-PCR. TaqMan is a form of qRT-PCR that incorporates a fluorogenic probe between the two primers that is activated when cleaved during DNA replication to enable the detection of a specific fluorescent product as it accumulates during the PCR process.

2.8.1 RT-PCR

For RT-PCR (where the reaction product is to be run on an agarose gel), the following protocol was used: 1 µl of cDNA was combined with 10 µl of Biomix Red PCR buffer (Bioline, UK), 0.2 µl of 20 µM 5' and 3' primers appropriate to the assay (detailed in Table 2-5, designed using Primer3 online software, synthesised by Eurofins MWG Operon, UK) and 8.6 µl of PCR-clean water in a sterile 0.2 ml thin-

walled tube (Continental Lab Products, Oxford, UK). Assays were run on a PCR machine using a programme of 94 °C for 3 minutes, followed by 35 cycles of 94 °C for 30 seconds, the appropriate pre-optimised annealing temperature (see Table 2-5) for 30 seconds and 72 °C for 30 seconds, followed by a final incubation at 72 °C for 5 minutes. Resulting products were run on an agarose gel (1% of agarose in 1x TAE buffer [section 2.9.2.3]) with a 100 base pair ladder (New England Biosciences, UK) as a size marker.

Table 2-5: Details of RT-PCR assays used in these studies

Assay	Ensembl gene ID	Sequences	Anneal temp	Product size
AR (exon 2)	ENSMUSG 00000046532	5' AAGCAGGTAGCTCTGGGACA 3' CGTTTCTGCTGGCACATAGA	62 °C	765 bp wild-type, 613 bp k/o
Acta2	ENSMUSG 00000035783	5' TCCCTGGAGAAGAGCTACGA 3' CTTCTGCATCCTGTCAGCAA	60°C	243 bp
Cdkn1b	ENSMUSG 00000003031	5' TTGGGTCTCAGGCAAACTCT 3' ACCGGAGCTGTTTACGTCTG	63 °C	250 bp
Ddx4	ENSMUSG 00000021758	5' TATGGAGGAACCCAGTTTGG 3' CTTTGATGGCATTCCTGGAC	56 °C	219 bp
Hsd3b1	ENSMUSG 00000027871	5' TGACACCCAGTACCTGAGGA 3' GCAACATCAACTGAGCTGGA	63 °C	195 bp

2.8.2 TaqMan® qRT-PCR

2.8.2.1 Primer and probe design

Expression of specific transcripts was determined using the Mouse Universal Probe Library ('UPL', Roche, UK), a set of probes labelled with carboxyfluorescein (FAM) fluorophore, and specific forward and reverse primers designed for the gene of interest using the online software at www.roche-applied-science.com/sis/rrpcr/upl/ezhome.html. Primers were ordered from Eurofins MWG Operon (UK). Validation of primer suitability for use with the ΔΔCt method (discussed in section 2.8.2.3) was performed by running the assay detailed in section 2.8.2.2 with a five-fold dilution series of a reference cDNA (either wild-type pituitary or wild-type epididymis, depending on the gene to be assayed). ΔCt should be the same for each concentration of cDNA, indicating a linear efficiency of amplification.

Table 2-6: Details of TaqMan assays used in these studies

Assay	Ensembl Gene ID	Primers	UPL probe number
Cga	ENSMUSG00000028298	5' AAATATGCAGCTGTCATTCTGG 3' GAAGAGAATGAAGAATATGCAGGAA	56
Lhb	ENSMUSG00000038194	5' CTCAGCCAGTGTGCACCTAC 3' GGAAAGGAGACTATGGGGTCTAC	71
Fshb	ENSMUSG00000027120	5' GTGCGGGCTACTGCTACACT 3' CAGGCAATCTTACGGTCTCG	17
Tshb	ENSMUSG00000027857	5' AAGAGCTGGGGTTGTTCAAA 3' TACAAAAGGATGCTGCTTGC	55
Prl	ENSMUSG00000021342	5' AGGGGTCAGCCCAGAAAG 3' GAGAAGTCTGGCAGTCACCAG	53
Pomc	ENSMUSG00000020660	5' CAGTGCCAGGACCTCACC 3' CAGCGAGAGGTCGAGTTTG	62
Gpr64	ENSMUSG00000031298	5' TCAAGATACAGCTAATGGCACCT 3' GAGTTTTGTTGAGCTCTGATCG	109

2.8.2.2 TaqMan assay

TaqMan reactions for each cDNA of interest were performed in duplicate. The expression level of the transcript of interest was related to an internal control (18s ribosomal RNA) with a probe labelled with VIC, a fluorophore that fluoresces at a different wavelength to the FAM labelled probe of the gene of interest, so levels of both the gene of interest and 18s control could be recorded after each cycle. Each plate included a 'no template control' that substituted water for cDNA template, and a positive 'normaliser' cDNA so assays performed on within and between plates

could be compared to each other (either wild-type pituitary cDNA or wild-type epididymis cDNA, depending on the assay).

The reaction mix for a duplicate reaction was as follows:

	Volume added
2x Express Supermix (ABI)	16 µl
5' primer (20 µM)	0.32 µl
3' primer (20 µM)	0.32 µl
Universal probe (10 µM)	0.32 µl
18s (ABI, mix contains primers at 1.33 µM, probe at 5.3 µM)	0.24 µl
cDNA	2 µl
PCR-clean water (BDH)	13.2 µl

This gave two duplicates of 15 µl (with 2 µl left over for error), which were aliquotted into a 96 well MicroAmp optical reaction plate (Applied Biosystems) sealed with an ABI prism optical adhesive cover (Applied Biosystems) and run on the default programme on the ABI prism with detection of both FAM and VIC.

2.8.2.3 Analysing TaqMan results

TaqMan PCR results were displayed as an amplification plot, which shows the amount of the fluorescent product generated during amplification: this is proportional to the amount of PCR product formed and thus the amount of target gene expressed in the target tissue. When analysing a TaqMan amplification plot three regions can be seen: the baseline, which indicates the basal fluorescence in the reaction plate, the exponential region where fluorescence is increasing exponentially associated with a corresponding increase of PCR product, and the plateau region, where the reaction is no longer exponential due to limiting reagents. The 'threshold level' is where the fluorescence that is generated during the reaction crosses the threshold where it is significantly above background fluorescence. The Ct (threshold cycle) is the cycle

number at which this has occurred. A lower Ct indicates that more of the transcript of interest was originally present in that sample.

A relative quantification assay was used to analyse any changes in gene expression in a given sample, relative to another reference sample (such as an untreated control sample). Relative quantification was achieved using the comparative ΔΔCt method (Schmittgen and Livak, 2008). For each sample, the ΔCt was first calculated by subtracting the Ct for the internal positive control gene (in this case 18s rRNA) from the ΔCt of the target gene. The two duplicates of each sample were then averaged and then compared to a reference sample. This was calculated by subtracting the ΔCt for the reference sample from the ΔCt for the target sample and was referred to as ΔΔCt. The formula $2^{-\Delta\Delta Ct}$ gives the relative fold change of the target gene in that particular sample compared to the reference sample. Values from at least 3 samples for each group (specific age, genotype either control or mutant) were averaged and plotted on a graph with the standard error of the mean. Groups were compared to each other in GraphPad Prism software (version 5; GraphPad Software Inc., San Diego, CA, USA) using a 2-tailed unpaired t test.

2.9 Commonly used solutions

Unless stated otherwise, all of the components of these solutions can be brought from Sigma-Aldrich, UK. Ultra-filtered water was provided by a Millipore water filter (Millipore, UK).

2.9.1 H&E solutions

2.9.1.1 Harris's haematoxylin

25 ml of 10% haematoxylin in absolute alcohol was added to 500 ml of 10% warm aluminium potassium sulphate solution. The solution was heated to boiling point and 1.25 g of mercuric oxide (1.25g) was added slowly. The haematoxylin solution was

plunged into ice to cool before filtering it into a staining dish. Finally, glacial acetic acid was added (4 ml per 100 ml haematoxylin).

2.9.1.2 Eosin

An aqueous eosin solution was made by dissolving 1% w/v eosin in water, and an alcohol solution was made by dissolving 1% w/v eosin in methylated spirit. The solutions were mixed at 1 part alcohol to 3 parts aqueous and filtered. 0.5 ml/L of formaldehyde was added to prevent bacterial growth.

2.9.1.3 Acid alcohol

1% concentrated hydrochloric acid was added to 70% ethanol.

2.9.1.4 Scotts tap water

0.2% w/v potassium hydrogen carbonate and 2% w/v magnesium sulphate were added to tap water.

2.9.2 Buffers

2.9.2.1 Phosphate-buffered saline (PBS)

One PBS tablet (Medicago, Sweden) was added to each litre of ultra-filtered water.

2.9.2.2 Tris-buffered saline (TBS)

To make a 10x solution, 60.5 g of Trizma base, 87.6 g NaCl and 300 ml hydrochloric acid were made up to 10 L with ultra-filtered water. The solution was adjusted to pH 7.4 and the stock solution was diluted to 1x with ultra-filtered water before use.

2.9.2.3 Tris-acetate-EDTA (TAE)

To make a 50x solution, 242 g of Tris base, 57.1 ml glacial acetic acid (BDH, UK) and 100 ml 0.5M EDTA (section 2.9.2.4) were made up to 1 L with ultra-filtered water. The solution was adjusted to pH 8.5 and the stock solution was diluted to 1x with ultra-filtered water before use.

2.9.2.4 0.5M EDTA

186.1 g EDTA was added to 800 ml of ultra-filtered water. The solution was adjusted to pH 8.0 with concentrated NaOH to allow the EDTA to dissolve then diluted to 1 L with ultra-filtered water.

2.9.2.5 Tris-EDTA-Tween (TE-Tween)

2.5 ml of Tris-HCl, 100 µl 0.5M EDTA (section 2.9.2.4) and 250 µl Tween were dissolved in 50 ml of distilled water.

2.9.3 Normal sera

Normal chicken and goat sera were obtained from Biosera, UK.

2.9.3.1 Normal serum: phosphate-buffered saline: bovine serum albumin (NS: PBS: BSA)

NS from the animal of choice was diluted 1 in 4 with PBS (section 2.9.2.1) containing 5% BSA.

2.9.3.2 Normal serum: tris-buffered saline: bovine serum albumin (NS: TBS: BSA)

NS from the animal of choice was diluted 1 in 4 with TBS (section 2.9.2.2) containing 5% BSA.

2.9.4 Tissue dissociation reagents

2.9.4.1 Collagenase solution

Collagenase A (Roche, UK) was reconstituted to a final concentration of 1mg/ml in PBS (2.9.2.1)

2.9.4.2 DNase solution

DNase I (Roche, UK) was reconstituted to a final concentration of 1 mg/ml in PBS (2.9.2.1).

2.9.4.3 Trypsin/DNase solution

Solution consisted of 50 µg/ml trypsin (Roche, UK), 40 µg/ml DNase I (Roche, UK) and 20 µg/ml EDTA reconstituted in PBS (2.9.2.1).

3. Generation and characterisation of novel testicular cell-specific ARKO mice

3.1 Introduction

Testes of mice with total ablation of androgen receptor (ARKO) are well characterised (Yeh et al., 2002), as are those from mice with a cell-specific ablation of AR in the Sertoli (Chang et al., 2004; De Gendt et al., 2004), PTM (Welsh et al., 2009a) and Leydig cells (Xu et al., 2007) (see Chapter 1). None of the cell-specific knock-outs has a phenotype as severe as the ubiquitous knock-out. This may be due to the additive effect of AR ablation in three cell types, or additional effects induced by the cryptorchidism of the total ARKO testis. However, two other cell types in the testis have been postulated to express androgen receptor: the germ cells and endothelial cells. It is generally accepted within the literature that germ cells of the adult testis do not express AR (O'Donnell et al., 2006) although some studies have demonstrated AR protein immunolocalisation in elongating spermatids of the adult testis (Vornberger et al., 1994). Whether or not AR is expressed in germ cells, evidence suggests that it is not necessary for normal spermatogenesis, as when spermatogonia from *Tfm* mice were transplanted into wild-type mice they proceeded through spermatogenesis normally (Johnston et al., 2001). Aquaporin-2 (Aqp2) is expressed by the post-meiotic germ cells of the testis (Nelson et al., 1998). Preceding these studies, an Aqp2-Cre line was available but had not yet been characterised in the testis. Mating of this line to the R26YFP reporter line would produce offspring that express YFP in cells where Cre is active, to confirm that expression of Aqp2-Cre mirrors that of endogenous Aqp2. Mating of the Aqp2-Cre line to the floxed androgen receptor (AR^{flox}) line would produce offspring with ablation of AR in post-meiotic germ cells. These mice can then be analysed to determine whether ablation of AR in these cells has an impact on spermatogenesis.

Vascular endothelial cells line blood vessels in the testis and are also found in the testicular interstitium as lymphatic endothelial cells (Kerr et al., 2006). Androgen receptor signalling promotes proliferation and augments key angiogenic events in

cultured vascular endothelial cells (Cai et al., 2011; Sieveking et al., 2010), but there is some debate in the literature as to whether testicular endothelial cells express AR or not (Nakhla et al., 1984; Pelletier et al., 2000; Vornberger et al., 1994). The endothelial-specific receptor tyrosine kinase (Tie2)-Cre line expresses Cre recombinase specifically in endothelial cells (Kisanuki et al., 2001). Targeting of the Cre line in the testis has not been tested, so this will be also be investigated using Tie2-YFP mice before the testicular impact of ablating endothelial AR will be analysed in Tie2-ARKO mice.

To study the effects of AR in Sertoli cells, it is advantageous to have a Sertoli cell line for *in vitro* experiments. It requires several days of seeding to isolate primary cultures of Sertoli cells free from contamination of germ and PTM cells (Buzzard et al., 2002), but Sertoli cells lose their expression of AR after a few days in culture (Sneddon et al., 2005). Immortalised Sertoli cells lines have been used as an alternative (Rahman and Huhtaniemi, 2004) but many of these lines also do not express AR, or aberrantly express mesenchymal cell-specific genes (Konrad et al., 2005). The Cre-*loxP* system is mostly utilised to for conditional ablation of a gene of interest. However, as shown in the experiments in chapters 3 to 6 of this thesis, it can also be used to label a cell type of interest with a fluorescent protein. This is most often used to identify cells in which Cre is or has been active, but has the potential for novel uses. Mice with fluorescently labelled Sertoli cells can be generated by mating males from the AMH-Cre line to females carrying the R26R-YFP transgene (Srinivas et al., 2001). Fluorescence-activated cell sorting (FACS) is a type of flow cytometry that can be used to sort a heterogeneous mixture of cells into two or more populations based upon the specific light scattering and fluorescent characteristics of each cell. FACS on a testicular cell suspension from the AMH-YFP line will therefore be investigated for the potential to assist in the isolation of a pure Sertoli cell population from the testis.

3.1.1 Aims

The aims of this chapter are:

- To investigate whether the endothelial and germ cells of the testis express androgen receptor, and what happens when AR is ablated in each of these two cell types.
- To investigate whether the AMH-YFP line can be used to isolate a pure population of Sertoli cells by FACS sorting.

3.2 Results

3.2.1 Use of a Tie2-Cre line to ablate AR from the endothelial cells of the testis

3.2.1.1 Localisation of YFP in Tie2-YFP testes

Immunostaining of thin sections of Tie2-YFP testes revealed that YFP was localised to the endothelial cells of the testicular blood vessels of d100 Tie2-YFP testes, and also to a population of interstitial cells not associated with blood vessels (Figure 3-1, n=3 sections for both Tie2-YFP and controls). YFP+ endothelial cells lining blood vessels and dispersed through the interstitium did not stain for AR.

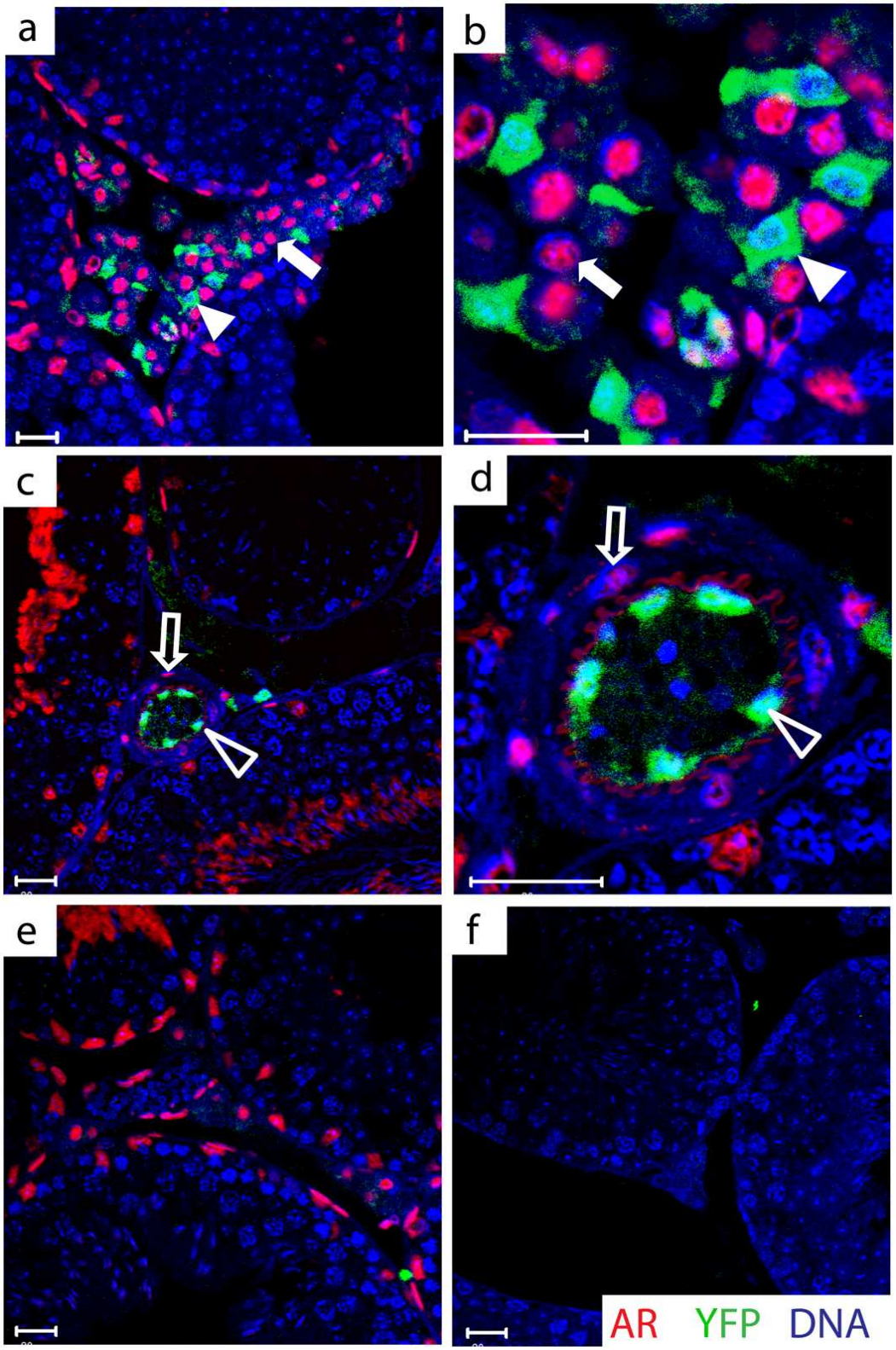

Figure 3-1: YFP immunolocalisation in cross-sections of d100 Tie2-YFP testes

Figure 3-1: YFP immunolocalisation in cross-sections of d100 Tie2-YFP testes (figure on preceding page)

(a, b) Endothelial cells of the interstitium of d100 Tie2-YFP testes stain for YFP, but do not stain for AR (solid arrowheads) whereas AR positive interstitial cells do not stain for YFP (solid arrows). (c, d) Endothelial cells of the blood vessels of d100 Tie2-YFP testes stain for YFP, but do not stain for AR (outline arrowheads) whereas AR positive blood vessel smooth muscle cells do not stain for YFP (outline arrows). (e) No YFP immunostaining is seen in testes of control littermates. (f) No-primary antibody control. Scale bars are 20µm.

3.2.1.2 Analysing ablation of AR expression in the testis of a TIAR mouse line

Tie2-ARKO mice did not differ significantly from controls in mean body weight, AGD and testicular weight (Table 3-1). d100 Tie2-ARKO testes d100 appeared histologically similar to controls with normal spermatogenesis (Figure 3-2). Mature spermatozoa were present in the cauda epididymides of d100 Tie2-ARKO mice, similar to controls. Testes of d100 Tie2-ARKO mice produced only wild-type full-length *Ar* transcript, and not the shorter transcript that results from Cre recombinase-mediated deletion of exon 2 (Figure 3-3). Recombination of *Ar* exon 2 was shown to have occurred at the genomic level in Tie2-ARKO testes (Figure 3-4).

Table 3-1: Mean body weight, AGD and testis weight of Tie2-ARKO compared to control.

n=3 mice for both Tie2-ARKO and controls, P>0.05

	Control	**Tie2-ARKO**
Body weight	24.2 g	25.0 g
AGD	15.6 mm	15.5 mm
Testicular weight	85.3 mg	86.2 mg

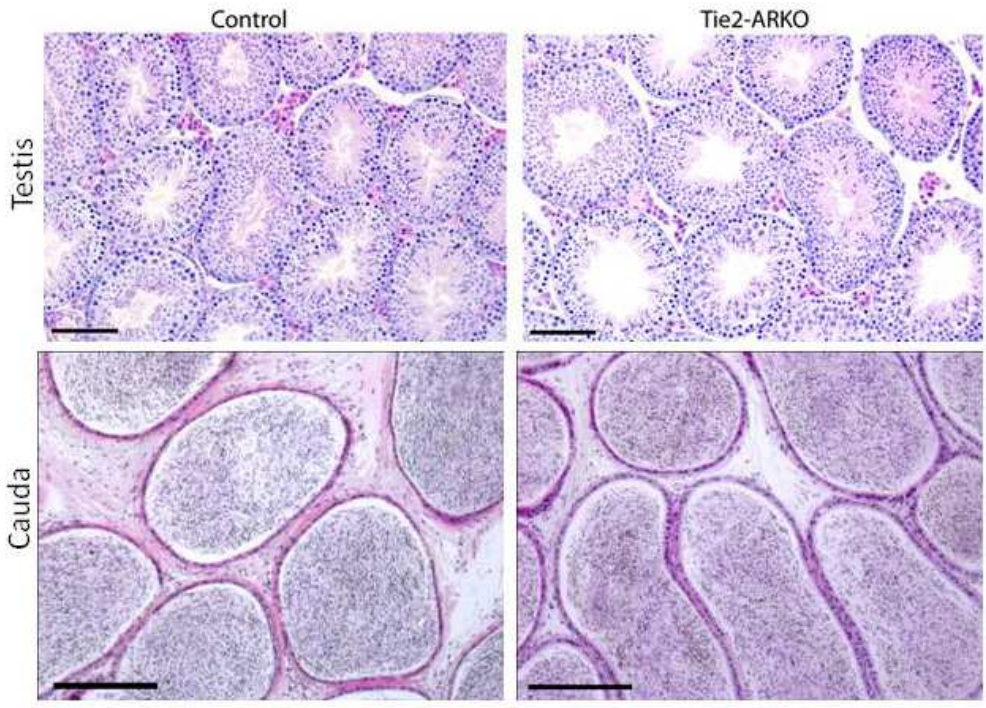

Figure 3-2: Histology of d100 control and Tie2-ARKO testes and cauda epididymides

Histology of Tie2-ARKO testes and cauda epididymides is similar to controls at d100. Scale bars are 200µm.

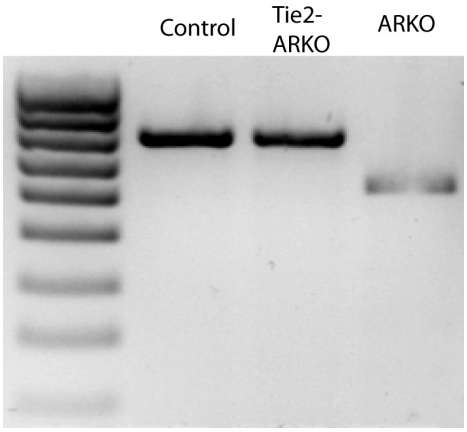

Figure 3-3: Presence of wild-type and/or Cre-recombined Ar transcript in d100 control and Tie2-ARKO testis

RT-PCR on d100 control testis confirms all Ar transcripts are wild-type (upper band). d100 Tie2-ARKO testis expresses only wild-type Ar transcripts. Total ARKO testis expresses only recombined AR (lower band).

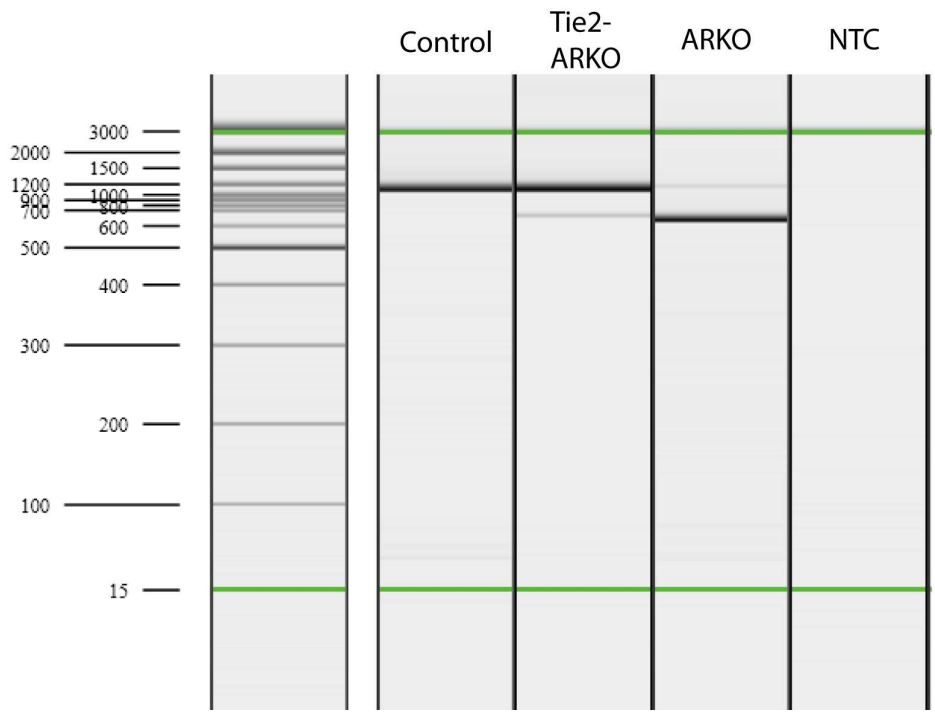

Figure 3-4 Presence of wild-type and/or Cre-recombined genomic Ar exon 2 in d100 control and Tie2-ARKO testis

PCR on d100 control testis confirms that genomic Ar exon 2 is not recombined (upper band, approx. 1.2 kb). PCR on d100 Tie2-ARKO testis reveals that some genomic Ar exon 2 is recombined (lower band, approx. 0.6 kb), although most genomic AR exon 2 is not recombined .Total ARKO testis contains only recombined genomic AR. NTC = no-template control.

3.2.2 Use of an Aqp2-Cre line to ablate AR from the post-meiotic germ cells of the testis

3.2.2.1 Localisation of YFP in Aqp2-YFP testes

Whole mount visualisation of YFP fluorescence in unfixed seminiferous tubules demonstrated that YFP was localised in germ cells. When viewed at a plane at the base of the tubule, the YFP was localised to the outline of hexagonal-shaped Sertoli cells (Figure 3-5a). When viewed in a more central plane the YFP was localised in clusters of germ cells in the centre of the tubule (Figure 3-5b). When embedded in paraffin, sectioned and stained with a GFP/YFP antibody, YFP immunostaining was specific to the cytoplasm of post-meiotic germ cells at d100 (Figure 3-6, n=3 sections for both Aqp2-YFP and controls).

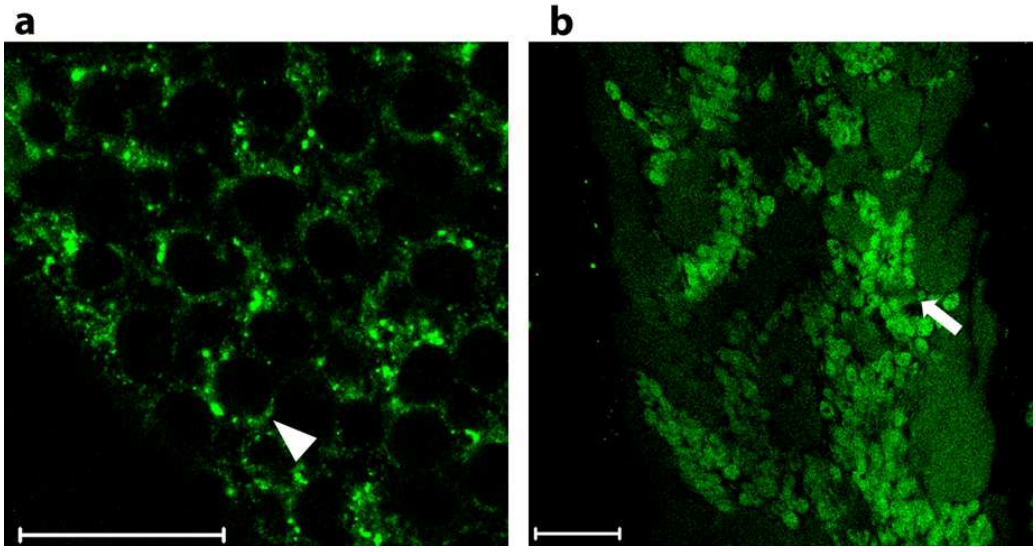

Figure 3-5: YFP fluorescence localisation in whole seminiferous tubules of d100 Aqp2-YFP testes

(a) At the periphery of a seminiferous tubule, YFP is localised outside the characteristic hexagonal-shaped basal aspects of Sertoli cells (arrowhead). (b) In a more central plane of a seminiferous tubule, YFP is localised to the clusters of germ cells (arrow). Scale bars are 50µm.

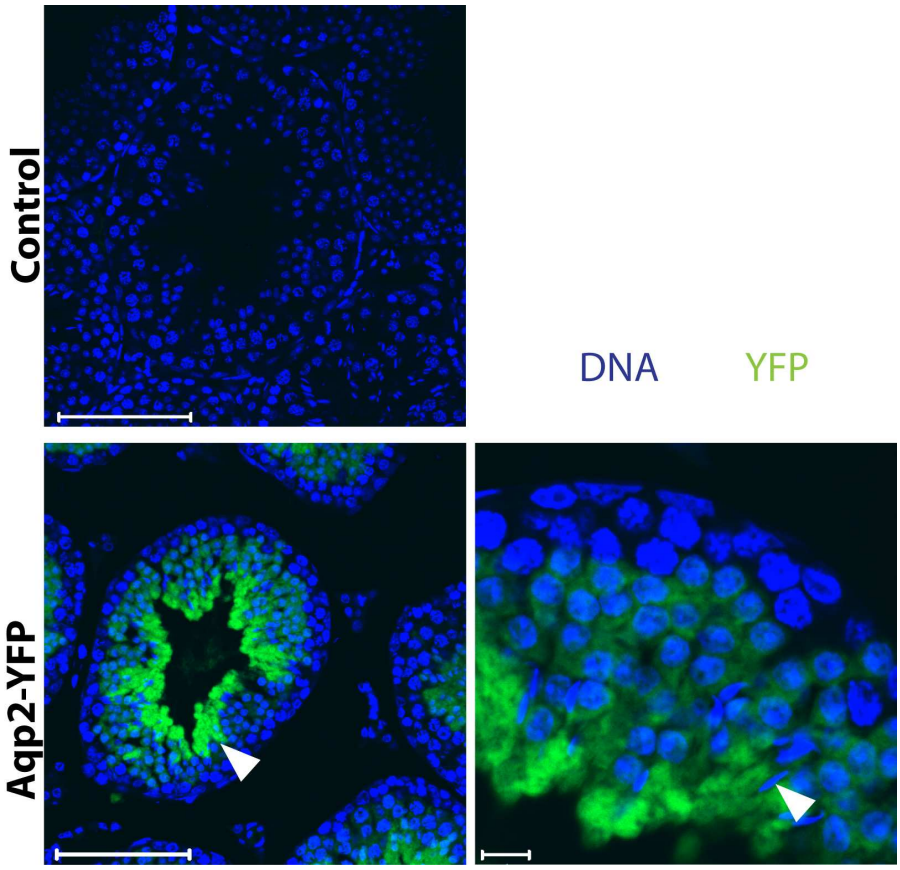

Figure 3-6: YFP immunolocalisation in cross-sections of d100 Aqp2-YFP testis

YFP is localised to the post-meiotic germ cells of the testis (arrowheads). No YFP staining is seen in testes of control littermates. Scale bars in left panels are 100µm for right panel is 10µm.

3.2.2.2 Analysing ablation of AR expression in the testis of an Aqp2-ARKO mouse line

AR immunostaining in a wild-type d100 testis revealed that elongating spermatids stained for AR with the antibody used in these studies (Figure 3-7). Aqp2-ARKO mice did not appear to be grossly different to controls in mean body weight (25.0 g control, 26.2 g Aqp2-ARKO) AGD (14.8 mm control, 15.6 mm Aqp2-ARKO) and testicular weight (64.3 mg control, 69.3 mg Aqp2-ARKO). However, whilst it was apparent that there was no phenotypic difference, low n numbers prohibited statistical analysis of these observations (n=3 mice for Aqp2-ARKO and n=1 for control). Aqp2-ARKO testes at d100 appeared similar to controls with normal spermatogenesis (Figure 3-8). Mature spermatozoa were present in the cauda epididymides of d100 controls and Aqp2-ARKO mice (Figure 3-8). Testes of d100 Aqp2-ARKO mice produced only wild-type full-length *Ar* transcript, and not the shorter transcript that results from Cre recombinase-mediated deletion of exon 2 (Figure 3-9).

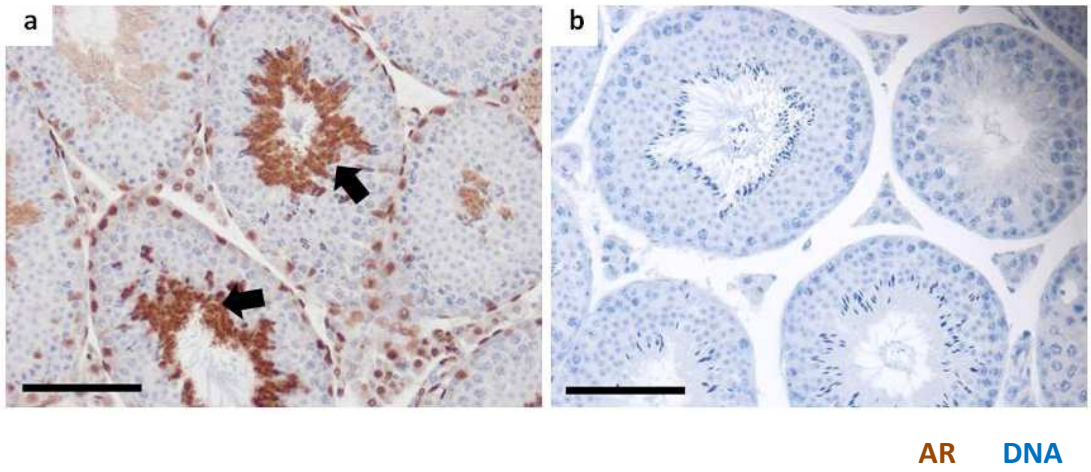

Figure 3-7: AR immunostaining in d100 control testis

(a*) Elongating spermatids of the testis show positive staining for androgen receptor (arrows). (b) No-primary control with no staining.*

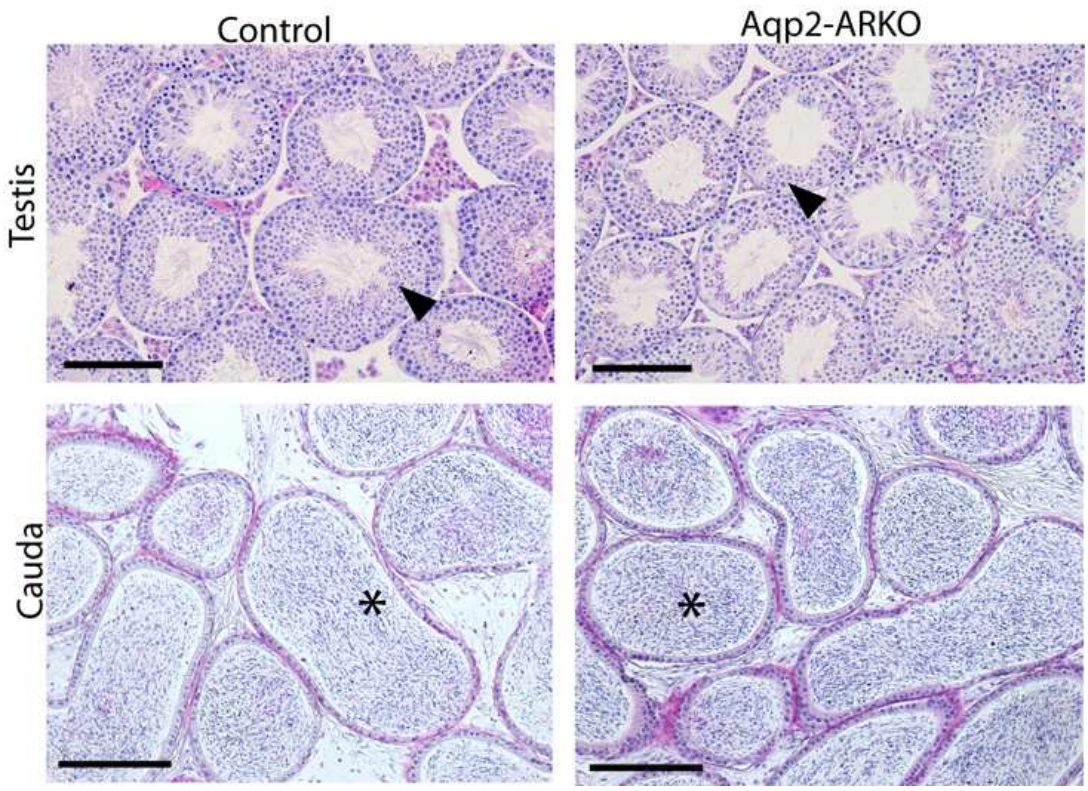

Figure 3-8: Histology of d100 control and Aqp2-ARKO testes and cauda epididymides

Histology of Aqp2-ARKO testes and cauda epididymides is similar to controls at d100. Scale bars are 200µm.

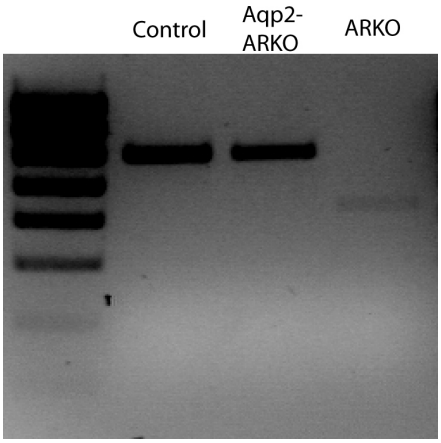

Figure 3-9: Presence of wild-type and/or Cre-recombined Ar transcript in d100 control and Aqp2-ARKO testis

RT-PCR on d100 control testis confirms all Ar transcripts are wild-type (upper band). d100 Aqp2-ARKO testis expresses only wild-type Ar transcripts. Total ARKO testis expresses only recombined AR (lower band).

3.2.3 Use of an AMH-Cre line to fluorescently label the Sertoli cells of the testis for subsequent isolation by FACS

3.2.3.1 Localisation of YFP in AMH-YFP testes

Whole mount visualisation of YFP in unfixed seminiferous tubules demonstrated that YFP is localised in hexagonal shaped cells, characteristic of Sertoli cell morphology (Figure 3-10a). When viewed in a more central plane the YFP appeared to 'project' into the centre of the tubule (Figure 3-10b). When embedded in paraffin, sectioned and stained with a GFP/YFP antibody, YFP staining was specific to the nucleus and cytoplasm of Sertoli cells of mice at d100 (Figure 3-11).

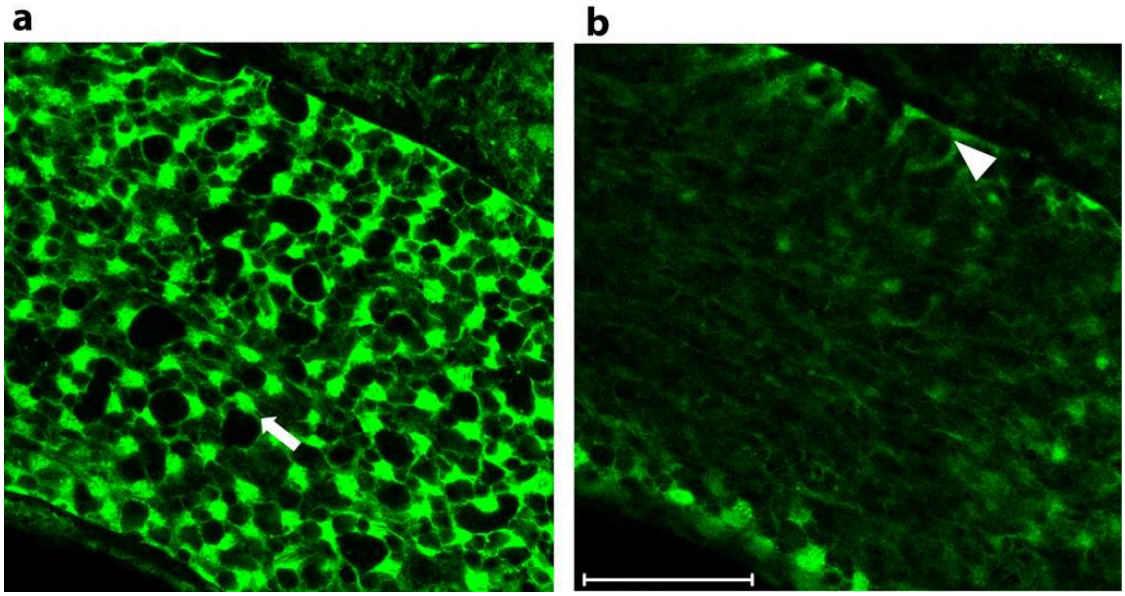

Figure 3-10: YFP localisation in whole seminiferous tubules of d100 AMH-YFP testes

(a) At the periphery of a seminiferous tubule, YFP is localised to the characteristic hexagonal-shaped basal aspects of Sertoli cells (arrow). (b) In a more central plane of a seminiferous tubule, YFP is localised to the Sertoli cell cytoplasm projecting into the centre of the tubule (arrowhead). Scale bar is 100µm.

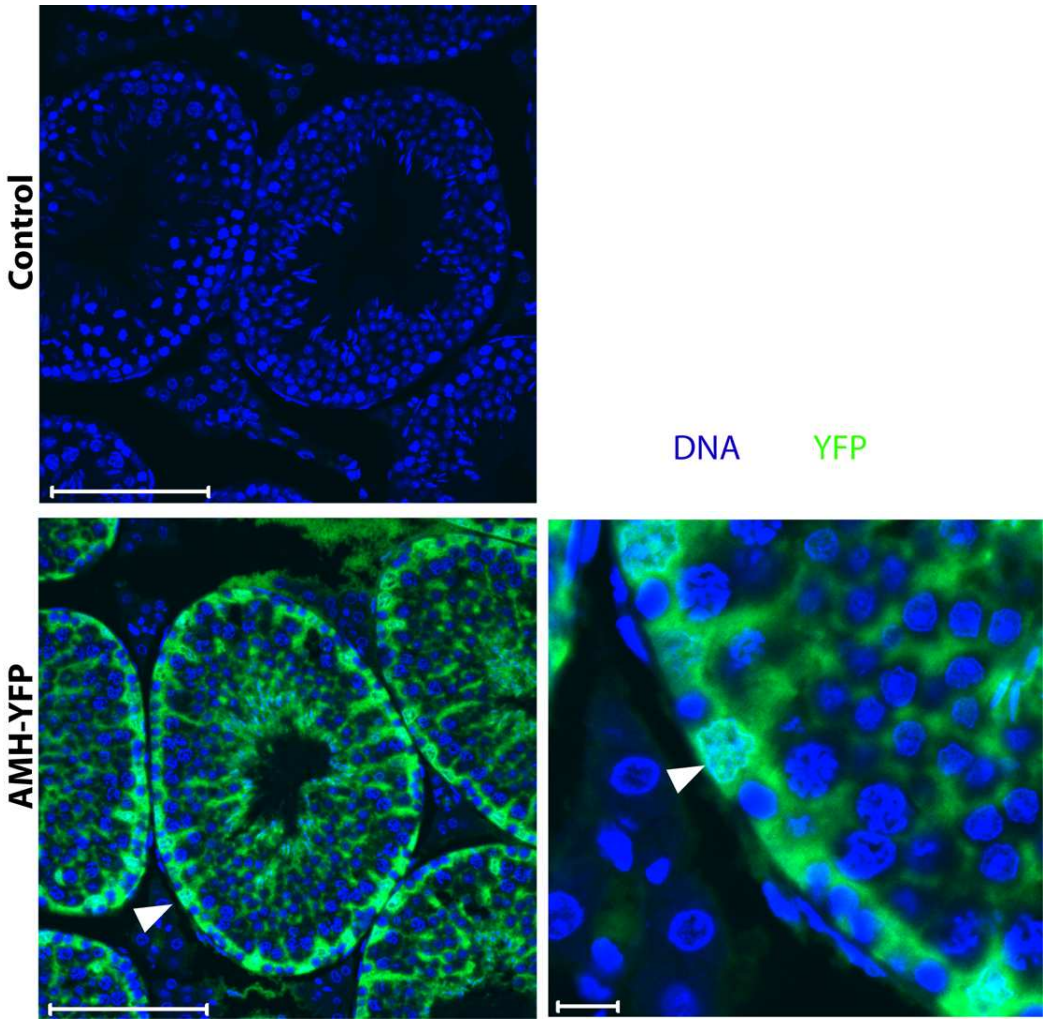

Figure 3-11: YFP localisation in cross-sections of seminiferous tubules of d100 AMH-YFP testes

No YFP staining is seen in testes of control littermates. Sertoli cells of AMH-YFP testes stain positive for YFP (arrowheads). Scale bars in left panels are 100µm, in right panel is 10µm

3.2.3.2 Isolation of a population of cells by FACS

AMH-YFP testes were distinguished from control littermates as they appeared to glow green under a dissecting microscope with a YFP-specific fluorescent filter, unlike control testes, which did not (Figure 3-12). Testes from two litters of mice, one at d15 and one at d21 were sorted into 4 groups, d15 AMH-YFP, d15 control, d22 AMH-YFP and d22 control based on their age and presence of YFP as established under a fluorescent scope.

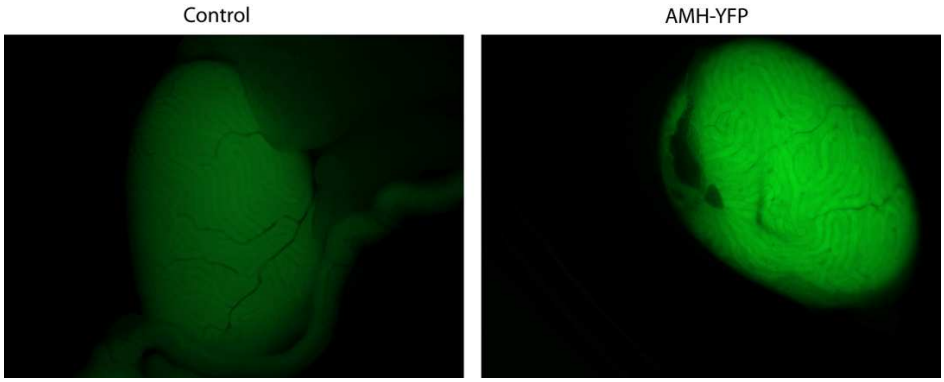

Figure 3-12: Distinguishing AMH-YFP testes from control testes using a dissecting microscope with fluorescent filter

When viewed under a dissecting microscope fitted with a fluorescent filter, AMH-YFP testes glow green as a result of YFP expression, whereas control testes do not.

Each group of testes was subjected to a combination of mechanical and enzymatic dissociation and subsequent sorting by FACS. Cells from both AMH-YFP and control testes were sorted into YFP+ and YFP- cell populations. 9.9 % of all events recorded by the FACS machine were classed as YFP+ cells using d15 AMH-YFP testes (Figure 3-13a), whereas 0% of all events were classed as YFP+ cells using d15 control testes (Figure 3-13b). 3% of all events recorded by the FACS machine were classed as YFP+ cells using d22 AMH-YFP testes (Figure 3-13c), whereas 0% of all events were classed as YFP+ cells using d22 control testes (Figure 3-13d).

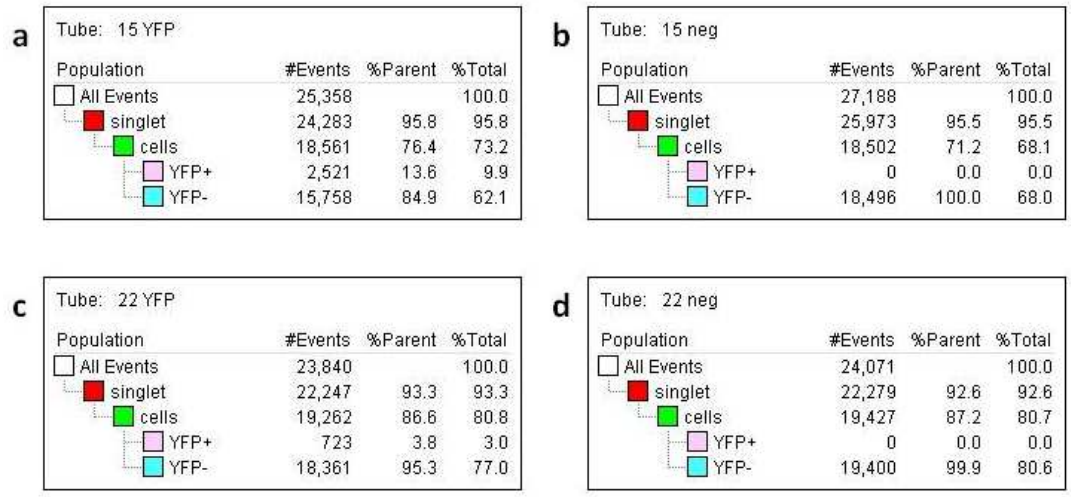

Figure 3-13: Numbers of cells generated by FACS on AMH-YFP and control testes at d15 and d22

The 'singlet' and 'cells' functions use size and shape algorithms to ensure only single whole cells are sorted. Fluorescence algorithms are then used to sort single whole cells into YFP+ and YFP- groups.

Cells from YFP+ and YFP- cell populations of AMH-YFP testes at both d15 and d22 were frozen and subjected to RNA extraction, reverse transcription and PCR for testicular cell type markers. P27/kip localisation is specific to Sertoli cells in the testis (Figure 3-14a). RT-PCR revealed that *Cdknb1* (the p27/kip transcript) was present in both the YFP+ and YFP- cell populations from both d15 and d22 testes, indicating that Sertoli cells were present in both YFP+ and YFP- cell populations from both ages (Figure 3-14b). Mouse Vasa homolog (MVH) localisation is specific to germ cells in the testis (Figure 3-15a). RT-PCR revealed that *Ddx4* (the MVH transcript) was present in both YFP+ and YFP- cell populations from both d15 and d22 testes, although expression was weaker in d15 YFP+ population (Figure 3-15b). This indicated that germ cells were present in both YFP+ and YFP- cell populations from both ages, but potentially fewer were present in the d15 YFP sample. SMA localisation is specific to PTM and vascular smooth muscle cells in the testis (Figure 3-16a). RT-PCR revealed that *Acta2* (the SMA transcript) was present in both the YFP+ and YFP- cell populations from both d15 and d22 testes, although expression was much weaker in the YFP+ cell populations when compared to the YFP- cell

populations at both ages (Figure 3-16b). This indicated that PTM cells were present in YFP+ cell populations at a much lower level than in YFP- cell populations. 3βHSD1 localisation is specific to Leydig cells in the testis (Figure 3-17a). RT-PCR revealed that *Hsd13b* (the 3βHSD1 transcript) was present in YFP- cell populations from both d15 and d22 testes but was not seen in YFP+ cell populations at either age (Figure 3-17b). This indicated that Leydig cells were only present in YFP- cell populations and not YFP+ cell populations.

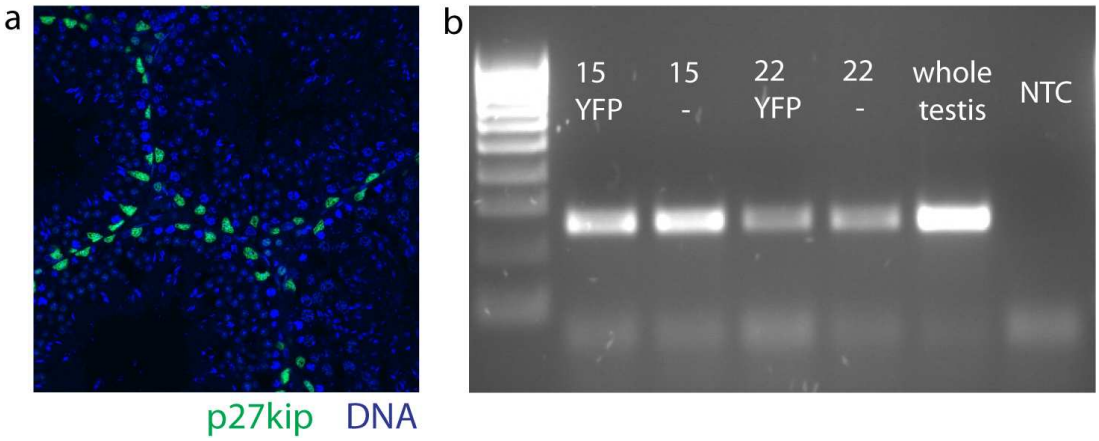

Figure 3-14: Presence of Cdkn1b transcript in YFP+ and YFP- FACS samples

(a) p27kip localisation is specific to Sertoli cells in the testis (b) Cdkn1b (the p27kip transcript) was present in both the YFP+ and YFP- cell populations from both d15 and d22 testes

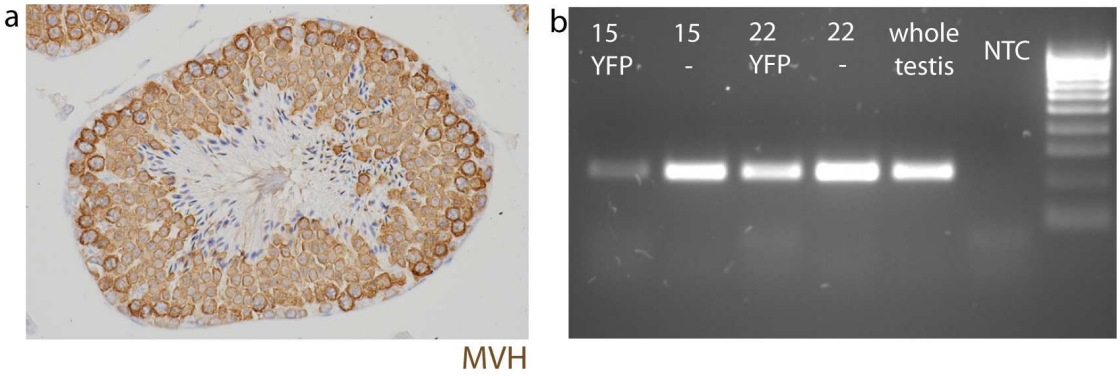

Figure 3-15: Presence of Ddx4 transcript in YFP+ and YFP- FACS samples

(a) MVH localisation is specific to germ cells in the testis. (b) Ddx4 (the MVH transcript) was present in both YFP+ and YFP- cell populations from both d15 and d22 testes, although expression was weaker in d15 YFP+ population.

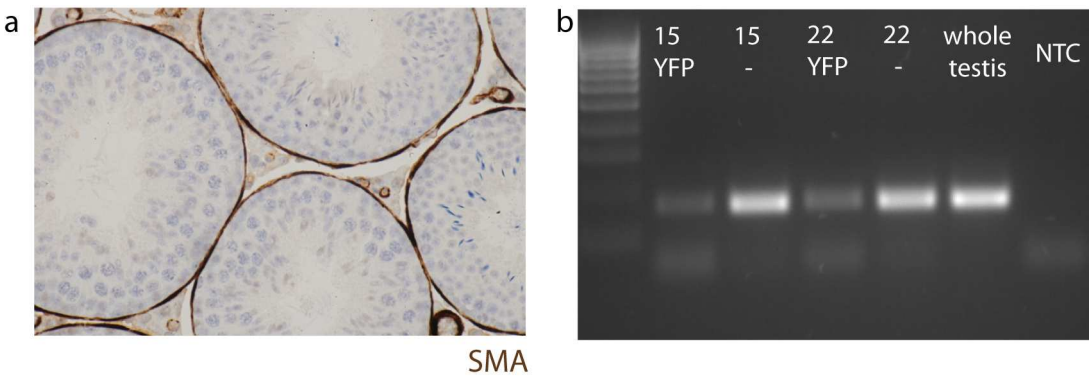

Figure 3-16: Presence of Acta2 transcript in YFP+ and YFP- FACS samples

(a) SMA localisation is specific to PTM and vascular smooth muscle cells in the testis. (b) Acta2 (the SMA transcript) was present in both the YFP+ and YFP- cell populations from both d15 and d22 testes, although expression was much weaker in the YFP+ cell populations when compared to the YFP- cell populations at both ages.

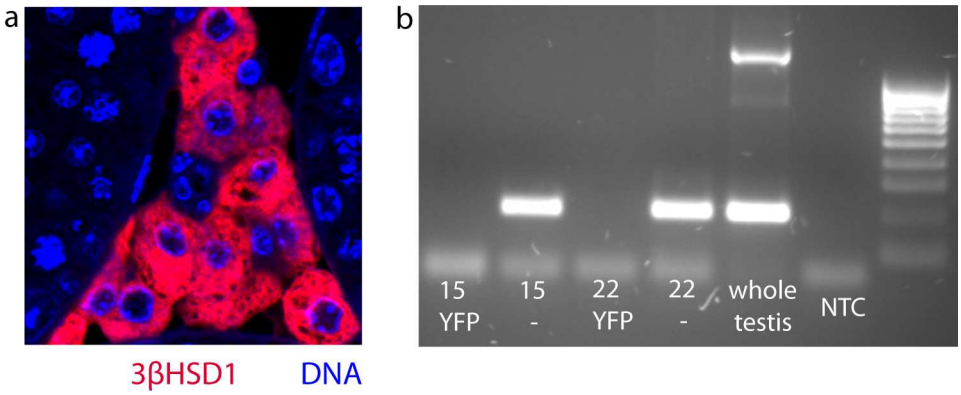

Figure 3-17: Presence of Hsd3b1 transcript in YFP+ and YFP- FACS samples

(a) 3βHSD1 localisation is specific to Leydig cells in the testis (b) Hsd3b1 (the 3βHSD1 transcript) was present in YFP- cell populations from both d15 and d22 testes but was not seen in YFP+ cell populations at either age.

3.3 Discussion

The aims of this chapter were to characterise the expression of both post-meiotic germ cell and endothelial cell-specific Cre lines using fluorescent reporters and use them to ablate AR in these cell types, and also to investigate the possibility of using FACS to sort Sertoli cells from testes expressing a Sertoli cells-specific fluorescent reporter.

The Tie2-Cre line was shown for the first time to be active in vascular and interstitial endothelial cells of the testis, based on the expression of a YFP reporter gene in Tie2-YFP mice. Vascular endothelial expression of the Tie2-Cre in several organs is well documented (Constien et al., 2001; Kisanuki et al., 2001), but its expression in both the vascular and interstitial endothelial cells is a novel finding. Based on these results, the Tie2-Cre line would be suitable for generating mice with testicular vascular and interstitial endothelial cell-specific ablation of a gene of interest by mating to a mouse line with a knock-in of a floxed version of that gene. Tie2-Cre was used to ablate AR in these cell types by mating to an AR^{flox} line. Testes from Tie2-ARKO mice have a phenotype similar to testes from control littermates, with a normal testicular histology including complete spermatogenesis and the presence of morphologically mature spermatozoa in the cauda epididymis. There is no Cre-recombined exon 2 band present in the RT-PCR of Tie2-ARKO testes. PCR on genomic DNA demonstrates that Cre has recombined *Ar* in the genome of the endothelial cells, but the endothelial cells do not express *Ar* so a recombined transcript is not seen. These results show that Tie2-Cre is effective at ablating the AR by recombination, but that the testicular endothelial cells do not express AR, which confirms reports in published literature (Vornberger et al., 1994). Since there is evidence in the literature that prostate vascular endothelial cells express AR (Godoy et al., 2008; Pelletier et al., 2000), then examination of the prostates of the Tie2-ARKO line could provide further information about the function of prostate vascular endothelial AR. As shown in Figure 3-1, vascular smooth muscle cells express AR, and when AR is ablated from this cell type using Cre-loxP, slight compensatory Leydig cell failure and a defect in testicular fluid exchange results, demonstrating

that AR action in vascular smooth muscle cells may locally regulated microvascular blood flow within the testis (Welsh et. al, 2010b).

The Aqp2-Cre line was shown for the first time to be active in post-meiotic germ cells based on the expression of a YFP reporter gene in Aqp2-YFP mice. This corroborates with the expression of endogenous Aqp2 (Nelson et al., 1998). Based on these results, the Aqp2-Cre line would be suitable for generating mice with post-meiotic germ cell ablation of a gene of interest by mating to a mouse line with a knock-in of a floxed version of that gene. Aqp2-Cre was used to ablate AR in post-meiotic germ cells by mating to an AR^{flox} line. Testes from Aqp2-ARKO mice have a phenotype similar to testes from control littermates, with a normal testicular histology including complete spermatogenesis and the presence of morphologically mature spermatozoa in the cauda epididymis. There is no Cre-recombined exon 2 band present in the RT-PCR of Aqp2-ARKO testes. Based on these results, either Cre has recombined AR in the genome of the post-meiotic germ cells, but they do not express AR so a recombined transcript is not seen, or post-meiotic germ cells do express AR but Cre ablation has not occurred at the genomic level which is why a recombined transcript is not seen. The way to definitively differentiate between these two possibilities would be to do a PCR across exon 2 of the genomic DNA rather than cDNA, as was performed on the Tie2-ARKO. In agreement with the hypothesis that germ cells do not express AR (O'Donnell et al., 2006), it is more likely that the Aqp2-Cre is effective at ablating the AR by recombination, but that post-meiotic germ cells do not express AR and that the elongating spermatid staining seen both in some areas of the literature with the AR antibody used in this study is non-specific staining (Vornberger et al., 1994).

Obtaining a fast, pure population of Sertoli cells by FAC-sorting cells from AMH-YFP testes shows promise, but the protocol needs to be further refined to ensure high purity. Based on analysis of cell-specific marker expression by RT-PCR, populations of YFP positive cells obtained from AMH-YFP testes have no Leydig cell contamination and very little PTM cell contamination at either d15 or d22. At both

ages, however, there is significant germ cell contamination. Experimentation with different protease enzymes and length and temperature of their digesting steps could potentially increase the dissociation of germ cells from Sertoli cells and therefore increase the purity of the cell population. Currently the protocol as it stands does not offer any advantages over other fast methods of isolating Sertoli cells. Mechanical dissociation and enzymatic digestion of neonatal rat testes followed by plating on *D. stramonium* lectin coated plates results in a population determined to be 95% Sertoli, 4% PTM and 1% Leydig cell with no germ cell contamination (Scarpino et al., 1998). However, a pure population of Sertoli cells is difficult to achieve when adult testes are used, and a combination of mechanical dissociation and enzymatic digestion on adult rat testes yields a population of cells that is determined to be 80% Sertoli cell, 10% germ cell and 10% PTM cell (Anway et al., 2003). It is likely that the germ cell contamination will be the most difficult to eliminate when attempting to isolate Sertoli cells from adult testes, due to the many diverse junction complexes that exist between the two cell types (Mruk and Cheng, 2004). If suitable Cre lines can be chosen then FACS isolation could be used to a greater effect for Leydig cell populations of the adult testis. As the cells are interstitial then seminiferous tubules would not need to be mechanically dissociated and a mild enzymatic treatment of a decapsulated testis would potentially be enough to release interstitial cells into a single-cell suspension. The maturation of adult Leydig cells proceeds through several precursor stages, each of which expresses a specific transcriptome (Chen et al., 2009a). Use of an appropriate Cre line could label one of these populations and allow for their isolation from the other Leydig cell populations and subsequent culture.

4. Characterisation of the testicular phenotype of the FoxG1-ARKO mouse

4.1 Introduction

The Cre/*loxP* transgenic system of cell-specific genetic ablation (section 1.1.2) has been an important tool in elucidating the action of androgen receptor (AR) within the male reproductive system. The Sertoli-cell androgen receptor knock-out (SCARKO) mouse line is a well-characterised model of cell-specific AR ablation using the Cre-lox system (Chang et al., 2004; De Gendt et al., 2004). Cre is driven by the AMH promoter, specific to Sertoli cells in the male during embryonic life. AR^{flox} mice are transgenically modified so that exon 2 of each copy of the *Ar* gene is flanked by *loxP* sites (De Gendt et al., 2004). Half of the male offspring from matings between AMH-Cre males and AR^{flox} females are SCARKO mice. Two separate groups have characterised the SCARKO model and although both report the mice to be infertile, with an absence of post-meiotic spermatocytes and spermatids, there is conflicting evidence as to whether SCARKO mice have a change in serum hormone levels. However, the De Gendt group report that the seminal vesicle weight of the SCARKO is similar to the controls (De Gendt et al., 2004), and the Chang group report there was no difference in most of the genitourinary organs' (Chang et al., 2004) between SCARKO and controls, suggesting that systemic testosterone levels are unchanged.

Expression of the AMH-Cre transgene in Sertoli cells occurs at e15 (Lecureuil et al., 2002) before AR is widely expressed in Sertoli cells at d5 (Willems et al.). The SCARKO model recombines genomic AR before transcription and translation has begun in embryonic Sertoli cells. Hence, the Sertoli cells in SCARKO mice never express functional AR protein and spermatocytes arrest at the beginning of meiosis. This prevents the elucidation of the action of AR *via* Sertoli cells on post-meiotic spermatids. Rodent models with a systemic decrease in testosterone levels demonstrate several problems with round spermatid adhesion and spermiation (Holdcraft and Braun, 2004; O'Donnell et al., 1996; Saito et al., 2000), and it would be interesting to discover whether spermatid maturation and spermiation are

mediated by Sertoli cell AR signalling. This could be achieved with the generation of an 'adult SCARKO' where the Sertoli cell-specific promoter is activated after mature spermatozoa are produced and the testicular phenotype is analysed shortly afterwards, thus allowing the effect of Sertoli cell-specific AR ablation on post-meiotic germ cells to be elucidated.

Establishment and analysis of a conditional gene ablation model requires a well-characterised Cre-line and thorough analysis of any resulting phenotype. In order to generate an adult SCARKO model, the Cre line used would have to be driven by a Sertoli-cell specific promoter so AR ablation would also be Sertoli-cell specific. It also needs to be expressed post-pubertally so Sertoli cells express AR for some time before it is ablated. Then, the Cre line should be fully tested using a fluorescent reporter to assess the penetrance of the Cre expression in the target cell population, as well as identifying the possibility of non-specific Cre expression in other cell types. The Cre line of interest can then be mated to the AR^{flox} mouse line and the resulting ablation of AR assessed using cell and molecular biology techniques. Finally, if an infertility phenotype has resulted from the knock-out, differences between the knock-out and the control must be characterised. Parameters to look at when assessing testis function and determining infertility include serum and intra-testicular hormone measurements, histological assessment of the testes and reproductive tract, and immunochemistry and quantitative RT-PCR for genes of interest that may be altered in the mutant line.

Preliminary data from the Smith group had suggested that FoxG1-Cre would be a good Cre line to use to generate an adult SCARKO model. FoxG1 is primarily characterised in the development of the cerebral hemispheres (Xuan et al., 1995), but FoxG1 transcript has also previously been identified in the testis of humans, but not rodents (Obendorf et al., 2007). Despite this finding, preliminary immunohistochemistry on adult wild-type mouse testis showed FoxG1 was localised to all Sertoli cells. With preliminary expression data and the FoxG1-Cre line available for use, the aim was to utilise it to create an adult SCARKO line.

4.1.1 Aims

- To analyse the pattern of expression of FoxG1 in the testis and determine its suitability for producing mice with an adult-onset Sertoli cell-specific knock-out of AR
- To generate 'FoxG1-ARKO' mice with an adult-onset Sertoli cell-specific knock-out of AR
- To analyse any resulting reproductive phenotype of these mice

4.2 Results

4.2.1 FoxG1 localisation in the embryonic and post-natal testis

To assess the localisation of FoxG1 during development of the testes, immunohistochemistry using FoxG1 antibody was performed at several developmental time-points (Figure 4-1). FoxG1 protein was present in the testis from e12.5, but was not consistently present in one particular testicular cell type during development. At e12.5 to e13.5 FoxG1 protein was observed in the somatic cells of the developing testis cords. Localisation was then seen to switch to a sub-population of interstitial cells starting at e15.5 until d2. FoxG1+ interstitial cells were also 3βHSD1+, demonstrating that they were fetal Leydig cells, but not all 3βHSD1+ cells were FoxG1+. One theory to explain this interesting staining pattern is that FoxG1 is transiently expressed in all fetal Leydig cells but not at the same time in all cells, another is that there is a sub-population of fetal Leydig cells that express FoxG1 and a sub-population that do not. By d12, FoxG1 was localised in the somatic cells of the seminiferous tubules, which at this age are morphologically identifiable as Sertoli cells. FoxG1 also continued to be localised to some interstitial cells. Expression was restricted to the nucleus rather than being both nuclear and cytoplasmic as it was in other cell types. FoxG1 continued to be localised in this pattern when assessed at d100. FoxG1 did not localise to the germ cells of the testis cords at any time-point observed.

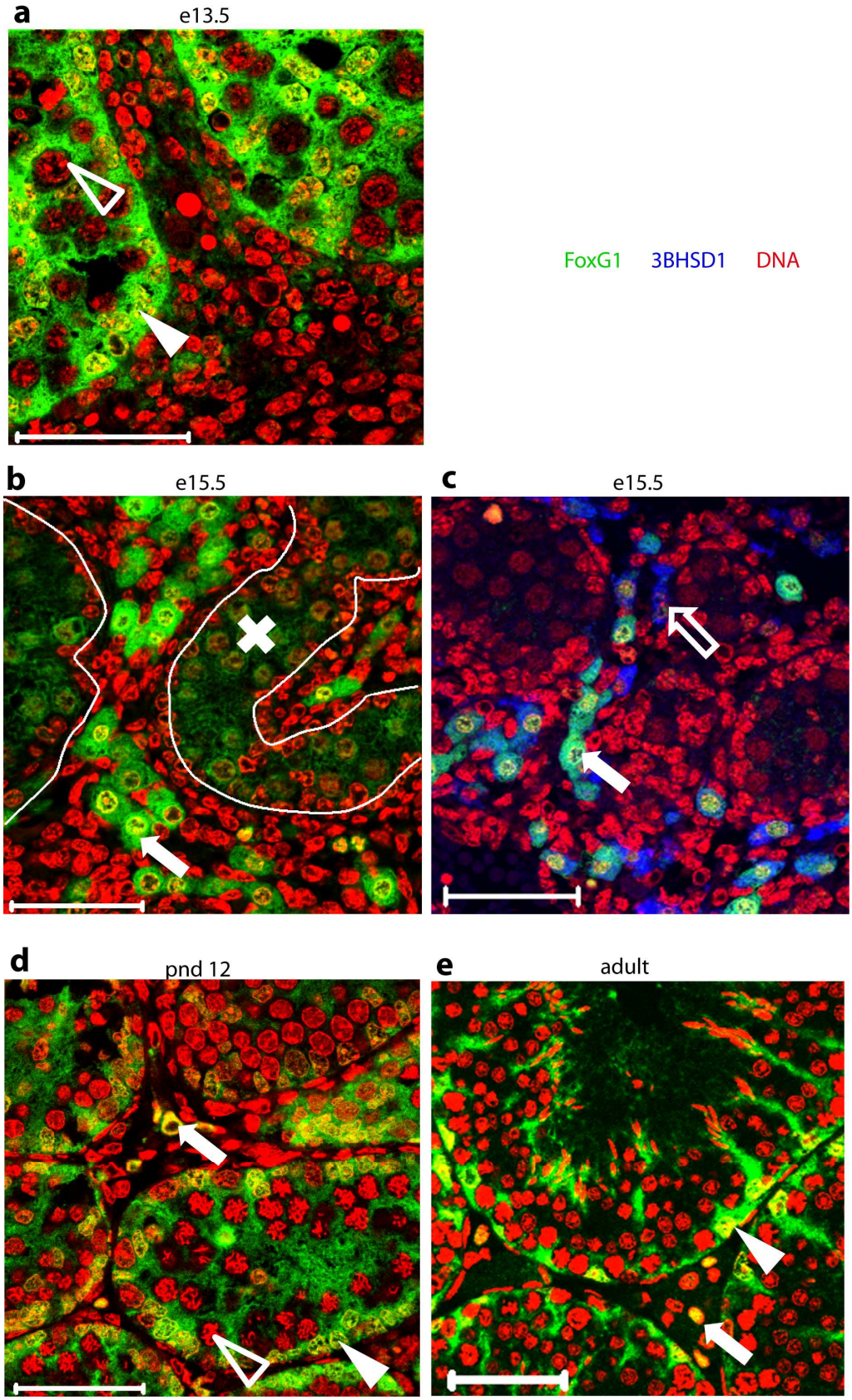

Figure 4-1: FoxG1 expression in pre and post-natal wild-type mouse testis

Figure 4-1: FoxG1 expression in pre and post-natal wild-type mouse testis (figure on preceding page)

(a): At e13.5 FoxG1 protein is localised to nucleus and cytoplasm of somatic cells of developing testis cords (solid arrowhead). FoxG1 does not localise to germ cells of testis cords (outline arrowhead). (b): By e15.5 FoxG1 staining is almost absent from testis cords (outlined in white and marked with an X), but staining is strong in nucleus and cytoplasm of a population of interstitial cells (arrow). This staining pattern is also seen at e17.5 and d2. (c): At e15.5 all FoxG1 positive cells stain positive for 3β HSD1 (solid arrow), but there is also a population of 3beta HSD1 positive cells that do not stain positive for FoxG1. (d): By d12, nucleus and cytoplasm of all Sertoli cells stain positive FoxG1 (solid arrowhead), and nuclei of some interstitial cells stain positive for FoxG1 (solid arrow). Germ cells do not stain for FoxG1 (outline arrowhead). (e)This pattern is persistent at d100. Scale bars are 50μm.

4.2.2 FoxG1-Cre stud males are fertile and do not display a reproductive phenotype

The FoxG1-Cre mouse line contains a knock-in of Cre recombinase at one of the FoxG1 loci, resulting in haploinsufficiency of FoxG1. Previous literature has stated that haploinsufficiency of another Fox gene, FoxA3 has resulted in a testicular phenotype (Behr et al., 2007). To confirm that the loss of one allele of FoxG1 did not induce a reproductive phenotype, reproductive tissues were examined from aged males carrying the FoxG1-Cre transgene but no floxed AR. The testes of all FoxG1-Cre males had no degeneration of the seminiferous epithelium and visually normal spermatogenesis, and were fertile with mature sperm in their cauda epididymis (Figure 4-2). That FoxG1-Cre males were used as studs to sire FoxG1-ARKO and FoxG1-YFP litters was further evidence that their reproductive function was not impaired.

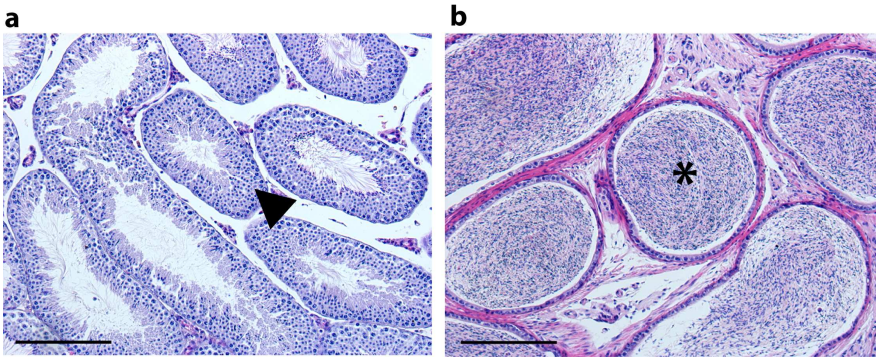

Figure 4-2: Phenotype of FoxG1-Cre mice compared to FoxG1-ARKO and control.
(a): d100 FoxG1-Cre mice have normal spermatogenesis (arrowhead) and no degeneration of the seminiferous epithelium. (b): d100 FoxG1-Cre mice have spermatozoa in the lumen of the cauda epididymis. Both (a) and (b) are stained with H&E. Scale bars are 200 µm.

4.2.3 Determining site of action of Cre recombinase in FoxG1-Cre testes

Testes from d100 FoxG1-YFP mice appeared fluorescent when viewed under a microscope with a YFP filter (Figure 4-3), with foci of YFP fluorescence in short lengths of tubules (Figure 4-3, arrow) as well as a fainter dispersed fluorescence throughout the tissue. To determine the localisation of this fluorescence, immunohistochemistry using a GFP/YFP antibody was performed on thin sections of FoxG1-YFP and control testes. This revealed that YFP expression in FoxG1-YFP testes was not localised to any one cell type (Figure 4-4). YFP was localised in some Sertoli cells, clusters of germ cells and some interstitial cells. Staining was heterogeneous and some tubule cross sections did not express YFP in any cell types. The pattern of YFP expression observed in these mice was not analogous to either endogenous FoxG1 expression (in which expression is seen in all Sertoli and some Leydig cells, see Figure 4-1), or YFP expression in an AMH-YFP mouse (in which expression is seen in all Sertoli cells, Figure 4-4).

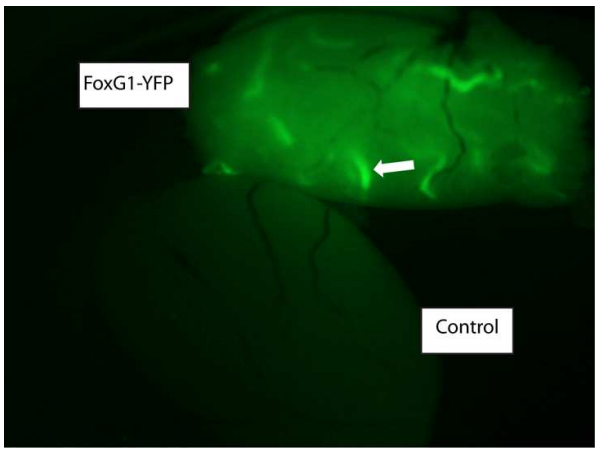

Figure 4-3: d100 FoxG1-YFP and control testes viewed under a fluorescent filter

FoxG1-YFP testes show foci of YFP fluorescence in short lengths of tubules (arrow) as well as a fainter dispersed fluorescence throughout the tissue. Control testis (below) is not fluorescent.

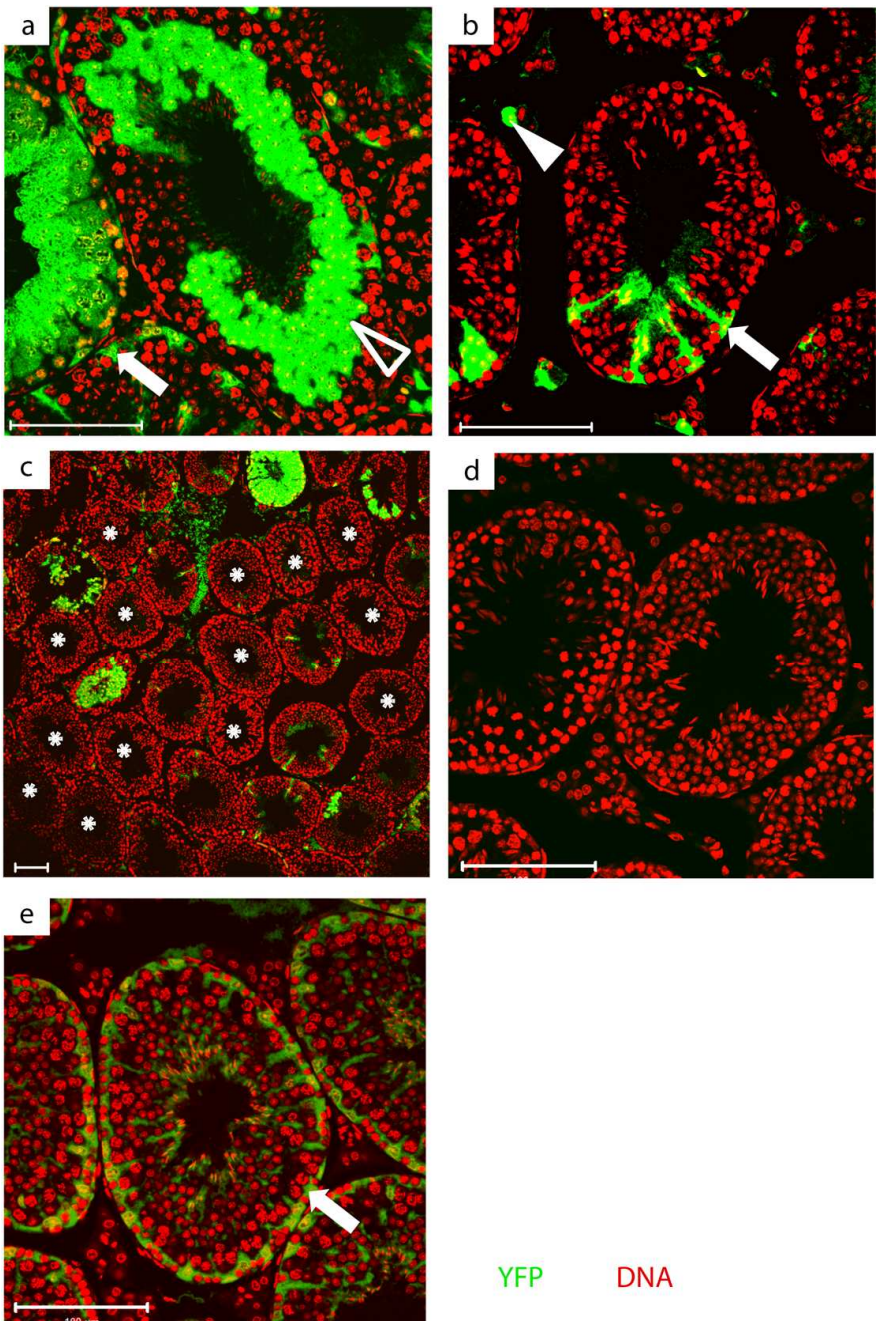

Figure 4-4: Localisation of YFP in FoxG1-YFP testes compared to AMH-YFP testes

(a) In d100 FoxG1-YFP testes, YFP is localised to some Sertoli cells (arrow) and also clusters of germ cells (outline arrowhead). (b) YFP is localised to some Sertoli cells (arrow) and some interstitial cells (solid arrowhead). (c) Staining is heterogeneous and some tubule cross-sections do not express YFP in any cell types (asterisks) (d) Testes from control littermates do not stain for YFP. (e) AMH-YFP mice express YFP in all Sertoli cells of the testis (arrow).Scale bars are all 100µm.

4.2.4 Testis phenotype of FoxG1-ARKO mice

FoxG1-ARKO mice were generated as described in materials and methods. As the original plan was to ablate AR in the adult testes, this was the first organ to be analysed. d100 testes were the first to be examined. Testes from d100 FoxG1-ARKO mice appeared visibly smaller than control testes during necroscopy, but all other reproductive tissues appeared similar to controls. Mean testis weight of FoxG1 mice was significantly reduced compared to controls at d100 (107.5 ± 3.9 mg control, 86.8 ± 5.8 mg FoxG1-ARKO, $P \leq 0.01$, Figure 4-5).

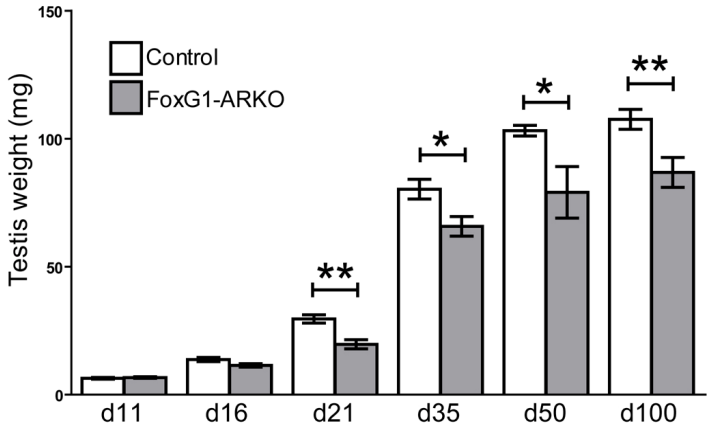

Figure 4-5: Mean weight of testes from control and FoxG1-ARKO mice measured at selected post-natal ages

*Mean weights of testes from FoxG1-ARKO mice are not significantly different to controls at d11 and d16. At d21, d35, d50 and d100, FoxG1-ARKO mice have significantly smaller testes compared to controls. n≥5 for each group. * P≤0.05, ** P≤0.01. All values are means ± SEM.*

When examined histologically, control testes appeared normal, with all stages of spermatogenesis present within a functioning seminiferous epithelium. By contrast, FoxG1-ARKO testes displayed tubules that had lost germ cells, appeared to have a lumen of increased diameter and the seminiferous epithelium of some tubules was almost completely atrophic (Figure 4-6). In control animals, the rete testis was normal and lacked spermatozoa as expected, compared to the FoxG1-ARKO rete which was distended and contained spermatozoa and pieces of sloughed seminiferous epithelium (Figure 4-6).

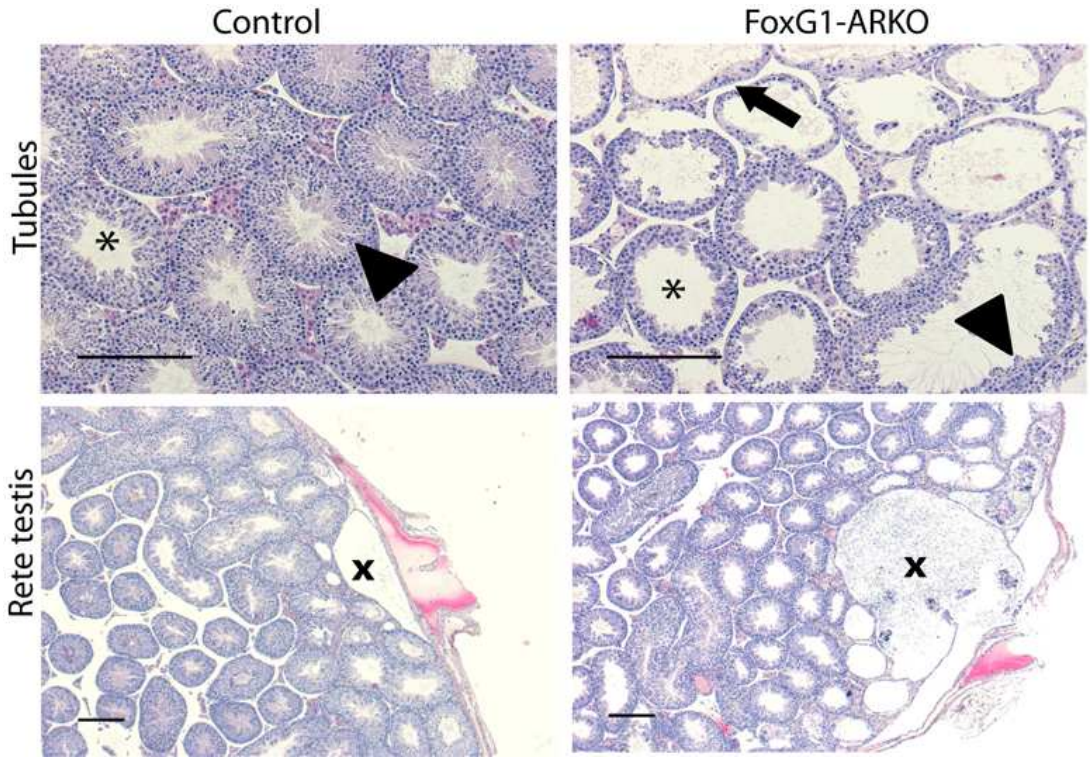

Figure 4-6: Histology of testes from control and FoxG1-ARKO mice at d100

At d100, all tubule cross-sections in the control appear to have a functioning seminiferous epithelium (arrowhead) and a lumen (asterisk). In the FoxG1-ARKO the tubule lumens appear bigger (asterisk), and although some areas of the seminiferous epithelium show normal spermatogenesis (arrowhead), others appear to be missing germ cells (arrow). In the control, the rete testis is small and empty of sperm (cross) compared to the FoxG1-ARKO rete which is distended and contains spermatozoa and pieces of sloughed seminiferous epithelium (cross).Scale bars are 200 µm.

Mean seminiferous tubule radius is significantly decreased in FoxG1-ARKO testes compared to control testes (106 µm control, 96 µm FoxG1-ARKO, $P \leq 0.05$, Figure 4-7a) and mean lumen diameter is significantly increased (38 µm control, 51 µm FoxG1-ARKO, $P \leq 0.001$, Figure 4-7a).

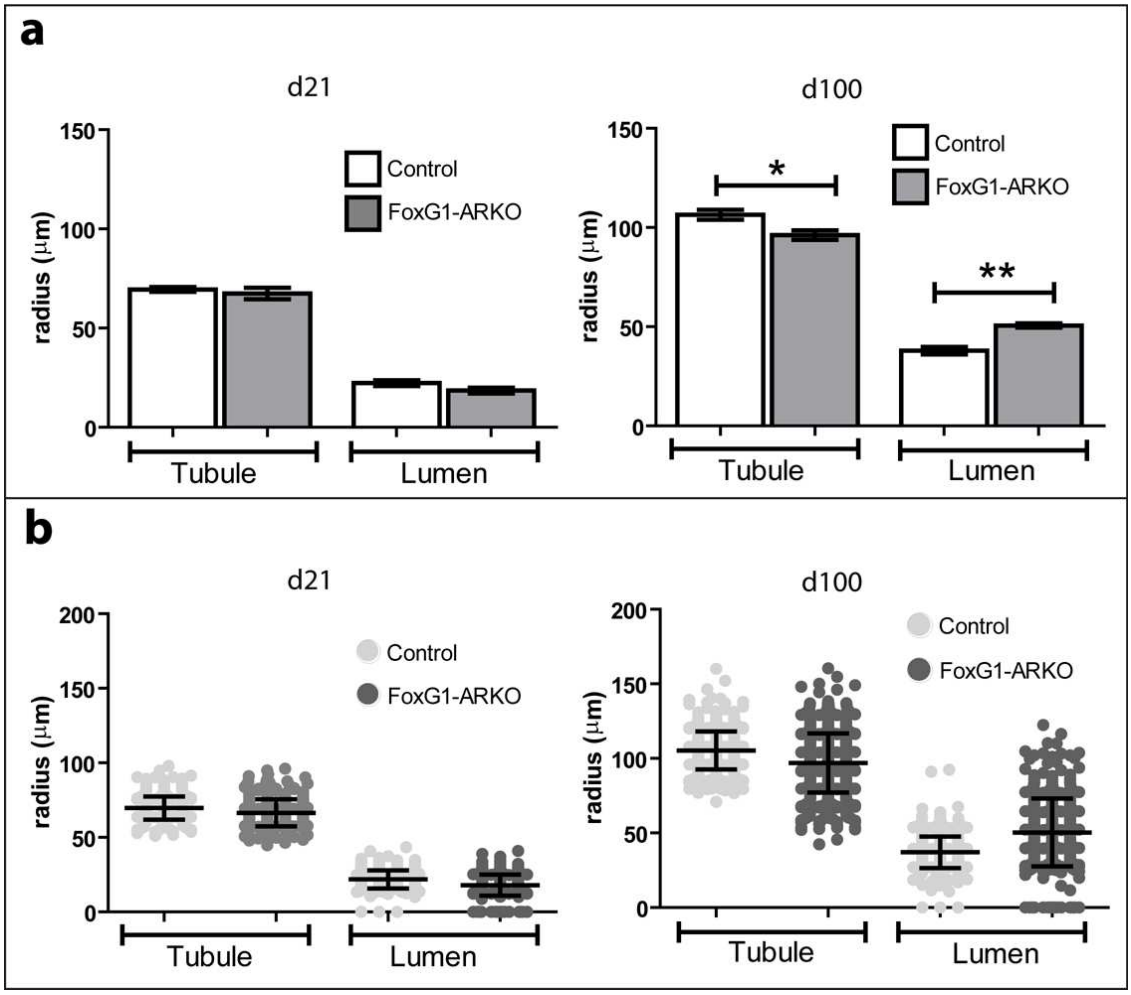

Figure 4-7: Radii of seminiferous tubule and tubule lumen cross-sections from d21 and d100 control and FoxG1-ARKO testes

*(a) At d21, FoxG1-ARKO mean seminiferous tubule radius and mean tubule lumen radius are not significantly different to controls, but at d100 FoxG1-ARKO tubules have a significantly smaller mean radius than controls but a significantly larger mean lumen radius. Values are means of 5 samples for each group consisting of the mean of 100 tubule/lumen radii measured per sample ± SEM. (b) Graphs represented as scatter plots, so all tubule lumen/radius measurements for each of the 5 samples in each group can be observed. Error bars are standard deviations. Note that at d100 the spread of data is much larger in FoxG1-ARKO tubule and lumen measurements. n=5 mice, ~100 tubule measurements from each. *P≤0.05, **P≤0.01.*

This data demonstrates that seminiferous tubules are not distended in the FoxG1-ARKO as appears in histological section and in fact are smaller. This can be explained by the presence of completely atrophied tubules that no longer appear circular in cross section but are flattened due to the loss of tubule structure after atrophy. The increase in tubule lumen diameter could imply that the seminiferous tubules are distended but because the tubule diameter itself is not also increased it is more likely to be explained by a loss of germ cells from the seminiferous epithelium, perhaps by sloughing. The standard deviations of both individual tubule radius (12.8 µm control, 19.8 µm FoxG1-ARKO) and lumen radius (10.7 µm control, 22.8 µm FoxG1-ARKO) measurements is larger for the FoxG1-ARKO data than the control data, implying that variation in FoxG1 ARKO tubules is greater (Figure 4-7b). This can be explained in tandem with the histological observations as normal, sloughed (normal tubule radius but larger lumen radius) and atrophied (reduced tubule and lumen radius 'collapsed' appearance) tubule cross sections can all be seen in the same FoxG1-ARKO testis thin-sections. Similar to the SCARKO mouse phenotype, there is also a reduction in weight compared to controls, but the histology of the phenotype is very different. The SCARKO mouse has a post-meiotic germ cell block (De Gendt et al., 2004), whereas the FoxG1-ARKO has all stages of spermatogenesis present, but sloughing of the seminiferous epithelium. With the aim to document the progression of this phenotype, weighing and histological analysis was performed on the testes at the selected post-natal ages of d2, d11, d16, d21, d35.

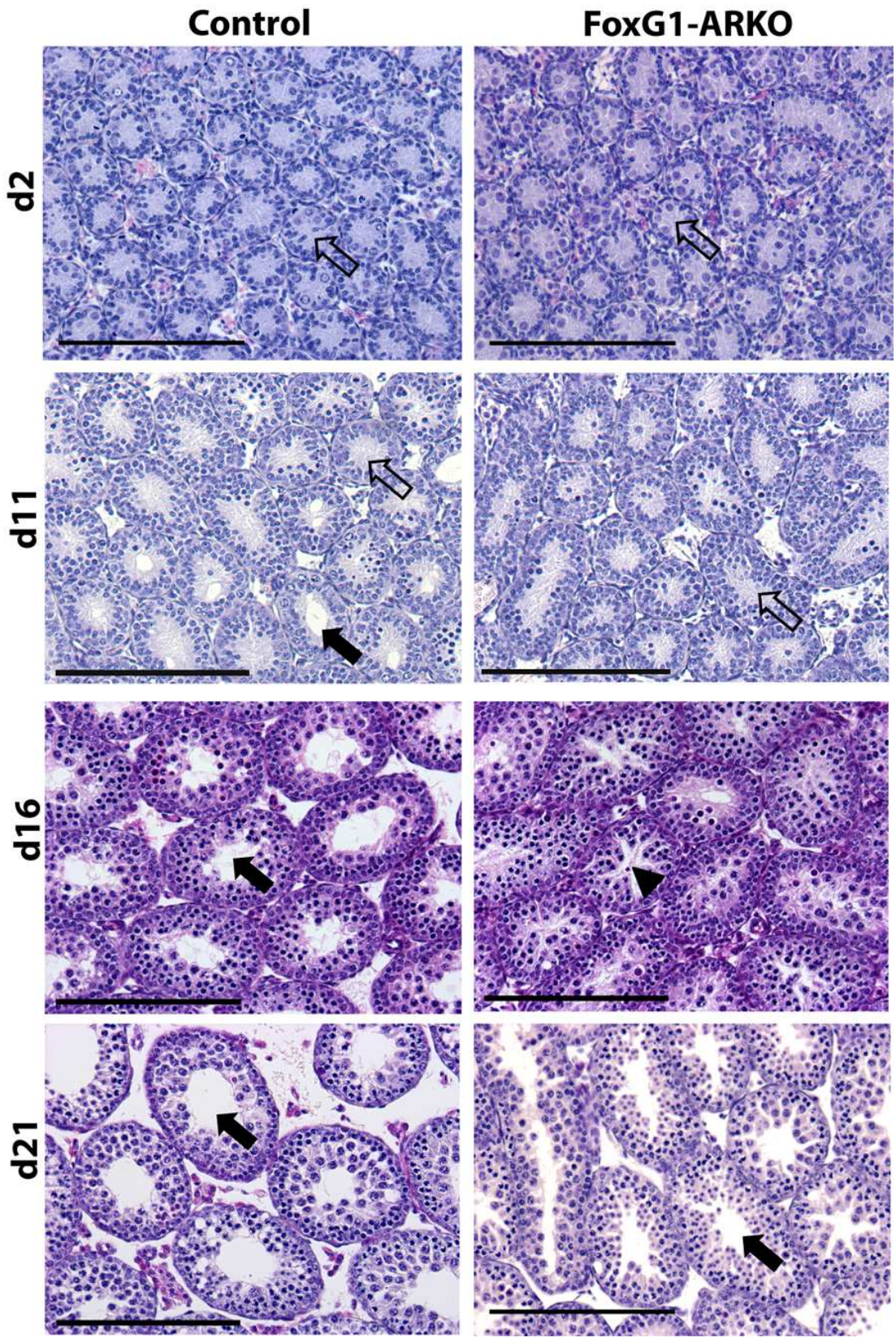

Figure 4-8: Histology of testes from control and FoxG1-ARKO mice at selected post-natal ages to d21

Figure 4-8: Histology of testes from control and FoxG1-ARKO mice at selected post-natal ages to d21 (figure on preceding page)

At d2 FoxG1-ARKO testes are morphologically similar to controls, with no seminiferous tubule lumens (outline arrows). At d11, some lumens are beginning to form in controls (solid arrows), but tubule lumens have not begun to develop in FoxG1-ARKO testes (outline arrows). At d16 nearly all tubules in control testes appear to have developed lumens (solid arrows), in the FoxG1-ARKO some tubules are beginning to develop cruciate lumens (arrowhead) whilst others are closed. At d21 seminiferous tubule lumens are patent in control and FoxG1-ARKO (solid arrows). Scale bars are 200μm.

At d2 FoxG1-ARKO testes were histologically similar to controls (Figure 4-8). Testes at this age were too small to register an accurate weight reading on the balance used, so weights were not taken, but FoxG1-ARKO testes appeared grossly similar to controls.

At d11, there was no significant difference in mean testis weight to controls (6.4 ± 0.3 mg control, 6.7 ± 0.3 mg FoxG1-ARKO, $P>0.05$, Figure 4-5), but differences in histology had become apparent. Some seminiferous tubule lumens were beginning to form in controls (Figure 4-8, solid arrows), but tubule lumens had not begun to develop in FoxG1-ARKO testes. When quantified, the mean percentage of tubule cross-sections with a lumen was significantly lower (23% in control testes compared to 7% in FoxG1-ARKO testes, $P\leq0.01$, Figure 4-9).

At d16 mean testis weight is lower in FoxG1-ARKO compared to controls (13.7 ± 0.8 mg control, 11.4 ± 0.7 mg FoxG1-ARKO, $P>0.05$, Figure 4-5). Though this difference is not significant, the *P* value is 0.0504 which is extremely close to being significant ($P\leq0.05$). When quantified, the mean percentage of tubule cross-sections with a lumen was again significantly lower (75% in control testes compared to 36% in FoxG1-ARKO testes, $P\leq0.05$, Figure 4-9). Nearly all tubules in control testes appear to have developed lumens. Lumens that have formed in control seminiferous tubules are round, but those that have formed in FoxG1-ARKO seminiferous tubules were stellate (Figure 4-8).

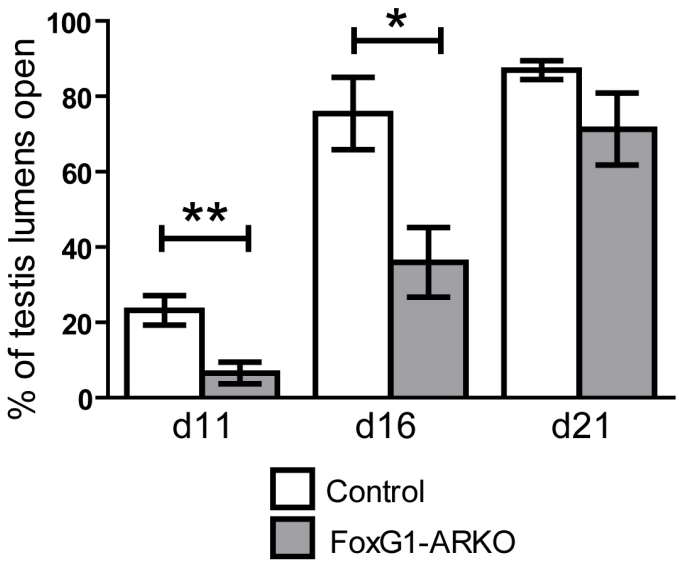

Figure 4-9: Mean percentage of seminiferous tubules lumens open in testis sections from d11, d16 and d21 control and FoxG1-ARKO testes

*At d11 and d16, the percentage of seminiferous tubule lumens open in sections of FoxG1-ARKO testes is significantly lower than controls. At d21 the percentage of seminiferous tubule lumens open in sections of FoxG1-ARKO testes is not significantly different to controls. n=5 mice, ~100 tubule measurements from each. *P≤0.05, **P≤0.01.*

At d21 mean FoxG1-ARKO testis weight was significantly less than control testis weight (29.5 ± 1.6 mg control, 19.7 ± 1.8 mg FoxG1-ARKO, $P \leq 0.01$, Figure 4-5). The mean percentage of open FoxG1 tubule lumens was not significantly different to the control (87% in control testes compared to 71% in FoxG1-ARKO testes, $P > 0.5$, Figure 4-9). FoxG1-ARKO seminiferous tubule radii (69.5 µm control, 67.5 µm FoxG1-ARKO, $P > 0.5$, Figure 4-7) and lumen radii (22.3 µm controls, 18.5 µm FoxG1-ARKO, $P > 0.5$, Figure 4-7) were not significantly different to controls, evidence that the apparent delay in lumen opening of the FoxG1-ARKO was resolved by d21. This is also apparent histologically, at d21 seminiferous tubule lumens are patent in control and FoxG1-ARKO (Figure 4-8).

At d35 mean FoxG1-ARKO testis weight is significantly less than controls. (80.3 ± 3.9 mg control, 65.8 ± 3.8 mg FoxG1-ARKO, $P \leq 0.01$, Figure 4-5). d35 control testes

had full spermatogenesis and patent seminiferous tubule lumens (Figure 4-10a). Of the seven d35 FoxG1-ARKO testes analysed, all appeared to have normal spermatogenesis, but three of these displayed a patent lumen akin to the control (Figure 4-10b), three had distended lumens that appeared larger than the control (Figure 4-10c) and one displayed evidence of the initiation of seminiferous epithelial sloughing (Figure 4-10d).

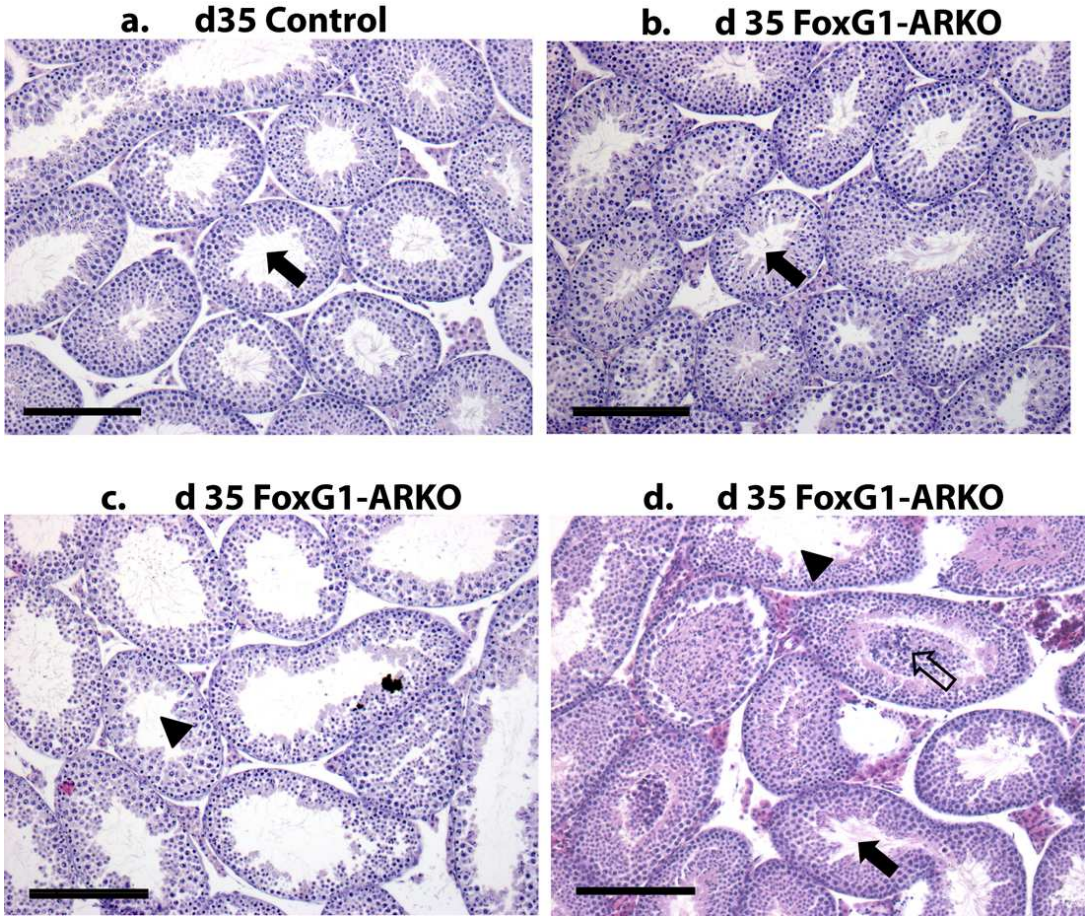

Figure 4-10: Histology of testes from control and FoxG1-ARKO mice d35

(a) d35 control testes have patent lumens (solid arrow). (b) An example of a d35 FoxG1-ARKO testis with morphology similar to control and patent lumens (solid arrow). (c) An example of a d35 FoxG1-ARKO testis with distended lumens but without tubule atrophy (arrowhead). (d) An example of a d35 FoxG1-ARKO testis with seminiferous epithelial sloughing (outline arrow) as well as normal (solid arrow) and distended (arrowhead) lumens. Scale bars are 200µm.

4.2.5 Systemic androgen-dependent phenotype of FoxG1-ARKO mice

Disruption of androgen signalling has quantifiable effects on whole body hormone levels as well as the structure and function of other reproductive organs. To determine if a systemic change in androgen levels had occurred, specific physiological parameters were quantified. Testosterone is produced by the Leydig cells of the testis. As well as acting within the testis it is also released into blood vessels in the testis for transport around the body. Its production is promoted by LH, which is produced in the pituitary gland in response to a decrease in circulating testosterone levels (section 1.5). Serum testosterone and LH concentration was measured at several key ages. Testosterone concentrations were not significantly different in FoxG1-ARKO males compared to controls ($P>0.05$) at d16, d21, d35 or d100 (Figure 4-11). Due to difficulty obtaining sufficient serum from smaller animals, LH was measured at d35 and d100, but no significant difference was seen between control and FoxG1-ARKO animals at these ages (Figure 4-11).

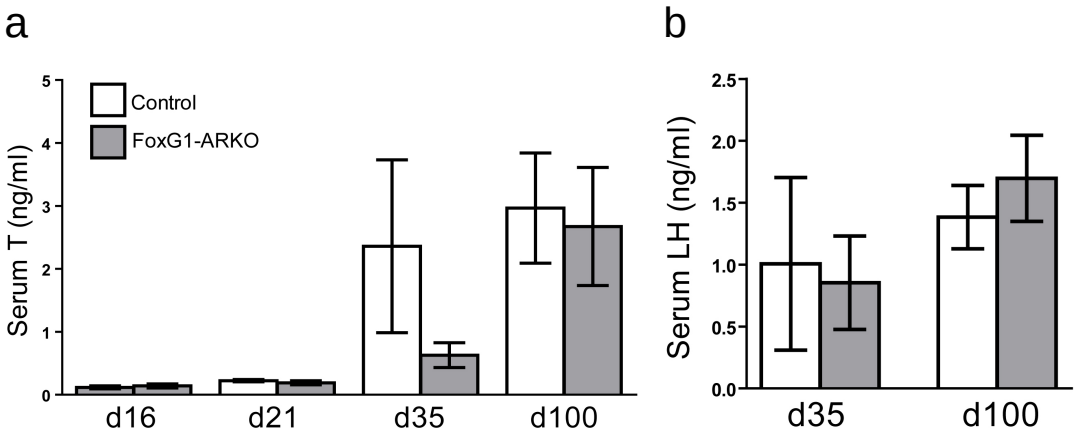

Figure 4-11: Serum T and LH concentrations of control and FoxG1-ARKO mice measured at selected post-natal ages

(a) Serum T concentration does not differ in FoxG1-ARKO mice compared to controls at d16, d21, d35 and d100. (b) Serum LH concentration does not differ in FoxG1-ARKO mice compared to controls at d35 and d100. n≥3 for each group. All values are means ± SEM.

Anogenital distance, seminal vesicle weight and body weight are all influenced by circulating androgen concentrations. Anogenital distance (AGD), the distance between the anus and base of the phallus, is greater in male mice than in female mice. A reduction in AGD is indicative of a decrease in exposure to androgens during the male programming window (Welsh et al., 2007), and total ARKO male mice have an AGD akin to females (Yeh et al., 2002). AGD of FoxG1-ARKO males did not differ significantly compared to controls at d11, d16, d21, d35 and d100 demonstrating that pre-natal androgen concentrations were normal (Figure 4-12).

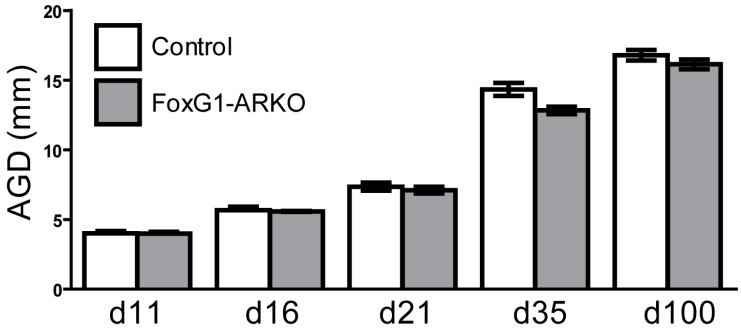

Figure 4-12: AGD of control and FoxG1-ARKO mice measured at selected post-natal ages

AGD is not significantly different in FoxG1-ARKO mice compared to controls at d11, d16, d21, d35 and d100. n≥4 for each group. All values are means ± SEM.

The seminal vesicles are Wolffian duct-derived structures. They are present in rudimentary form until puberty, when they begin to grow and produce seminal plasma, which contributes to the ejaculate. Seminal vesicles are dependent on androgen signalling for development and subsequent maintenance of their structure and function. When this is perturbed they are smaller and weigh less than controls (Simanainen et al., 2008; Welsh et al., 2010a). Weight of seminal vesicles of FoxG1-ARKO males did not differ significantly compared to controls at d11, d16, d21, d35 and d100 implying that post-natal androgen levels were normal (Figure 4-13).

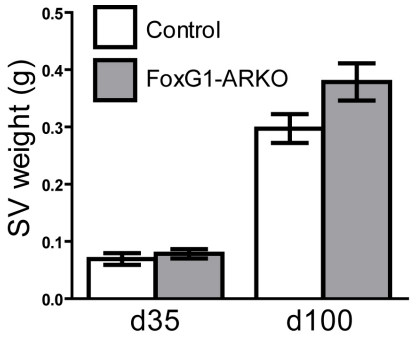

Figure 4-13: SV weight of control and FoxG1-ARKO mice measured at selected post-natal ages

SV weight does not significantly differ in FoxG1-ARKO mice compared to controls at d35 and d100. n≥5 for each group. All values are means ± SEM.

Body-weight is androgen dependent, and was measured to check that there was no growth or metabolic effects of the knock-out. ARKO males weigh less than controls due to a reduction in weight of bone (Yeh et al., 2002) and muscle (MacLean et al., 2008). Body weight of FoxG1-ARKO males did not differ significantly compared to controls at d11, d16, d21, d35 and d100 (Figure 4-14). Based on these observations, it was concluded that the testicular phenotype noted in the FoxG1-ARKO males was not due to a reduction in circulating testosterone levels.

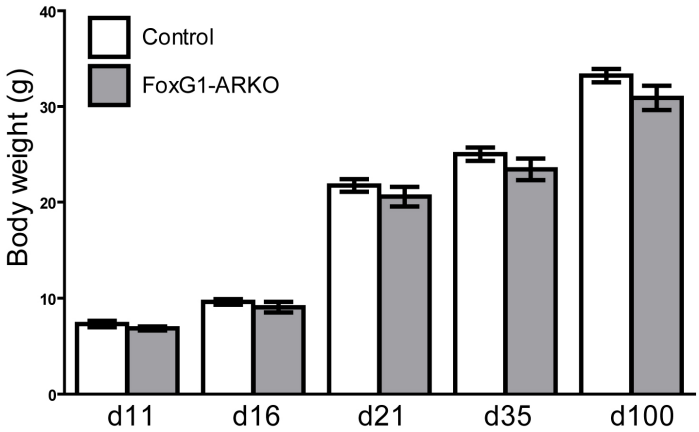

Figure 4-14: Body weight of control and FoxG1-ARKO mice measured at selected post-natal ages

Body weight does not differ in FoxG1-ARKO mice compared to controls at d11, d16, d21, d35 and d100. n≥5 for each group. All values are means ± SEM.

4.2.6 Investigating fertility in FoxG1-ARKO mice

Since the FoxG1-ARKO had a severe testicular phenotype, experiments were undertaken to investigate its fertility. Spermatozoa are stored in the cauda epididymis before entering the vas deferens prior to ejaculation. In d100 FoxG1-ARKO mice very few spermatozoa were present although proteinaceous material could be widely detected (Figure 4-15, asterisks). A few spermatozoa could be observed in the cauda epididymis (Figure 4-15, arrow).

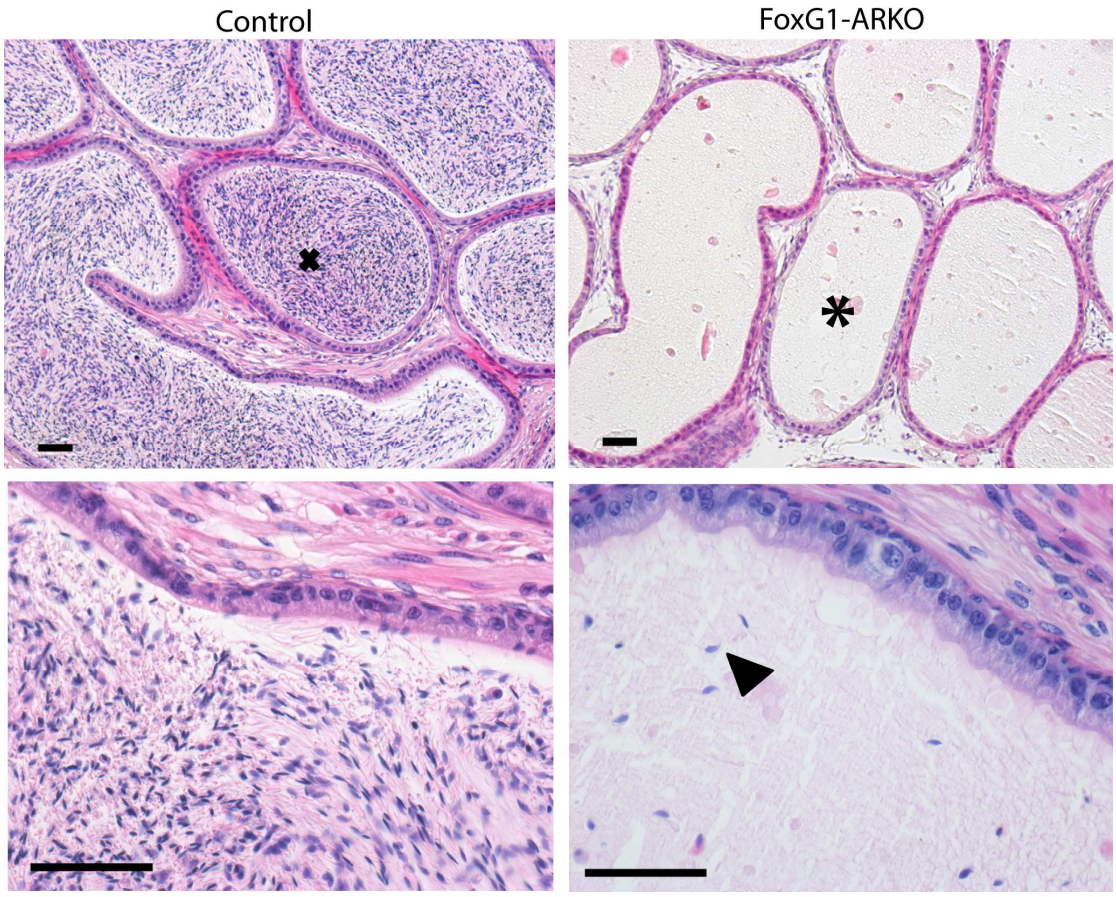

Figure 4-15: Histology of cauda epididymides from d100 control FoxG1-ARKO mice

d100 control mice have densely-packed spermatozoa in the lumen of their cauda epididymides (cross). Cauda epididymides of d100 FoxG1-ARKOs contain proteinaceous material (asterisks) and a few sperm-heads (higher magnification, arrowhead)
Scale bars are 200 µm.

FoxG1-ARKO males sired significantly fewer litters, (with just a single mating proving successful, representing 6% of total matings undertaken) than controls (83% of matings; χ^2 $P \leq 0.001$, Figure 4-16). Furthermore, the sole FoxG1-ARKO male that did produce a litter failed to produce litters in three further matings. However, postcopulatory vaginal plugs were evident after FoxG1-ARKO males were paired with females overnight, implying that normal mating behaviour and ejaculation had occurred. Moreover, the frequency of plugs in females paired overnight with FoxG1-ARKO males (50%) was no lower than in those paired with control males (33%).

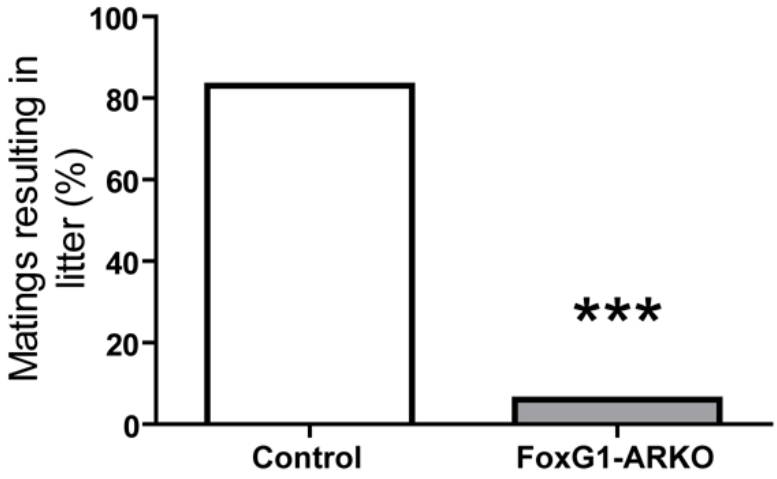

Figure 4-16: Fertility testing of d100 control and FoxG1-ARKO mice

*Significantly fewer matings between d100 FoxG1-ARKO males and wild-type females sire litters (6%) when compared to matings between d100 control males and wild-type females (83%) ***P≤0.001.*

Histological examination of the efferent ducts and rete testis junction of the d100 FoxG1-ARKO revealed that spermatozoa have accumulated in the efferent ducts, whereas the control efferent ducts contain few spermatozoa (Figure 4-17).

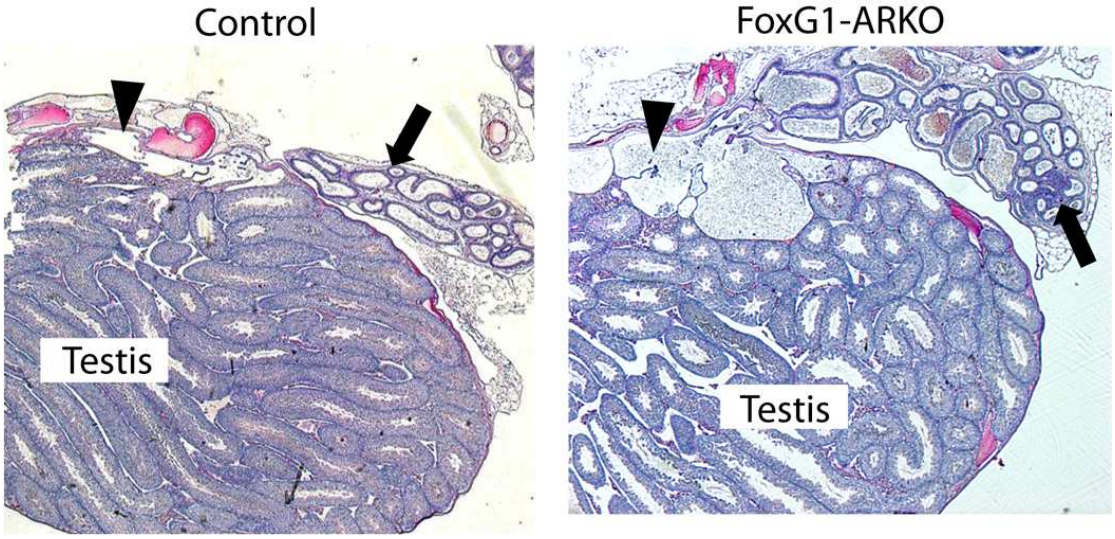

Figure 4-17: Low magnification comparison of rete and efferent ducts of control and FoxG1-ARKO at d100

The rete of the FoxG1-ARKO is distended with spermatozoa, unlike the rete of the control which is smaller and lacks spermatozoa (arrowheads). The efferent ducts of the FoxG1-ARKO are distended with spermatozoa, unlike the efferent ducts of the controls which contain few spermatozoa (arrows).

4.2.7 Identifying the location of AR ablation in FoxG1-ARKO testis

To determine if the phenotype seen in the testis of FoxG1-ARKO mice was caused by ablation of AR in any of the testicular cell types, presence of wild-type AR in the testis was assessed at both the transcript and protein level. Presence of recombined and full-length *Ar* exon 2 in the testis as indicated by RT-PCR indicated that there was ablation of AR in a population of cells in the testis, but that ablation is not total (Figure 4-18). Percentage of cells ablated cannot be determined from an RT-PCR as it is not quantitative (see section 2.8). To determine the cell-types in which AR is ablated, immunohistochemistry for AR was performed both as immunohistochemistry for AR only and as a double with testis cell markers.

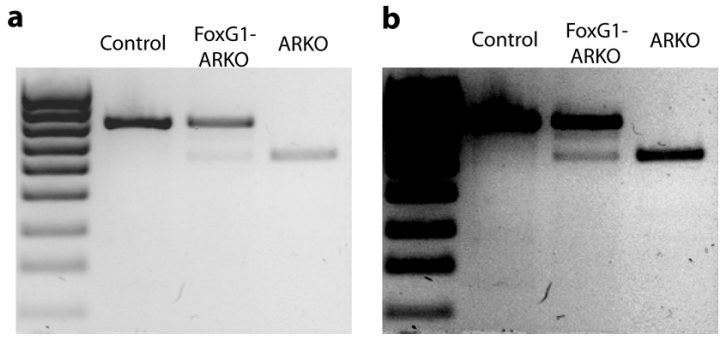

Figure 4-18: Presence of wild-type and/or Cre-recombined Ar transcript in d100 control and FoxG1-ARKO testis

RT-PCR on d100 control testes confirms all Ar transcripts are wild-type (upper band). d100 FoxG1-ARKO testes express both full length and recombined (lower band) Ar transcripts. Total ARKO testis expresses only recombined AR. Gel is shown both underexposed (a) and overexposed (b) so the presence of all stated bands can be confirmed.

Sertoli cells express AR from d5 (Willems et al., 2010). A single AR immuno revealed the presence of AR+ cells with Sertoli cell morphology in the testes of d100 control and FoxG1-ARKO mice (Figure 4-19). AR was not identified in any intratubular cells at d2 in either control or FoxG1-ARKO testes. Double immunohistochemistry for AR with the Sertoli-cell specific markers Wilms' tumour suppressor (WT1) or Cyclin-dependent kinase inhibitor 1B (p27/kip) was attempted to quantify any ablation but was unsuccessful in both cases.

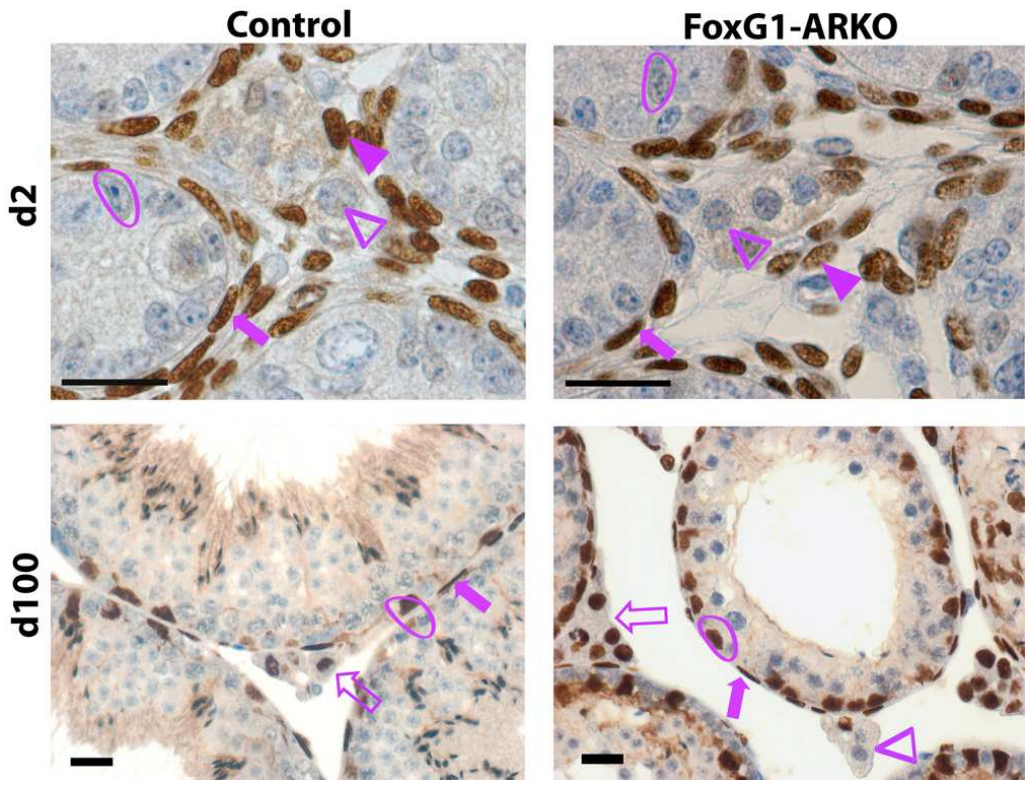

Figure 4-19: Localisation of AR protein in testes from control and FoxG1-ARKO mice at d2 and d100

Control testes at d2 stain positive for androgen receptor in both the PTM cells (solid arrows) and a population of the interstitial cells (solid arrowheads). Staining in FoxG1-ARKO testes is similar to the control. At this age Sertoli cells do not strongly express AR in either the control or FoxG1-ARKO testes (circled). There are also populations of interstitial cells with Leydig cell morphology that do not express AR in both the control and the FoxG1-ARKO (outline arrowhead). At d100, AR staining is present in some interstitial cells with Leydig cell morphology in both the control and FoxG1-ARKO (outline arrow), all PTM cells in both control and FoxG1-ARKO (solid arrows) and is now strong in Sertoli cells in both control and FoxG1-ARKO (circled). Some cells with Leydig cell morphology in the FoxG1-ARKO do not express AR (outline arrowhead). Scale bars are 100 µm.

Adult Leydig cells are thought to express AR from the precursor Leydig cell (PLC) stage (Chen et al., 2009a). Cells with definitive Leydig cell morphology can be seen to stain positive for AR from d21 in the mouse (Zhou et al., 2002). At early postnatal ages involuting AR-negative fetal Leydig cells may also be seen in the testis (Kerr and Knell, 1988), as well as AR-positive cells with a mesenchymal morphology (Willems et al., 2009). A single AR immuno revealed the presence of AR+

interstitial cells at both d2 and d100 in both the control and FoxG1-ARKO (Figure 4-19). To determine whether any ablation of AR had occurred in Leydig cells, double-antibody immunohistochemistry of AR with 3βHSD1 (a Leydig cell-specific protein involved in steroidogenesis) was performed on d100 control and FoxG1-ARKO testes (Figure 4-20). In d100 controls, all 3betaHSD1+ cells were also AR+. In FoxG1-ARKO testes at d100, some 3betaHSD1+ cells were AR+ and some were AR-. This ablation was not quantified.

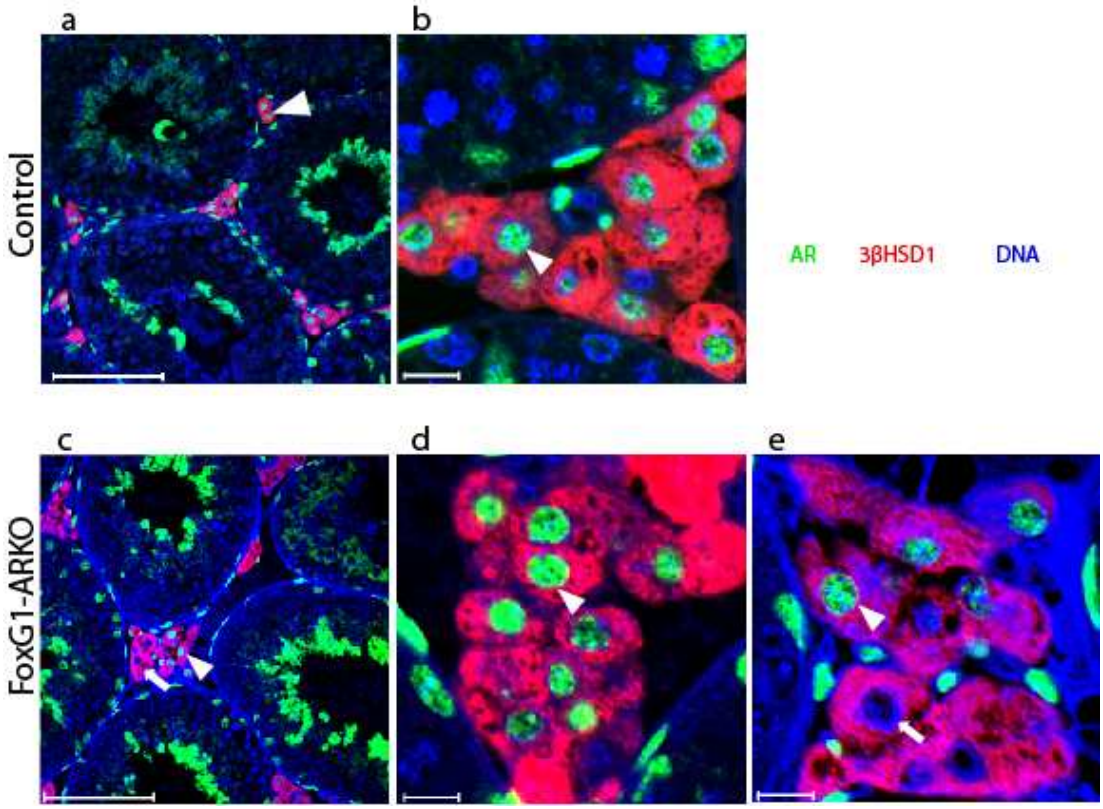

Figure 4-20: Localisation of AR protein in Leydig cells of control and FoxG1-ARKO mice at d100

(a and b): In d100 controls, all 3betaHSD1+ cells are also AR+ (arrowheads). (c): In FoxG1-ARKO testes at d100, some 3betaHSD1+ cells are AR+ (arrowhead), but some are AR- (arrow) (d) High magnification of a group of AR+ 3betaHSD1+ interstitial cells (arrowhead) in a d100 FoxG1-ARKO testis (e) High magnification of a group of interstitial cells in a d100 FoxG1-ARKO testis containing both AR+3betaHSD1+ cells (arrowhead) and AR-3betaHSD1+ cells (arrow). Scale bars for a and c are 100 µm, for b, d and e are 10 µm.

PTM cells express AR from at or before e16.5 in the mouse (Drews et al., 2001). A single AR immuno revealed the presence of AR+ peritubular cells in the testes of both d2 and d100 control and FoxG1 mice (Figure 4-19). To determine whether any ablation of AR had occurred in PTM cells, a double immuno of AR with SMA (a smooth muscle cell-specific protein) was performed on d100 control and FoxG1-ARKO testes (Figure 4-21). All SMA+ cells are also AR+ in all testes examined for both control and FoxG1-ARKO testes at d100.

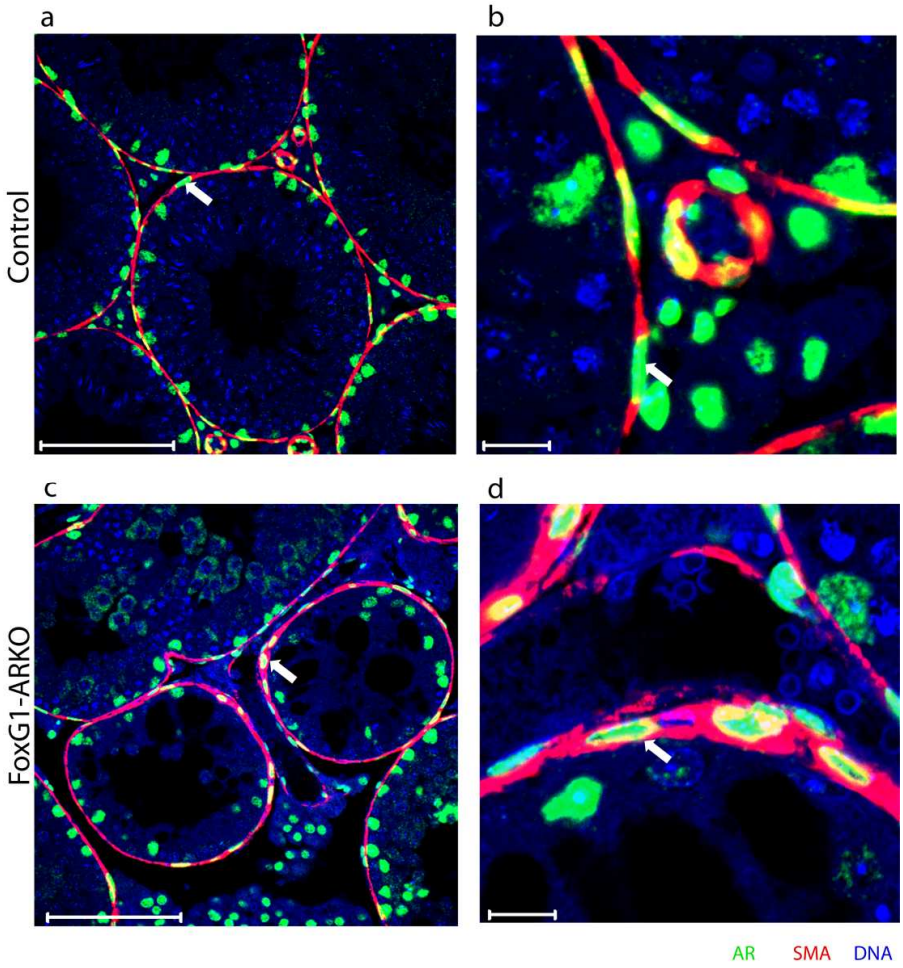

Figure 4-21: Localisation of AR protein in PTM cells of control and FoxG1-ARKO mice at d100

(a and b): In control testes at d100, all SMA+ cells are also AR+(arrows).

(c and d): In FoxG1-ARKO testes at d100, all SMA+ cells are also AR+. Scale bars for a and c are 100 µm, for b and d are 10 µm.

4.2.8 Identification of other sites of AR ablation in the FoxG1-ARKO mouse

To determine whether ablation had occurred in any other tissues known to express AR, RT-PCR for *Ar* exon 2 was performed on tissues from d100 FoxG1-ARKO mice (Figure 4-22). Wild-type *Ar* transcript only was observed in the epididymis/efferent ducts and prostate, recombination of some, but not all *Ar* transcript was noted in testis, brain, penis, kidney, adrenal and seminal vesicle, and recombination of AR RNA in almost all cells was noted in the pituitary.

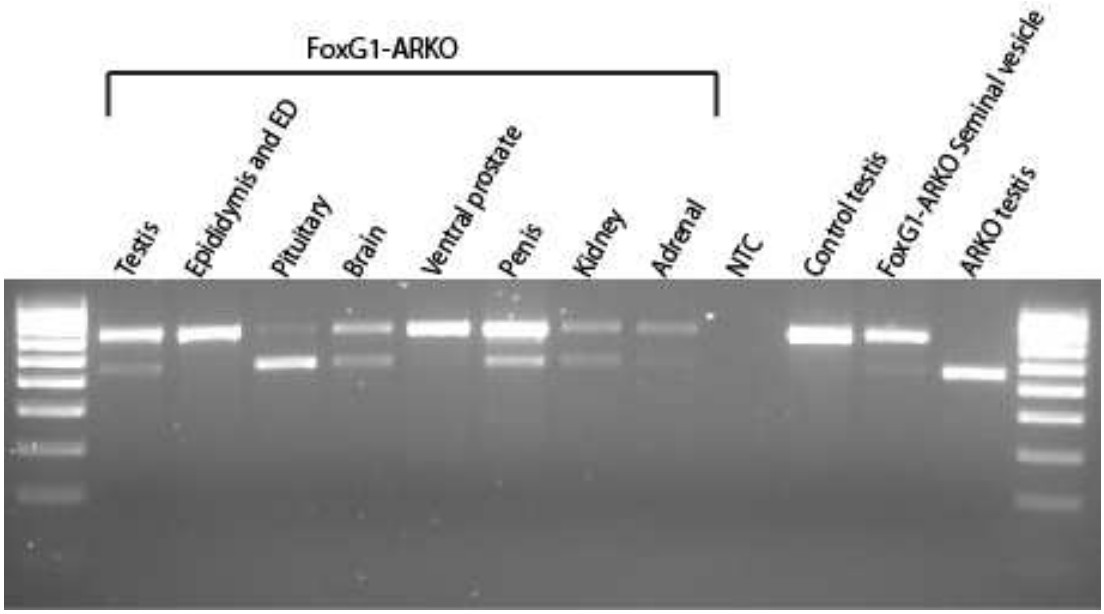

Figure 4-22: Presence of wild-type and/or Cre-recombined Ar transcript in a panel of tissues from d100 FoxG1-ARKO mice

Expression of wild-type full-length Ar transcript (upper band) only is noted in control testis, as well as FoxG1-ARKO epididymis and ventral prostate. Some recombination of Ar exon 2, resulting in a truncated Ar transcript (lower band) is noted in FoxG1-ARKO testis, brain, penis, kidney, adrenal and seminal vesicles. The majority of Ar transcript in the FoxG1-ARKO pituitary is recombined (lower band). All Ar transcript in the ARKO testis is recombined (lower band).

4.3 Discussion

The aims of this chapter were to characterise the expression of FoxG1 in the testis, determine the suitability of FoxG1-Cre for producing mice with an adult-onset Sertoli cell-specific knock-out of AR, and to generate and analyse the phenotype of FoxG1-ARKO male mice. FoxG1-Cre was initially utilised to produce an 'adult-SCARKO' ablation of AR in post-pubertal Sertoli cells based on immunohistochemistry confirming its expression in adult Sertoli cells. Immunohistochemistry on further ages demonstrated that endogenous FoxG1 is not present in fetal or neonatal Sertoli cells from e15.5 until d2, but is present in Sertoli cells from d12 onwards. Endogenous FoxG1 is also present in the somatic cells of the developing testicular cords at e12.5 and e13.5, in fetal Leydig cells from e15.5 until d2, and is still seen in some interstitial cells at d12 and d100 (the nature of these interstitial cells could not be determined due to a lack of sufficient FoxG1 antibody for double immunohistochemistry experiments to be performed). The characterisation pattern of expression of FoxG1 in the testis is a novel result, previous literature has reported that it is present in the human but not rodent testes when examined by Northern blot, and cellular localisation has not previously been characterised (Obendorf et al., 2007). Full analysis of the expression pattern of FoxG1 at embryonic, perinatal and adult ages before a FoxG1-Cre was used to selectively ablate AR would have excluded it from being suitable for both Sertoli cell-specific gene ablation (as it is also expressed in fetal Leydig cells and interstitial cells of the adult) and adult-SCARKO generation (as it is expressed from d12 and mature spermatozoa are not generated until between d30 and d35 in the mouse (Borg et al., 2010). However, by the time this immunohistochemical study had been performed, tissue from FoxG1-YFP and FoxG1-ARKO mice was already being analysed.

FoxG1-Cre has been used to ablate ten different genes in the developing forebrain but has not been used in gene ablation studies in tissues other than the brain (Arnold et al., 2006; Barrionuevo et al., 2008; Chen et al., 2006; Chen et al., 2009b; Fuccillo

et al., 2004; Gordon et al.; Hurd et al.; Hwang et al.; Pirvola et al., 2002; Wang et al.). Genetic background has previously been shown to affect the expression of FoxG1-Cre. 129SvJ embryos demonstrate a pattern of FoxG1-Cre action almost exclusively in the forebrain, whereas BALB/c embryos demonstrate Cre recombination in most tissues observed (Hebert and McConnell, 2000). Analysis of the expression pattern of YFP in FoxG1-YFP reporter mice revealed that FoxG1-Cre is not expressed in the same cell types as endogenous FoxG1 in the testis. Whereas endogenous FoxG1 is present in all adult Sertoli cells, YFP is only present in a few adult Sertoli cells, demonstrating that FoxG1-Cre has been active in these cells during their development. Endogenous FoxG1 is expressed in fetal Leydig cells and adult interstitial cells. YFP is present in some adult interstitial cells demonstrating that FoxG1-Cre has been active in these cells during their development. Since endogenous FoxG1 is present in both fetal Leydig cells and postnatal interstitial cells and it is not known if the interstitial cells are Leydig cells or mesenchymal cells, the activation of FoxG1-Cre could have happened at any age. It appears that Leydig cell FoxG1-Cre activation more accurately mirrors endogenous FoxG1 Leydig cell expression than the Sertoli cell FoxG1-Cre. Endogenous FoxG1 is not seen in germ cells at any age, but YFP expression is present in clones of germ cells, indicating that FoxG1-Cre has been active in these cells during their development. Ectopic Cre activity during gametogenesis has been recorded in some lines (including FoxG1-Cre, also known as BF1-Cre) and has been hypothesised to occur when progenitor germ cells commit to terminal differentiation and enter gametogenesis, at which time the floxed allele may undergo Cre-mediated recombination (Weng et al., 2008). The inconsistent expression pattern of FoxG1-Cre compared to FoxG1 is novel compared to its activity in the developing brain, where it faithfully reproduce the expression of endogenous FoxG1 (Hebert and McConnell, 2000). The differences in FoxG1-Cre expression in the testis could be due to a testis-specific promoter element within the FoxG1 gene that has been deleted in the FoxG1-Cre allele. The lack of a reproducible immunohistochemistry protocol for Cre means that its localisation can't be determined and expression of YFP in FoxG1-YFP mice must be used. This has its limitations as the continuing YFP acts as a lineage tracer to label cells that have

expressed Cre at any point during their development, and also the daughter cells of cells where Cre is active.

When the FoxG1-Cre line was mated to the AR^{flox} line to generate a cell-specific knock-out of AR (FoxG1-ARKO), the ablation pattern of AR followed the same expression pattern of YFP in the FoxG1-YFP testis rather than the pattern of endogenous FoxG1 expression. Virtually no AR ablation was noted in Sertoli cells of FoxG1-ARKO mice, just as very few cells of the FoxG1-YFP mouse express YFP, despite ubiquitous expression of endogenous FoxG1 in adult Sertoli cells. There is evidence in the literature of studies where reporter gene expression and gene ablation lines show different localisation of Cre recombination; this is thought to be due to differences in recombination efficiency due to differing epigenetic modifications at the divergent genomic locations of *loxP* sites (Smith, 2011). However in this case the reporter gene and gene ablation lines show a similar pattern of recombination, but both are different from the endogenous gene expression. Since the FoxG1-Cre is a knock-in of Cre recombinase to one copy of the FoxG1 locus, removing the sequence downstream of the FoxG1 promoter, it is possible that the Cre is not expressed in the same spatio-temporal pattern as the endogenous FoxG1 due to loss of promoter or modifier sequences downstream of the 'classical' FoxG1 promoter that is thought to be driving expression. It is interesting to note that recent data from our lab suggests that the FoxG1 antibody our lab and other labs have used for immunohistochemistry may not be consistent between lot numbers: the most recent vial of antibody used stains germ cells specifically, and FoxG1 antibody from another company stains Leydig cells specifically. A transgenic line with a knock-in of β-galactosidase at the FoxG1 locus could be used to definitively determine the localisation of endogenous FoxG1.

FoxG1-ARKO mice also have a partial ablation of AR in the brain, kidney, penis, adrenal and seminal vesicle, as well as a near total ablation of AR in the pituitary. These data lead to the conclusion that FoxG1-Cre is a Cre line with low specificity. Partial ablation of AR in the pituitary and brain of the FoxG1-ARKO is an

interesting result due to the role of the hypothalamus and pituitary in the control of testicular hormone production (see section 1.5). This will be investigated further in Chapter 5.

Despite the lack of a complete ablation of AR in any one testicular cell type, the phenotype of the FoxG1-ARKO testis is relatively severe, and does not have the same progression as any published cell-specific knock-outs of AR. The embryonic SCARKO exhibits a meiotic block that precludes formation of round or elongating spermatids (Chang et al., 2004; De Gendt et al., 2004). By contrast, the FoxG1-ARKO undergoes normal spermatogenesis which is only disrupted by the onset of seminiferous epithelium sloughing from day 35. The peri-tubular myoid cell (PTM)-ARKO mouse has testes with a reduction in numbers of all germ cell stages including the spermatogonia (Welsh et al., 2009a), but this phenotype is present from early in development and is not a degenerative change associated with seminiferous epithelial sloughing as in the FoxG1-ARKO. The published Leydig cell ARKO (Xu et al., 2007) has a block at the round spermatid stage whereas the FoxG1-ARKO has complete spermatogenesis up until the onset of seminiferous epithelial sloughing. It is important to note that the Leydig cell ARKO phenotype is complicated by the contribution of an ablation of AR in Sertoli cells, as the Cre line used in this paper (AMHR2-Cre) is present in both cell types (Jeyasuria et al., 2004). However, other experiments elucidating the effect of AR in Leydig cells have suggested that it works in tandem with LHR signalling to support pubertal maturation of PLCs to steroidogenically active ILCs (Hardy et al., 1990; Murphy et al., 1994). Since the FoxG1-ARKO has a similar serum testosterone level to the control it is unlikely that the partial ablation of AR in Leydig cells is having an effect on their maturation and therefore steroidogenic output. In conclusion, the FoxG1-ARKO does not have a phenotype analogous to any of the published cell-specific knock-outs of AR.

The FoxG1-Cre line has a knock-in of Cre downstream of the promoter of one of its two FoxG1 loci. This results in haploinsufficiency of FoxG1. Haploinsufficiency of another Fox gene (FoxA3), results in a severe testicular phenotype (Behr et al., 2007)

and FoxG1 has been noted to be an AR co-repressor (Obendorf et al., 2007), so haploinsufficiency of FoxG1 could potentially be interfering with normal testicular function. Despite this, FoxG1-Cre mice did not display a testicular phenotype or infertility; in fact they were used as efficient breeding studs to produce both FoxG1-YFP and FoxG1-ARKO offspring. However, haploinsufficiency of FoxG1 in the FoxG1-Cre line has resulted in problems for groups using FoxG1-Cre for brain-specific ablation, as the FoxG1-Cre line itself displays a brain phenotype that complicates resulting phenotypic analysis of knock-out lines (Eagleson et al., 2007).

Phenotypes similar to the FoxG1-ARKO testis are seen in rodents with ligations or occlusions of the efferent ducts, epididymis or vas deferens, resulting in fluid back-pressure damage to the seminiferous epithelium of the testis (Anton, 2003; Flickinger et al., 1999; Hess and Nakai, 2000; Peng et al., 2010). When the efferent ducts of the FoxG1-ARKO were investigated they were found to contain a large number of spermatozoa, whereas the efferent ducts of control mice contained few spermatozoa. When considered along with the observation that FoxG1-ARKO contain very few spermatozoa in their cauda epididymis, the implication is that the spermatozoa are stalling in their transit upstream in the efferent ducts or caput epididymis. This will be investigated further in Chapter 6.

5. Characterisation of the effects of AR ablation in the FoxG1-ARKO pituitary

5.1 Introduction

FoxG1-ARKO mice have a near-total ablation of AR in the pituitary and a partial ablation in the brain (see section 4.2.8). FoxG1-Cre is expressed in the pharyngeal pouches (that give rise to the anterior pituitary) from e9.5 (Hebert and McConnell, 2000). The pituitary plays an important role in the HPG axis as the site of gonadotropin synthesis and release (see section 1.5). FoxG1-ARKO shows no change in serum testosterone or LH levels (see section 4.2.5). Testosterone is thought to act at the hypothalamus rather than the pituitary to modify the release of LH (Pitteloud et al., 2008; Tilbrook and Clarke, 2001). In *Tfm* mice, levels of serum LH and FSH are increased (Amador et al., 1986) due to a failure of testosterone to limit LH expression. Despite this, pituitaries of ARKO mice have apparently normal pituitary expression of LHβ and FSHβ at both the mRNA and protein levels (Miyamoto et al., 2007), but this was recorded qualitatively not quantitatively. Mice with cell-specific inactivation of AR in the nervous system (but not pituitary) also have increased testosterone and LH levels and a slight decline in the number of sperm present in the epididymis (Raskin et al., 2009). Their reduction in fertility is due to abnormal mating behaviours that lead to fewer matings and delayed ejaculation. Despite the partial ablation of AR in the brain of the FoxG1-ARKO male, its mating behaviour was normal as the frequency of post-copulatory plugs produced by FoxG1-ARKO males was no less than for control males (see section 4.2.6). Since it appears that the levels of serum gonadotropins and sexual behaviour are not affected in FoxG1-ARKO mice, despite the total pituitary ablation of AR and partial brain ablation, pituitary hormone output other than gonadotropins could be the cause of the phenotype.

As well as the gonadotropins which are vital for normal testicular function, the pituitary produces other endocrine hormones that have been noted to have potential

testicular effects, either *via* direct stimulation of their receptors in testicular cells, or *via* indirect effects on other target organs that have a subsequent testicular effect. Thyroid stimulating hormone (TSH) is produced by the anterior pituitary and consists of the common glycoprotein α subunit and the specific TSHβ subunit. It stimulates the thyroid gland to release the hormones thyroxine (T_4) and triiodothyronine (T_3). TSH receptor knock-out mice die within 1 week of weaning unless fed a diet supplemented with thyroid powder. However, diet-supplemented mice are fertile, suggesting that TSH does not have any direct testicular effects on male fertility (Marians et al., 2002). However, T_3 is known to inhibit Sertoli cell proliferation and promote Leydig cell differentiation via receptors present in the testis, so it is likely that the absence of TSH stimulation of T_3 would result in testicular effects (Wagner et al., 2008).

Prolactin is produced by the anterior pituitary and is involved in lactogenesis in females. Both prolactin (Steger et al., 1998) and prolactin receptor (Binart et al., 2003) knock-out males are fertile (though prolactin knock-out males display reduced LH levels and weights of seminal vesicles and ventral prostate) suggesting that prolactin does not have any vital effects on male fertility. Pro-opiomelanocortin (POMC) is a precursor polypeptide hormone produced by the anterior pituitary that is post-translationally cleaved by prohormone convertase enzymes to form adrenocorticotropin (ACTH), β-endorphin and α and β melanocyte stimulating hormones (MSH). POMC knock-out mice display obesity, defective adrenal development and altered pigmentation (Yaswen et al., 1999). ACTH has been shown to stimulate fetal Leydig cell function through the melanocortin type-2 receptor, however POMC-null mice have normal FLC development, so it is likely that FLCs, whilst responsive to ACTH, are not dependent on it (O'Shaughnessy et al., 2003). Investigation of the onset of AR deletion in the pituitary of FoxG1-ARKO mice and the levels of pituitary hormone transcripts produced compared to the control would help elucidate the effects of AR in the mouse pituitary on levels of hormones it produces and any potential endocrine effects of these hormones on the testis.

5.1.1 Aims

- To determine the onset of AR ablation in the pituitary of the FoxG1-ARKO.
- To determine whether ablation of AR from the pituitary impacts upon hormone output.

5.2 Results

5.2.1 Onset of activity of FoxG1-Cre in the forebrain and pituitary

When e12.5 FoxG1-YFP embryos were examined under a dissecting scope fitted with a fluorescent filter, strong YFP expression could be detected in the developing forebrain and weaker YFP expression in the remainder of the embryo (Figure 5-1a). Localisation of YFP by immunohistochemistry was identified in Rathke's pouch, the embryonic anlagen of the pituitary (Figure 5-2b, c). YFP was not observed in littermate control embryos either when viewed whole under a fluorescent filter or sectioned and stained with an antibody to YFP.

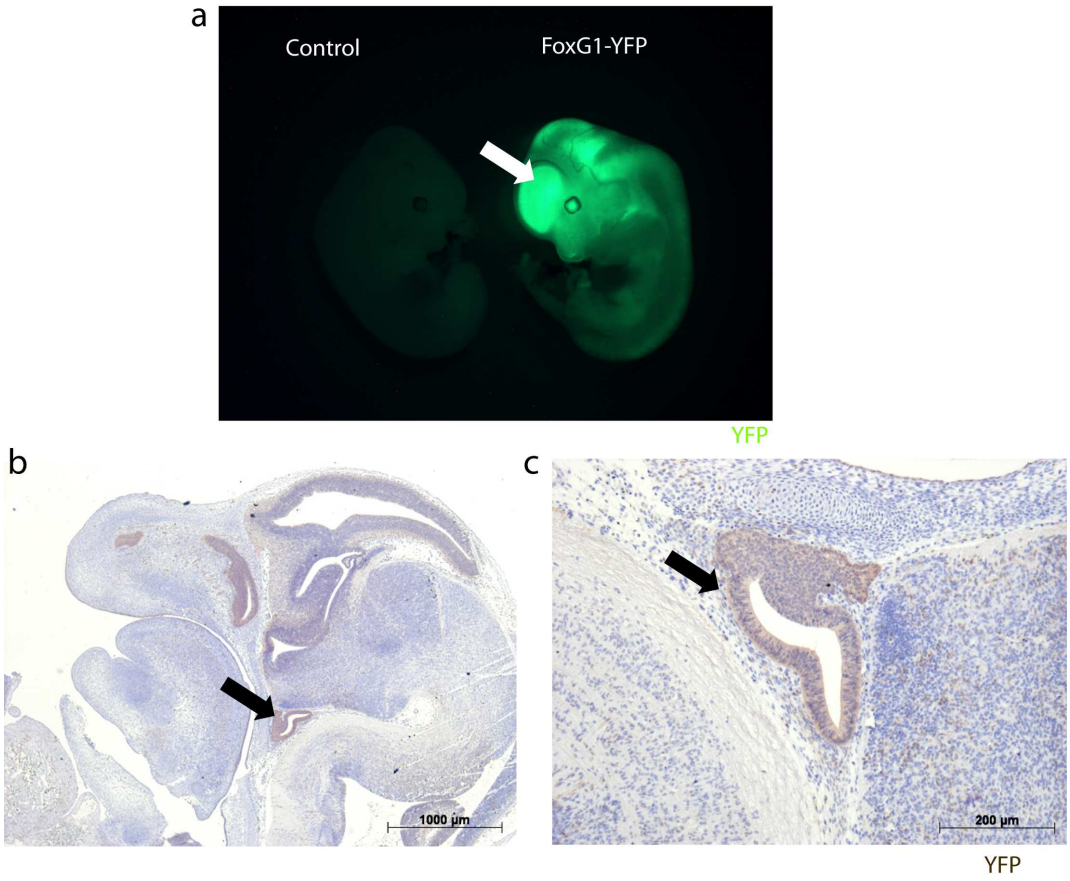

Figure 5-1: YFP expression in the forebrain and pituitary of e12.5 FoxG1-YFP embryos

(a) Comparison of control and FoxG1-YFP e12.5 embryos when viewed under a fluorescent scope. YFP expression is particularly strong in the developing forebrain (arrow). (b and c) YFP is present in the epithelium of Rathke's pouch in an e12.5 FoxG1-YFP embryo (arrows). Scale bar for b is 1mm, c is 200 µm.

5.2.2 Analysing ablation of AR in the pituitary of the FoxG1-ARKO

To confirm and determine the onset and localisation of pituitary AR ablation, presence of full-length AR in the pituitary was assessed at both the transcript and protein level. Presence of recombined *Ar* exon 2 in the pituitary confirmed by RT-PCR indicated that there was ablation of AR from the FoxG1-ARKO pituitary at d11 (Figure 5-2). d11 was the earliest age that RNA extraction and RT-PCR was performed due to the difficulty obtaining a clean dissection of the pituitary from embryonic or neonatal mice.

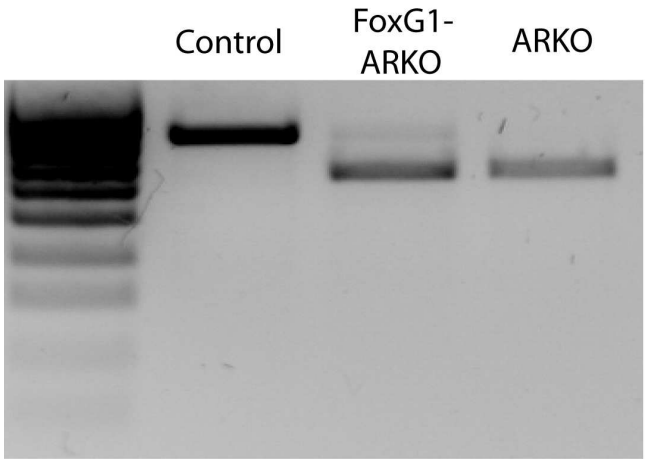

Figure 5-2: Presence of wild-type and/or Cre-recombined Ar transcript in d11 control and FoxG1-ARKO pituitary

RT-PCR on d11 control pituitary confirms all Ar transcripts are wild-type (upper band). d11 FoxG1-ARKO pituitaries express mostly a recombined (lower band) Ar transcripts. d11 total ARKO pituitary expresses only recombined AR.

Immunohistochemistry for AR on d100 control and FoxG1-ARKO mice indicated that AR protein was completely absent from the FoxG1-ARKO pituitary at this age, whereas the control pituitary displayed AR staining in a scattered sub-population of cells (Figure 5-3).

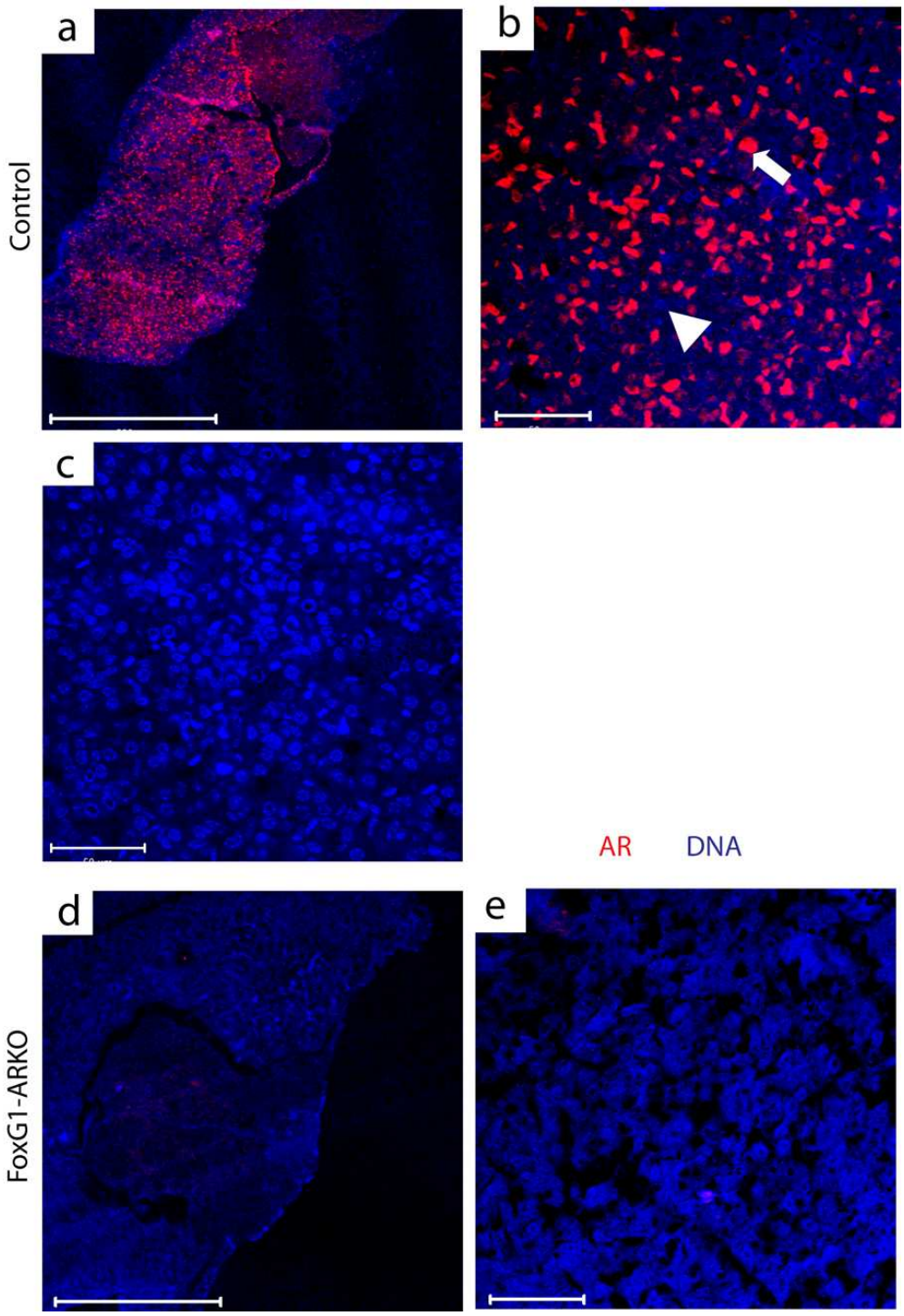

Figure 5-3: Immunohistochemistry for AR on d100 control and FoxG1-ARKO pituitary

(a, b) d100 control pituitary shows immunostaining for AR in some cells (arrow) whereas other cells are AR negative (arrowhead). (c) d100 control pituitary with no primary antibody control does not show immunostaining for AR. (d, e) d100 FoxG1-ARKO pituitary does not show immunostaining for AR. Scale bars are 500 µm for a and d and 50 µm for b, c and e.

5.2.3 Morphology of the FoxG1-ARKO pituitary

To determine whether ablation of AR was coincident with a change in morphology of the FoxG1-ARKO pituitary, H&E stained sections of d100 pituitary were examined (Figure 5-4). Posterior, intermediate and anterior lobes were present in both the d100 control and FoxG1-ARKO pituitaries. Pituitaries were too small to be accurately weighed but FoxG1-ARKO pituitaries did not appear grossly different to controls.

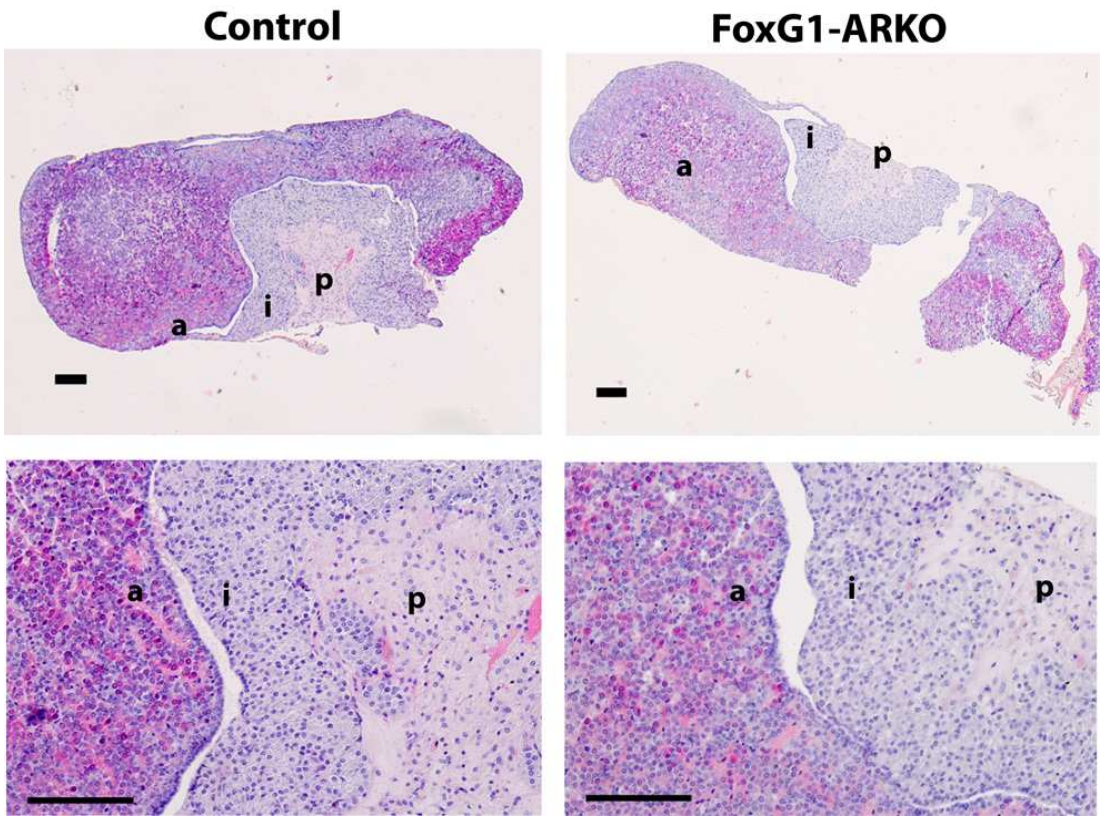

Figure 5-4: H&E stain of d100 control and FoxG1-ARKO pituitaries

Note that pituitary morphology is normal in both control and FoxG1-ARKO tissue, with posterior (p), intermediate (i) and anterior (a) lobes present. Scale bars are 100μm.

5.2.4 Levels of pituitary hormone transcripts in the FoxG1-ARKO mouse

To investigate the levels of pituitary hormone transcripts in the FoxG1-ARKO pituitary, TaqMan qRT-PCR was performed on d16, d21, d35 and d100 pituitary cDNA for the transcripts of *Cga* (glycoprotein hormone α-subunit, the common subunit for LH, FSH and TSH, Figure 5-5a), *Lhb* (LHβ transcript, Figure 5-5b), *Fshb* (FSHβ transcript, Figure 5-5c), *Prl* (prolactin transcript, Figure 5-5d), *Tshb* (TSHβ transcript, Figure 5-5e), and *Pomc* (POMC transcript, Figure 5-5f). Mean relative expression of these genes did not significantly differ between control and FoxG1-ARKO samples for any of these transcripts at any of the ages examined.

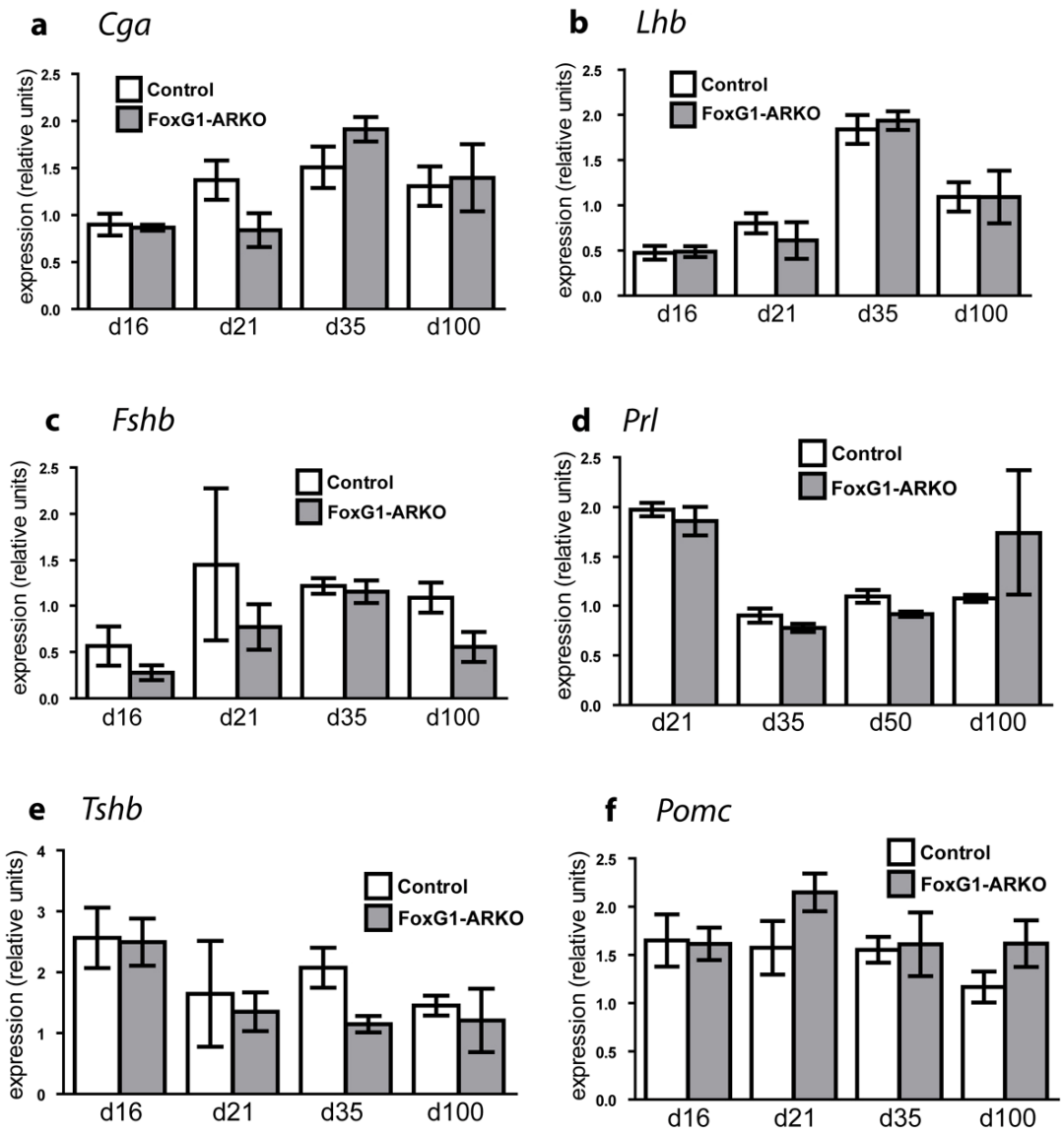

Figure 5-5: Expression levels of pituitary hormone transcripts in control and FoxG1-ARKO mice pituitaries at selected post-natal ages

(a) There is no significant difference in Cga transcript levels between control and FoxG1-ARKO pituitaries at d16, d21, d35 or d100. (b) There is no significant difference in Lhb transcript levels between control and FoxG1-ARKO pituitaries at d16, d21, d35 or d100. (c) There is no significant difference in Fshb transcript levels between control and FoxG1-ARKO pituitaries at d16, d21, d35 or d100. (d) There is no significant difference in Prl transcript levels between control and FoxG1-ARKO pituitaries at d21, d35, d50 or d100. (e) There is no significant difference in Tshb transcript levels between control and FoxG1-ARKO pituitaries at d16, d21, d35 or d100. (f) There is no significant difference in Pomc transcript levels between control and FoxG1-ARKO pituitaries at d16, d21, d35 or d100. Values are mean ± SEM, n≥3 for each group.

5.3 Discussion

The aims of this chapter were to determine the onset of AR ablation in the FoxG1-ARKO pituitary, and to determine whether ablation of AR from the pituitary impacts upon hormone output. Androgen receptor mRNA has been shown to be expressed in the pituitary of e18.5 mouse embryos (Crocoll et al., 1998) but the HPG axis does not start to control testis function until after birth in the mouse (O'Shaughnessy et al., 2009). FoxG1-Cre expression in the pituitary was present at e12.5. By d11 nearly all AR is ablated in the pituitary. Confirmation of onset at earlier ages was hampered by the difficulty of obtaining a clean dissection of pituitaries from embryonic and perinatal mice so exon 2 PCR could not be performed. AR immunohistochemistry confirmed that AR protein was absent from the d100 FoxG1-ARKO pituitary.

As was noted in Chapter 4, FoxG1-ARKO mice do not have significantly different serum testosterone and LH levels to controls. As well as the gonadotropins which are vital for normal testicular function, the pituitary produces other endocrine hormones that have been noted to have potential testicular effects, but none have been shown to directly regulate male fertility (Binart et al., 2003; Marians et al., 2002; O'Shaughnessy et al., 2003; Steger et al., 1998). When pituitary hormone transcripts were examined at ages from d16 onwards there were no differences between levels in FoxG1-ARKO and controls, demonstrating that pituitary AR does not have a direct feedback effect on *Cga, Lhb, Fshb, Prl, Tshb* or *Pomc* transcript levels. However, it must be noted that concentrations of FSH, prolactin, ACTH or TSH proteins in the serum were not measured, and may differ between control and FoxG1-ARKO even if the transcript levels are not significantly different. The morphology of the FoxG1-ARKO pituitary was normal, which is also reported for the pituitary morphology in the ARKO mouse (Miyamoto et al., 2007). Current theory is that AR acts on kisspeptin neurons, which regulate release of GnRH from AR-negative GnRH neurons into the anterior pituitary (Raskin et al., 2009). The expression of AR in pituitary gonadotrophs (Okada et al., 2003) despite its apparent redundancy in gonadotropin synthesis and release begs the question: what exactly is its role?

The FoxG1-ARKO mouse also demonstrated partial ablation of AR in the brain. As discussed above, site of action of AR feedback on the HPG axis is thought to be at the level of kisspeptin hormones in the hypothalamus. AR is also thought to act to promote male-specific sexual behaviour, and mice with ablation of neural AR show dysfunction in both the HPG axis regulation and sexual behaviour (Raskin et al., 2009). Time and technical limitations prevented the analysis of the sites of AR ablation in the brain, but since FoxG1-ARKO mice do not appear to have dysfunction in either HPG axis regulation or sexual behaviour it is unlikely that complete ablation of AR has occurred in the neural populations that control these function.

Examination of the pituitary and hypothalamus-specific function of AR is complicated in FoxG1-ARKO mice by the lack of Cre specificity and therefore ablation of AR in multiple sites. More appropriate Cre lines to use to ablate AR would be ones that specifically target gonadotrophs, GnRH neurons or kisspeptin neurons. Gonadotroph-specific Cre lines include a glycoprotein α subunit-Cre controlled by doxycycline (Naik et al., 2006) or a Cre knock in to the 3' end of one copy of the *Gnrhr* gene (Wen et al., 2008). A random insertion GnRH-Cre line is available that active specifically in GnRH neurons whilst not interfering with GnRH production (Wolfe et al., 2008). Finally a Kisspeptin-Cre line is available with a Cre knock in to the 3' end of one copy of the *Kiss1* gene.

6. Characterisation of the effects AR ablation in the FoxG1-ARKO epididymis

6.1 Introduction

As demonstrated in section 4.2.6, spermatozoa fail to transit the efferent ducts of the FoxG1-ARKO, which implies that the origin of the phenotype may be with dysfunction in the efferent ducts or downstream in the epididymis. Obstructive azoospermia (OA) is the absence of sperm in the ejaculate due to a post-testicular obstruction of the genital tract. Four to six percent of infertile men have obstructive azoospermia (Anon, 2008). Some cases of OA have been linked to congenital bilateral absence of vas deferens due to mutations in the cystic fibrosis transmembrane conductance receptor (Lopez et al., 2010), but most cases of OA have no definitive cause.

Several mouse models of OA exist. Mice with a knock-out of LGR4/GPR48 fail to undergo proper epididymal convolution, and exhibit persistence of an undifferentiated epithelium in the epididymis resulting in OA (Mendive et al., 2006). Male mice with persistent Müllerian ducts develop spermatoceles (spermatozoal cysts in the reproductive tract) in the caput epididymis due to physical inhibition of the coiling and integrity of the epididymis by the aberrant Müllerian duct derived tissue (Tanwar et al., 2010). Mice with homozygous or heterozygous knock-outs of three of the bone morphogenetic protein (BMP) genes display obstructive azoospermia (Hu et al., 2004; Zhao et al., 2001). Other reported models of obstructive azoospermia implicate epithelial dysregulation of the efferent ducts and caput epididymis due to abnormal trans-epithelial fluid transport (Wong, 1990). One such example is the phenotype of mice with a knock-out of GPR64, an orphan GPCR located on the apical membrane of efferent ducts and stereocilia of epididymal caput principal cells (Kirchhoff et al., 2008). GPR64 knock-out mice display a similar stasis of spermatozoa in their efferent ducts, and incorrect fluid transport by the efferent ducts and epididymis is implicated (Davies et al., 2004). Obstructive

azoospermia also occurs in mice treated with the fungicides Benomyl or Carbendazim (Hess and Nakai, 2000; Nakai et al., 1992).

The diverse causes of these OA models implies that the disorder can be caused by specific ablation of a particular gene but also by a failure in the correct morphological development of the epididymis leading to dysregulation of epididymal coiling and segmentation or epithelial function. Testicular dysfunction in the progression of the phenotype is also implicated in the case of chemical insult to the seminiferous epithelium, but this is thought to be in tandem with dysregulation occurring in the efferent ducts and epididymis, implying that these organs play the key role in OA development.

RT-PCR targeting *Ar* exon 2 demonstrates that AR has not been ablated in the epididymis/efferent ducts of the FoxG1-ARKO mouse (section 4.2.8), but this has not been confirmed by immunohistochemistry. Expression of FoxG1 or FoxG1-Cre has also not been documented in the efferent ducts or epididymis. Determination of the action of FoxG1-Cre in the efferent ducts and epididymis will assist in the elucidation of the cause of the phenotype in the FoxG1-ARKO, and whether it can be explained by the partial ablation of AR in the testis alone, or also has a contribution from ablation in the efferent ducts or epididymis.

6.1.1 Aims

- To characterise the expression of FoxG1-Cre in the efferent ducts and epididymis, and determine if this has resulted in an ablation of AR in the FoxG1-ARKO efferent ducts or epididymis.
- To characterise the OA phenotype and determine if it has been caused by dysfunction in the efferent ducts or epididymis.

6.2 Results

6.2.1 Spermatozoa progressively block the efferent ducts

Characterisation of the progression of the FoxG1-ARKO efferent duct block was undertaken by histological examination of the efferent ducts at d11, d21 and d100 (Figure 6-1). At d11, the efferent ducts of FoxG1-ARKO mice were indistinguishable from those in controls. In both cases, the efferent ducts appeared patent, with cellular debris within the lumen. At d21, an increase in the amount of cellular debris and proteinaceous exudate was observed in the efferent ducts of FoxG1-ARKO mice compared with that in controls. At d100, clusters of spermatozoa were evident in the efferent ducts of the FoxG1-ARKO and these appeared to have formed a physical ‘block’, preventing spermatozoa from passing through the lumen. Conversely, control efferent duct lumens did not contain obvious groups of cells/spermatozoa at d21 or d100.

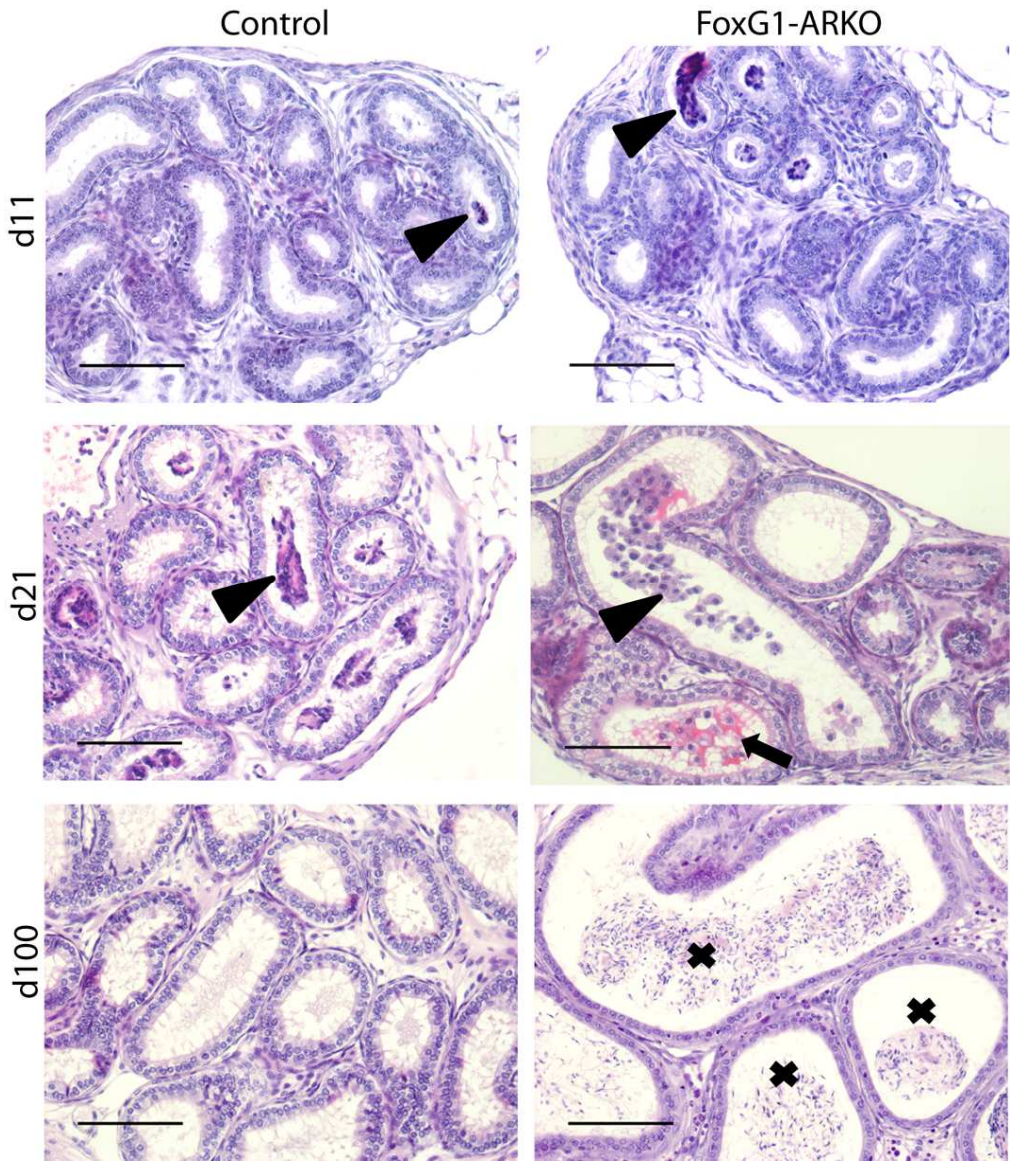

Figure 6-1: Comparison of histology of efferent ducts at d11, d21 and d100

d11 control and FoxG1-ARKO efferent ducts are visibly similar, with cellular debris present in the lumens of both (arrowheads). Efferent ducts of d21 control and FoxG1-ARKOs also contain cellular debris (arrowheads) but d21 FoxG1-ARKO efferent ducts are beginning to accumulate eosinophilic proteinaceous material (arrow). d100 control efferent ducts have empty, patent lumens, unlike d100 FoxG1-ARKO efferent ducts which are distended and contain spermatozoa and cellular debris in their lumens (crosses). Scale bars are 100 µm.

6.2.2 Macroscopic comparison of FoxG1-ARKO and control testis, efferent ducts and epididymis

During dissection, it was noted that epididymides of FoxG1-ARKO mice were smaller and a different shape to controls. When compared at d11 and d16, control and FoxG1-ARKO epididymides were morphologically similar (Figure 6-2). At d21 the FoxG1-ARKO caput epididymis appeared to be smaller than that of the control. At d100, the whole epididymis of the FoxG1-ARKO was smaller than the control. The FoxG1-ARKO caput was narrower and flatter than that of the control and the efferent ducts appeared to connect to the epididymis at the top of the epididymal tunica rather than at the side as seen in the control.

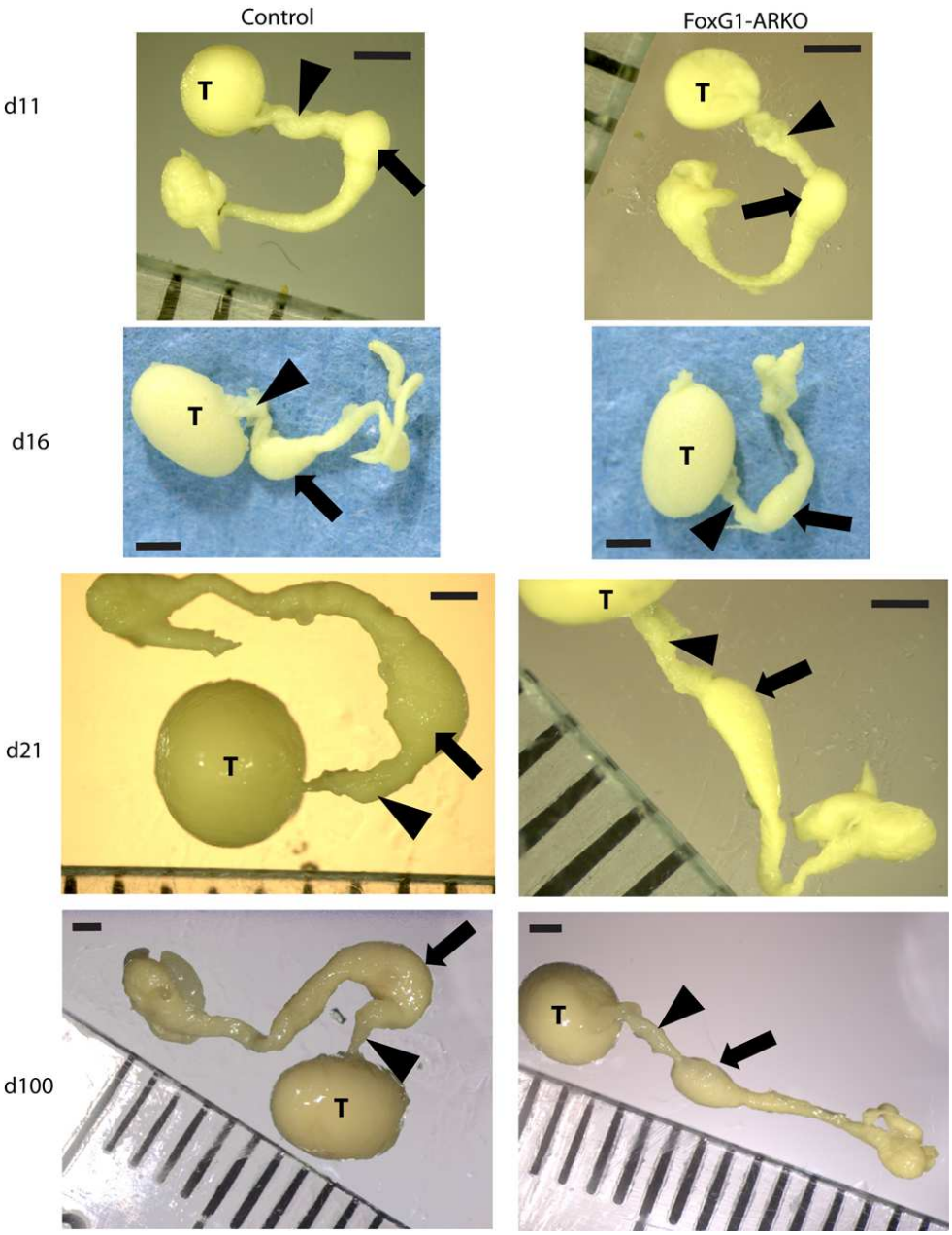

Figure 6-2: Macroscopic comparison of testis, efferent ducts and epididymis of control and FoxG1-ARKO mice at d11, d16, d21 and d100

At d11 and d16 FoxG1-ARKO testes (T), efferent ducts (arrowheads) and proximal epididymis are a similar size to controls. At d21 and d100 a decrease in the size of the FoxG1-ARKO caput epididymis is apparent when compared to the control. Scale bars are 1mm.

This apparent visual difference in size was also reflected in a difference in weight (Table 6-1, Figure 6-3). The mean post-fixation weight of FoxG1-ARKO efferent ducts and epididymis together (ED/epi) did not significantly differ from controls at d11 and d16. FoxG1-ARKO mean ED/epi weight was significantly smaller than controls at d21, d35 and d100. Reduction in weight could have been due to the lack of sperm in the epididymis, therefore the weights of epididymides from SCARKO mice were measured and compared to control littermates (the SCARKO does not have post-meiotic germ cells hence no spermatozoa in epididymis, but with no epididymal ablation of AR). The weight of SCARKO ED/epi at d100 was not significantly different to their control littermates despite lacking spermatozoa, which implied that the difference in mean weight of the FoxG1-ARKO ED/epi to the control was not due solely to lack of spermatozoa.

Table 6-1: Mean weights of control and FoxG1-ARKO epididymides (including efferent ducts) at d11, d16, d21 and d100

**Key: Control-F = FoxG1-ARKO control littermates, Control-S= SCARKO littermates*

	d11	**d16**	**d21**	**d35**	**d100**
Control-F*	2.2 mg	4.5 mg	8.1 mg	18.3 mg	47.4 mg
FoxG1-ARKO	1.8 mg	3.7 mg,	4.5 mg	8.0 mg	25.5 mg
***P* value**	*P*>0.05	*P*>0.05	*P*≤0.05	*P*≤0.001	*P*≤0.001
Control-S*	/	/	/	/	38.2 mg
SCARKO	/	/	/	/	34.1 mg
***P* value**	/	/	/	/	*P*>0.05

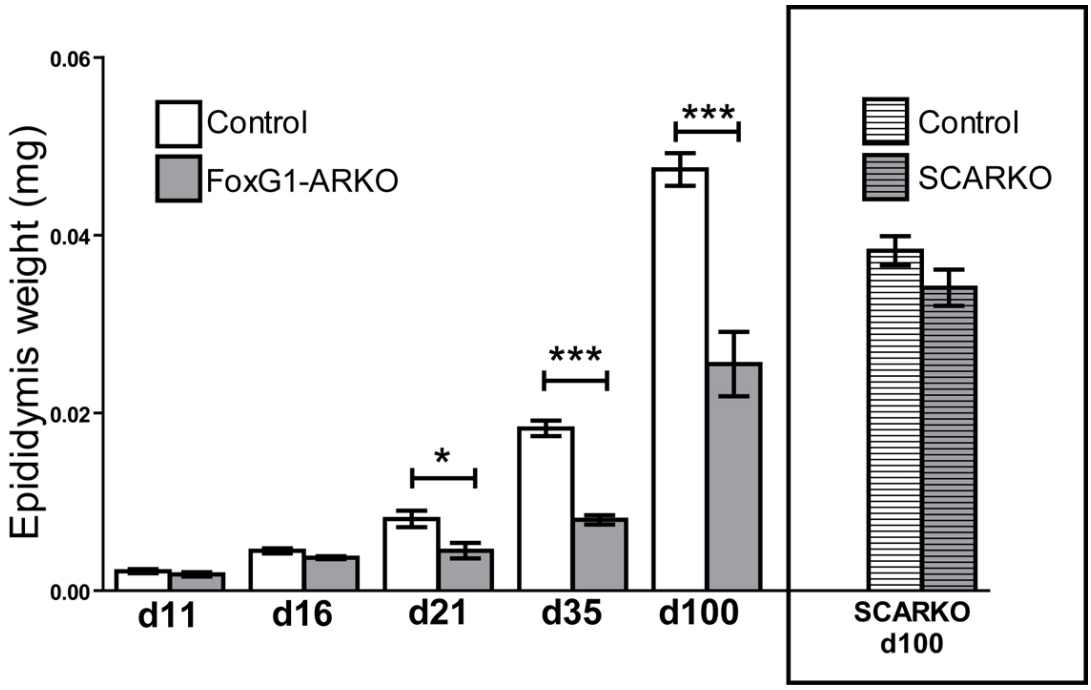

Figure 6-3: Mean weights of control and FoxG1-ARKO epididymides (including efferent ducts) at d11, d16, d21 and d100

*At d11 and d16, mean FoxG1-ARKO epididymis weight is not significantly different to mean control epididymis weight. At d21, d35 and d100 mean FoxG1-ARKO epididymis weight is significantly reduced compared to control. Mean d100 SCARKO epididymis weight is not significantly different to its corresponding littermate control. n≥5 for each group. All values are means ± SEM.*P≤0.05, ***P≤0.001.*

6.2.3 Gross and histological comparison of whole FoxG1-ARKO and control epididymides

FoxG1-ARKO epididymides were visibly smaller compared to controls when examined at d100 (Figure 6-4a). Histological examination, of longitudinal sections through the epididymis of FoxG1-ARKO and control animals revealed that the initial segment (IS) was absent from d100 FoxG1-ARKO epididymides (Figure 6-4b). The caput, corpus and cauda epididymis regions of the FoxG1-ARKO all appeared smaller both in gross and thin-section.

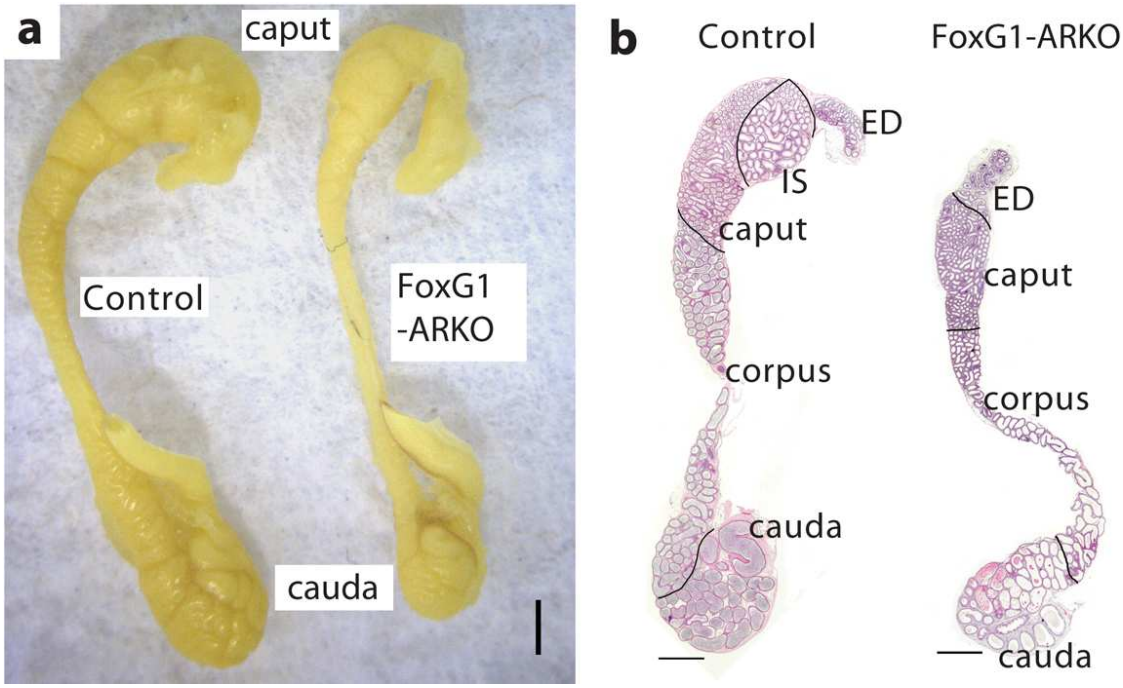

Figure 6-4: Gross and histological comparison of whole d100 control and FoxG1-ARKO epididymides

(a) Gross image of Bouin's-fixed d100 control and FoxG1-ARKO epididymides: note that the FoxG1-ARKO epididymis appears smaller when compared to the control. (b) Histological analysis of d100 control and FoxG1-ARKO epididymides shows that the FoxG1-ARKO epididymis is missing the initial segment of the proximal caput (segment I) that is distinctly present in the control. Scale bars are 1 mm.

6.2.4 FoxG1 protein localisation in wild-type efferent ducts and epididymis

Thin sections of d100 wild-type efferent ducts and epididymis were immunostained for FoxG1 protein to identify/establish where it was localised in these tissues (Figure 6-5). FoxG1 was localised to the nucleus and cytoplasm of the ciliated cells of the efferent ducts, and to the nucleus and cytoplasm of sporadic cell groups of the epithelium of the caput segment III, corpus and cauda epididymis. It was not localised at all to the initial segment I, and was only localised to the nucleus of some apical cells of the caput segment II. FoxG1 protein was however localised to the proximal part of the epididymis at d2.

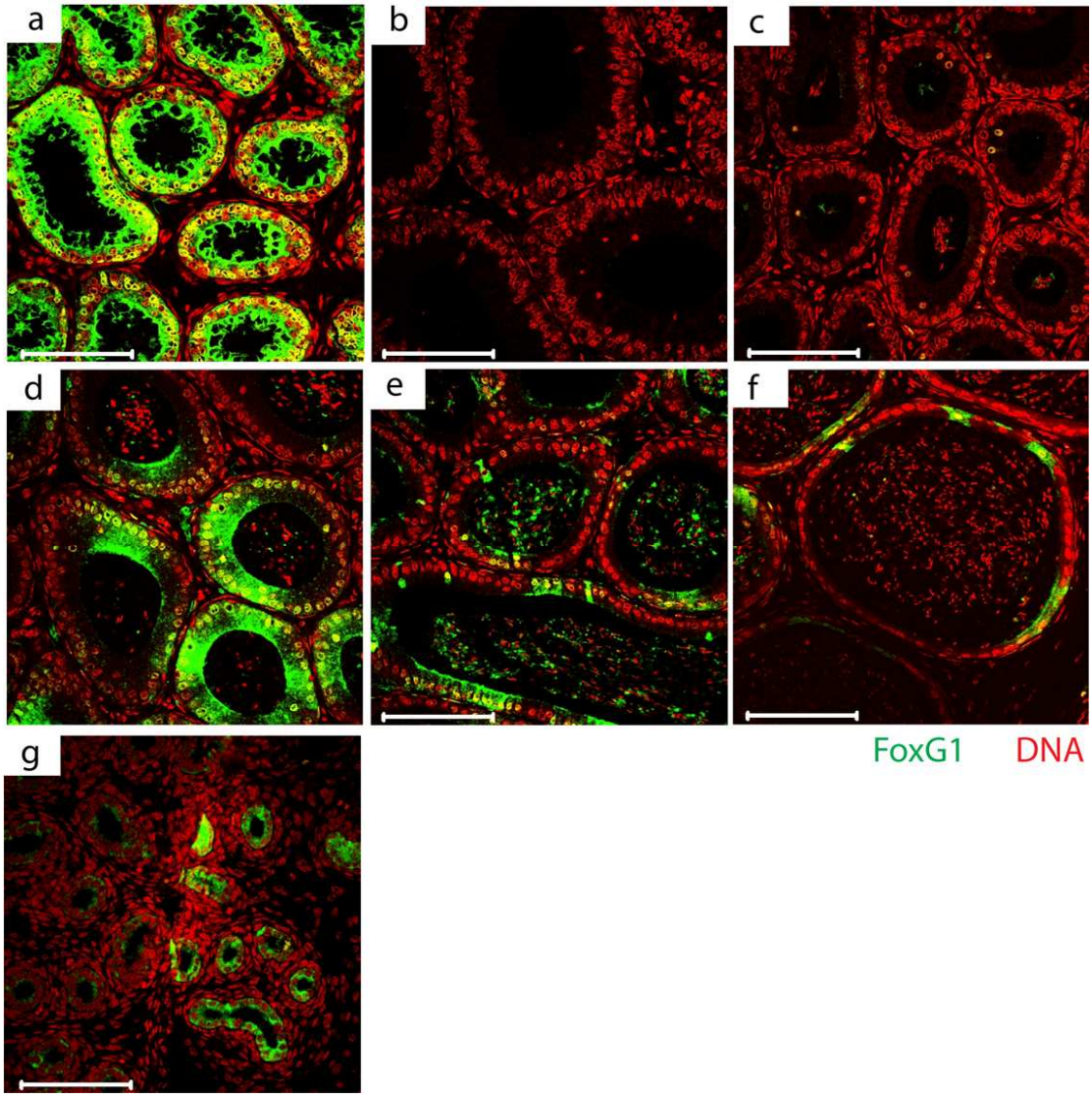

Figure 6-5: FoxG1 immunolocalisation in d100 wild-type efferent ducts and epididymis

FoxG1 is present in the epithelium of d100 efferent ducts (a), caput segment III (d), corpus (e) and cauda (f) epididymis, as well as in tubules of the d2 proximal epididymis (g). FoxG1 is not present in the epithelium of the d100 epididymal caput segment I (b) or segment II (c). Scale bars are 100 µm.

6.2.5 YFP protein localisation in FoxG1-YFP efferent ducts and epididymides

FoxG1-Cre stud males were mated to females carrying a Cre Recombinase inducible YFP reporter gene, to demonstrate Cre Recombinase functional expression. Immunohistochemistry for YFP in the efferent ducts and epididymis of d100 FoxG1-YFP mice revealed that expression of YFP could be detected in the proximal efferent duct and epididymal epithelium. This expression was mosaic and was not detected in stromal cells. YFP is not expressed in the epithelium of distal efferent ducts of FoxG1-YFP mice.

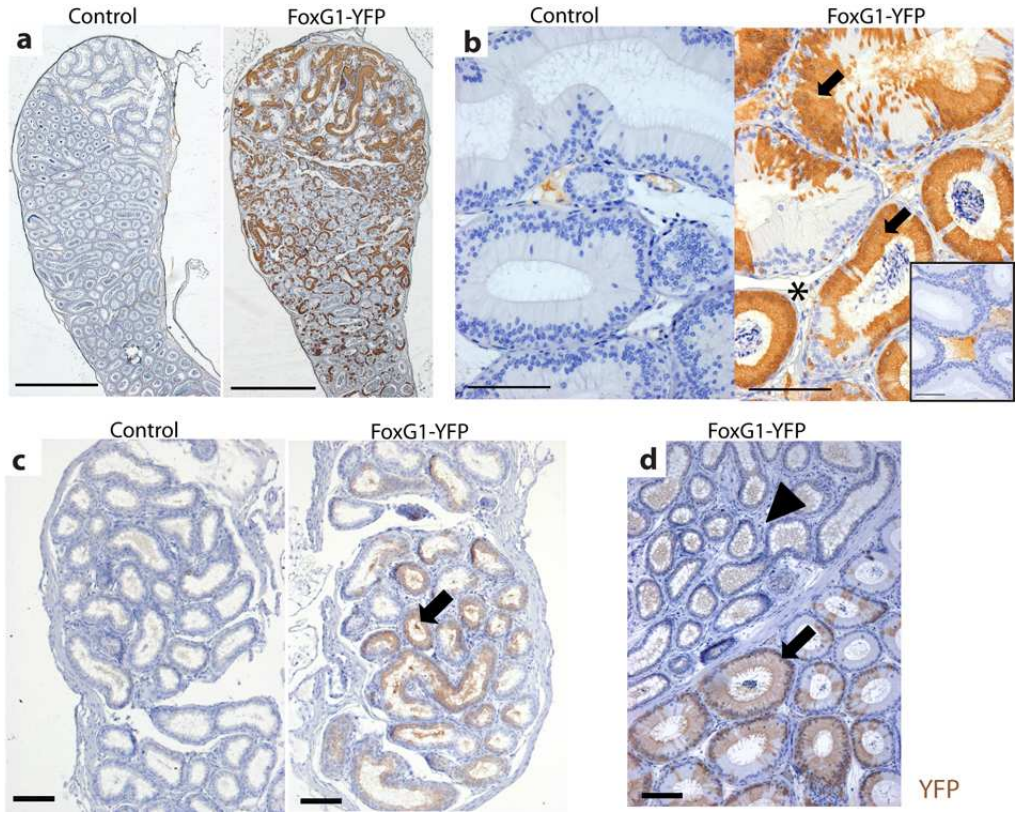

Figure 6-6: YFP immuno-localisation in d100 control and FoxG1-YFP epididymis and efferent ducts

(a) YFP is present in the post-natal caput epididymis of FoxG1-YFP mice, but not in control littermates. (b) YFP expression is confined to the epithelium of the epididymis (arrow) and is not expressed in the stroma (asterisk). Inset: no-primary control showing interstitial non-specific staining. (c) YFP is present in the epithelium of the post-natal proximal efferent ducts of FoxG1-YFP mice, but not in control littermates. (d) YFP is not expressed in the epithelium of distal efferent ducts of FoxG1-YFP mice (arrowhead) whereas it can be seen in the initial segment of the same mouse (arrow). Scale bars are 1 mm for a and 100 µm for b, c and d.

6.2.6 AR protein localisation in control and FoxG1-ARKO efferent ducts and epididymides

AR immunostaining and quantification revealed that AR protein was not expressed in 37% of the principal epithelial cells of the proximal caput epididymis at d2 and 67% at d100 (Figure 6-7).

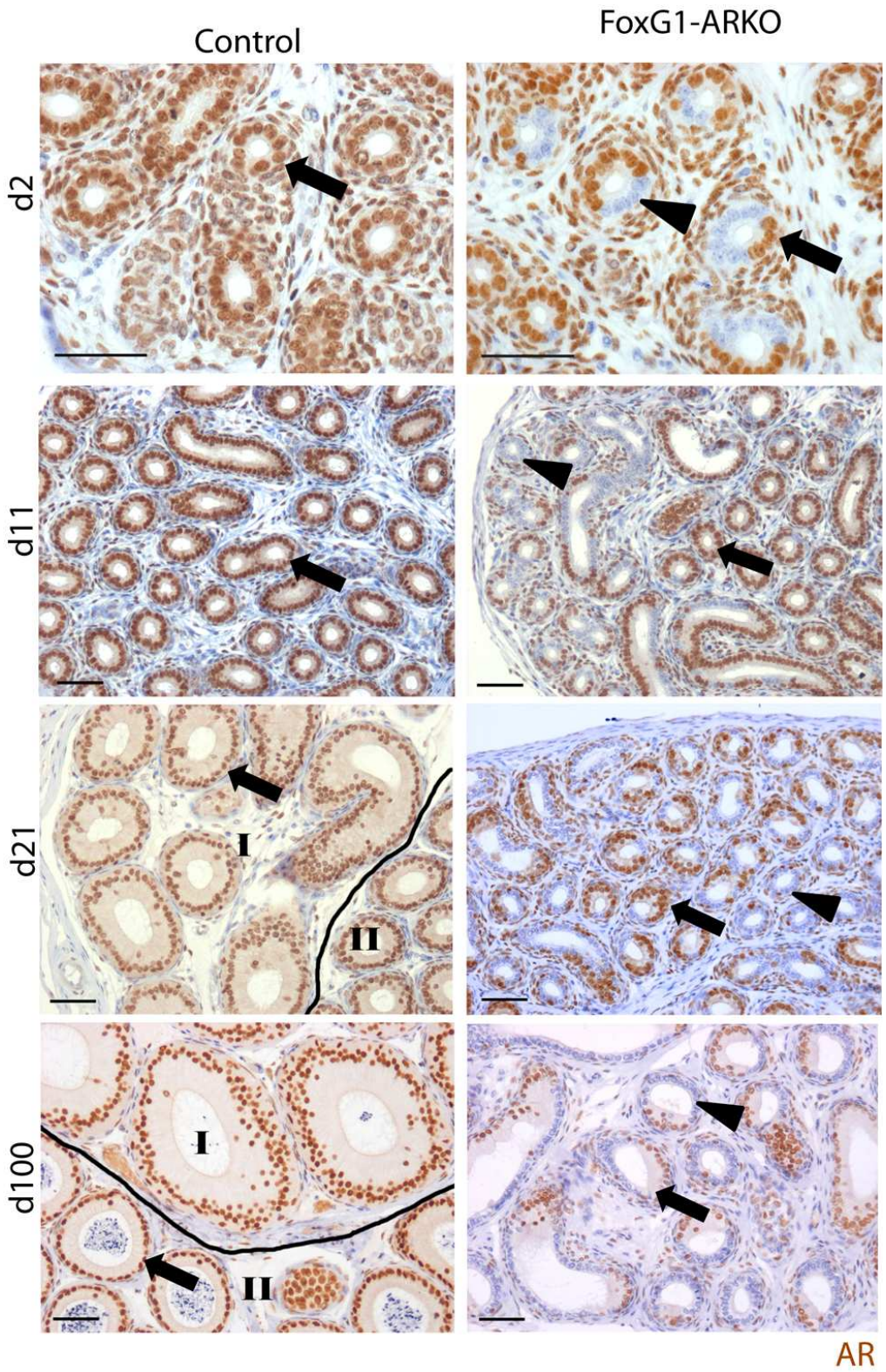

Figure 6-7: AR immuno-localisation in d2, d11, d21 and d100 control and FoxG1-ARKO proximal caput epididymis

Figure 6-7: AR immuno-localisation in d2, d11, d21 and d100 control and FoxG1-ARKO proximal caput epididymis (figure on preceding page)

d11 control caput epididymal epithelium is low columnar and AR-positive (arrow). d11 FoxG1-ARKO caput epididymal epithelium appears grossly similar to that in controls but with areas of epithelial AR ablation (arrowheads). d21 control caput epididymal epithelium has begun to increase in height where the initial segment (I) will develop, and is distinguishable from the proximal caput (II), conversely epididymal epithelium of the d21 FoxG1-ARKO remains low columnar. d100 control proximal epididymis is segmented with epithelium characteristic of the tall pseudo-stratified columnar epithelium of the IS (I) next to the lower columnar epithelium of the proximal caput (II). d100 FoxG1-ARKO proximal epididymis is disordered with no epithelial characteristics of the IS. AR-negative areas (arrowhead) of d100 FoxG1-ARKO epithelium are shorter, with more columnar cells (arrowhead), compared to AR-positive epithelial cells which are taller (arrow) and visibly similar to segment II rather than segment I of the control. Scale bars = 50 µm.

Ablation of AR was limited to principal cells whereas basal epithelial cells were all positive for AR in FoxG1-ARKO mice, as in controls (Figure 6-8). Small foci of AR ablation were occasionally noted in the remainder of the epididymis in FoxG1-ARKO, but these were too irregular and few to merit quantification. All epididymal epithelial cells were immunopositive for AR in controls.

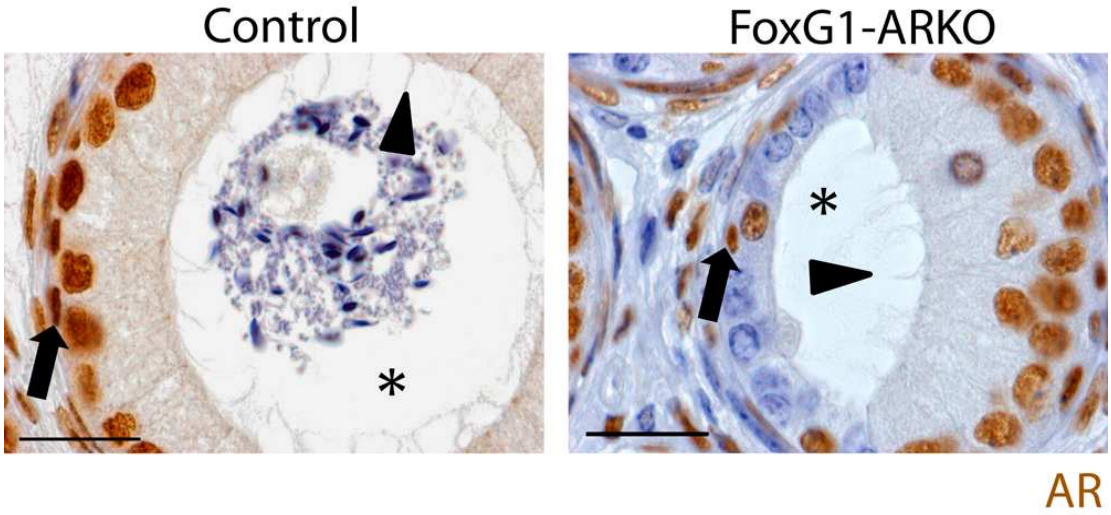

Figure 6-8: Histological comparison of the epithelium and lumen of segment II of d100 control and FoxG1-ARKO

d100 FoxG1-ARKO epididymides have a visible reduction in height of AR-negative compared to AR-positive epithelial cells. Basal cells in the proximal epididymal epithelium of the FoxG1-ARKO are AR-positive (arrows). The proximal epididymal lumen in the FoxG1-ARKO is irregularly shaped compared to the circular lumen of controls (asterisks). Microvilli are present on the apical surface of AR-positive epithelial cells in d100 control and FoxG1-ARKO (arrowheads) but are absent in AR-negative epithelial cells of the FoxG1-ARKO. Scale bars are 20 µm.

Immunostaining for AR protein in the efferent ducts demonstrated that neither control nor FoxG1-ARKO efferent duct epithelia displayed areas of ablation of AR at d11, d21 or d100 (Figure 6-9).

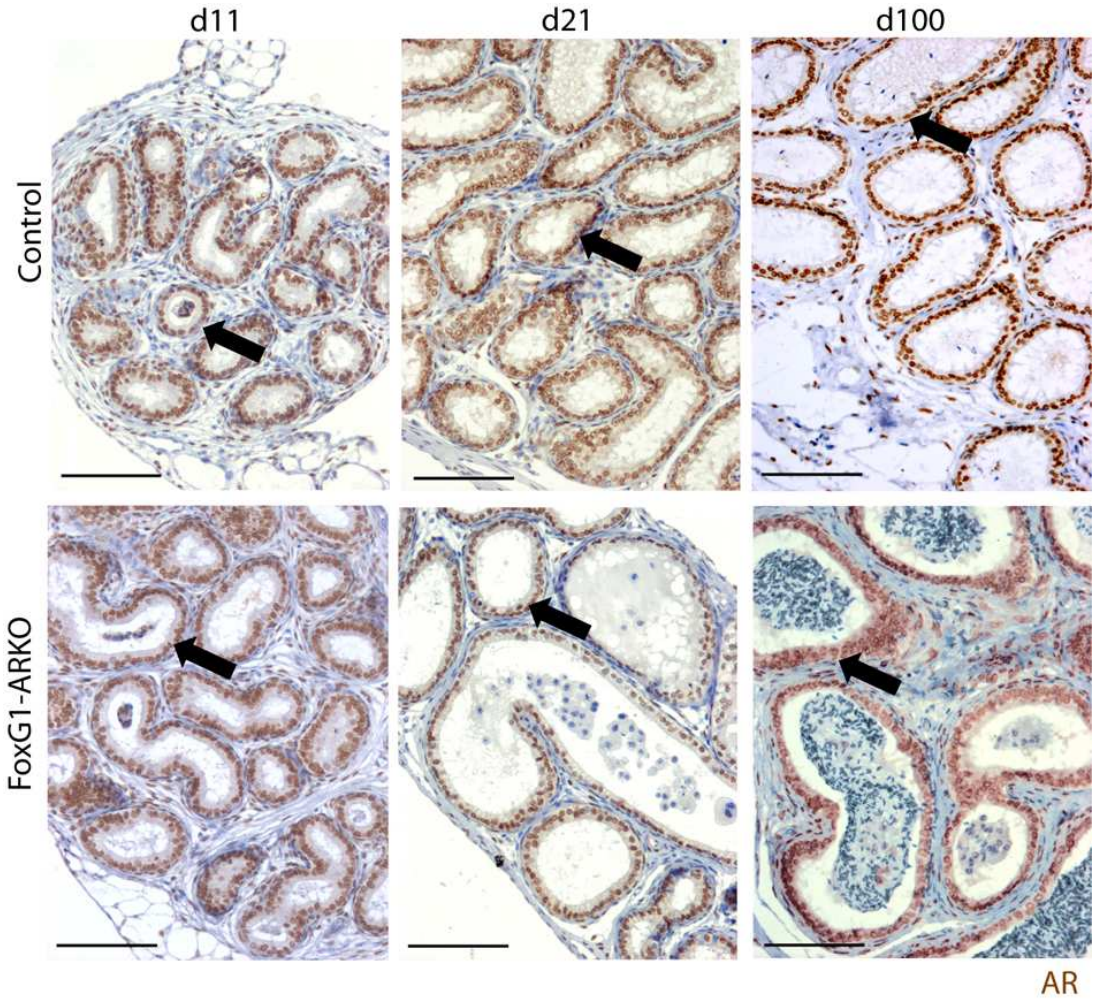

Figure 6-9: AR immuno-localisation in d11, d21 and d100 control and FoxG1-ARKO efferent ducts

Note that AR is expressed in all cells of the control and FoxG1-ARKO efferent duct epithelium at d11, d21 and d100 (arrows).

6.2.7 Development of control and FoxG1-ARKO epididymides

Control and FoxG1-ARKO caput epididymides were examined at d11, d21 and d100 to determine if the initial segment failed to develop or developed and later regressed (Figure 6-7). At d11 the proximal caput epididymal epithelium in the FoxG1-ARKO appeared morphologically similar to that in controls. Mosaic loss of epithelial AR was already apparent in the d11 FoxG1-ARKO. At d21, differentiation of the caput epididymal epithelium was observed in controls; evidence of this includes the development of a visibly distinguishable initial segment precursor, characterised by increasing epithelial cell height and lumen diameter. The initial segment precursor was not obvious in the FoxG1-ARKO at d21 and the AR-negative cells in the proximal caput epithelium did not display an increase in height. At d100, control animals displayed a well developed IS characterised by tall pseudo-stratified columnar epithelia and large tubule lumen. Conversely, epithelial cells in the FoxG1-ARKO segment immediately distal to the efferent ducts resembled those found in segment II, the proximal caput of the control; as a result, the single lobe of efferent ducts within the epididymal tunica of FoxG1- ARKO mice connected directly to segment II, the proximal caput.

6.2.8 Epithelial cell morphology and lumen diameter in segment II of d100 control and FoxG1-ARKO epididymides

On histological examination, AR-positive epithelial cells in the FoxG1-ARKO caput epididymis were visibly increased in height compared to AR-negative epithelial cells (Figure 6-8). This was confirmed when measurements of cell heights were taken (Table 6-2, Figure 6-10). Mean height of FoxG1-ARKO AR- epithelial cells in segment II was significantly reduced compared to AR+ epithelial cells in segment II at d11, d21 and d100. AR positive epithelial cells in FoxG1-ARKO mice did not differ significantly in height from the AR-positive epithelial cells in control epididymides at d11, d21 or d100.

Table 6-2: Comparison of mean heights of control epididymal segment II epithelium with both AR+ and AR- cells in the FoxG1-ARKO epididymal segment II epithelium

	d11	**d21**	**d100**
FoxG1-ARKO (AR+)	14.1 µm	17.3 µm	23.4 µm
FoxG1-ARKO (AR-)	10.9 µm	10.5 µm,	13.4 µm
***P* value** (FoxG1-ARKO AR+ vs FoxG1-ARKO AR-)	*P*≤0.001	*P*≤0.005	*P*≤0.005
Control (AR+)	14.3 µm	20.3 µm	25.8 µm
***P* value** (control AR+ vs FoxG1-ARKO AR+)	*P*>0.05	*P*>0.05	*P*>0.05

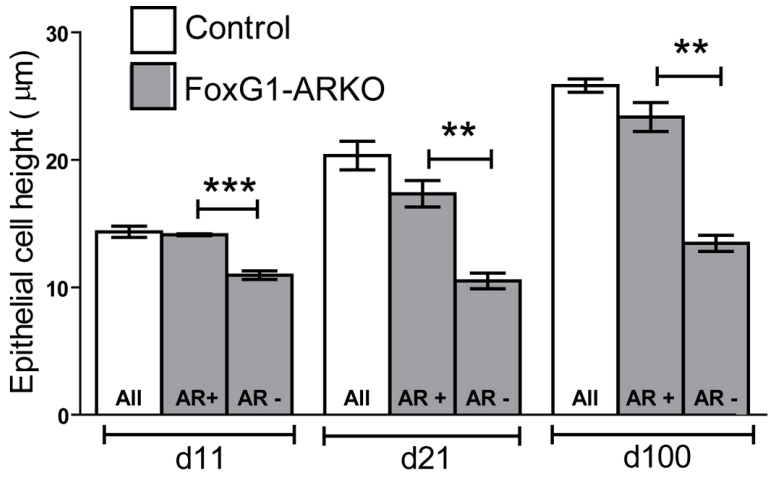

Figure 6-10: Comparison of mean heights of control epididymal segment II epithelium with both AR+ and AR- cells in the FoxG1-ARKO epididymal segment II epithelium

*The height of AR-negative epithelial cells is significantly smaller than that of AR-positive epithelial cells within FoxG1-ARKO proximal caput epididymis at d11, d21 and d100. There was no significant difference between the AR-positive cells of the proximal caput epididymis in controls and FoxG1-ARKOs at any age examined. Values are means ± SEM, n= 3 mice for each group. (*** P≤0.001, ** P≤0.005).*

Upon histological examination, the mean lumen radius in the proximal caput region in d100 FoxG1-ARKO mice appeared smaller than those of the comparable segment

II region in d100 control mice. Quantification revealed that at d11, mean epididymal lumen radius in segment II of FoxG1-ARKO mice was similar to that of the controls, but at d21 and d100 the FoxG1-ARKO lumen radius was significantly smaller than controls (Table 6-3, Figure 6-11).

Table 6-3: Comparison of control and FoxG1-ARKO mean epididymal segment II lumen radius

	d11	**d21**	**d100**
Control	8.2 µm	15.1 µm	32.5 µm
FoxG1-ARKO	8.2 µm	9.5 µm	17.3 µm
***P* value**	*P*>0.05	*P*≤0.001	*P*≤0.001

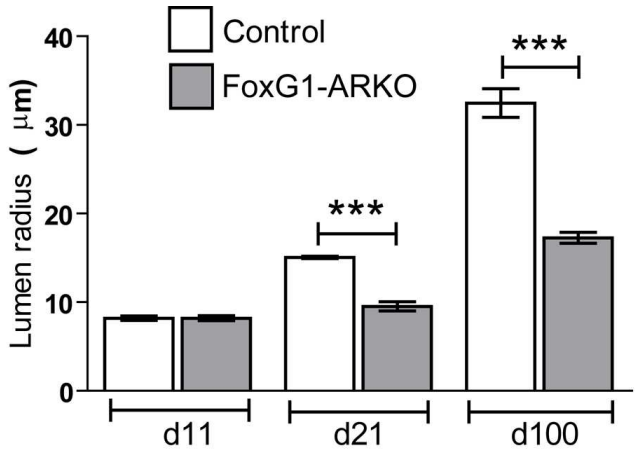

Figure 6-11: Comparison of control and FoxG1-ARKO mean epididymal segment II lumen radius

*At d11 the caput epididymal lumen radius of FoxG1-ARKO mice is not significantly different to that of control mice. At d21 and d100 proximal caput epididymal lumen of FoxG1-ARKO mice is significantly smaller than that of control mice (*** P≤0.001). Values are means ± SEM, n= 3 mice for each group.*

6.2.9 ERα protein localisation in segment II of control and FoxG1-ARKO epididymides

ERα is thought to be a regulator of fluid absorption in the efferent ducts and proximal epididymis (Joseph et al., 2010a). To investigate whether the expression of ERα was affected by the disruption to the epididymal epithelium, thin sections of epididymis and efferent ducts from d100 FoxG1-ARKO mice were immunostained for ERα (Figure 6-12). ERα staining in controls correlated with previously published literature (Zhou et al., 2002). ERα immunostaining was strong in the efferent duct epithelium of the control and FoxG1-ARKO. Only apical and narrow cells of the epithelium of segment I of the control stained positive for ERα, whereas the FoxG1-ARKO did not develop a segment I so staining could not be assessed. Only apical and narrow cells of the epithelium of the control segment II stained positive for ERα, whereas all AR-ablated cells of the FoxG1-ARKO segment II stained strongly for ERα. In segment III of the control, all apical cells and some principal cells stained for ERα but all principal cells in the FoxG1-ARKO are ERα positive.

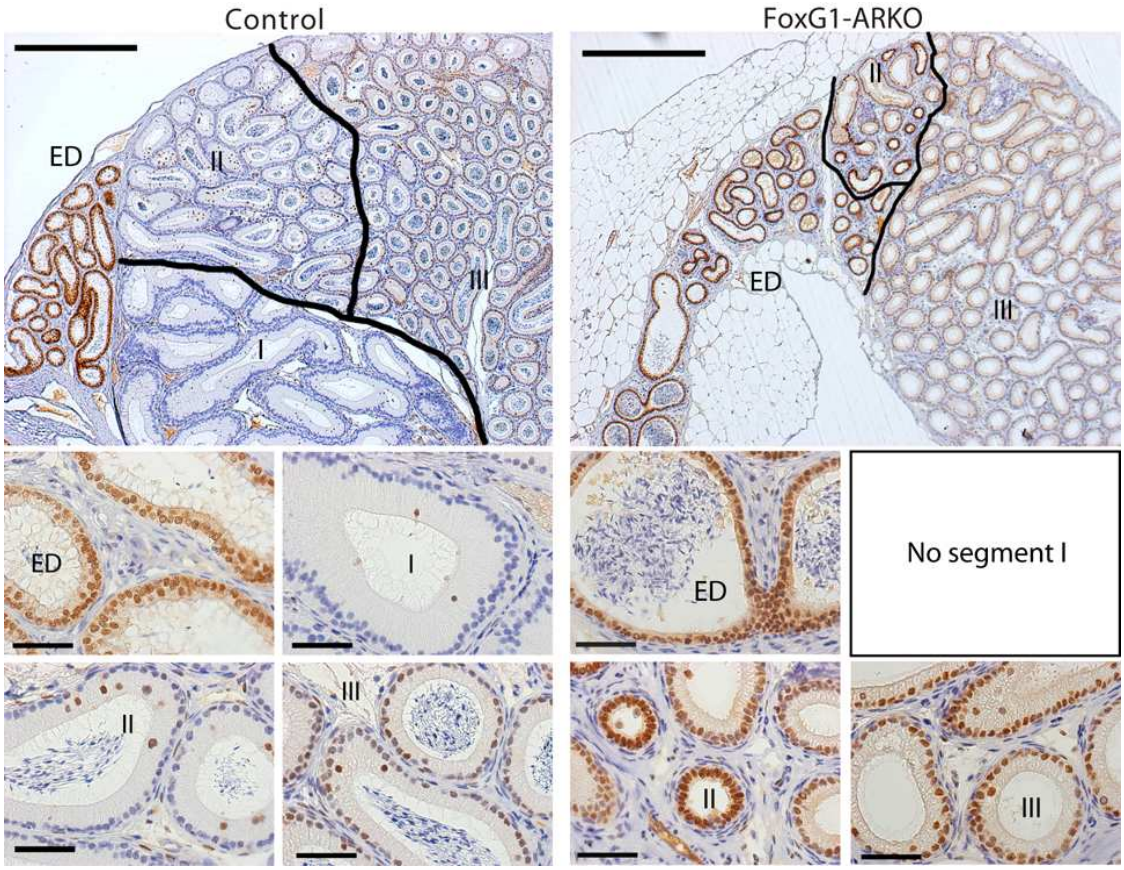

Figure 6-12: ERα immunostaining in d100 control and FoxG1-ARKO efferent ducts and proximal epididymis

ERα immunostaining is strong in the efferent duct epithelium of the control and FoxG1-ARKO. Only apical and narrow cells of the epithelium of segment I of the control stain positive for ER, whereas the FoxG1-ARKO does not develop a segment I. Only apical and narrow cells of the epithelium of the control segment II stain positive for ERα, whereas all AR-ablated cells of the FoxG1-ARKO segment II stain strongly for ERα. In segment III of the control, all apical cells and some principal cells stain for ERα but all principal cells in the FoxG1-ARKO appear to stain for ERα. Key: ED = efferent ducts, I, II and III are segments I, II or III. Scale bars are 500 µm for main images and 50 µm for high magnification insets.

6.2.10 SMA protein localisation in segment II of control and FoxG1-ARKO epididymides

Dysregulation in the epithelial layer of hormone responsive tissues is known to affect the underlying stromal layer (Cunha et al., 1996), so to investigate whether the

smooth muscle interface between the stroma and epithelium was affected by the disruption to the epididymal epithelium, thin sections of epididymis from d11 and d100 FoxG1-ARKO mice were immunostained for SMA (Figure 6-13). At d11, SMA immunostaining was similar in control and FoxG1-ARKO epididymides, appearing as a strongly staining ring around the tubules. However, at d100 the smooth muscle layer of the FoxG1-ARKO epididymis was disorganised with evidence of disruption at specific foci.

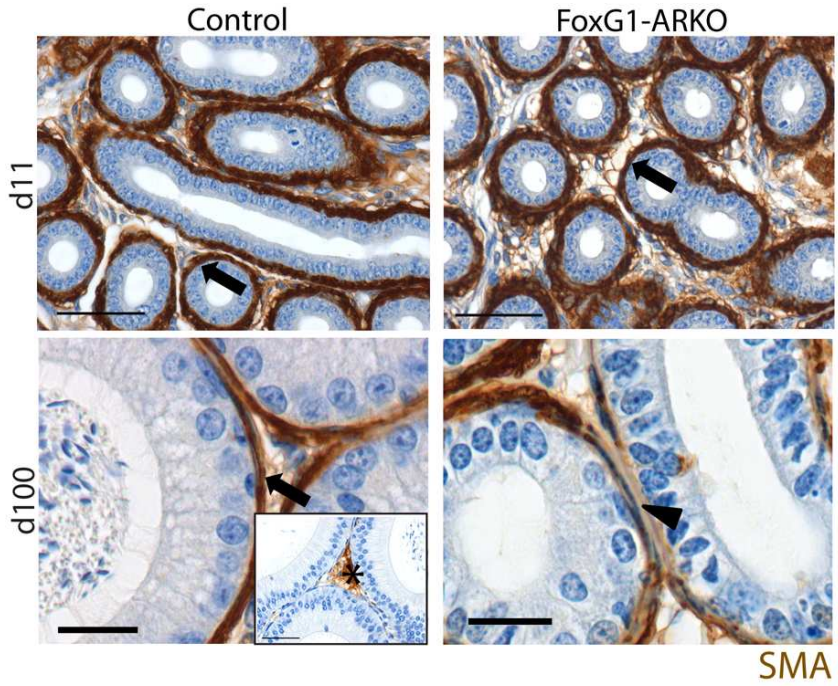

Figure 6-13: SMA staining in caput epididymides of d11 and d100 control and FoxG1-ARKO mice

At d11, SMA immunostaining appears as a thick layer around the outside of the tubule in both control and FoxG1-ARKO caput epididymides (arrows). At d100, SMA immunostaining is an unbroken thinner layer around the tubules in segment II of control epididymides (arrow) but staining is interrupted around the tubules in the caput region of FoxG1-ARKO (arrowhead). Inset: no-primary control non-specific interstitial staining (asterisks). Scale bars = 20µm.

6.2.11 Levels of *Gpr64* in FoxG1-ARKO epididymis

Since the GPR64 knockout mouse has a similar phenotype to the FoxG1-ARKO (Davies et al., 2004), the levels of *Gpr64* transcript in the control and the FoxG1-ARKO were quantified using TaqMan qRT-PCR (Figure 6-14). Levels of *Gpr64*

transcript were lower that the control at d11, d16, d21 and d100, but the difference was only significant at d21.

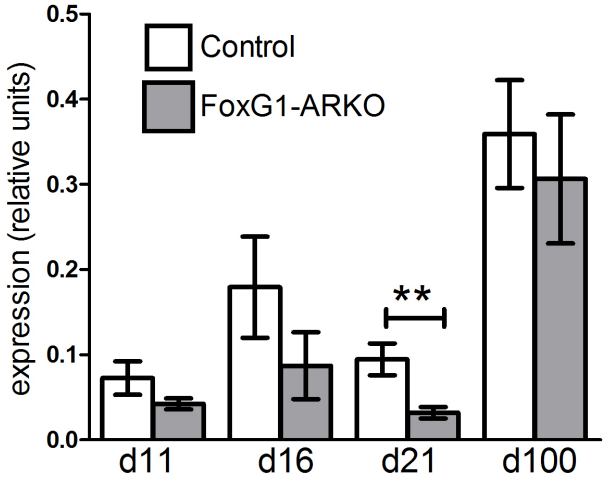

Figure 6-14: Expression levels of Gpr64 transcript in control and FoxG1-ARKO epididymides at selected post-natal ages

Levels of Gpr64 transcript were lower that the control at d11, d16, d21 and d100, but the difference was only significant at d21.Values are mean ± SEM, n≥4 for each group.

6.2.12 Effects of efferent duct block on FoxG1-ARKO efferent ducts

The efferent ducts of the FoxG1-ARKO do not have an ablation of AR. Despite this, the spermatozoal block occurs in the efferent ducts. The morphology and function of the efferent ducts was assessed to elucidate whether the dysfunction in the efferent ducts was contributing to the phenotype in the FoxG1-ARKO. Development of the efferent ducts of the FoxG1-ARKO has resulted in patent connection to the epididymis, as a low concentration of spermatozoa is still present in the cauda epididymis despite the block that has formed in the efferent ducts (see section 4.2.6). The number of efferent ducts emerging from the testis was between three and five in both the FoxG1-ARKO and the control (Figure 6-15). Cilia present on the apical surface of some cells in the control efferent ducts were also noted in the FoxG1-ARKO (Figure 6-16).

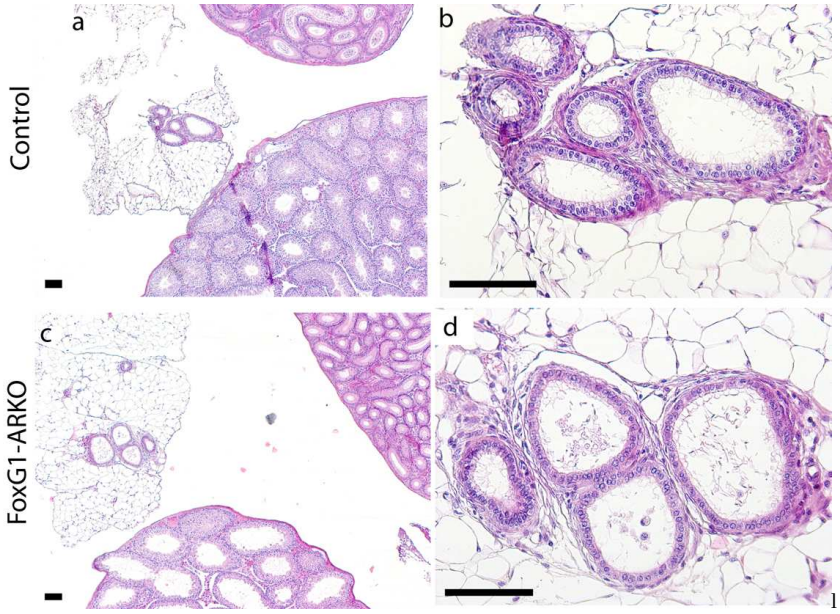

Figure 6-15: Representative images of histology of d35 control and FoxG1-ARKO initial efferent ducts

A transverse section of testis attached to epididymis close to the rete testis shows the number and form of efferent ducts that exit the rete testis. Both control (a, c) and FoxG1-ARKO (b, d) mice typically have from three to five efferent ducts. Scale bars are 100 µm.

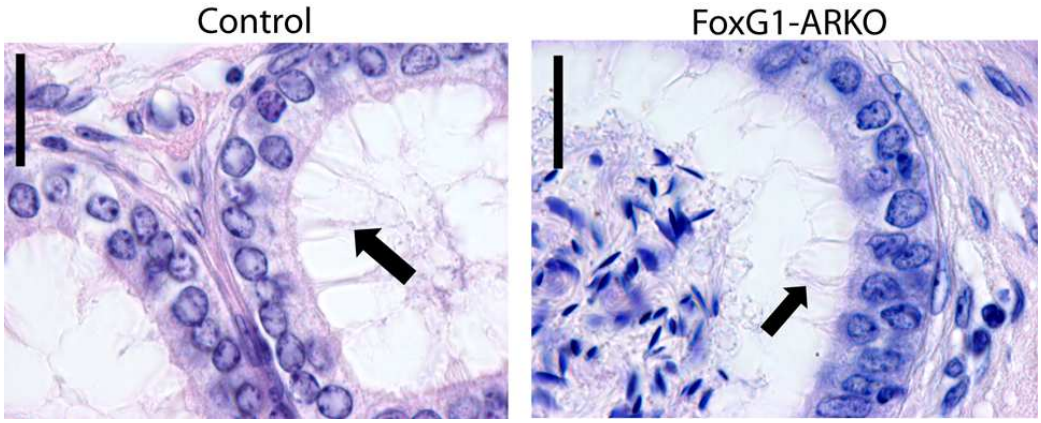

Figure 6-16: Presence of cilia in control and FoxG1-ARKO efferent ducts

Cilia (arrows) are present on the apical surface of some cells in the control efferent ducts, and are also found in the FoxG1-ARKO. Scale bars are 20µm.

6.2.13 Immunostaining for CD45 in control and FoxG1-ARKO efferent ducts

A common feature of efferent duct blockage is immune cell infiltration and phagocytosis of sperm by the epithelium (Hess and Nakai, 2000; Mendive et al.,

2006; Nakai et al., 1992). Therefore immunostaining for CD45 (a pan-immune cell marker) was utilised to determine if inflammation was occurring in the efferent ducts as a consequence of the sperm block (Figure 6-17). The occasional cell was CD45+ in the efferent duct stroma of d100 controls. Conversely, the efferent ducts of d100 FoxG1-ARKO mice displayed widespread CD45 immunostaining in stromal, epithelial and luminal compartments of the efferent ducts. Phagocytosis of stagnant sperm was apparent in the epithelia of some efferent duct cross-sections, as shown by dense accumulations of the characteristic 'hooked' spermatozoa heads inside CD45+ cells in the epithelium.

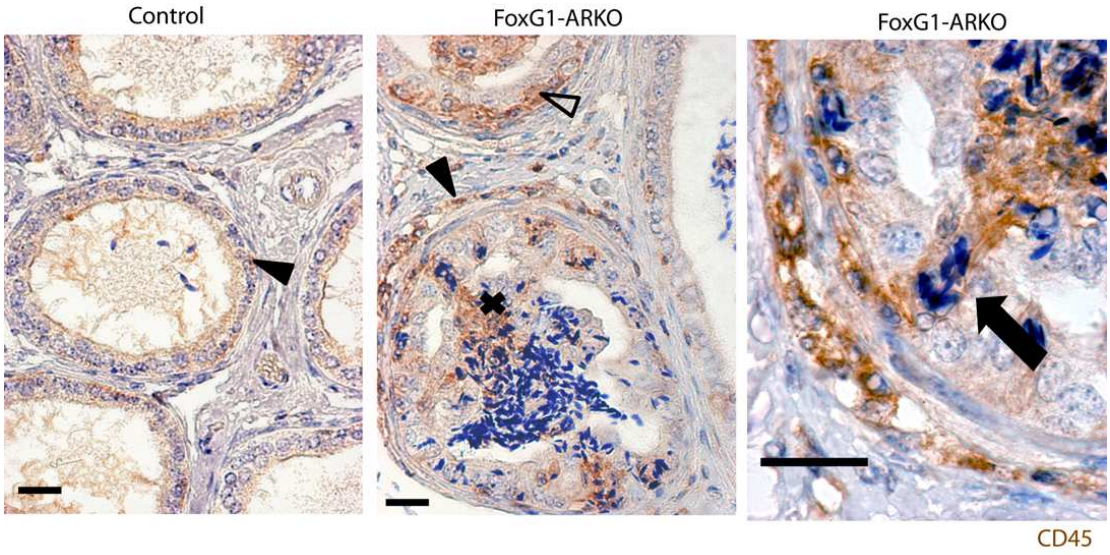

Figure 6-17: CD45 staining in control and FoxG1-ARKO efferent ducts

Specific staining for CD45 can be seen in the occasional stromal cell in d100 control efferent ducts (solid arrowhead) but can be seen in stromal (solid arrowhead), epithelial (outline arrowhead) and luminal (cross) cells in the d100 FoxG1-ARKO efferent ducts. Higher magnification image shows phagocytosis of spermatozoa heads by the FoxG1-ARKO efferent duct epithelium (arrow). Scale bars are 20 µm.

6.3 Discussion

The aims of this chapter were to characterise the expression of FoxG1-Cre in the efferent ducts and epididymis, and determine if this has resulted in an ablation of AR in the FoxG1-ARKO efferent ducts or epididymis, and to characterise the efferent duct block phenotype and determine if it has been caused by dysfunction in the efferent ducts or epididymis. Lack of ablation of *Ar* exon 2 in the epididymis (see section 4.2.8) implied that there was no ablation of AR protein in the epididymis. However, on immunohistochemical staining, FoxG1-ARKO mice were found to have a partial ablation of AR in the caput epithelium of the epididymis, with 67% of cells lacking AR at d100. This has also been noted in the seminal vesicles of the MHC-Cre ARKO mouse, which displays AR ablation at the protein level that is unable to be detected at the transcript level (Smith group, unpublished data). This observation could be due to the silencing of transcription of the *Ar* gene in a cell due to lack of functional AR protein or the loss of cell identity resulting in suppression of AR expression. A reduced level of mutant *Ar* transcript has previously been noted in gonadal fibroblasts from patients with CAIS (Hellwinkel et al., 1999).

Ablation of AR in the caput epididymis was in a mosaic pattern similar to that seen for endogenous FoxG1 expression and FoxG1-Cre expression. It has been noted that several proteins present in the epididymal epithelium including sulphated glycoprotein 2 (Hermo et al., 1991), immobilin (Hermo et al., 1992) and cyclin D1 (Darwanto et al., 2008) are expressed in this ‘checkerboard’ pattern with the potential explanation that the epididymal epithelium acts as a syncytium to control some functions and that only a percentage of the epithelial cells need to express the protein of interest for the epithelium as a whole to respond.

FoxG1-Cre expression pattern in the epididymis generally followed the expression of endogenous FoxG1. Although endogenous FoxG1 appears to be present throughout the efferent duct epithelium, FoxG1-Cre is present in a mosaic pattern. Both FoxG1 and FoxG1-Cre are present in a mosaic pattern throughout the distal caput, corpus and cauda epithelium, with no expression in mesenchymal tissues. However, at d100,

YFP is not seen in the initial segment or proximal caput (segment I or segment II) of the FoxG1-YFP epididymis. Since YFP is a lineage tracing marker it is probable that endogenous FoxG1 is expressed in segments I and II earlier than d100, but switches off before this age, whereas transgenic YFP activated by FoxG1-Cre persists. Expression of both endogenous FoxG1 and FoxG1-Cre is found in the efferent ducts, whereas ablation of AR does not occur in the efferent ducts. This could potentially be due to strain background effects (the FoxG1-Cre may be active in the efferent ducts in the FoxG1-YFP background but not in the FoxG1-ARKO background) or AR ablation in the developing efferent ducts may have occurred earlier than the age first examined (d2) resulting in apoptosis of the ablated cells and their failure to contribute to the adult efferent ducts. This could be determined by performing immunohistochemistry for AR on efferent ducts of prenatal FoxG1-ARKO mice. It is unlikely that any prenatal ablation of AR in the efferent ducts would contribute to the phenotype, as the efferent ducts appear to develop and function normally prior to and despite the formation of the efferent duct block. Since AR ablation is confirmed and persistent in the epithelium of the caput epididymis, it is likely that dysregulation in this region is the primary cause of the spermatozoa block upstream in the efferent ducts.

The epididymis in FoxG1-ARKO mice is grossly and histologically indistinguishable from that of controls at d2, despite AR ablation in 37% of caput epithelial cells. Normal epididymal development is known to be under the control of androgens, as Wolffian duct-derived tissues are absent at birth in genetic models of ablation of AR function (He et al., 1991; Yeh et al., 2002) and the epididymis fails to coil in male rats treated prenatally with the AR antagonist flutamide (Welsh et al., 2006). However, prenatal androgen action is mediated by stromal AR in the WD, and epithelial androgen receptor is not detected until after the WD has stabilised and begun to coil. These results are consistent with our observation that neonatal development of the FoxG1-ARKO epididymis appears normal. Conversely, early post-natal maturation of the epididymis is compromised in FoxG1-ARKO mice. At d11, control and FoxG1-ARKO epididymides appear grossly similar with no

significant difference in weight, but histological abnormalities were already evident at this age. There is a significant difference in epithelial cell height between AR-positive and AR-negative cells in FoxG1-ARKO epididymides at d11. Previously published literature suggested that the epididymal epithelium in mice exists in an undifferentiated state from d7 to d14 (Avram and Cooper, 2004), at which point a 'precursor' epithelium arises. However our data suggests that the epithelium is already responsive to androgens at d11 and possibly even earlier, as AR-ablated and AR-positive cells at this age display different morphology.

By adulthood, gross abnormalities can be identified in FoxG1-ARKO epididymides. At d100, FoxG1-ARKO mice lack the initial segment (IS, segment I) of the epididymis, so the proximal caput epididymis (segment II) is located immediately distal to the efferent ducts. Analysis of epididymal histology at d11, d21 and d100 demonstrated that the IS was not absent because it had regressed, but rather that it had completely failed to develop in FoxG1-ARKO mice. By d21, the initial segment precursor is obvious in control mice, characterised by increasing epithelial cell height and lumen diameter. However, in the d21 FoxG1-ARKO epididymis, epithelial cells lacking AR failed to increase in height or develop stereocilia in the principal cells of the proximal caput, maintaining a similar morphology to that of the pre-differentiated epithelium at d11. Previously published studies have shown that IS development is under the control of a number of factors including circulating androgens, the product of the gene *Cros* and testicular lumicrine factors (Avram and Cooper, 2004). At day 16, the epithelium of segment I (IS) is reported to become visually distinct from the remaining caput epithelium, whilst segment II (proximal caput) and III (distal caput) of the epididymis appear differentiated by day 21. Acute withdrawal of androgens following orchidectomy results in regression of segment I and de-differentiation of segments II and III to a 'precursor' state, suggesting that continuous androgen exposure is required to maintain a differentiated epididymal epithelium (Avram et al., 2004). Consistent with this, we conclude that in the absence of epithelial AR, the proximal epithelium of the caput is unable to undergo correct terminal differentiation, resulting in complete failure of development of the initial segment.

Since lumicrine factors from the testis are also thought to be needed for maintenance of the initial segment (Abe and Takano, 1989), the presence of an obstruction in the efferent ducts at later ages likely compounds this phenotype by preventing testicular lumicrine factors from passing into the epididymis. This requires further investigation.

AR-negative epithelial cells within the remainder of the FoxG1-ARKO caput epididymis also fail to mature. This resulted in the persistence of areas of undifferentiated epithelium with reduced cell height compared to the AR-positive epithelial cells, and a decrease in lumen size at d11, d21 and d100 in the FoxG1-ARKO caput. The striking difference in both epithelial cell height and morphology between AR-positive and AR-negative cells suggests that the impact of AR-dependent signalling on epithelial cells is predominantly autocrine, not paracrine. Despite lumen diameter differences between the FoxG1-ARKO and control, AR-positive FoxG1-ARKO epithelial cells in the remaining proximal caput of the FoxG1-ARKO did not significantly differ in height compared to cells in segment II of the ubiquitously AR-positive control epididymal epithelium. This suggests that AR-positive caput epithelium in the FoxG1-ARKO is comparable to segment II in the control. The initial segment is believed to develop from a different anlage to the rest of the epididymis, namely the mesonephric tubules, while the remaining caput develops from the Wolffian duct (Marshall et al., 1979). This divergent origin may explain the differential response of the two epididymal regions to AR ablation in FoxG1-ARKO mice, with epithelial AR signalling a fundamental requirement for development of the IS but not the caput; epithelial AR is however important in regulating epithelial cell function in the remainder of the caput.

Previous models of epididymal androgen deprivation by orchidectomy reported apoptosis in the epididymal epithelium (Fan and Robaire, 1998; Takagi-Morishita et al., 2002). In contrast, the epithelium of FoxG1-ARKO mice did not display the characteristic histological signs of apoptosis. It is possible that epithelial cells in FoxG1-ARKO epididymides do not undergo apoptosis because AR has been ablated

from birth and the epithelia never develop correctly, whereas in previous studies androgen withdrawal took place after the differentiation of the epididymal epithelium (Fan and Robaire, 1998; Takagi-Morishita et al., 2002). This suggests that apoptosis either occurs in epithelial cells that have developed under the influence of androgens as a direct response to acute androgen withdrawal or that it is a secondary response to a reduction in androgens in the stromal compartment resulting in a disruption in mesenchymal-epithelial signalling.

The failure of the proximal epithelium of the FoxG1-ARKO epididymis to differentiate correctly results in an obstruction developing in the efferent ducts. From d21, FoxG1-ARKO efferent ducts begin to accumulate proteinaceous and cellular debris that would normally pass through the epididymis and be phagocytosed in the cauda in controls. When spermiation occurs at around d35 in the mouse, some FoxG1-ARKO mice had spermatozoa in the epididymis despite having developed these histological changes in the efferent ducts. However, by d100 all FoxG1-ARKO epididymides examined were near azoospermic with spermatozoa stasis in the efferent ducts, suggesting that the phenotype was progressively degenerative. Previous reports suggest that the absence of an initial segment *per se* does not cause obstructive azoospermia. For example although the *c-ros* -/- mutant mouse fails to develop an initial segment, the spermatozoa progress straight from the efferent ducts to the distal caput of the epididymis (Sonnenberg-Riethmacher et al., 1996). Although spermatozoa from *c-ros* -/- male mice reach the cauda epididymis they have angulated tails and swollen heads due to problems with volume regulation (Yeung et al., 1999). However the remaining caput epithelium in *c-ros* -/- mice developed and differentiated normally under the influence of androgens, suggesting obstructive azoospermia in FoxG1-ARKO mice is likely to result from persistence of an incorrectly differentiated epididymal epithelium rather than absence of an initial segment. A further morphological characteristic that may have contributed to stasis of spermatozoa in the FoxG1-ARKO efferent ducts was the visibly smaller and more irregular lumen diameter of the FoxG1-ARKO caput epididymis. This could cause a ‘bottleneck’ point for spermatozoa and testicular fluids, slowing down their transit

and resulting in accumulation upstream in the efferent ducts. This could result in a self-perpetuating stasis, leading to changes in the composition of testicular fluid and spermatozoa in the efferent ducts and further blockage. This view is supported both through our own observations and other published models of obstructive azoospermia. For example, mice with a knock-out of LGR4/GPR48 fail to undergo proper epididymal convolution, and exhibit persistence of an undifferentiated epithelium in the epididymis (Mendive et al., 2006). Other reported models of obstructive azoospermia implicate epithelial dysregulation of the efferent ducts and caput epididymis due to abnormal trans-epithelial fluid transport (Wong, 1990). One such example is the phenotype of mice with a knock-out of GPR64, an orphan GPCR located on the apical membrane of efferent ducts and stereocilia of epididymal caput principal cells (Kirchhoff et al., 2008). GPR64 knock-out mice display a similar stasis of spermatozoa in their efferent ducts, and incorrect fluid transport by the efferent ducts and epididymis is implicated (Davies et al., 2004). Androgens are known to control the height of epididymal stereocilia (Primiani et al., 2007) and the AR-ablated immature epithelium of the proximal epididymis of FoxG1-ARKO mice lacked stereocilia which are characteristic of mature epididymal epithelial cells of this region. It is therefore probable that the localisation of many important fluid and solute transport proteins are compromised in the FoxG1-ARKO. ERα is expressed aberrantly and strongly by all cells of the epididymal epithelium in segments II and III of the FoxG1-ARKO, and increase in its expression may be causing a dysregulation of the fluid absorption function of the caput epididymis and contributing to the phenotype.

To establish whether AR ablation in the caput epididymal epithelium impacts upon the surrounding stroma, SMA expression was investigated as a marker of epididymal smooth muscle cells (Welsh et al., 2006). At d11 the staining for SMA in FoxG1-ARKO caput epididymides appeared similar to that in controls. However, at day 100 the smooth muscle layer of the FoxG1-ARKO epididymis was disorganised with evidence of disruption at specific foci, suggesting that smooth muscle function may be compromised in the FoxG1-ARKO epididymis and that this could be

compounding the problems with spermatozoa transport. This observation is likely to be an effect rather than a cause of the impaired development of the epithelium, since there is no observable difference in SMA staining in FoxG1-ARKO mice epididymides compared to controls at d11. Reciprocal homeostatic interaction between epithelium and smooth muscle in the adult prostate has been previously demonstrated (Cunha et al., 1996), so it is probable that disruption of epithelium in the epididymis also causes dysfunction in the surrounding smooth muscle layer, this requires further investigation.

Previous studies have noted that the physical blockage of the efferent ducts by sperm stasis results in inflammation and phagocytosis by the ductal epithelium (Hess and Nakai, 2000; Nakai et al., 1992). This is also apparent in the FoxG1-ARKO model at d100, with more cells immunostaining CD45+ compared to controls. Of particular interest is the morphology and locations of the CD45+ cells, noted in the stroma, dispersed throughout the efferent duct epithelium and also interspersed with spermatozoa in the lumen of efferent duct cross-sections in the conus region of the efferent ducts. Foci of dense spermatozoa heads can also be noted inside epithelial cells that stain CD45+, showing that they are being phagocytosed by immune cells within the ductal epithelium. The presence of similar CD45+ cell syncytia has been noted in efferent duct block phenotype of the LGR4 knock-out mouse (Mendive et al., 2006).

In conclusion, the mosaic ablation of AR in 67% of the cells of the caput epididymis is likely to be contributing to the phenotype of obstructive azoospermia through preventing maturation of the cells of the caput epididymal epithelium, reducing the lumen diameter of the epididymal tubule and interfering with fluid reabsorbtion in the caput epididymis.

7. General Discussion

The action of androgens via their receptor AR is essential for the correct development and function of the male reproductive system. Studies using rodents with systemic ablation of androgen-action including mice with a systemic genetic ablation of AR (*Tfm* and ARKO) (Lyon and Hawkes, 1970; Yeh et al., 2002) or rats treated with the anti-androgen flutamide (Welsh et al., 2008; Welsh et al., 2006) have been very informative in gaining information on the function of androgens during development and function of the testis. But as adult spermatogenesis is incomplete, the testes of these animals are cryptorchid, and Wolffian duct-derived structures (epididymis, vas deferens and seminal vesicles) are absent, it is difficult to draw conclusions about the relative contributions of androgen action in specific cells to the overall androgen-dependent function and development of the male reproductive system. Models in which AR is genetically ablated in specific cell types have contributed to an exponential increase in our understanding of its role in different organs of the body, but, perhaps unsurprisingly, no one cell specific knockout has a phenotype that recapitulates every aspect of the global ablation models.

This leads to the hypothesis of this thesis: that ablation of AR action in previously untargeted cell types of the male reproductive system, or in previously characterised cell types at different ages, will have significant and novel effects on reproductive development and function that have not been previously documented by current models of androgen disruption. This final chapter aims to pool together the conclusions derived by each results chapter and address the initial objectives in light of these results, as well as suggesting further directions for the research.

The experimental approach used in this thesis, and in other cell-specific knock-out of AR was the transgenic Cre-*loxP* system. Cre-*loxP* transgenic mice are appropriate models for elucidating the specific roles of androgens in different cell types, as the promoter that drives Cre can be selected to be active in a specific cell type, or at a specific age (Smith, 2011). Mouse lines with cell-specific knock-outs of AR have

been generated for several different cell types in the testis and wider reproductive system (Chang et al., 2004; De Gendt et al., 2004; Holdcraft and Braun, 2004; Raskin et al., 2009; Simanainen et al., 2008; Tsai et al., 2006; Welsh et al., 2010a; Welsh et al., 2009a; Welsh et al., 2010b; Wu et al., 2007; Xu et al., 2007; Zhang et al., 2006) have been characterised, with varying success, proving that the *Cre loxP* system is an appropriate method for cell-specific AR ablation that has resulted in new insights into signalling of AR in several of the cell types of the testis and male reproductive tract.

In this thesis, three lines expressing Cre Recombinase were used with the intention of ablating AR in the vascular endothelial cells, the post-meiotic germ cells and the adult Sertoli cells of the mouse. Although the latter aim was not fully realised the experiments had the serendipitous result of AR ablation in the pituitary and caput epididymal epithelium, both of which were cell types in which the effect of AR had not previously been examined by cell specific ablation.

7.1 The importance of empirical validation of Cre lines

It is important to note that, regardless of where it is supposed to function, the utility of a Cre line should be decided upon only following empirical validation of its spatiotemporal expression pattern, which can be achieved by using reporter genes such as β-galactosidase or fluorescent proteins to label the cells in which it is expressed or functioning. The expression of a transgene driven by a cell-specific promoter may not mirror the expression of the endogenous gene driven by the promoter, demonstrated by the discrepancy between the expression of endogenous FoxG1 and the FoxG1-Cre transgene in these studies, so it is important that the site of ablation of a gene of interest is not automatically assumed from the expression pattern of the gene downstream of the endogenous promoter that is driving Cre. Reasons for this include the ablation of any transcription enhancer or repressor sites internal to the ORF of the gene that is replaced by Cre so the transgenic promoter may no longer behave like the endogenous promoter (Smith, 2011).

The R26YFP reporter line activated by Cre expression is used to good effect in these studies to identify where the Cre is going to be active: the ablation of AR in the FoxG1-ARKO is an example of this. However, some caveats are attached. Since reporter genes and the floxed gene of interest are at different loci and may be in different strains, it cannot be assumed that Cre recombinase is going to have the same affect in both a reporter gene and a floxed gene of interest. Reasons for this may be the silencing of chromatin at different loci that prevents Cre recombinase from accessing the DNA, or the presence of modifier sequences in the vicinity of the loci.

Empirical validation using a fluorescent reporter line determined that two of the three Cre lines (Tie2-Cre and Aqp2-Cre) used in this thesis for cell-specific ablation of AR were suitable for the cell-type they were predicted to be active in. Tie2-Cre was used to target endothelial cells, a cell type which is not widely thought to express AR the testis (Pelletier et al., 2000; Vornberger et al., 1994), although the literature contains some disagreement. Through validation of the Tie2-Cre line using a fluorescent reporter that labelled Tie2-Cre positive cells, it was shown that both the vascular and interstitial endothelial cells of the testis do not express AR, but that Tie2-Cre appeared to specifically target testicular endothelial cells, a novel finding. To confirm that loss of AR from testicular endothelial cells was indeed dispensable for normal function of the testis, the Tie2-Cre line was used to genetically ablate AR in endothelial cells, and this was shown to have no effect on spermatogenesis and morphologically mature spermatozoa were found in the cauda epididymis. No truncated *Ar* transcript was recorded in the testis of the Tie2-ARKO, confirming the general consensus in the literature that AR is not expressed by endothelial cells. Aqp2-Cre was used to target post-meiotic germ cells, another cell type which is generally agreed to lack AR (O'Donnell et al., 2006), although again the literature contains some disagreement (Vornberger et al., 1994) and the AR antibody used in these studies was found to stain elongating spermatids. Validation of the Aqp2-Cre line using a fluorescent reporter confirmed that it was suitable for targeting genes in post-meiotic germ cells. Although the original paper that set out to characterise

Aqp2-Cre expression in the testis could confirm that endogenous Aqp2 was present in post-meiotic germ cells, attempts to tag Cre with a herpes simplex virus (HSV) glycoprotein epitope tag and discover its localisation by immunostaining with an antibody against the tag failed in the testis due to high background levels (Nelson et al., 1998). Localisation of YFP to the post-meiotic germ cells of the Aqp2-YFP testis is therefore the first demonstration of the suitability of Aqp2-Cre for targeting this cell type, validating it for the purpose of genetic ablation of AR. To confirm that loss of AR from post-meiotic germ cells was indeed dispensable for normal function of the testis Aqp2-Cre was used to genetically ablate AR in this cell type. Ablation had no effect on spermatogenesis and morphologically mature spermatozoa were found in the cauda epididymis. No truncated *Ar* transcript was recorded in the testis of the Aqp2-ARKO, confirming the literature consensus that AR is not expressed by post-meiotic germ cells.

FoxG1-Cre was the third Cre line used for cell-specific AR ablation in this thesis, and although validation using a FoxG1-YFP reporter did not determine that the Cre was suitable for its originally intended use in generating an adult SCARKO model, it assisted in determining where the FoxG1-Cre was in fact active and therefore promoting focus on its action in the pituitary and epididymis. A preliminary study that had shown FoxG1 to be expressed in adult but not embryonic Sertoli cells suggested that FoxG1-Cre, a line previously used for ablation in the developing telencephalon (Hebert and McConnell, 2000), would be a suitable Cre line to use to generate an ablation of AR in adult post-pubertal Sertoli cells. However FoxG1-Cre expression did not mirror endogenous FoxG1 expression and was not active in the majority of adult Sertoli cells, so was determined to be unsuitable to generate an adult SCARKO. Despite this, observation of dissected whole organs of FoxG1-YFP mice under a microscope with a fluorescent filter, and immunostaining of tissues for YFP helped confirm that the FoxG1-Cre was active in the pituitary and epididymis and that AR ablation should be explored in these organs.

7.2 The phenotype of the FoxG1-ARKO

The aim of using FoxG1-Cre to ablate AR in post-pubertal Sertoli cells was hampered by the failure of the Cre line to mirror endogenous FoxG1 in the testes. The FoxG1-Cre did not target all Sertoli cells but instead targeted a mosaic of germ cells, Leydig cells and a small number of Sertoli cells. Despite this, when FoxG1-ARKO mice were generated, they had a severe age-dependent phenotype in which failure of spermatozoa to transit the efferent ducts leading to atrophy of the seminiferous epithelium due to a build up of pressure. Further investigation revealed that the FoxG1-ARKO line had a partial ablation of AR in several reproductive organs, including the epididymis and a total ablation of AR in the pituitary. The contribution of ablation in different organs to the observed phenotype was investigated.

The ablation of AR in the testis appeared to be confined to approximately 20% of Leydig cells and occasional Sertoli cells, but the phenotype of the FoxG1-ARKO was unlike the phenotype of previously published cell-specific knock-outs. The Leydig cell ARKO paper published by Xu *et al.* (2007) has a block at the round spermatid stage whereas the FoxG1-ARKO has complete spermatogenesis up until the onset of seminiferous epithelial sloughing. The Leydig cell ARKO phenotype is complicated by the contribution of an ablation of AR in Sertoli cells, as the Cre line used in this paper (AMHR2-Cre) is present in both cell types (Jeyasuria et al., 2004). Other experiments elucidating the effect of AR in Leydig cells have suggested that it works in tandem with LHR signalling to support pubertal maturation of PLCs to steroidogenically active ILCs (Hardy et al., 1990; Murphy et al., 1994). Since the FoxG1-ARKO has a similar serum testosterone level to the control it is unlikely that the partial ablation of AR in Leydig cells is having an effect on their steroidogenic output. The FoxG1-ARKO also has a very different phenotype to the published embryonic SCARKO, which exhibits a meiotic block that precludes formation of round or elongating spermatids (Chang et al., 2004; De Gendt et al., 2004). By contrast, the FoxG1-ARKO undergoes normal spermatogenesis which is only disrupted by the onset of seminiferous epithelium sloughing from day 35. The peri-

tubular myoid cell (PTM)-ARKO mouse has testes with a reduction in numbers of all germ cell stages including the spermatogonia (Welsh et al., 2009a), but this phenotype is present from early in development and is not a degenerative change associated with seminiferous epithelial sloughing as is the FoxG1-ARKO.

The total ablation of AR in the pituitary gland did not have an effect on LH serum hormone levels or the levels of any other pituitary hormone transcript measured so was unlikely to be impacting on the function of the testis or excurrent duct system. The focus of the analysis of the FoxG1-ARKO phenotype was the ablation in the caput epithelium of the epididymis, as it was immediately downstream of the block that was forming in the efferent ducts. Acute withdrawal of androgens following orchidectomy has previously been observed to result in apoptosis of epididymal epithelial principal cells (Fan and Robaire, 1998; Takagi-Morishita et al., 2002) and de-differentiation of the caput epididymal epithelium to a 'precursor' state (Avram et al., 2004), demonstrating that androgens are important for maintenance of epithelial cell identity. Although action of androgens in Wolffian duct stabilisation and early development is known to be mediated by stromal AR (Archambeault et al., 2009), it was not known if maintenance of the epididymis in adults was due to stromal or epithelial AR (or a combination of the two).

In the FoxG1-ARKO, ablation of AR in the caput epididymal epithelium resulted in the failure of the epithelium to mature. The initial segment did not develop, and the remaining caput epithelium had a reduction in luminal diameter, cell height and development of apical stereocilia. These results were a novel demonstration of the vital effects of epididymal epithelial AR in promoting differentiation and terminal maturation of this cell type. The result of these effects would be likely to cause the efferent duct block, as an epididymal phenotype is apparent from d11 but the efferent duct block does not begin to develop until later ages. Also, obstructive azoospermia is also seen in other mouse models with perturbation of the epididymal epithelium or epididymal development and morphology (Davies et al., 2004; Mendive et al., 2006; Tanwar et al., 2010; Zhao et al., 2001). The phenotype seen appears to be a

concentration of sperm in the efferent ducts, unlike the ERα ablation mouse model which exhibits efferent duct distension due to malabsorbtion of fluid in the efferent ducts (Lee et al., 2000) and infertility due to aberrant sperm morphology (Joseph et al., 2010a).

The testicular phenotype seen in FoxG1-ARKO mice is most probably a secondary effect due to the efferent duct block, rather than the primary cause of the block in the first place, though it is likely that the two events are perpetuating each other. The development of a physical block in the efferent ducts induced both gross and histological changes in the testis of the FoxG1-ARKO from d35. Stereological quantification revealed a reduction in tubule diameter with an increase in lumen diameter at d100 consistent with atrophy of the seminiferous tubules and sloughing of the seminiferous epithelium in FoxG1-ARKO testes. This late-stage testicular phenotype is similar to that found following acute efferent duct blockage (Anton, 2003; Flickinger et al., 1999; Hess and Nakai, 2000; Peng et al., 2010) and suggests that the degeneration seen in the testis is a consequence of the efferent duct block. However, the transient increase in testis weight predicted from this model was not observed in the FoxG1-ARKO model. This may be due to the observed epithelial phagocytosis relieving fluid pressure and accumulation of sperm to some extent. Further to this, the FoxG1-ARKO model represents a ‘chronic treatment’ with a progressively worsening phenotype in a developing system rather than an ‘acute treatment’ whose impacts are widespread and immediate (e.g. efferent duct ligation or chemical insult).

However, the predicted sequence of events (epididymal dysfunction causes efferent duct block causes testicular disruption) does not preclude the contribution of a testicular phenotype to the generation of the efferent duct block in the first place. There is a delay in lumen opening of the FoxG1-ARKO testis compared to controls that is resolved by d21. The reason behind this was not fully investigated. It could potentially be the consequence of AR ablation in testis, a consequence of the early stages of the epididymal phenotype or a result of the FoxG1 haploinsufficiency.

Though adult FoxG1-Cre stud males at the end of their breeding life had normal spermatogenesis with no evidence of the phenotype that FoxG1-ARKO mice display, earlier ages were not investigated for any potential effect of the haploinsufficiency on testicular phenotype. Even if testicular effects from either the FoxG1 haploinsufficiency or ablation of AR in a few Leydig and Sertoli cells were causing germ cell sloughing this would probably not be enough to block efferent ducts without a coincident dysfunction in the epididymis. Several models of germ cell sloughing demonstrate that the sloughed cells pass through the efferent ducts and epididymis as mature spermatozoa would, and are noted in the cauda, where they are phagocytosed. Despite these observations, widespread sloughing of germ cells is not seen in the FoxG1-ARKO until after the seminiferous epithelium degradation occurs, so it is unlikely to be contributing to the initial progression of the efferent duct block. Although a few sloughed immature germ cells have accumulated in the efferent ducts when observed at d21, epididymal ablation of AR has already caused a phenotype in the epididymal epithelium from d11 implying that the initial stages of the block are likely to be already due to epididymal dysfunction. Another contribution to the early stages of the efferent duct block could be the reduction in testicular luminal fluid that would occur with a delay in the opening of the seminiferous tubule lumen. Since lumen opening is due to fluid produced by the Sertoli cells, which is dependent on AR signalling, it could be postulated that ablation of AR in Sertoli cells is causing this. Analysis of any ablation of AR in Sertoli cells has been one of the main problems encountered in this thesis, as a double immunostaining protocol for AR and a Sertoli-cell marker was consistently unsuccessful, despite several attempts at optimisation with several different antibodies used as Sertoli cell markers (p27/kip, WT1 and β-tubulin were all attempted, with limited success). However, immunohistochemistry with an AR antibody alone combined with identification of Sertoli cells by their distinctive morphology demonstrated that very few, if any Sertoli cells had AR ablation, although this was further compounded by the fluctuation of the intensity of AR immunostaining at different stages of the spermatogenic cycle (Zhou et al., 2002). It could be possible that the partial ablation

of AR in the Leydig cell population causes a delay in lumen opening by limiting a trophic factor that stimulates the Sertoli cells.

The FoxG1-ARKO mouse has utility as a novel model of obstructive azoospermia (OA). OA is the absence of sperm in the ejaculate due to a post-testicular obstruction of the genital tract. Four to six percent of infertile men have obstructive azoospermia (Anon, 2008). Some cases of OA have been linked to congenital bilateral absence of vas deferens due to mutations in the cystic fibrosis transmembrane conductance receptor (Lopez et al., 2010), but most cases of OA have no definitive cause. The FoxG1-ARKO model introduces the idea that OA results from epithelial dysregulation in the epididymis. Since cell-specific gene ablation of AR is extremely unlikely to occur in humans, a possible cause could be a mutation in an epididymis-specific gene controlled by AR signalling, or another developmental problem that has lead to incorrect maturation of the epididymal epithelium, or epithelial degeneration with age.

7.3 Future perspectives

Several of the results in this thesis would benefit from further exploration. The morphology of the caput epididymal epithelium was clearly affected in the FoxG1-ARKO mice, and this in itself is likely to contribute to the efferent duct spermatozoal block by narrowing the lumen diameter of the epididymal tubule. But the aberrant expression of ERα noted in the caput epididymal epithelium implies that there may also be dysregulation in absorption of testicular fluid in the epididymis that may be contributing to the block. There is abundant speculation in the literature about an optimal 'balance' between androgens and estrogens that affects spermatogenesis, but balance between expression of their equivalent receptors in certain tissues could be contributing to this. Since the FoxG1-ARKO and the ERα knockout have 'opposite' phenotypes and aberrant ERα expression is implicated in the phenotype of the FoxG1-ARKO, it would be interesting to treat FoxG1-ARKO and control mice with an ERα inhibitor such as ICI 182,780 (Lee et al., 2000) and see whether this

positively or negatively impacts on the phenotype. The expression of *Gpr64* (a novel receptor whose systemic ablation caused a phenotype similar to that seen in the FoxG1-ARKO (Davies et al., 2004)) was decreased in FoxG1-ARKO epididymides compared to controls at d21. Performing a microarray on epididymis tissue at an age between d21 and d35 could identify genes that are differentially regulated between the FoxG1-ARKO and controls and that may contribute to the obstructive azoospermia phenotype. Studies of gene expression in the FoxG1-ARKO mouse could prove useful for identifying downstream pathways and molecules for potential therapeutics for obstructive azoospermia. The epididymis is also being investigated as a site for potential novel post-testicular contraceptives (Sipila et al., 2009; Turner et al., 2006), and although the phenotype generated by the FoxG1-ARKO would be an undesirable side-effect of any novel male contraceptive, any information generated about the epididymis and its response to changes in gene expression could help pinpoint proteins that are potential contraceptive targets.

Another aspect of the FoxG1-ARKO that was under-explored is the presence of a partial brain ablation of androgen receptor. Due to time and tissue constraints the location of this ablation was not established. Complete neural ablation of AR in males (Raskin et al., 2009) is linked to problems with both mating behaviour (due to AR ablation in the medial amygdala, lateral septum, bed nucleus of stria terminalis and medial preoptic area) and the HPG axis (due to AR ablation in the kisspeptin neurons of the hypothalamus). Since FoxG1-ARKO mice did not demonstrate either of these problems it is unlikely that the ablation seen is in either of these areas, but pinpointing the localisation of the ablation in these mice may help draw a map of the regions of the brain that have redundant AR expression. Growth hormone (GH) is a pituitary hormone that was not investigated in these studies. GH receptor knock-out (GHR-KO) mice have a delayed puberty (Keene et al., 2002), with conflicting reports of either a slight decrease (Chandrashekar et al., 1999) or no decrease (Zhou et al., 1997) in fertility. However GHR-KO mice are approximately half the weight of their wild-type controls (Keene et al., 2002); and a decrease in body weight is not

seen in the FoxG1-ARKO implying that GH expression is unlikely to be altered in this model.

The Tie2-ARKO also presents interesting opportunities for further investigation. In this model the endothelial AR is ablated throughout the body, not just in the testis. Evidence suggests that AR is causally involved in the homeostasis of human prostate endothelial cells (Godoy et al., 2008), suggesting that the observation of the prostates of Tie2-ARKO mice could yield some interesting results.

The use of a FoxG1-Cre line to ablate AR did not result in an 'adult SCARKO', so the generation of this line has still not been achieved. Potential suitable Cre lines are difficult to select for this task because most Sertoli cell-specific genes are induced either embryonically or at the advent of puberty, rather than after the first full round of spermatogenesis has occurred (Ojeda and Skinner, 2006). A potential way of circumnavigating this problem is to use a Cre line that is dependent on a ligand such as tamoxifen, interferon or tetracycline for activation (Garcia and Mills, 2002), but also under the control of a Sertoli-cell specific promoter, so would not be expressed in Sertoli cells until the animals were treated with the ligand of choice. Furthermore, preliminary investigations in the Lee Smith group are underway to assess the suitability of using a lentiviral vector carrying a Sertoli cell-specific Cre, to be injected into the efferent ducts of an AR^{flox} mouse. Lentiviral vectors injected into seminiferous tubules are preferentially taken up by the Sertoli cells (Ikawa et al., 2002), and so Cre expression should be specific to these cells.

7.4 General thesis conclusions

The original hypothesis of this thesis was that ablation of AR action in previously untargeted cell types of the male reproductive system, or in previously characterised cell types at different ages, will have significant and novel effects on reproductive development and function that have not been previously documented by current models of androgen disruption. This hypothesis has been proven with the FoxG1-ARKO, which has resulted in the following novel observations:

- AR signalling in the caput epididymal epithelium of the mouse is vital for normal differentiation of the epithelium, including the development of the initial segment.
- Disruption of AR signalling the caput epididymal epithelium of the mouse contributes to a novel model of obstructive azoospermia in which most spermatozoa do not transit the efferent ducts.
- AR signalling in the pituitary is not required for normal regulation of serum LH and testosterone, or for regulation of other pituitary endocrine hormone transcripts in the mouse.

Other novel, previously unreported observations through the course of this thesis have been:

- FoxG1 is present in the fetal Leydig cells and post-pubertal Sertoli cells of the mouse testis. Previously, FoxG1 had been shown to be expressed in the human but not mouse testis, and localisation had not been determined (Obendorf et al., 2007).
- Tie2-Cre is an appropriate line to use to ablate a gene of interest in both the vascular and interstitial endothelial cells of the testis.
- Ablation of endothelial AR has no effect on normal spermatogenesis in the mouse.
- Ablation of AR in post-meiotic germ cells has no effect on normal spermatogenesis in the mouse.

The FoxG1-ARKO has also demonstrated that the Cre/*loxP* system is a useful tool for cell-specific genetic ablation, but careful empirical validation must be performed to determine the site of action of the Cre line used in studies. However, because we conducted detailed empirical analysis we were able to exploit this line extremely successfully to provide significant novel findings relevant to male reproductive health. Although it was not the original intention of the study to target the epididymis or pituitary in the FoxG1-ARKO, the targeting of both provided novel results. Analysis of the epididymal phenotype of the FoxG1-ARKO has been published in a

recent paper (O'Hara et al., 2011). This manuscript was published back-to-back with another group who independently targeted AR in the caput epididymis from d25 using an RNase10-Cre line, resulting in a similar phenotype of obstructive azoospermia. (Krutskikh et al., 2011).

8. Bibliography

Abe, K., and Takano, H. (1989). Cytological response of the principal cells in the initial segment of the epididymal duct to efferent duct cutting in mice. Arch Histol Cytol *52*, 321-326.

Abel, M.H., Baker, P.J., Charlton, H.M., Monteiro, A., Verhoeven, G., De Gendt, K., Guillou, F., and O'Shaughnessy, P.J. (2008). Spermatogenesis and sertoli cell activity in mice lacking sertoli cell receptors for follicle-stimulating hormone and androgen. Endocrinology *149*, 3279-3285.

Abel, M.H., Wootton, A.N., Wilkins, V., Huhtaniemi, I., Knight, P.G., and Charlton, H.M. (2000). The effect of a null mutation in the follicle-stimulating hormone receptor gene on mouse reproduction. Endocrinology *141*, 1795-1803.

Abou-Haila, A., and Fain-Maurel, M.A. (1984). Regional differences of the proximal part of mouse epididymis: morphological and histochemical characterization. Anat Rec *209*, 197-208.

Abou-Haila, A., and Tulsiani, D.R. (2000). Mammalian sperm acrosome: formation, contents, and function. Arch Biochem Biophys *379*, 173-182.

Adamali, H.I., and Hermo, L. (1996). Apical and narrow cells are distinct cell types differing in their structure, distribution, and functions in the adult rat epididymis. J Androl *17*, 208-222.

Akingbemi, B.T., Ge, R., Rosenfeld, C.S., Newton, L.G., Hardy, D.O., Catterall, J.F., Lubahn, D.B., Korach, K.S., and Hardy, M.P. (2003). Estrogen receptor-alpha gene deficiency enhances androgen biosynthesis in the mouse Leydig cell. Endocrinology *144*, 84-93.

Albertelli, M.A., Scheller, A., Brogley, M., and Robins, D.M. (2006). Replacing the mouse androgen receptor with human alleles demonstrates glutamine tract length-dependent effects on physiology and tumorigenesis in mice. Mol Endocrinol *20*, 1248-1260.

Allan, C.M., Garcia, A., Spaliviero, J., Zhang, F.P., Jimenez, M., Huhtaniemi, I., and Handelsman, D.J. (2004). Complete Sertoli cell proliferation induced by follicle-stimulating hormone (FSH) independently of luteinizing hormone activity: evidence from genetic models of isolated FSH action. Endocrinology *145*, 1587-1593.

Allan, C.M., Haywood, M., Swaraj, S., Spaliviero, J., Koch, A., Jimenez, M., Poutanen, M., Levallet, J., Huhtaniemi, I., Illingworth, P., *et al.* (2001). A novel transgenic model to characterize the specific effects of follicle-stimulating hormone on gonadal physiology in the absence of luteinizing hormone actions. Endocrinology *142*, 2213-2220.

Allard, S., Adin, P., Gouedard, L., di Clemente, N., Josso, N., Orgebin-Crist, M.C., Picard, J.Y., and Xavier, F. (2000). Molecular mechanisms of hormone-mediated Mullerian duct regression: involvement of beta-catenin. Development *127*, 3349-3360.

Amador, A.G., Parkening, T.A., Beamer, W.G., Bartke, A., and Collins, T.J. (1986). Testicular LH receptors and circulating hormone levels in three mouse models for inherited diseases (Tfm/y, lit/lit and hyt/hyt). Endocrinol Exp *20*, 349-358.

Andersson, S., Berman, D.M., Jenkins, E.P., and Russell, D.W. (1991). Deletion of steroid 5 alpha-reductase 2 gene in male pseudohermaphroditism. Nature *354*, 159-161.

Andersson, S., and Russell, D.W. (1990). Structural and biochemical properties of cloned and expressed human and rat steroid 5 alpha-reductases. Proc Natl Acad Sci U S A *87*, 3640-3644.

Anon (2008). The management of infertility due to obstructive azoospermia. In Fertil Steril (Practise Committee of the American Society for Reproductive Medicine in collaboration with the Society for Male Reproduction and Urology), pp. S121-124.

Anton, E. (2003). Arrested apoptosis without nuclear fragmentation produced by efferent duct ligation in round spermatids and multinucleated giant cells of rat testis. Reproduction *125*, 879-887.

Anway, M.D., Folmer, J., Wright, W.W., and Zirkin, B.R. (2003). Isolation of sertoli cells from adult rat testes: an approach to ex vivo studies of Sertoli cell function. Biol Reprod *68*, 996-1002.

Archambeault, D.R., Tomaszewski, J., Joseph, A., Hinton, B.T., and Yao, H.H. (2009). Epithelial-mesenchymal crosstalk in Wolffian duct and fetal testis cord development. Genesis *47*, 40-48.

Arnold, J.S., Braunstein, E.M., Ohyama, T., Groves, A.K., Adams, J.C., Brown, M.C., and Morrow, B.E. (2006). Tissue-specific roles of Tbx1 in the development of the outer, middle and inner ear, defective in 22q11DS patients. Hum Mol Genet *15*, 1629-1639.

Avram, C., Yeung, C.H., Nieschlag, E., and Cooper, T.G. (2004). Regulation of the initial segment of the murine epididymis by dihydrotestosterone and testicular exocrine secretions studied by expression of specific proteins and gene expression. Cell Tissue Res *317*, 13-22.

Avram, C.E., and Cooper, T.G. (2004). Development of the caput epididymidis studied by expressed proteins (a glutamate transporter, a lipocalin and beta-galactosidase) in the c-ros knockout and wild-type mice with prepubertally ligated efferent ducts. Cell Tissue Res *317*, 23-34.

Baarends, W.M., van Helmond, M.J., Post, M., van der Schoot, P.J., Hoogerbrugge, J.W., de Winter, J.P., Uilenbroek, J.T., Karels, B., Wilming, L.G., Meijers, J.H., *et al.* (1994). A novel member of the transmembrane serine/threonine kinase receptor family is specifically expressed in the gonads and in mesenchymal cells adjacent to the mullerian duct. Development *120*, 189-197.

Badran, H.H., and Hermo, L.S. (2002). Expression and regulation of aquaporins 1, 8, and 9 in the testis, efferent ducts, and epididymis of adult rats and during postnatal development. J Androl *23*, 358-373.

Baker, P.J., and O'Shaughnessy, P.J. (2001). Role of gonadotrophins in regulating numbers of Leydig and Sertoli cells during fetal and postnatal development in mice. Reproduction *122*, 227-234.

Baker, P.J., Pakarinen, P., Huhtaniemi, I.T., Abel, M.H., Charlton, H.M., Kumar, T.R., and O'Shaughnessy, P.J. (2003). Failure of normal Leydig cell development in follicle-stimulating hormone (FSH) receptor-deficient mice, but not FSHbeta-deficient mice: role for constitutive FSH receptor activity. Endocrinology *144*, 138-145.

Baker, P.J., Sha, J.A., McBride, M.W., Peng, L., Payne, A.H., and O'Shaughnessy, P.J. (1999). Expression of 3beta-hydroxysteroid dehydrogenase type I and type VI isoforms in the mouse testis during development. Eur J Biochem *260*, 911-917.

Barbulescu, K., Geserick, C., Schuttke, I., Schleuning, W.D., and Haendler, B. (2001). New androgen response elements in the murine pem promoter mediate selective transactivation. Mol Endocrinol *15*, 1803-1816.

Barrionuevo, F., Naumann, A., Bagheri-Fam, S., Speth, V., Taketo, M.M., Scherer, G., and Neubuser, A. (2008). Sox9 is required for invagination of the otic placode in mice. Dev Biol *317*, 213-224.

Bartlett, J.M., Kerr, J.B., and Sharpe, R.M. (1986). The effect of selective destruction and regeneration of rat Leydig cells on the intratesticular distribution of testosterone and morphology of the seminiferous epithelium. J Androl *7*, 240-253.

Beardsley, A., and O'Donnell, L. (2003). Characterization of normal spermiation and spermiation failure induced by hormone suppression in adult rats. Biol Reprod *68*, 1299-1307.

Beato, M., Truss, M., and Chavez, S. (1996). Control of transcription by steroid hormones. Ann N Y Acad Sci *784*, 93-123.

Beck, J.A., Lloyd, S., Hafezparast, M., Lennon-Pierce, M., Eppig, J.T., Festing, M.F., and Fisher, E.M. (2000). Genealogies of mouse inbred strains. Nat Genet *24*, 23-25.

Behr, R., Sackett, S.D., Bochkis, I.M., Le, P.P., and Kaestner, K.H. (2007). Impaired male fertility and atrophy of seminiferous tubules caused by haploinsufficiency for Foxa3. Dev Biol *306*, 636-645.

Bendel-Stenzel, M., Anderson, R., Heasman, J., and Wylie, C. (1998). The origin and migration of primordial germ cells in the mouse. Semin Cell Dev Biol *9*, 393-400.

Benson, G.V., Lim, H., Paria, B.C., Satokata, I., Dey, S.K., and Maas, R.L. (1996). Mechanisms of reduced fertility in Hoxa-10 mutant mice: uterine homeosis and loss of maternal Hoxa-10 expression. Development *122*, 2687-2696.

Bentvelsen, F.M., Brinkmann, A.O., van der Schoot, P., van der Linden, J.E., van der Kwast, T.H., Boersma, W.J., Schroder, F.H., and Nijman, J.M. (1995). Developmental pattern and regulation by androgens of androgen receptor expression in the urogenital tract of the rat. Mol Cell Endocrinol *113*, 245-253.

Berg, J.M. (1989). DNA binding specificity of steroid receptors. Cell *57*, 1065-1068.

Billig, H., Furuta, I., Rivier, C., Tapanainen, J., Parvinen, M., and Hsueh, A.J. (1995). Apoptosis in testis germ cells: developmental changes in gonadotropin dependence and localization to selective tubule stages. Endocrinology *136*, 5-12.

Binart, N., Melaine, N., Pineau, C., Kercret, H., Touzalin, A.M., Imbert-Bollore, P., Kelly, P.A., and Jegou, B. (2003). Male reproductive function is not affected in prolactin receptor-deficient mice. Endocrinology *144*, 3779-3782.

Blackburn, W.R., Chung, K.W., Bullock, L., and Bardin, C.W. (1973). Testicular feminization in the mouse: studies of Leydig cell structure and function. Biol Reprod *9*, 9-23.

Borg, C.L., Wolski, K.M., Gibbs, G.M., and O'Bryan, M.K. (2010). Phenotyping male infertility in the mouse: how to get the most out of a 'non-performer'. Hum Reprod Update *16*, 205-224.

Braun, R.E. (2001). Packaging paternal chromosomes with protamine. Nat Genet *28*, 10-12.

Breed, W.G. (2004). The spermatozoon of Eurasian murine rodents: Its morphological diversity and evolution. J Morphol *261*, 52-69.

Brennan, J., Tilmann, C., and Capel, B. (2003). Pdgfr-alpha mediates testis cord organization and fetal Leydig cell development in the XY gonad. Genes Dev *17*, 800-810.

Brewer, L.R., Corzett, M., and Balhorn, R. (1999). Protamine-induced condensation and decondensation of the same DNA molecule. Science *286*, 120-123.

Brinkmann, A.O. (2009). Chapter 3: Androgen Physiology: Receptor and Metabolic Disorders. In Endotext (http://wwwendotextorg).

Brooks, D.E. (1979). Influence of androgens on the weights of the male accessory reproductive organs and on the activities of mitochondrial enzymes in the epididymis of the rat. J Endocrinol *82*, 293-303.

Brown, C.J., Goss, S.J., Lubahn, D.B., Joseph, D.R., Wilson, E.M., French, F.S., and Willard, H.F. (1989). Androgen receptor locus on the human X chromosome: regional localization to Xq11-12 and description of a DNA polymorphism. Am J Hum Genet *44*, 264-269.

Burger, H.G. (1988). Inhibin: definition and nomenclature, including related substances. J Endocrinol *117*, 159-160.

Buzzard, J.J., Wreford, N.G., and Morrison, J.R. (2002). Marked extension of proliferation of rat Sertoli cells in culture using recombinant human FSH. Reproduction *124*, 633-641.

Cai, J., Hong, Y., Weng, C., Tan, C., Imperato-McGinley, J.L., and Zhu, Y.S. (2011). Androgen Stimulates Endothelial Cell Proliferation via an Androgen Receptor-VEGF/Cyclin A Mediated Mechanism. Am J Physiol Heart Circ Physiol.

Carreau, S., and Hess, R.A. (2010). Oestrogens and spermatogenesis. Philos Trans R Soc Lond B Biol Sci *365*, 1517-1535.

Cattanach, B.M., Iddon, C.A., Charlton, H.M., Chiappa, S.A., and Fink, G. (1977). Gonadotrophin-releasing hormone deficiency in a mutant mouse with hypogonadism. Nature *269*, 338-340.

Chandrashekar, V., Bartke, A., Coschigano, K.T., and Kopchick, J.J. (1999). Pituitary and testicular function in growth hormone receptor gene knockout mice. Endocrinology *140*, 1082-1088.

Chang, C., Chen, Y.T., Yeh, S.D., Xu, Q., Wang, R.S., Guillou, F., Lardy, H., and Yeh, S. (2004). Infertility with defective spermatogenesis and hypotestosteronemia in male mice lacking the androgen receptor in Sertoli cells. Proc Natl Acad Sci U S A *101*, 6876-6881.

Charest, N.J., Zhou, Z.X., Lubahn, D.B., Olsen, K.L., Wilson, E.M., and French, F.S. (1991). A frameshift mutation destabilizes androgen receptor messenger RNA in the Tfm mouse. Mol Endocrinol *5*, 573-581.

Chauvin, T.R., and Griswold, M.D. (2004). Androgen-regulated genes in the murine epididymis. Biol Reprod *71*, 560-569.

Chen, H., Ge, R.S., and Zirkin, B.R. (2009a). Leydig cells: From stem cells to aging. Mol Cell Endocrinol *306*, 9-16.

Chen, L., Liao, G., Yang, L., Campbell, K., Nakafuku, M., Kuan, C.Y., and Zheng, Y. (2006). Cdc42 deficiency causes Sonic hedgehog-independent holoprosencephaly. Proc Natl Acad Sci U S A *103*, 16520-16525.

Chen, L., Melendez, J., Campbell, K., Kuan, C.Y., and Zheng, Y. (2009b). Rac1 deficiency in the forebrain results in neural progenitor reduction and microcephaly. Dev Biol *325*, 162-170.

Chen, M., Wolfe, A., Wang, X., Chang, C., Yeh, S., and Radovick, S. (2009c). Generation and characterization of a complete null estrogen receptor alpha mouse using Cre/LoxP technology. Mol Cell Biochem *321*, 145-153.

Cheng, C.Y., and Mruk, D.D. (2009). An intracellular trafficking pathway in the seminiferous epithelium regulating spermatogenesis: a biochemical and molecular perspective. Crit Rev Biochem Mol Biol *44*, 245-263.

Cheng, J., Watkins, S.C., and Walker, W.H. (2007). Testosterone activates mitogen-activated protein kinase via Src kinase and the epidermal growth factor receptor in sertoli cells. Endocrinology *148*, 2066-2074.

Clulow, J., Jones, R.C., and Hansen, L.A. (1994). Micropuncture and cannulation studies of fluid composition and transport in the ductuli efferentes testis of the rat: comparisons with the homologous metanephric proximal tubule. Exp Physiol *79*, 915-928.

Collins, F.S., Rossant, J., and Wurst, W. (2007). A mouse for all reasons. Cell *128*, 9-13.

Combes, A.N., Wilhelm, D., Davidson, T., Dejana, E., Harley, V., Sinclair, A., and Koopman, P. (2009). Endothelial cell migration directs testis cord formation. Dev Biol *326*, 112-120.

Constien, R., Forde, A., Liliensiek, B., Grone, H.J., Nawroth, P., Hammerling, G., and Arnold, B. (2001). Characterization of a novel EGFP reporter mouse to monitor Cre recombination as demonstrated by a Tie2 Cre mouse line. Genesis *30*, 36-44.

Cooke, P.S., Young, P., and Cunha, G.R. (1991). Androgen receptor expression in developing male reproductive organs. Endocrinology *128*, 2867-2873.

Cool, J., Carmona, F.D., Szucsik, J.C., and Capel, B. (2008). Peritubular myoid cells are not the migrating population required for testis cord formation in the XY gonad. Sex Dev *2*, 128-133.

Cooper, T.G., and Yeung, C.H. (2003). Acquisition of volume regulatory response of sperm upon maturation in the epididymis and the role of the cytoplasmic droplet. Microsc Res Tech *61*, 28-38.

Cooper, T.G., Yeung, C.H., Wagenfeld, A., Nieschlag, E., Poutanen, M., Huhtaniemi, I., and Sipila, P. (2004). Mouse models of infertility due to swollen spermatozoa. Mol Cell Endocrinol *216*, 55-63.

Corker, C.S., and Davidson, D.W. (1978). A radioimmunoassay for testosterone in various biological fluids without chromatography. J Steroid Biochem *9*, 373-374.

Cornwall, G.A. (2009). New insights into epididymal biology and function. Hum Reprod Update *15*, 213-227.

Cornwall, G.A., and Hann, S.R. (1995). Specialized gene expression in the epididymis. J Androl *16*, 379-383.

Crocoll, A., Zhu, C.C., Cato, A.C., and Blum, M. (1998). Expression of androgen receptor mRNA during mouse embryogenesis. Mech Dev *72*, 175-178.

Cunha, G.R., Hayward, S.W., Dahiya, R., and Foster, B.A. (1996). Smooth muscle-epithelial interactions in normal and neoplastic prostatic development. Acta Anat (Basel) *155*, 63-72.

d'Anglemont de Tassigny, X., and Colledge, W.H. (2010). The role of kisspeptin signaling in reproduction. Physiology (Bethesda) *25*, 207-217.

Darwanto, A., Kitazawa, R., Mori, K., Kondo, T., and Kitazawa, S. (2008). MeCP2 expression and promoter methylation of cyclin D1 gene are associated with cyclin D1 expression in developing rat epididymal duct. Acta Histochem Cytochem *41*, 135-142.

Davidoff, M.S., Middendorff, R., Enikolopov, G., Riethmacher, D., Holstein, A.F., and Muller, D. (2004). Progenitor cells of the testosterone-producing Leydig cells revealed. J Cell Biol *167*, 935-944.

Davies, B., Baumann, C., Kirchhoff, C., Ivell, R., Nubbemeyer, R., Habenicht, U.F., Theuring, F., and Gottwald, U. (2004). Targeted deletion of the epididymal receptor HE6 results in fluid dysregulation and male infertility. Mol Cell Biol *24*, 8642-8648.

De Gendt, K., Atanassova, N., Tan, K.A., de Franca, L.R., Parreira, G.G., McKinnell, C., Sharpe, R.M., Saunders, P.T., Mason, J.I., Hartung, S., *et al.* (2005). Development and function of the adult generation of Leydig cells in mice with Sertoli cell-selective or total ablation of the androgen receptor. Endocrinology *146*, 4117-4126.

De Gendt, K., Swinnen, J.V., Saunders, P.T., Schoonjans, L., Dewerchin, M., Devos, A., Tan, K., Atanassova, N., Claessens, F., Lecureuil, C., *et al.* (2004). A Sertoli cell-selective knockout of the androgen receptor causes spermatogenic arrest in meiosis. Proc Natl Acad Sci U S A *101*, 1327-1332.

de Rooij, D.G. (2009). The spermatogonial stem cell niche. Microsc Res Tech *72*, 580-585.

Deitch, A.D., Goldberg, S.D., and DeVere White, R. (1986). Flow cytometric analysis of testicular tissue: Detection of injury and recovery. World J Urol *4*, 71-76.

Denolet, E., De Gendt, K., Allemeersch, J., Engelen, K., Marchal, K., Van Hummelen, P., Tan, K.A., Sharpe, R.M., Saunders, P.T., Swinnen, J.V., *et al.* (2006). The effect of a sertoli cell-selective knockout of the androgen receptor on testicular gene expression in prepubertal mice. Mol Endocrinol *20*, 321-334.

Dierich, A., Sairam, M.R., Monaco, L., Fimia, G.M., Gansmuller, A., LeMeur, M., and Sassone-Corsi, P. (1998). Impairing follicle-stimulating hormone (FSH) signaling in vivo: targeted disruption of the FSH receptor leads to aberrant gametogenesis and hormonal imbalance. Proc Natl Acad Sci U S A *95*, 13612-13617.

Drews, U., Sulak, O., and Oppitz, M. (2001). Immunohistochemical localisation of androgen receptor during sex-specific morphogenesis in the fetal mouse. Histochem Cell Biol *116*, 427-439.

Dufau, M.L. (1988). Endocrine regulation and communicating functions of the Leydig cell. Annu Rev Physiol *50*, 483-508.

Dupont, E., Labrie, F., Luu-The, V., and Pelletier, G. (1993). Ontogeny of 3 beta-hydroxysteroid dehydrogenase/delta 5-delta 4 isomerase (3 beta-HSD) in rat testis as studied by immunocytochemistry. Anat Embryol (Berl) *187*, 583-589.

Dupont, S., Krust, A., Gansmuller, A., Dierich, A., Chambon, P., and Mark, M. (2000). Effect of single and compound knockouts of estrogen receptors alpha (ERalpha) and beta (ERbeta) on mouse reproductive phenotypes. Development *127*, 4277-4291.

Dym, M., and Fawcett, D.W. (1970). The blood-testis barrier in the rat and the physiological compartmentation of the seminiferous epithelium. Biol Reprod *3*, 308-326.

Dyson, A.L., and Orgebin-Crist, M.C. (1973). Effect of hypophysectomy, castration and androgen replacement upon the fertilizing ability of rat epididymal spermatozoa. Endocrinology *93*, 391-402.

Eacker, S.M., Shima, J.E., Connolly, C.M., Sharma, M., Holdcraft, R.W., Griswold, M.D., and Braun, R.E. (2007). Transcriptional profiling of androgen receptor (AR) mutants suggests instructive and permissive roles of AR signaling in germ cell development. Mol Endocrinol *21*, 895-907.

Eagleson, K.L., Schlueter McFadyen-Ketchum, L.J., Ahrens, E.T., Mills, P.H., Does, M.D., Nickols, J., and Levitt, P. (2007). Disruption of Foxg1 expression by knock-in of cre recombinase: effects on the development of the mouse telencephalon. Neuroscience *148*, 385-399.

Eddy, E.M., Washburn, T.F., Bunch, D.O., Goulding, E.H., Gladen, B.C., Lubahn, D.B., and Korach, K.S. (1996). Targeted disruption of the estrogen receptor gene in male mice causes alteration of spermatogenesis and infertility. Endocrinology *137*, 4796-4805.

Ehmcke, J., Wistuba, J., and Schlatt, S. (2006). Spermatogonial stem cells: questions, models and perspectives. Hum Reprod Update *12*, 275-282.

Emmen, J.M., McLuskey, A., Grootegoed, J.A., and Brinkmann, A.O. (1998). Androgen action during male sex differentiation includes suppression of cranial suspensory ligament development. Hum Reprod *13*, 1272-1280.

Evaul, K., and Hammes, S. R. (2008). Cross-talk between G protein-coupled and epidermal growth factor receptors regulates gonadotropin-mediated steroidogenesis in Leydig cells. J Biol Chem *283*, 27525-27533.

Ezer, N., and Robaire, B. (2003). Gene expression is differentially regulated in the epididymis after orchidectomy. Endocrinology *144*, 975-988.

Faber, P.W., King, A., van Rooij, H.C., Brinkmann, A.O., de Both, N.J., and Trapman, J. (1991). The mouse androgen receptor. Functional analysis of the protein and characterization of the gene. Biochem J *278 (Pt 1)*, 269-278.

Faber, P.W., Kuiper, G.G., van Rooij, H.C., van der Korput, J.A., Brinkmann, A.O., and Trapman, J. (1989). The N-terminal domain of the human androgen receptor is encoded by one, large exon. Mol Cell Endocrinol *61*, 257-262.

Fan, X., and Robaire, B. (1998). Orchidectomy induces a wave of apoptotic cell death in the epididymis. Endocrinology *139*, 2128-2136.

Farr, C.H., and Ellis, L.C. (1980). In-vitro contractility of rat seminiferous tubules in response to prostaglandins, cyclic GMP, testosterone and 2,4'-dibromoacetophenone. J Reprod Fertil *58*, 37-42.

Fawcett, D.W., and Hoffer, A.P. (1979). Failure of exogenous androgen to prevent regression of the initial segments of the rat epididymis after efferent duct ligation or orchidectomy. Biol Reprod *20*, 162-181.

Fisher, C.R., Graves, K.H., Parlow, A.F., and Simpson, E.R. (1998a). Characterization of mice deficient in aromatase (ArKO) because of targeted disruption of the cyp19 gene. Proc Natl Acad Sci U S A *95*, 6965-6970.

Fisher, J.S., Turner, K.J., Fraser, H.M., Saunders, P.T., Brown, D., and Sharpe, R.M. (1998b). Immunoexpression of aquaporin-1 in the efferent ducts of the rat and marmoset monkey during development, its modulation by estrogens, and its possible role in fluid resorption. Endocrinology *139*, 3935-3945.

Fix, C., Jordan, C., Cano, P., and Walker, W.H. (2004). Testosterone activates mitogen-activated protein kinase and the cAMP response element binding protein transcription factor in Sertoli cells. Proc Natl Acad Sci U S A *101*, 10919-10924.

Flickinger, C.J., Baran, M.L., Howards, S.S., and Herr, J.C. (1999). Degeneration of the seminiferous epithelium following epididymal obstruction in prepubertal rats. Anat Rec *254*, 76-86.

Freedman, L.P. (1992). Anatomy of the steroid receptor zinc finger region. Endocr Rev *13*, 129-145.

Friedrich, G., and Soriano, P. (1991). Promoter traps in embryonic stem cells: a genetic screen to identify and mutate developmental genes in mice. Genes Dev *5*, 1513-1523.

Frojdman, K., Paranko, J., Virtanen, I., and Pelliniemi, L.J. (1992). Intermediate filaments and epithelial differentiation of male rat embryonic gonad. Differentiation *50*, 113-123.

Fuccillo, M., Rallu, M., McMahon, A.P., and Fishell, G. (2004). Temporal requirement for hedgehog signaling in ventral telencephalic patterning. Development *131*, 5031-5040.

Gama Sosa, M.A., De Gasperi, R., and Elder, G.A. (2010). Animal transgenesis: an overview. Brain Struct Funct *214*, 91-109.

Garcia, E.L., and Mills, A.A. (2002). Getting around lethality with inducible Cre-mediated excision. Semin Cell Dev Biol *13*, 151-158.

Gaspar, M.L., Meo, T., Bourgarel, P., Guenet, J.L., and Tosi, M. (1991). A single base deletion in the Tfm androgen receptor gene creates a short-lived messenger RNA that directs internal translation initiation. Proc Natl Acad Sci U S A *88*, 8606-8610.

Gaspar, M.L., Meo, T., and Tosi, M. (1990). Structure and size distribution of the androgen receptor mRNA in wild-type and Tfm/Y mutant mice. Mol Endocrinol *4*, 1600-1610.

Ge, R., Chen, G., and Hardy, M.P. (2008). The role of the Leydig cell in spermatogenic function. Adv Exp Med Biol *636*, 255-269.

Ge, R.S., and Hardy, M.P. (1998). Variation in the end products of androgen biosynthesis and metabolism during postnatal differentiation of rat Leydig cells. Endocrinology *139*, 3787-3795.

Geissler, W.M., Davis, D.L., Wu, L., Bradshaw, K.D., Patel, S., Mendonca, B.B., Elliston, K.O., Wilson, J.D., Russell, D.W., and Andersson, S. (1994). Male pseudohermaphroditism caused by mutations of testicular 17 beta-hydroxysteroid dehydrogenase 3. Nat Genet *7*, 34-39.

Georget, V., Lobaccaro, J.M., Terouanne, B., Mangeat, P., Nicolas, J.C., and Sultan, C. (1997). Trafficking of the androgen receptor in living cells with fused green fluorescent protein-androgen receptor. Mol Cell Endocrinol *129*, 17-26.

Ghadessy, F.J., Lim, J., Abdullah, A.A., Panet-Raymond, V., Choo, C.K., Lumbroso, R., Tut, T.G., Gottlieb, B., Pinsky, L., Trifiro, M.A., *et al.* (1999). Oligospermic infertility associated with an androgen receptor mutation that disrupts interdomain and coactivator (TIF2) interactions. J Clin Invest *103*, 1517-1525.

Ghyselinck, N.B., Vernet, N., Dennefeld, C., Giese, N., Nau, H., Chambon, P., Viville, S., and Mark, M. (2006). Retinoids and spermatogenesis: lessons from mutant mice lacking the plasma retinol binding protein. Dev Dyn *235*, 1608-1622.

Gioeli, D., Ficarro, S.B., Kwiek, J.J., Aaronson, D., Hancock, M., Catling, A.D., White, F.M., Christian, R.E., Settlage, R.E., Shabanowitz, J., *et al.* (2002). Androgen receptor phosphorylation. Regulation and identification of the phosphorylation sites. J Biol Chem *277*, 29304-29314.

Gobinet, J., Poujol, N., and Sultan, C. (2002). Molecular action of androgens. Mol Cell Endocrinol *198*, 15-24.

Godoy, A., Watts, A., Sotomayor, P., Montecinos, V.P., Huss, W.J., Onate, S.A., and Smith, G.J. (2008). Androgen receptor is causally involved in the homeostasis of the human prostate endothelial cell. Endocrinology *149*, 2959-2969.

Goldstein, J.L., and Wilson, J.D. (1972). Studies on the pathogenesis of the pseudohermaphroditism in the mouse with testicular feminization. J Clin Invest *51*, 1647-1658.

Gordon, J., Patel, S.R., Mishina, Y., and Manley, N.R. (2010). Evidence for an early role for BMP4 signaling in thymus and parathyroid morphogenesis. Dev Biol *339*, 141-154.

Gottlieb, B., Beitel, L.K., Wu, J.H., and Trifiro, M. (2004). The androgen receptor gene mutations database (ARDB): 2004 update. Hum Mutat *23*, 527-533.

Goyal, H.O., Bartol, F.F., Wiley, A.A., Khalil, M.K., Chiu, J., and Vig, M.M. (1997). Immunolocalization of androgen receptor and estrogen receptor in the developing testis and excurrent ducts of goats. Anat Rec *249*, 54-62.

Greco, T.L., and Payne, A.H. (1994). Ontogeny of expression of the genes for steroidogenic enzymes P450 side-chain cleavage, 3 beta-hydroxysteroid dehydrogenase, P450 17 alpha-hydroxylase/C17-20 lyase, and P450 aromatase in fetal mouse gonads. Endocrinology *135*, 262-268.

Grino, P.B., Griffin, J.E., and Wilson, J.D. (1990). Testosterone at high concentrations interacts with the human androgen receptor similarly to dihydrotestosterone. Endocrinology *126*, 1165-1172.

Griswold, S.L., and Behringer, R.R. (2009). Fetal Leydig cell origin and development. Sex Dev *3*, 1-15.

Guttman, J.A., Kimel, G.H., and Vogl, A.W. (2000). Dynein and plus-end microtubule-dependent motors are associated with specialized Sertoli cell junction plaques (ectoplasmic specializations). J Cell Sci *113 (Pt 12)*, 2167-2176.

Guttman, J.A., Takai, Y., and Vogl, A.W. (2004). Evidence that tubulobulbar complexes in the seminiferous epithelium are involved with internalization of adhesion junctions. Biol Reprod *71*, 548-559.

Guttroff, R.F., Cooke, P.S., and Hess, R.A. (1992). Blind-ending tubules and branching patterns of the rat ductuli efferentes. Anat Rec *232*, 423-431.

Hamzeh, M., and Robaire, B. (2009). Effect of testosterone on epithelial cell proliferation in the regressed rat epididymis. J Androl *30*, 200-212.

Hannema, S.E., Scott, I.S., Rajpert-De Meyts, E., Skakkebaek, N.E., Coleman, N., and Hughes, I.A. (2006). Testicular development in the complete androgen insensitivity syndrome. J Pathol *208*, 518-527.

Hansen, L.A., Clulow, J., and Jones, R.C. (1999). The role of Na+-H+ exchange in fluid and solute transport in the rat efferent ducts. Exp Physiol *84*, 521-527.

Hardy, M.P., Kelce, W.R., Klinefelter, G.R., and Ewing, L.L. (1990). Differentiation of Leydig cell precursors in vitro: a role for androgen. Endocrinology *127*, 488-490.

Haywood, M., Spaliviero, J., Jimemez, M., King, N.J., Handelsman, D.J., and Allan, C.M. (2003). Sertoli and germ cell development in hypogonadal (hpg) mice expressing transgenic follicle-stimulating hormone alone or in combination with testosterone. Endocrinology *144*, 509-517.

Haywood, M., Tymchenko, N., Spaliviero, J., Koch, A., Jimenez, M., Gromoll, J., Simoni, M., Nordhoff, V., Handelsman, D.J., and Allan, C.M. (2002). An activated human follicle-stimulating hormone (FSH) receptor stimulates FSH-like activity in gonadotropin-deficient transgenic mice. Mol Endocrinol *16*, 2582-2591.

He, W.W., Kumar, M.V., and Tindall, D.J. (1991). A frame-shift mutation in the androgen receptor gene causes complete androgen insensitivity in the testicular-feminized mouse. Nucleic Acids Res *19*, 2373-2378.

Hebert, J.M., and McConnell, S.K. (2000). Targeting of cre to the Foxg1 (BF-1) locus mediates loxP recombination in the telencephalon and other developing head structures. Dev Biol *222*, 296-306.

Heckert, L.L., and Griswold, M.D. (1991). Expression of follicle-stimulating hormone receptor mRNA in rat testes and Sertoli cells. Mol Endocrinol *5*, 670-677.

Heldring, N., Pike, A., Andersson, S., Matthews, J., Cheng, G., Hartman, J., Tujague, M., Strom, A., Treuter, E., Warner, M., *et al.* (2007). Estrogen receptors: how do they signal and what are their targets. Physiol Rev *87*, 905-931.

Hellwinkel, O.J., Bull, K., Holterhus, P.M., Homburg, N., Struve, D., and Hiort, O. (1999). Complete androgen insensitivity caused by a splice donor site mutation in intron 2 of the human androgen receptor gene resulting in an exon 2-lacking transcript with premature stop-codon and reduced expression. J Steroid Biochem Mol Biol *68*, 1-9.

Herbison, A.E. (2006). Physiology of the Gonadotropin-Releasing Hormone Neuronal Network. In Knobil and Neill's Physiology of Reproduction, 3rd Edition, J.D. Neill, ed. (Elsevier), pp. 1415-1456.

Hermo, L., Dworkin, J., and Oko, R. (1988). Role of epithelial clear cells of the rat epididymis in the disposal of the contents of cytoplasmic droplets detached from spermatozoa. Am J Anat *183*, 107-124.

Hermo, L., Krzeczunowicz, D., and Ruz, R. (2004). Cell specificity of aquaporins 0, 3, and 10 expressed in the testis, efferent ducts, and epididymis of adult rats. J Androl *25*, 494-505.

Hermo, L., Oko, R., and Robaire, B. (1992). Epithelial cells of the epididymis show regional variations with respect to the secretion of endocytosis of immobilin as revealed by light and electron microscope immunocytochemistry. Anat Rec *232*, 202-220.

Hermo, L., Pelletier, R.M., Cyr, D.G., and Smith, C.E. (2010). Surfing the wave, cycle, life history, and genes/proteins expressed by testicular germ cells. Part 1: background to spermatogenesis, spermatogonia, and spermatocytes. Microsc Res Tech *73*, 241-278.

Hermo, L., Wright, J., Oko, R., and Morales, C.R. (1991). Role of epithelial cells of the male excurrent duct system of the rat in the endocytosis or secretion of sulfated glycoprotein-2 (clusterin). Biol Reprod *44*, 1113-1131.

Hess, R.A. (1998). Effects of environmental toxicants on the efferent ducts, epididymis and fertility. J Reprod Fertil Suppl *53*, 247-259.

Hess, R.A., Bunick, D., Lee, K.H., Bahr, J., Taylor, J.A., Korach, K.S., and Lubahn, D.B. (1997). A role for oestrogens in the male reproductive system. Nature *390*, 509-512.

Hess, R.A., and Nakai, M. (2000). Histopathology of the male reproductive system induced by the fungicide benomyl. Histol Histopathol *15*, 207-224.

Higgins, S.J., Young, P., and Cunha, G.R. (1989). Induction of functional cytodifferentiation in the epithelium of tissue recombinants. II. Instructive induction of Wolffian duct epithelia by neonatal seminal vesicle mesenchyme. Development *106*, 235-250.

Hiort, O., and Holterhus, P.M. (2003). Androgen insensitivity and male infertility. Int J Androl *26*, 16-20.

Holdcraft, R.W., and Braun, R.E. (2004). Androgen receptor function is required in Sertoli cells for the terminal differentiation of haploid spermatids. Development *131*, 459-467.

Hsieh-Li, H.M., Witte, D.P., Weinstein, M., Branford, W., Li, H., Small, K., and Potter, S.S. (1995). Hoxa 11 structure, extensive antisense transcription, and function in male and female fertility. Development *121*, 1373-1385.

Hu, J., Chen, Y.X., Wang, D., Qi, X., Li, T.G., Hao, J., Mishina, Y., Garbers, D.L., and Zhao, G.Q. (2004). Developmental expression and function of Bmp4 in spermatogenesis and in maintaining epididymal integrity. Dev Biol *276*, 158-171.

Hu, R., Dunn, T.A., Wei, S., Isharwal, S., Veltri, R.W., Humphreys, E., Han, M., Partin, A.W., Vessella, R.L., Isaacs, W.B., *et al.* (2009). Ligand-independent androgen receptor variants derived from splicing of cryptic exons signify hormone-refractory prostate cancer. Cancer Res *69*, 16-22.

Hu, Z., Dandekar, D., O'Shaughnessy, P.J., De Gendt, K., Verhoeven, G., and Wilkinson, M.F. Androgen-induced Rhox homeobox genes modulate the expression of AR-regulated genes. Mol Endocrinol *24*, 60-75.

Hughes, I.A., and Acerini, C.L. (2008). Factors controlling testis descent. Eur J Endocrinol *159 Suppl 1*, S75-82.

Hurd, E.A., Poucher, H.K., Cheng, K., Raphael, Y., and Martin, D.M. The ATP-dependent chromatin remodeling enzyme CHD7 regulates pro-neural gene expression and neurogenesis in the inner ear. Development *137*, 3139-3150.

Hwang, C.H., Guo, D., Harris, M.A., Howard, O., Mishina, Y., Gan, L., Harris, S.E., and Wu, D.K. Role of bone morphogenetic proteins on cochlear hair cell formation: analyses of Noggin and Bmp2 mutant mice. Dev Dyn *239*, 505-513.

Ikawa, M., Tergaonkar, V., Ogura, A., Ogonuki, N., Inoue, K., and Verma, I.M. (2002). Restoration of spermatogenesis by lentiviral gene transfer: offspring from infertile mice. Proc Natl Acad Sci U S A *99*, 7524-7529.

Ilio, K.Y., and Hess, R.A. (1992). Localization and activity of Na+,K(+)-ATPase in the ductuli efferentes of the rat. Anat Rec *234*, 190-200.

Ilio, K.Y., and Hess, R.A. (1994). Structure and function of the ductuli efferentes: a review. Microsc Res Tech *29*, 432-467.

Imperato-McGinley, J., and Zhu, Y.S. (2002). Androgens and male physiology the syndrome of 5alpha-reductase-2 deficiency. Mol Cell Endocrinol *198*, 51-59.

Janulis, L., Hess, R.A., Bunick, D., Nitta, H., Janssen, S., Asawa, Y., and Bahr, J.M. (1996). Mouse epididymal sperm contain active P450 aromatase which decreases as sperm traverse the epididymis. J Androl *17*, 111-116.

Jenkins, E.P., Hsieh, C.L., Milatovich, A., Normington, K., Berman, D.M., Francke, U., and Russell, D.W. (1991). Characterization and chromosomal mapping of a human steroid 5 alpha-reductase gene and pseudogene and mapping of the mouse homologue. Genomics *11*, 1102-1112.

Jenster, G., Trapman, J., and Brinkmann, A.O. (1993). Nuclear import of the human androgen receptor. Biochem J *293 (Pt 3)*, 761-768.

Jenster, G., van der Korput, H.A., Trapman, J., and Brinkmann, A.O. (1995). Identification of two transcription activation units in the N-terminal domain of the human androgen receptor. J Biol Chem *270*, 7341-7346.

Jeyasuria, P., Ikeda, Y., Jamin, S.P., Zhao, L., De Rooij, D.G., Themmen, A.P., Behringer, R.R., and Parker, K.L. (2004). Cell-specific knockout of steroidogenic factor 1 reveals its essential roles in gonadal function. Mol Endocrinol *18*, 1610-1619.

Johnson, M.H., and Everitt, B.J. (2000). Essential Reproduction, 5th edn (Blackwell Science).

Johnston, D.S., Russell, L.D., Friel, P.J., and Griswold, M.D. (2001). Murine germ cells do not require functional androgen receptors to complete spermatogenesis following spermatogonial stem cell transplantation. Endocrinology *142*, 2405-2408.

Jones, N. (1990). Transcriptional regulation by dimerization: two sides to an incestuous relationship. Cell *61*, 9-11.

Jorgensen, J.S., and Nilson, J.H. (2001). AR suppresses transcription of the LHbeta subunit by interacting with steroidogenic factor-1. Mol Endocrinol *15*, 1505-1516.

Joseph, A., Hess, R.A., Schaeffer, D.J., Ko, C., Hudgin-Spivey, S., Chambon, P., and Shur, B.D. (2010a). Absence of estrogen receptor alpha leads to physiological alterations in the mouse epididymis and consequent defects in sperm function. Biol Reprod *82*, 948-957.

Joseph, A., Shur, B.D., and Hess, R.A. (2010b). Estrogen, Efferent Ductules, and the Epididymis. Biol Reprod.

Joseph, A., Yao, H., and Hinton, B.T. (2009). Development and morphogenesis of the Wolffian/epididymal duct, more twists and turns. Dev Biol *325*, 6-14.

Joseph, D.R. (1994). Structure, function, and regulation of androgen-binding protein/sex hormone-binding globulin. Vitam Horm *49*, 197-280.

Kampa, M., Papakonstanti, E.A., Hatzoglou, A., Stathopoulos, E.N., Stournaras, C., and Castanas, E. (2002). The human prostate cancer cell line LNCaP bears functional membrane testosterone receptors that increase PSA secretion and modify actin cytoskeleton. FASEB J *16*, 1429-1431.

Karl, J., and Capel, B. (1998). Sertoli cells of the mouse testis originate from the coelomic epithelium. Dev Biol *203*, 323-333.

Katz, M.D., Kligman, I., Cai, L.Q., Zhu, Y.S., Fratianni, C.M., Zervoudakis, I., Rosenwaks, Z., and Imperato-McGinley, J. (1997). Paternity by intrauterine insemination with sperm from a man with 5alpha-reductase-2 deficiency. N Engl J Med *336*, 994-997.

Keene, D.E., Suescun, M.O., Bostwick, M.G., Chandrashekar, V., Bartke, A., and Kopchick, J.J. (2002). Puberty is delayed in male growth hormone receptor gene-disrupted mice. J Androl *23*, 661-668.

Keeney, D. S., Mendis-Handagama, S. M. L. C., Zirkin, B. R., and Ewing, L. L. (1988). Effect of long-term deprivation of luteinizing hormone on Leydig cell volume, Leydig cell number and steroidogenic capacity of the rat testis. Endocrinology *123*, 2906-2915.

Kent, J., Wheatley, S.C., Andrews, J.E., Sinclair, A.H., and Koopman, P. (1996). A male-specific role for SOX9 in vertebrate sex determination. Development *122*, 2813-2822.

Kerr, J.B., and Knell, C.M. (1988). The fate of fetal Leydig cells during the development of the fetal and postnatal rat testis. Development *103*, 535-544.

Kerr, J.B., Loveland, K.L., O'Bryan, M.K., and de Kretser, D.M. (2006). Cytology of the Testis and Intrinsic Control Mechanisms. In Physiology of Reproduction (Third Edition), K. Knobil, and J.D. Neill, eds. (Gulf Professional Publishing).

Kierszenbaum, A.L. (2002). Sperm axoneme: a tale of tubulin posttranslation diversity. Mol Reprod Dev *62*, 1-3.

Kim, H.J., and Lee, W.J. (2009). Ligand-independent activation of the androgen receptor by insulin-like growth factor-I and the role of the MAPK pathway in skeletal muscle cells. Mol Cells *28*, 589-593.

Kim, Y., Kobayashi, A., Sekido, R., DiNapoli, L., Brennan, J., Chaboissier, M.C., Poulat, F., Behringer, R.R., Lovell-Badge, R., and Capel, B. (2006). Fgf9 and Wnt4 act as antagonistic signals to regulate mammalian sex determination. PLoS Biol *4*, e187.

Kirchhoff, C., Osterhoff, C., and Samalecos, A. (2008). HE6/GPR64 adhesion receptor co-localizes with apical and subapical F-actin scaffold in male excurrent duct epithelia. Reproduction *136*, 235-245.

Kisanuki, Y.Y., Hammer, R.E., Miyazaki, J., Williams, S.C., Richardson, J.A., and Yanagisawa, M. (2001). Tie2-Cre transgenic mice: a new model for endothelial cell-lineage analysis in vivo. Dev Biol *230*, 230-242.

Kitamura, K., Yanazawa, M., Sugiyama, N., Miura, H., Iizuka-Kogo, A., Kusaka, M., Omichi, K., Suzuki, R., Kato-Fukui, Y., Kamiirisa, K., *et al.* (2002). Mutation of ARX causes abnormal development of forebrain and testes in mice and X-linked lissencephaly with abnormal genitalia in humans. Nat Genet *32*, 359-369.

Kobayashi, A., and Behringer, R.R. (2003). Developmental genetics of the female reproductive tract in mammals. Nat Rev Genet *4*, 969-980.

Kojima, M., and Ohe, H. (1986). Experimental study on the regulation of testicular function by the cremaster reflex in rats. Tohoku J Exp Med *150*, 175-180.

Konrad, L., Munir Keilani, M., Cordes, A., Volck-Badouin, E., Laible, L., Albrecht, M., Renneberg, H., and Aumuller, G. (2005). Rat Sertoli cells express epithelial but also mesenchymal genes after immortalization with SV40. Biochim Biophys Acta *1722*, 6-14.

Kotsuji, F., Winters, S.J., Attardi, B., Keeping, H.S., Oshima, H., and Troen, P. (1988). Effects of gonadal steroids on gonadotropin secretion in males: studies with perifused rat pituitary cells. Endocrinology *123*, 2683-2689.

Krege, J.H., Hodgin, J.B., Couse, J.F., Enmark, E., Warner, M., Mahler, J.F., Sar, M., Korach, K.S., Gustafsson, J.A., and Smithies, O. (1998). Generation and reproductive phenotypes of mice lacking estrogen receptor beta. Proc Natl Acad Sci U S A *95*, 15677-15682.

Krishnamurthy, H., Kats, R., Danilovich, N., Javeshghani, D., and Sairam, M.R. (2001). Intercellular communication between Sertoli cells and Leydig cells in the absence of follicle-stimulating hormone-receptor signaling. Biol Reprod *65*, 1201-1207.

Krutskikh, A., De Gendt, K., Sharp, V., Verhoeven, G., Poutanen, M., and Huhtaniemi, I. (2011). Targeted inactivation of the androgen receptor gene in murine proximal epididymis causes epithelial hypotrophy and obstructive azoospermia. Endocrinology *152*, 689-696.

Kuil, C.W., and Mulder, E. (1995). Effects of androgens and antiandrogens on the conformation of the androgen receptor. Ann N Y Acad Sci *761*, 351-354.

Kuiper, G.G., and Brinkmann, A.O. (1995). Phosphotryptic peptide analysis of the human androgen receptor: detection of a hormone-induced phosphopeptide. Biochemistry *34*, 1851-1857.

Kumar, T.R., Wang, Y., Lu, N., and Matzuk, M.M. (1997). Follicle stimulating hormone is required for ovarian follicle maturation but not male fertility. Nat Genet *15*, 201-204.

Kuure, S., Vuolteenaho, R., and Vainio, S. (2000). Kidney morphogenesis: cellular and molecular regulation. Mech Dev *92*, 31-45.

La Spada, A.R., Wilson, E.M., Lubahn, D.B., Harding, A.E., and Fischbeck, K.H. (1991). Androgen receptor gene mutations in X-linked spinal and bulbar muscular atrophy. Nature *352*, 77-79.

Labrie, F., Sugimoto, Y., Luu-The, V., Simard, J., Lachance, Y., Bachvarov, D., Leblanc, G., Durocher, F., and Paquet, N. (1992). Structure of human type II 5 alpha-reductase gene. Endocrinology *131*, 1571-1573.

Lavoie, H.A., and King, S.R. (2009). Transcriptional regulation of steroidogenic genes: STARD1, CYP11A1 and HSD3B. Exp Biol Med (Maywood) *234*, 880-907.

Layman, L.C., Porto, A.L., Xie, J., da Motta, L.A., da Motta, L.D., Weiser, W., and Sluss, P.M. (2002). FSH beta gene mutations in a female with partial breast development and a male sibling with normal puberty and azoospermia. J Clin Endocrinol Metab *87*, 3702-3707.

Lecureuil, C., Fontaine, I., Crepieux, P., and Guillou, F. (2002). Sertoli and granulosa cell-specific Cre recombinase activity in transgenic mice. Genesis *33*, 114-118.

Lee, K.H., Finnigan-Bunick, C., Bahr, J., and Bunick, D. (2001). Estrogen regulation of ion transporter messenger RNA levels in mouse efferent ductules are mediated differentially through estrogen receptor (ER) alpha and ER beta. Biol Reprod *65*, 1534-1541.

Lee, K.H., Hess, R.A., Bahr, J.M., Lubahn, D.B., Taylor, J., and Bunick, D. (2000). Estrogen receptor alpha has a functional role in the mouse rete testis and efferent ductules. Biol Reprod *63*, 1873-1880.

Lei, Z.M., Mishra, S., Zou, W., Xu, B., Foltz, M., Li, X., and Rao, C.V. (2001). Targeted disruption of luteinizing hormone/human chorionic gonadotropin receptor gene. Mol Endocrinol *15*, 184-200.

Leung, G.P., Gong, X.D., Cheung, K.H., Cheng-Chew, S.B., and Wong, P.Y. (2001). Expression of cystic fibrosis transmembrane conductance regulator in rat efferent duct epithelium. Biol Reprod *64*, 1509-1515.

Li, M.W., Xia, W., Mruk, D.D., Wang, C.Q., Yan, H.H., Siu, M.K., Lui, W.Y., Lee, W.M., and Cheng, C.Y. (2006). Tumor necrosis factor {alpha} reversibly disrupts the blood-testis barrier and impairs Sertoli-germ cell adhesion in the seminiferous epithelium of adult rat testes. J Endocrinol *190*, 313-329.

Lie, P.P., Mruk, D.D., Lee, W.M., and Cheng, C.Y. (2010). Cytoskeletal dynamics and spermatogenesis. Philos Trans R Soc Lond B Biol Sci *365*, 1581-1592.

Lieberman, A.P., Harmison, G., Strand, A.D., Olson, J.M., and Fischbeck, K.H. (2002). Altered transcriptional regulation in cells expressing the expanded polyglutamine androgen receptor. Hum Mol Genet *11*, 1967-1976.

Lim, P., Robson, M., Spaliviero, J., McTavish, K.J., Jimenez, M., Zajac, J.D., Handelsman, D.J., and Allan, C.M. (2009). Sertoli cell androgen receptor DNA binding domain is essential for the completion of spermatogenesis. Endocrinology *150*, 4755-4765.

Lopez, E., Viart, V., Guittard, C., Templin, C., Rene, C., Mechin, D., Georges, M.D., Claustres, M., Romey-Chatelain, M.C., and Taulan, M. (2010). Variants in CFTR untranslated regions are associated with congenital bilateral absence of the vas deferens. J Med Genet.

Lording, D.W., and De Kretser, D.M. (1972). Comparative ultrastructural and histochemical studies of the interstitial cells of the rat testis during fetal and postnatal development. J Reprod Fertil *29*, 261-269.

Lui, W.Y., Wong, C.H., Mruk, D.D., and Cheng, C.Y. (2003). TGF-beta3 regulates the blood-testis barrier dynamics via the p38 mitogen activated protein (MAP) kinase pathway: an in vivo study. Endocrinology *144*, 1139-1142.

Lumbroso, S., Lobaccaro, J.M., Vial, C., Sassolas, G., Ollagnon, B., Belon, C., Pouget, J., and Sultan, C. (1997). Molecular analysis of the androgen receptor gene in Kennedy's disease. Report of two families and review of the literature. Horm Res *47*, 23-29.

Lyng, F.M., Jones, G.R., and Rommerts, F.F. (2000). Rapid androgen actions on calcium signaling in rat sertoli cells and two human prostatic cell lines: similar biphasic responses between 1 picomolar and 100 nanomolar concentrations. Biol Reprod *63*, 736-747.

Lyon, M.F., and Hawkes, S.G. (1970). X-linked gene for testicular feminization in the mouse. Nature *227*, 1217-1219.

Ma, X., Dong, Y., Matzuk, M.M., and Kumar, T.R. (2004). Targeted disruption of luteinizing hormone beta-subunit leads to hypogonadism, defects in gonadal steroidogenesis, and infertility. Proc Natl Acad Sci U S A *101*, 17294-17299.

MacLean, H.E., Chiu, W.S., Notini, A.J., Axell, A.M., Davey, R.A., McManus, J.F., Ma, C., Plant, D.R., Lynch, G.S., and Zajac, J.D. (2008). Impaired skeletal muscle development and function in male, but not female, genomic androgen receptor knockout mice. FASEB J *22*, 2676-2689.

Maddocks, S., Hargreave, T.B., Reddie, K., Fraser, H.M., Kerr, J.B., and Sharpe, R.M. (1993). Intratesticular hormone levels and the route of secretion of hormones from the testis of the rat, guinea pig, monkey and human. Int J Androl *16*, 272-278.

Mahendroo, M.S., Cala, K.M., Hess, D.L., and Russell, D.W. (2001). Unexpected virilization in male mice lacking steroid 5 alpha-reductase enzymes. Endocrinology *142*, 4652-4662.

Majdic, G., Millar, M.R., and Saunders, P.T. (1995). Immunolocalisation of androgen receptor to interstitial cells in fetal rat testes and to mesenchymal and epithelial cells of associated ducts. J Endocrinol *147*, 285-293.

Malinowska, K., Neuwirt, H., Cavarretta, I.T., Bektic, J., Steiner, H., Dietrich, H., Moser, P.L., Fuchs, D., Hobisch, A., and Culig, Z. (2009). Interleukin-6 stimulation of growth of prostate cancer in vitro and in vivo through activation of the androgen receptor. Endocr Relat Cancer *16*, 155-169.

Mangelsdorf, D.J., Thummel, C., Beato, M., Herrlich, P., Schutz, G., Umesono, K., Blumberg, B., Kastner, P., Mark, M., Chambon, P., *et al.* (1995). The nuclear receptor superfamily: the second decade. Cell *83*, 835-839.

Marcelli, M., Ittmann, M., Mariani, S., Sutherland, R., Nigam, R., Murthy, L., Zhao, Y., DiConcini, D., Puxeddu, E., Esen, A., *et al.* (2000). Androgen receptor mutations in prostate cancer. Cancer Res *60*, 944-949.

Marians, R.C., Ng, L., Blair, H.C., Unger, P., Graves, P.N., and Davies, T.F. (2002). Defining thyrotropin-dependent and -independent steps of thyroid hormone synthesis by using thyrotropin receptor-null mice. Proc Natl Acad Sci U S A *99*, 15776-15781.

Marker, P.C., Donjacour, A.A., Dahiya, R., and Cunha, G.R. (2003). Hormonal, cellular, and molecular control of prostatic development. Dev Biol *253*, 165-174.

Marshall, F.F., Reiner, W.G., and Goldberg, B.S. (1979). The embryologic origin of the caput epididymidis in the rat. Invest Urol *17*, 78-82.

Mason, A.J., Hayflick, J.S., Zoeller, R.T., Young, W.S., 3rd, Phillips, H.S., Nikolics, K., and Seeburg, P.H. (1986). A deletion truncating the gonadotropin-releasing hormone gene is responsible for hypogonadism in the hpg mouse. Science *234*, 1366-1371.

Matthaei, K.I. (2007). Genetically manipulated mice: a powerful tool with unsuspected caveats. J Physiol *582*, 481-488.

Matthiesson, K.L., McLachlan, R.I., O'Donnell, L., Frydenberg, M., Robertson, D.M., Stanton, P.G., and Meachem, S.J. (2006). The relative roles of follicle-stimulating hormone and luteinizing hormone in maintaining spermatogonial maturation and spermiation in normal men. J Clin Endocrinol Metab *91*, 3962-3969.

McEwan, I.J. (2004). Molecular mechanisms of androgen receptor-mediated gene regulation: structure-function analysis of the AF-1 domain. Endocr Relat Cancer *11*, 281-293.

McKenna, N.J., Lanz, R.B., and O'Malley, B.W. (1999). Nuclear receptor coregulators: cellular and molecular biology. Endocr Rev *20*, 321-344.

McLachlan, R.I., O'Donnell, L., Meachem, S.J., Stanton, P.G., de Kretser, D.M., Pratis, K., and Robertson, D.M. (2002). Identification of specific sites of hormonal regulation in spermatogenesis in rats, monkeys, and man. Recent Prog Horm Res *57*, 149-179.

McNeilly, J.R., Saunders, P.T., Taggart, M., Cranfield, M., Cooke, H.J., and McNeilly, A.S. (2000). Loss of oocytes in Dazl knockout mice results in maintained ovarian steroidogenic function but altered gonadotropin secretion in adult animals. Endocrinology *141*, 4284-4294.

Meachem, S.J., Nieschlag, E., and Simoni, M. (2001). Inhibin B in male reproduction: pathophysiology and clinical relevance. Eur J Endocrinol *145*, 561-571.

Mendive, F., Laurent, P., Van Schoore, G., Skarnes, W., Pochet, R., and Vassart, G. (2006). Defective postnatal development of the male reproductive tract in LGR4 knockout mice. Dev Biol *290*, 421-434.

Millar, R.P. (2005). GnRHs and GnRH receptors. Anim Reprod Sci *88*, 5-28.

Miyamoto, J., Matsumoto, T., Shiina, H., Inoue, K., Takada, I., Ito, S., Itoh, J., Minematsu, T., Sato, T., Yanase, T., *et al.* (2007). The pituitary function of androgen receptor constitutes a glucocorticoid production circuit. Mol Cell Biol *27*, 4807-4814.

Moore, H.D., and Bedford, J.M. (1979a). The differential absorptive activity of epithelial cells of the rat epididymus before and after castration. Anat Rec *193*, 313-327.

Moore, H.D., and Bedford, J.M. (1979b). Short-term effects of androgen withdrawal on the structure of different epithelial cells in the rat epididymis. Anat Rec *193*, 293-311.

Morais da Silva, S., Hacker, A., Harley, V., Goodfellow, P., Swain, A., and Lovell-Badge, R. (1996). Sox9 expression during gonadal development implies a conserved role for the gene in testis differentiation in mammals and birds. Nat Genet *14*, 62-68.

Mruk, D.D., and Cheng, C.Y. (2004). Sertoli-Sertoli and Sertoli-germ cell interactions and their significance in germ cell movement in the seminiferous epithelium during spermatogenesis. Endocr Rev *25*, 747-806.

Muller, J. (1984). Morphometry and histology of gonads from twelve children and adolescents with the androgen insensitivity (testicular feminization) syndrome. J Clin Endocrinol Metab *59*, 785-789.

Munell, F., Suarez-Quian, C.A., Selva, D.M., Tirado, O.M., and Reventos, J. (2002). Androgen-binding protein and reproduction: where do we stand? J Androl *23*, 598-609.

Munsterberg, A., and Lovell-Badge, R. (1991). Expression of the mouse anti-mullerian hormone gene suggests a role in both male and female sexual differentiation. Development *113*, 613-624.

Murphy, L., Jeffcoate, I.A., and O'Shaughnessy, P.J. (1994). Abnormal Leydig cell development at puberty in the androgen-resistant Tfm mouse. Endocrinology *135*, 1372-1377.

Murphy, L., and O'Shaughnessy, P.J. (1991). Testicular steroidogenesis in the testicular feminized (Tfm) mouse: loss of 17 alpha-hydroxylase activity. J Endocrinol *131*, 443-449.

Nagy, A. (2000). Cre recombinase: the universal reagent for genome tailoring. Genesis *26*, 99-109.

Naik, K., Pittman, I., Wolfe, A., Miller, R.S., Radovick, S., and Wondisford, F.E. (2006). A novel technique for temporally regulated cell type-specific Cre expression and recombination in the pituitary gonadotroph. Journal of Molecular Endocrinology *37*, 63-69.

Nakagawa, T., Nabeshima, Y., and Yoshida, S. (2007). Functional identification of the actual and potential stem cell compartments in mouse spermatogenesis. Dev Cell *12*, 195-206.

Nakai, M., Hess, R.A., Moore, B.J., Guttroff, R.F., Strader, L.F., and Linder, R.E. (1992). Acute and long-term effects of a single dose of the fungicide carbendazim (methyl 2-benzimidazole carbamate) on the male reproductive system in the rat. J Androl *13*, 507-518.

Nakajin, S., and Hall, P.F. (1981). Microsomal cytochrome P-450 from neonatal pig testis. Purification and properties of A C21 steroid side-chain cleavage system (17 alpha-hydroxylase-C17,20 lyase). J Biol Chem *256*, 3871-3876.

Nakhla, A.M., Mather, J.P., Janne, O.A., and Bardin, C.W. (1984). Estrogen and androgen receptors in Sertoli, Leydig, myoid, and epithelial cells: effects of time in culture and cell density. Endocrinology *115*, 121-128.

Nef, S., and Parada, L.F. (1999). Cryptorchidism in mice mutant for Insl3. Nat Genet *22*, 295-299.

Nef, S., and Vassalli, J.D. (2009). Complementary pathways in mammalian female sex determination. J Biol *8*, 74.

Nelson, R.D., Stricklett, P., Gustafson, C., Stevens, A., Ausiello, D., Brown, D., and Kohan, D.E. (1998). Expression of an AQP2 Cre recombinase transgene in kidney and male reproductive system of transgenic mice. Am J Physiol *275*, C216-226.

Nicander, L., and Glover, T.D. (1973). Regional histology and fine structue of the epididymal duct in the golden hamster (Mesocricetus auratus). J Anat *114*, 347-364.

Nitta, H., Bunick, D., Hess, R.A., Janulis, L., Newton, S.C., Millette, C.F., Osawa, Y., Shizuta, Y., Toda, K., and Bahr, J.M. (1993). Germ cells of the mouse testis express P450 aromatase. Endocrinology *132*, 1396-1401.

Norton, J.N., and Skinner, M.K. (1989). Regulation of Sertoli cell function and differentiation through the actions of a testicular paracrine factor P-Mod-S. Endocrinology *124*, 2711-2719.

Norton, J.N., Vigne, J.L., and Skinner, M.K. (1994). Regulation of Sertoli cell differentiation by the testicular paracrine factor PModS: analysis of common signal transduction pathways. Endocrinology *134*, 149-157.

Notini, A.J., Davey, R.A., McManus, J.F., Bate, K.L., and Zajac, J.D. (2005). Genomic actions of the androgen receptor are required for normal male sexual differentiation in a mouse model. J Mol Endocrinol *35*, 547-555.

O'Donnell, L., McLachlan, R.I., Wreford, N.G., de Kretser, D.M., and Robertson, D.M. (1996). Testosterone withdrawal promotes stage-specific detachment of round spermatids from the rat seminiferous epithelium. Biol Reprod *55*, 895-901.

O'Donnell, L., McLachlan, R.I., Wreford, N.G., and Robertson, D.M. (1994). Testosterone promotes the conversion of round spermatids between stages VII and VIII of the rat spermatogenic cycle. Endocrinology *135*, 2608-2614.

O'Donnell, L., Meachem, S.J., Stanton, P.G., and McLachlan, R.I. (2006). Endocrine Regulation of Spermatogenesis. In Knobil and Neill's Physiology of Reproduction (Third Edition), K. Knobil, and J.D. Neill, eds. (Gulf Professional Publishing).

O'Donnell, L., Stanton, P.G., Bartles, J.R., and Robertson, D.M. (2000). Sertoli cell ectoplasmic specializations in the seminiferous epithelium of the testosterone-suppressed adult rat. Biol Reprod *63*, 99-108.

O'Hara, L., Welsh, M., Saunders, P.T., and Smith, L.B. (2011). Androgen receptor expression in the caput epididymal epithelium is essential for development of the initial segment and epididymal spermatozoa transit. Endocrinology *152*, 718-729.

O'Shaughnessy, P.J., Abel, M., Charlton, H.M., Hu, B., Johnston, H., and Baker, P.J. (2007). Altered expression of genes involved in regulation of vitamin A metabolism, solute transportation, and cytoskeletal function in the androgen-insensitive tfm mouse testis. Endocrinology *148*, 2914-2924.

O'Shaughnessy, P.J., Baker, P.J., Heikkila, M., Vainio, S., and McMahon, A.P. (2000). Localization of 17beta-hydroxysteroid dehydrogenase/17-ketosteroid reductase isoform expression in the developing mouse testis--androstenedione is the major androgen secreted by fetal/neonatal leydig cells. Endocrinology *141*, 2631-2637.

O'Shaughnessy, P.J., Baker, P.J., and Johnston, H. (2006). The foetal Leydig cell-- differentiation, function and regulation. Int J Androl *29*, 90-95; discussion 105-108.

O'Shaughnessy, P.J., Fleming, L.M., Jackson, G., Hochgeschwender, U., Reed, P., and Baker, P.J. (2003). Adrenocorticotropic hormone directly stimulates testosterone production by the fetal and neonatal mouse testis. Endocrinology *144*, 3279-3284.

O'Shaughnessy, P.J., Johnston, H., Willerton, L., and Baker, P.J. (2002a). Failure of normal adult Leydig cell development in androgen-receptor-deficient mice. J Cell Sci *115*, 3491-3496.

O'Shaughnessy, P. J., Monteiro, A., Verhoeven, G., De Gendt, K., and Abel, M. H. (2010). Effect of FSH on testicular morphology and spermatogenesis in gonadotrophin-deficient hypogonadal mice lacking androgen receptors. Reproduction *139*, 177-184.

O'Shaughnessy, P.J., Morris, I.D., and Baker, P.J. (2008). Leydig cell re-generation and expression of cell signaling molecules in the germ cell-free testis. Reproduction *135*, 851-858.

O'Shaughnessy, P.J., Morris, I.D., Huhtaniemi, I., Baker, P.J., and Abel, M.H. (2009). Role of androgen and gonadotrophins in the development and function of the Sertoli cells and Leydig cells: data from mutant and genetically modified mice. Mol Cell Endocrinol *306*, 2-8.

O'Shaughnessy, P.J., and Sheffield, J.W. (1991). Effect of temperature and the role of testicular descent on post-natal testicular androgen production in the mouse. J Reprod Fertil *91*, 357-364.

O'Shaughnessy, P.J., Willerton, L., and Baker, P.J. (2002b). Changes in Leydig cell gene expression during development in the mouse. Biol Reprod *66*, 966-975.

Oakberg, E.F. (1956). Duration of spermatogenesis in the mouse and timing of stages of the cycle of the seminiferous epithelium. Am J Anat *99*, 507-516.

Oatley, J.M., and Brinster, R.L. (2008). Regulation of spermatogonial stem cell self-renewal in mammals. Annu Rev Cell Dev Biol *24*, 263-286.

Obendorf, M., Meyer, R., Henning, K., Mitev, Y.A., Schroder, J., Patchev, V.K., and Wolf, S.S. (2007). FoxG1, a member of the forkhead family, is a corepressor of the androgen receptor. J Steroid Biochem Mol Biol *104*, 195-207.

Ojeda, S.R., and Skinner, M.K. (2006). Puberty in the Rat. In Knobil and Neill's Physiology of Reproduction (Third Edition), E. Knobil, ed. (Gulf Professional Publishing).

Okada, Y., Fujii, Y., Moore, J.P., and Winters, S.J. (2003). Androgen Receptors in Gonadotrophs in Pituitary Cultures from Adult Male Monkeys and Rats. Endocrinology *144*, 267-273.

Oliveira, C.A., Mahecha, G.A., Carnes, K., Prins, G.S., Saunders, P.T., Franca, L.R., and Hess, R.A. (2004). Differential hormonal regulation of estrogen receptors ERalpha and ERbeta and androgen receptor expression in rat efferent ductules. Reproduction *128*, 73-86.

Olson, G.E., Winfrey, V.P., and Nagdas, S.K. (2003). Structural modification of the hamster sperm acrosome during posttesticular development in the epididymis. Microsc Res Tech *61*, 46-55.

Page, R.B. (2006). Anatomy of the Hypothalamo-Hypophysial Complex. In Knobil and Neill's Physiology of Reproduction, 3rd Edition, J.D. Neill, ed. (Elsevier), pp. 1309-1380.

Paigen, K. (2003a). One hundred years of mouse genetics: an intellectual history. I. The classical period (1902-1980). Genetics *163*, 1-7.

Paigen, K. (2003b). One hundred years of mouse genetics: an intellectual history. II. The molecular revolution (1981-2002). Genetics *163*, 1227-1235.

Pakarinen, P., Kimura, S., El-Gehani, F., Pelliniemi, L.J., and Huhtaniemi, I. (2002). Pituitary hormones are not required for sexual differentiation of male mice: phenotype of the T/ebp/Nkx2.1 null mutant mice. Endocrinology *143*, 4477-4482.

Palmer, S.J., and Burgoyne, P.S. (1991). In situ analysis of fetal, prepuberal and adult XX----XY chimaeric mouse testes: Sertoli cells are predominantly, but not exclusively, XY. Development *112*, 265-268.

Park, W.H., and Hutson, J.M. (1991). The gubernaculum shows rhythmic contractility and active movement during testicular descent. J Pediatr Surg *26*, 615-617.

Pastor-Soler, N., Bagnis, C., Sabolic, I., Tyszkowski, R., McKee, M., Van Hoek, A., Breton, S., and Brown, D. (2001). Aquaporin 9 expression along the male reproductive tract. Biol Reprod *65*, 384-393.

Pelletier, G., Labrie, C., and Labrie, F. (2000). Localization of oestrogen receptor alpha, oestrogen receptor beta and androgen receptors in the rat reproductive organs. J Endocrinol *165*, 359-370.

Peng, B., Mao, Y., Tang, X.-F., Shang, Y., Shen, C.-Y., Guo, Y.X., Xiang, Y., and Yang, Z.-W. (2010). Comparison of spermatogenic damage induced at 6 months after ligation of the vas deferens at proximal and distal locations in the rabbit. Andrologia.

Phillip, M., Arbelle, J.E., Segev, Y., and Parvari, R. (1998). Male hypogonadism due to a mutation in the gene for the beta-subunit of follicle-stimulating hormone. N Engl J Med *338*, 1729-1732.

Picard, D., Khursheed, B., Garabedian, M.J., Fortin, M.G., Lindquist, S., and Yamamoto, K.R. (1990). Reduced levels of hsp90 compromise steroid receptor action in vivo. Nature *348*, 166-168.

Pirvola, U., Ylikoski, J., Trokovic, R., Hebert, J.M., McConnell, S.K., and Partanen, J. (2002). FGFR1 is required for the development of the auditory sensory epithelium. Neuron *35*, 671-680.

Pitteloud, N., Dwyer, A.A., DeCruz, S., Lee, H., Boepple, P.A., Crowley, W.F., Jr., and Hayes, F.J. (2008). Inhibition of luteinizing hormone secretion by testosterone in men requires aromatization for its pituitary but not its hypothalamic effects: evidence from the tandem study of normal and gonadotropin-releasing hormone-deficient men. J Clin Endocrinol Metab *93*, 784-791.

Pointis, G., Gilleron, J., Carette, D., and Segretain, D. (2010). Physiological and physiopathological aspects of connexins and communicating gap junctions in spermatogenesis. Philos Trans R Soc Lond B Biol Sci *365*, 1607-1620.

Porter, T.D., and Coon, M.J. (1991). Cytochrome P-450. Multiplicity of isoforms, substrates, and catalytic and regulatory mechanisms. J Biol Chem *266*, 13469-13472.

Primiani, N., Gregory, M., Dufresne, J., Smith, C.E., Liu, Y.L., Bartles, J.R., Cyr, D.G., and Hermo, L. (2007). Microvillar size and espin expression in principal cells of the adult rat epididymis are regulated by androgens. J Androl *28*, 659-669.

Quigley, C.A., De Bellis, A., Marschke, K.B., el-Awady, M.K., Wilson, E.M., and French, F.S. (1995). Androgen receptor defects: historical, clinical, and molecular perspectives. Endocr Rev *16*, 271-321.

Rahman, F., and Christian, H.C. (2007). Non-classical actions of testosterone: an update. Trends Endocrinol Metab *18*, 371-378.

Rahman, N.A., and Huhtaniemi, I.T. (2004). Testicular cell lines. Mol Cell Endocrinol *228*, 53-65.

Raskin, K., de Gendt, K., Duittoz, A., Liere, P., Verhoeven, G., Tronche, F., and Mhaouty-Kodja, S. (2009). Conditional inactivation of androgen receptor gene in the nervous system: effects on male behavioral and neuroendocrine responses. J Neurosci *29*, 4461-4470.

Rato, L., Socorro, S., Cavaco, J.E., and Oliveira, P.F. (2010). Tubular fluid secretion in the seminiferous epithelium: ion transporters and aquaporins in Sertoli cells. J Membr Biol *236*, 215-224.

Ribeiro, R.C., Kushner, P.J., and Baxter, J.D. (1995). The nuclear hormone receptor gene superfamily. Annu Rev Med *46*, 443-453.

Richardson, L.L., Kleinman, H.K., and Dym, M. (1995). Basement membrane gene expression by Sertoli and peritubular myoid cells in vitro in the rat. Biol Reprod *52*, 320-330.

Robaire, B., and Henderson, N.A. (2006). Actions of 5alpha-reductase inhibitors on the epididymis. Mol Cell Endocrinol *250*, 190-195.

Robaire, B., and Hermo, L. (1988). Efferent Ducts, Epididymis, and Vas Deferens: Structure, Functions and Their Regulation. In The Physiology of Reproduction, 1st Edition, K. Knobil, and J.D. Neill, eds. (Raven Press), pp. 999-1065.

Robaire, B., Hinton, B.T., and Orgebin-Crist, M.C. (2006). The Epididymis. In Knobil and Neill's Physiology of Reproduction, 3rd Edition, J.D. Neill, ed. (Elsevier), p. 1071.

Robaire, B., Seenundun, S., Hamzeh, M., and Lamour, S.A. (2007). Androgenic regulation of novel genes in the epididymis. Asian J Androl *9*, 545-553.

Robaire, B., and Viger, R.S. (1995). Regulation of epididymal epithelial cell functions. Biol Reprod *52*, 226-236.

Robertson, K.M., O'Donnell, L., Jones, M.E., Meachem, S.J., Boon, W.C., Fisher, C.R., Graves, K.H., McLachlan, R.I., and Simpson, E.R. (1999). Impairment of spermatogenesis in mice lacking a functional aromatase (cyp 19) gene. Proc Natl Acad Sci U S A *96*, 7986-7991.

Roche, P.J., Hoare, S.A., and Parker, M.G. (1992). A consensus DNA-binding site for the androgen receptor. Mol Endocrinol *6*, 2229-2235.

Romano, F., Tripiciano, A., Muciaccia, B., De Cesaris, P., Ziparo, E., Palombi, F., and Filippini, A. (2005). The contractile phenotype of peritubular smooth muscle cells is locally controlled: possible implications in male fertility. Contraception *72*, 294-297.

Roselli, C.E., West, N.B., and Brenner, R.M. (1991). Androgen receptor and 5 alpha-reductase activity in the ductuli efferentes and epididymis of adult rhesus macaques. Biol Reprod *44*, 739-745.

Rosenfeld, C.S., Cooke, P.S., Welsh, T.H., Jr., Simmer, G., Hufford, M.G., Gustafsson, J.A., Hess, R.A., and Lubahn, D.B. (2000). The differential fate of mesonephric tubular-derived efferent ductules in estrogen receptor-alpha knockout versus wild-type female mice. Endocrinology *141*, 3792-3798.

Rugh, R. (1964). A Laboratory Manual of Vertebrate Embryology, 5th edn. (Harcourt, Brace and World, New York).

Russell, L.D. (1979). Spermatid-Sertoli tubulobulbar complexes as devices for elimination of cytoplasm from the head region late spermatids of the rat. Anat Rec *194*, 233-246.

Russell, L.D., and Clermont, Y. (1977). Degeneration of germ cells in normal, hypophysectomized and hormone treated hypophysectomized rats. Anat Rec *187*, 347-366.

Russell, L.D., Ettlin, R.A., Sinha Hikim, A.P., and Clegg, E.D. (1990). The classification and timing of spermatogenesis. In Histological and histopathological evaluation of the testis (Clearwater, FL, Cache River Press).

Russell, L.D., Malone, J.P., and Karpas, S.L. (1981). Morphological pattern elicited by agents affecting spermatogenesis by stimulation. Tissue Cell *13*, 369-380.

Ruz, R., Gregory, M., Smith, C.E., Cyr, D.G., Lubahn, D.B., Hess, R.A., and Hermo, L. (2006). Expression of aquaporins in the efferent ductules, sperm counts, and sperm motility in estrogen receptor-alpha deficient mice fed lab chow versus casein. Mol Reprod Dev *73*, 226-237.

Ryan, R.J., Charlesworth, M.C., McCormick, D.J., Milius, R.P., and Keutmann, H.T. (1988). The glycoprotein hormones: recent studies of structure-function relationships. FASEB J *2*, 2661-2669.

Sainio, K., Hellstedt, P., Kreidberg, J.A., Saxen, L., and Sariola, H. (1997). Differential regulation of two sets of mesonephric tubules by WT-1. Development *124*, 1293-1299.

Saito, K., O'Donnell, L., McLachlan, R.I., and Robertson, D.M. (2000). Spermiation failure is a major contributor to early spermatogenic suppression caused by hormone withdrawal in adult rats. Endocrinology *141*, 2779-2785.

Sato, T., Matsumoto, T., Kawano, H., Watanabe, T., Uematsu, Y., Sekine, K., Fukuda, T., Aihara, K., Krust, A., Yamada, T., *et al.* (2004). Brain masculinization requires androgen receptor function. Proc Natl Acad Sci U S A *101*, 1673-1678.

Savage, J.J., Yaden, B.C., Kiratipranon, P., and Rhodes, S.J. (2003). Transcriptional control during mammalian anterior pituitary development. Gene *319*, 1-19.

Scarpino, S., Morena, A.R., Petersen, C., Froysa, B., Soder, O., and Boitani, C. (1998). A rapid method of Sertoli cell isolation by DSA lectin, allowing mitotic analyses. Mol Cell Endocrinol *146*, 121-127.

Schmittgen, T.D., and Livak, K.J. (2008). Analyzing real-time PCR data by the comparative C(T) method. Nat Protoc *3*, 1101-1108.

Sekido, R., and Lovell-Badge, R. (2009). Sex determination and SRY: down to a wink and a nudge? Trends Genet *25*, 19-29.

Serre, V., and Robaire, B. (1999). Distribution of immune cells in the epididymis of the aging Brown Norway rat is segment-specific and related to the luminal content. Biol Reprod *61*, 705-714.

Shan, L., Hardy, D.O., Catterall, J.F., and Hardy, M.P. (1995). Effects of luteinizing hormone (LH) and androgen on steady state levels of messenger ribonucleic acid for LH receptors, androgen receptors, and steroidogenic enzymes in rat Leydig cell progenitors in vivo. Endocrinology *136*, 1686-1693.

Shayu, D., and Rao, A.J. (2006). Expression of functional aromatase in the epididymis: role of androgens and LH in modulation of expression and activity. Mol Cell Endocrinol *249*, 40-50.

Shono, T., Suita, S., Kai, H., and Yamaguchi, Y. (2004). Short-time exposure to vinclozolin in utero induces testicular maldescent associated with a spinal nucleus alteration of the genitofemoral nerve in rats. J Pediatr Surg *39*, 217-219; discussion 217-219.

Shum, W.W., Da Silva, N., Brown, D., and Breton, S. (2009). Regulation of luminal acidification in the male reproductive tract via cell-cell crosstalk. J Exp Biol *212*, 1753-1761.

Sieveking, D.P., Lim, P., Chow, R.W., Dunn, L.L., Bao, S., McGrath, K.C., Heather, A.K., Handelsman, D.J., Celermajer, D.S., and Ng, M.K. (2010). A sex-specific role for androgens in angiogenesis. J Exp Med *207*, 345-352.

Silver, L.M. (1995). Mouse Genetics: Concepts and Applications (Oxford University Press).

Simanainen, U., McNamara, K., Davey, R.A., Zajac, J.D., and Handelsman, D.J. (2008). Severe subfertility in mice with AR inactivation in sex accessory organs, but not in testis. Endocrinology.

Sinclair, A.H., Berta, P., Palmer, M.S., Hawkins, J.R., Griffiths, B.L., Smith, M.J., Foster, J.W., Frischauf, A.M., Lovell-Badge, R., and Goodfellow, P.N. (1990). A gene from the human sex-determining region encodes a protein with homology to a conserved DNA-binding motif. Nature *346*, 240-244.

Singh, J., and Handelsman, D.J. (1996a). The effects of recombinant FSH on testosterone-induced spermatogenesis in gonadotrophin-deficient (hpg) mice. J Androl *17*, 382-393.

Singh, J., and Handelsman, D.J. (1996b). Neonatal administration of FSH increases Sertoli cell numbers and spermatogenesis in gonadotropin-deficient (hpg) mice. J Endocrinol *151*, 37-48.

Singh, J., O'Neill, C., and Handelsman, D.J. (1995). Induction of spermatogenesis by androgens in gonadotropin-deficient (hpg) mice. Endocrinology *136*, 5311-5321.

Sinkevicius, K.W., Laine, M., Lotan, T.L., Woloszyn, K., Richburg, J.H., and Greene, G.L. (2009). Estrogen-dependent and -independent estrogen receptor-alpha signaling separately regulate male fertility. Endocrinology *150*, 2898-2905.

Sipila, P., Jalkanen, J., Huhtaniemi, I.T., and Poutanen, M. (2009). Novel epididymal proteins as targets for the development of post-testicular male contraception. Reproduction *137*, 379-389.

Sipila, P., Pujianto, D.A., Shariatmadari, R., Nikkila, J., Lehtoranta, M., Huhtaniemi, I.T., and Poutanen, M. (2006). Differential endocrine regulation of genes enriched in initial segment and distal caput of the mouse epididymis as revealed by genome-wide expression profiling. Biol Reprod *75*, 240-251.

Siril Ariyaratne, H.B., Chamindrani Mendis-Handagama, S., Buchanan Hales, D., and Ian Mason, J. (2000). Studies on the onset of Leydig precursor cell differentiation in the prepubertal rat testis. Biol Reprod *63*, 165-171.

Skinner, M.K., Fetterolf, P.M., and Anthony, C.T. (1988). Purification of a paracrine factor, P-Mod-S, produced by testicular peritubular cells that modulates Sertoli cell function. J Biol Chem *263*, 2884-2890.

Skinner, M.K., and Fritz, I.B. (1985). Testicular peritubular cells secrete a protein under androgen control that modulates Sertoli cell functions. Proc Natl Acad Sci U S A *82*, 114-118.

Skinner, M.K., Tung, P.S., and Fritz, I.B. (1985). Cooperativity between Sertoli cells and testicular peritubular cells in the production and deposition of extracellular matrix components. J Cell Biol *100*, 1941-1947.

Smith, C., and Mackay, S. (1991). Morphological development and fate of the mouse mesonephros. J Anat *174*, 171-184.

Smith, L. (2011). Good planning and serendipity: exploiting the Cre/Lox system in the testis. Reproduction *141*, 151-161.

Sneddon, S.F., Walther, N., and Saunders, P.T. (2005). Expression of androgen and estrogen receptors in sertoli cells: studies using the mouse SK11 cell line. Endocrinology *146*, 5304-5312.

Snyder, E.M., Small, C.L., Li, Y., and Griswold, M.D. (2009). Regulation of gene expression by estrogen and testosterone in the proximal mouse reproductive tract. Biol Reprod *81*, 707-716.

Soler, C., de Monserrat, J.J., Nunez, M., Gutierrez, R., Nunez, J., Sancho, M., and Cooper, T.G. (2005). Regionalization of epididymal duct and epithelium in rats and mice by automatic computer-aided morphometric analysis. Asian J Androl *7*, 267-275.

Sonnenberg-Riethmacher, E., Walter, B., Riethmacher, D., Godecke, S., and Birchmeier, C. (1996). The c-ros tyrosine kinase receptor controls regionalization and differentiation of epithelial cells in the epididymis. Genes Dev *10*, 1184-1193.

Srinivas, S., Watanabe, T., Lin, C.S., William, C.M., Tanabe, Y., Jessell, T.M., and Costantini, F. (2001). Cre reporter strains produced by targeted insertion of EYFP and ECFP into the ROSA26 locus. BMC Dev Biol *1*, 4.

Staack, A., Donjacour, A.A., Brody, J., Cunha, G.R., and Carroll, P. (2003). Mouse urogenital development: a practical approach. Differentiation *71*, 402-413.

Starzec, A.B., Lerrant, Y., Berault, A., and Counis, R. (1996). Testosterone inhibits the basal and gonadotropin-releasing hormone-stimulated synthesis and release of newly synthesized alpha- and lutropin (LH) beta-subunit but not release of stored LH in cultured rat pituitary cells. Biochim Biophys Acta *1310*, 348-354.

Steger, R.W., Chandrashekar, V., Zhao, W., Bartke, A., and Horseman, N.D. (1998). Neuroendocrine and reproductive functions in male mice with targeted disruption of the prolactin gene. Endocrinology *139*, 3691-3695.

Stocco, D.M. (2001). Tracking the role of a star in the sky of the new millennium. Mol Endocrinol *15*, 1245-1254.

Sugimura, Y., Cunha, G.R., and Bigsby, R.M. (1986). Androgenic induction of DNA synthesis in prostatic glands induced in the urothelium of testicular feminized (Tfm/Y) mice. Prostate *9*, 217-225.

Sun, E.L., and Flickinger, C.J. (1979). Development of cell types and of regional differences in the postnatal rat epididymis. Am J Anat *154*, 27-55.

Sylvester, S.R., and Griswold, M.D. (1994). The testicular iron shuttle: a "nurse" function of the Sertoli cells. J Androl *15*, 381-385.

Tadokoro, Y., Yomogida, K., Ohta, H., Tohda, A., and Nishimune, Y. (2002). Homeostatic regulation of germinal stem cell proliferation by the GDNF/FSH pathway. Mech Dev *113*, 29-39.

Takagi-Morishita, Y., Kuhara, A., Sugihara, A., Yamada, N., Yamamoto, R., Iwasaki, T., Tsujimura, T., Tanji, N., and Terada, N. (2002). Castration induces apoptosis in the mouse epididymis during postnatal development. Endocr J *49*, 75-84.

Tan, K.A., De Gendt, K., Atanassova, N., Walker, M., Sharpe, R.M., Saunders, P.T., Denolet, E., and Verhoeven, G. (2005). The role of androgens in sertoli cell proliferation and functional maturation: studies in mice with total or Sertoli cell-selective ablation of the androgen receptor. Endocrinology *146*, 2674-2683.

Tanwar, P.S., Zhang, L., Tanaka, Y., Taketo, M.M., Donahoe, P.K., and Teixeira, J.M. (2010). Focal Mullerian duct retention in male mice with constitutively activated beta-catenin expression in the Mullerian duct mesenchyme. Proc Natl Acad Sci U S A *107*, 16142-16147.

Tapanainen, J.S., Aittomaki, K., Min, J., Vaskivuo, T., and Huhtaniemi, I.T. (1997). Men homozygous for an inactivating mutation of the follicle-stimulating hormone (FSH) receptor gene present variable suppression of spermatogenesis and fertility. Nat Genet *15*, 205-206.

Temple, J.L., Scordalakes, E.M., Bodo, C., Gustafsson, J.A., and Rissman, E.F. (2003). Lack of functional estrogen receptor beta gene disrupts pubertal male sexual behavior. Horm Behav *44*, 427-434.

Thomson, A.A., and Marker, P.C. (2006). Branching morphogenesis in the prostate gland and seminal vesicles. Differentiation *74*, 382-392.

Tilbrook, A.J., and Clarke, I.J. (2001). Negative feedback regulation of the secretion and actions of gonadotropin-releasing hormone in males. Biol Reprod *64*, 735-742.

Tilmann, C., and Capel, B. (1999). Mesonephric cell migration induces testis cord formation and Sertoli cell differentiation in the mammalian gonad. Development *126*, 2883-2890.

Toda, K., Okada, T., Hayashi, Y., and Saibara, T. (2008). Preserved tissue structure of efferent ductules in aromatase-deficient mice. J Endocrinol *199*, 137-146.

Tomaszewski, J., Joseph, A., Archambeault, D., and Yao, H.H. (2007). Essential roles of inhibin beta A in mouse epididymal coiling. Proc Natl Acad Sci U S A *104*, 11322-11327.

Toshimori, K., and Ito, C. (2003). Formation and organization of the mammalian sperm head. Arch Histol Cytol *66*, 383-396.

Tripiciano, A., Filippini, A., Giustiniani, Q., and Palombi, F. (1996). Direct visualization of rat peritubular myoid cell contraction in response to endothelin. Biol Reprod *55*, 25-31.

Tsai, M.Y., Yeh, S.D., Wang, R.S., Yeh, S., Zhang, C., Lin, H.Y., Tzeng, C.R., and Chang, C. (2006). Differential effects of spermatogenesis and fertility in mice lacking androgen receptor in individual testis cells. Proc Natl Acad Sci U S A *103*, 18975-18980.

Turner, T.T., Bomgardner, D., Jacobs, J.P., and Nguyen, Q.A. (2003). Association of segmentation of the epididymal interstitium with segmented tubule function in rats and mice. Reproduction *125*, 871-878.

Turner, T.T., Johnston, D.S., Finger, J.N., and Jelinsky, S.A. (2007). Differential gene expression among the proximal segments of the rat epididymis is lost after efferent duct ligation. Biol Reprod *77*, 165-171.

Turner, T.T., Johnston, D.S., and Jelinsky, S.A. (2006). Epididymal genomics and the search for a male contraceptive. Mol Cell Endocrinol *250*, 178-183.

Turner, T.T., and Riley, T.A. (1999). p53 independent, region-specific epithelial apoptosis is induced in the rat epididymis by deprivation of luminal factors. Mol Reprod Dev *53*, 188-197.

Ungefroren, H., Ivell, R., and Ergun, S. (1997). Region-specific expression of the androgen receptor in the human epididymis. Mol Hum Reprod *3*, 933-940.

van der Schoot, P., and Elger, W. (1992). Androgen-induced prevention of the outgrowth of cranial gonadal suspensory ligaments in fetal rats. J Androl *13*, 534-542.

Vannier, B., Loosfelt, H., Meduri, G., Pichon, C., and Milgrom, E. (1996). Anti-human FSH receptor monoclonal antibodies: immunochemical and immunocytochemical characterization of the receptor. Biochemistry *35*, 1358-1366.

Vergouwen, R.P., Jacobs, S.G., Huiskamp, R., Davids, J.A., and de Rooij, D.G. (1991). Proliferative activity of gonocytes, Sertoli cells and interstitial cells during testicular development in mice. J Reprod Fertil *93*, 233-243.

Verhoeven, G., Hoeben, E., and De Gendt, K. (2000). Peritubular cell-Sertoli cell interactions: factors involved in PmodS activity. Andrologia *32*, 42-45.

Vogl, A.W., Pfeiffer, D.C., Redenbach, D.M., and Grove, B.D. (1993). Sertoli cell cytoskeleton. In The Sertoli cell, L.D. Russell, and G.M. D, eds. (Cache River Press), pp. 39-86.

Vornberger, W., Prins, G., Musto, N.A., and Suarez-Quian, C.A. (1994). Androgen receptor distribution in rat testis: new implications for androgen regulation of spermatogenesis. Endocrinology *134*, 2307-2316.

Wagner, M.S., Wajner, S.M., and Maia, A.L. (2008). The role of thyroid hormone in testicular development and function. J Endocrinol *199*, 351-365.

Walker, W.H. (2010). Non-classical actions of testosterone and spermatogenesis. Philos Trans R Soc Lond B Biol Sci *365*, 1557-1569.

Wang, R.S., Yeh, S., Chen, L.M., Lin, H.Y., Zhang, C., Ni, J., Wu, C.C., di Sant'Agnese, P.A., deMesy-Bentley, K.L., Tzeng, C.R., *et al.* (2006). Androgen receptor in sertoli cell is essential for germ cell nursery and junctional complex formation in mouse testes. Endocrinology *147*, 5624-5633.

Wang, Y., Song, L., and Zhou, C.J. The canonical Wnt/beta-catenin signaling pathway regulates Fgf signaling for early facial development. Dev Biol *349*, 250-260.

Ward, W.S. (2010). Function of sperm chromatin structural elements in fertilization and development. Mol Hum Reprod *16*, 30-36.

Waterston, R.H., Lindblad-Toh, K., Birney, E., Rogers, J., Abril, J.F., Agarwal, P., Agarwala, R., Ainscough, R., Alexandersson, M., An, P., *et al.* (2002). Initial sequencing and comparative analysis of the mouse genome. Nature *420*, 520-562.

Welsh, M., Moffat, L., Belling, K., de Franca, L.R., Segatelli, T.M., Saunders, P.T.K., Sharpe, R.M., and Smith, L.B. (2011). Androgen receptor Signaling in Peritubular Myoid Cells is Essential for Normal Differentiation and Function of Adult Leydig Cells. Int J Androl *In Press*.

Welsh, M., Moffat, L., Jack, L., McNeilly, A., Brownstein, D., Saunders, P.T., Sharpe, R.M., and Smith, L.B. (2010a). Deletion of Androgen Receptor in the Smooth Muscle of the Seminal Vesicles Impairs Secretory Function and Alters Its Responsiveness to Exogenous Testosterone and Estradiol. Endocrinology.

Welsh, M., Saunders, P.T., Atanassova, N., Sharpe, R.M., and Smith, L.B. (2009a). Androgen action via testicular peritubular myoid cells is essential for male fertility. FASEB J *23*, 4218-4230.

Welsh, M., Saunders, P.T., Fisken, M., Scott, H.M., Hutchison, G.R., Smith, L.B., and Sharpe, R.M. (2008). Identification in rats of a programming window for reproductive tract masculinization, disruption of which leads to hypospadias and cryptorchidism. J Clin Invest *118*, 1479-1490.

Welsh, M., Saunders, P.T., Marchetti, N.I., and Sharpe, R.M. (2006). Androgen-dependent mechanisms of Wolffian duct development and their perturbation by flutamide. Endocrinology *147*, 4820-4830.

Welsh, M., Saunders, P.T., and Sharpe, R.M. (2007). The critical time window for androgen-dependent development of the Wolffian duct in the rat. Endocrinology *148*, 3185-3195.

Welsh, M., Sharpe, R.M., Moffat, L., Atanassova, N., Saunders, P.T., Kilter, S., Bergh, A., and Smith, L.B. (2010b). Androgen action via testicular arteriole smooth muscle cells is important for Leydig cell function, vasomotion and testicular fluid dynamics. PLoS One *5*, e13632.

Welsh, M., Sharpe, R.M., Walker, M., Smith, L.B., and Saunders, P.T. (2009b). New insights into the role of androgens in wolffian duct stabilization in male and female rodents. Endocrinology *150*, 2472-2480.

Wen, S., Schwarz, J.R., Niculescu, D., Dinu, C., Bauer, C.K., Hirdes, W., and Boehm, U. (2008). Functional characterization of genetically labeled gonadotropes. Endocrinology *149*, 2701-2711.

Weng, D.Y., Zhang, Y., Hayashi, Y., Kuan, C.Y., Liu, C.Y., Babcock, G., Weng, W.L., Schwemberger, S., and Kao, W.W. (2008). Promiscuous recombination of LoxP alleles during gametogenesis in cornea Cre driver mice. Mol Vis *14*, 562-571.

Wiater, E., Lewis, K.A., Donaldson, C., Vaughan, J., Bilezikjian, L., and Vale, W. (2009). Endogenous betaglycan is essential for high-potency inhibin antagonism in gonadotropes. Mol Endocrinol *23*, 1033-1042.

Wickings, E. J., and Nieschlag, E. (1978). The effects of active immunization with testosterone on pituitary-gonadal feedback in the male rhesus monkey (Macaca mulatta). Biol Reprod *18*, 602-607.

Wilhelm, D., Palmer, S., and Koopman, P. (2007). Sex determination and gonadal development in mammals. Physiol Rev *87*, 1-28.

Willems, A., Batlouni, S.R., Esnal, A., Swinnen, J.V., Saunders, P.T., Sharpe, R.M., Franca, L.R., De Gendt, K., and Verhoeven, G. (2010). Selective ablation of the androgen receptor in mouse sertoli cells affects sertoli cell maturation, barrier formation and cytoskeletal development. PLoS One *5*, e14168.

Willems, A., De Gendt, K., Allemeersch, J., Smith, L.B., Welsh, M., Swinnen, J.V., and Verhoeven, G. (2009). Early effects of Sertoli cell-selective androgen receptor ablation on testicular gene expression. Int J Androl *33*, 507-517.

Wolfe, A., Divall, S., Singh, S.P., Nikrodhanond, A.A., Baria, A.T., Le, W.W., Hoffman, G.E., and Radovick, S. (2008). Temporal and spatial regulation of CRE recombinase expression in gonadotrophin-releasing hormone neurones in the mouse. Journal of Neuroendocrinology *20*, 909-916.

Wong, E.W., Mruk, D.D., and Cheng, C.Y. (2008). Biology and regulation of ectoplasmic specialization, an atypical adherens junction type, in the testis. Biochim Biophys Acta *1778*, 692-708.

Wong, P.Y. (1990). Abnormal fluid transport by the epididymis as a cause of obstructive azoospermia. Reprod Fertil Dev *2*, 115-127.

Wreford, N.G., Rajendra Kumar, T., Matzuk, M.M., and de Kretser, D.M. (2001). Analysis of the testicular phenotype of the follicle-stimulating hormone beta-subunit knockout and the activin type II receptor knockout mice by stereological analysis. Endocrinology *142*, 2916-2920.

Wu, C.T., Altuwaijri, S., Ricke, W.A., Huang, S.P., Yeh, S., Zhang, C., Niu, Y., Tsai, M.Y., and Chang, C. (2007). Increased prostate cell proliferation and loss of cell differentiation in mice lacking prostate epithelial androgen receptor. Proc Natl Acad Sci U S A *104*, 12679-12684.

Wu, X., Arumugam, R., Zhang, N., and Lee, M.M. (2010). Androgen profiles during pubertal Leydig cell development in mice. Reproduction *140*, 113-121.

Xu, Q., Lin, H.Y., Yeh, S.D., Yu, I.C., Wang, R.S., Chen, Y.T., Zhang, C., Altuwaijri, S., Chen, L.M., Chuang, K.H., *et al.* (2007). Infertility with defective spermatogenesis and steroidogenesis in male mice lacking androgen receptor in Leydig cells. Endocrine *32*, 96-106.

Xuan, S., Baptista, C.A., Balas, G., Tao, W., Soares, V.C., and Lai, E. (1995). Winged helix transcription factor BF-1 is essential for the development of the cerebral hemispheres. Neuron *14*, 1141-1152.

Yamashita, S. (2004). Localization of estrogen and androgen receptors in male reproductive tissues of mice and rats. Anat Rec A Discov Mol Cell Evol Biol *279*, 768-778.

Yao, H.H., and Capel, B. (2002). Disruption of testis cords by cyclopamine or forskolin reveals independent cellular pathways in testis organogenesis. Dev Biol *246*, 356-365.

Yao, H.H., Whoriskey, W., and Capel, B. (2002). Desert Hedgehog/Patched 1 signaling specifies fetal Leydig cell fate in testis organogenesis. Genes Dev *16*, 1433-1440.

Yaswen, L., Diehl, N., Brennan, M.B., and Hochgeschwender, U. (1999). Obesity in the mouse model of pro-opiomelanocortin deficiency responds to peripheral melanocortin. Nat Med *5*, 1066-1070.

Yeh, S., Tsai, M.Y., Xu, Q., Mu, X.M., Lardy, H., Huang, K.E., Lin, H., Yeh, S.D., Altuwaijri, S., Zhou, X., *et al.* (2002). Generation and characterization of androgen receptor knockout (ARKO) mice: an in vivo model for the study of androgen functions in selective tissues. Proc Natl Acad Sci U S A *99*, 13498-13503.

Yeung, C.H., Anapolski, M., Sipila, P., Wagenfeld, A., Poutanen, M., Huhtaniemi, I., Nieschlag, E., and Cooper, T.G. (2002). Sperm volume regulation: maturational changes in fertile and infertile transgenic mice and association with kinematics and tail angulation. Biol Reprod *67*, 269-275.

Yeung, C.H., Sonnenberg-Riethmacher, E., and Cooper, T.G. (1999). Infertile spermatozoa of c-ros tyrosine kinase receptor knockout mice show flagellar angulation and maturational defects in cell volume regulatory mechanisms. Biol Reprod *61*, 1062-1069.

You, L., and Sar, M. (1998). Androgen receptor expression in the testes and epididymides of prenatal and postnatal Sprague-Dawley rats. Endocrine *9*, 253-261.

Zambrowicz, B.P., Imamoto, A., Fiering, S., Herzenberg, L.A., Kerr, W.G., and Soriano, P. (1997). Disruption of overlapping transcripts in the ROSA beta geo 26 gene trap strain leads to widespread expression of beta-galactosidase in mouse embryos and hematopoietic cells. Proc Natl Acad Sci U S A *94*, 3789-3794.

Zhang, C., Yeh, S., Chen, Y.T., Wu, C.C., Chuang, K.H., Lin, H.Y., Wang, R.S., Chang, Y.J., Mendis-Handagama, C., Hu, L., *et al.* (2006). Oligozoospermia with normal fertility in male mice lacking the androgen receptor in testis peritubular myoid cells. Proc Natl Acad Sci U S A *103*, 17718-17723.

Zhang, F.P., Hamalainen, T., Kaipia, A., Pakarinen, P., and Huhtaniemi, I. (1994). Ontogeny of luteinizing hormone receptor gene expression in the rat testis. Endocrinology *134*, 2206-2213.

Zhang, F.P., Pakarainen, T., Zhu, F., Poutanen, M., and Huhtaniemi, I. (2004). Molecular characterization of postnatal development of testicular steroidogenesis in luteinizing hormone receptor knockout mice. Endocrinology *145*, 1453-1463.

Zhang, F.P., Poutanen, M., Wilbertz, J., and Huhtaniemi, I. (2001). Normal prenatal but arrested postnatal sexual development of luteinizing hormone receptor knockout (LuRKO) mice. Mol Endocrinol *15*, 172-183.

Zhao, G.Q., Chen, Y.X., Liu, X.M., Xu, Z., and Qi, X. (2001). Mutation in Bmp7 exacerbates the phenotype of Bmp8a mutants in spermatogenesis and epididymis. Dev Biol *240*, 212-222.

Zhou, Q., Clarke, L., Nie, R., Carnes, K., Lai, L.W., Lien, Y.H., Verkman, A., Lubahn, D., Fisher, J.S., Katzenellenbogen, B.S., *et al.* (2001). Estrogen action and male fertility: roles of the sodium/hydrogen exchanger-3 and fluid reabsorption in reproductive tract function. Proc Natl Acad Sci U S A *98*, 14132-14137.

Zhou, Q., Nie, R., Prins, G.S., Saunders, P.T., Katzenellenbogen, B.S., and Hess, R.A. (2002). Localization of androgen and estrogen receptors in adult male mouse reproductive tract. J Androl *23*, 870-881.

Zhou, X., Kudo, A., Kawakami, H., and Hirano, H. (1996). Immunohistochemical localization of androgen receptor in mouse testicular germ cells during fetal and postnatal development. Anat Rec *245*, 509-518.

Zhou, Y., Xu, B.C., Maheshwari, H.G., He, L., Reed, M., Lozykowski, M., Okada, S., Cataldo, L., Coschigamo, K., Wagner, T.E., *et al.* (1997). A mammalian model for Laron syndrome produced by targeted disruption of the mouse growth hormone receptor/binding protein gene (the Laron mouse). Proc Natl Acad Sci U S A *94*, 13215-13220.

Zickler, D., and Kleckner, N. (1999). Meiotic chromosomes: integrating structure and function. Annu Rev Genet *33*, 603-754.

Zimmermann, S., Steding, G., Emmen, J.M., Brinkmann, A.O., Nayernia, K., Holstein, A.F., Engel, W., and Adham, I.M. (1999). Targeted disruption of the Insl3 gene causes bilateral cryptorchidism. Mol Endocrinol *13*, 681-691.